Deltares

Enabling Delta Life

Derivation of the semi-probabilistic safety assessment rule for inner slope stability

Deltares

Derivation of the semi-probabilistic safety assessment rule for inner slope stability

WTI 2017: Cluster C, macrostability

Wim Kanning
Maximilian Huber
Mark van der Krogt
Timo Schweckendiek
Ana Martins Teixeira

1220080-003

Deltares

Title
Derivation of the semi-probabilistic
safety assessment rule for inner slope stability

Client	Project	Reference	Pages
Rijkswaterstaat Water, Verkeer en Leefomgeving Locatie Lelystad	1220080-003	1220080-003-ZWS-0019	197

Keywords
WTI 2017, safety factors, calibration, levees, slope stability, probabilistic analysis, reliability

Summary
In the Netherlands, all primary flood defences are periodically tested against statutory safety standards. The new safety assessment framework WTI 2017 (defined in terms of allowable probabilities of flooding) allows for probabilistic as well as semi-probabilistic assessments, which are based on a partial safety factor approach. To ensure consistency between probabilistic and semi-probabilistic assessments, the semi-probabilistic rules have to be (re)calibrated in order give similar results as probabilistic assessments.

This report presents the safety format, calibration procedure and results of the calibration of the semi-probabilistic assessment rule for inner slope stability (STBI) within the WTI 2017. The calibration procedure involves the following steps: 1) establish a reliability requirement for the cross-section, 2) establish the safety format, 3) establish the safety factors and 4) compare the calibration results with present-day rules. The slope stability computations have been based on an undrained material model for low permeable materials (peat, clay) and a drained material model for sand. Uplift Van has been used method to determine the critical slip circle. The effects of overtopping have not been considered in the calibration. Hence, the safety factors are valid only for cases without overtopping.

For the calibration of safety factors, 11 dikes have been analysed. For each dike, the berm lengths have been varied to obtain the right order of reliability. This resulted in a total of 33 analysed cases. The factor of safety, reliability index and FORM sensitivity factors have been computed for each case. This has resulted in the choice of a safety format that entails the computation of a factor of safety (determined by Uplift Van) using characteristic (5%) values of the strength parameters, and furthermore a model factor (1.06 for Uplift Van), a normative water level (MHW) and one, target reliability dependent, overall safety factor that a dike has to comply with. The target reliability dependent safety factor (γ_n) is γ_n = 0.161 · $\beta_{T,cross}$ + 0.463; in which $\beta_{T,cross}$ is the target reliability. The main difference with the current safety format is the absence of material factors mainly because the uncertainties in material parameters are covered sufficiently by using characteristic values. The safety format only applies to computations with Uplift Van.

The analysed cases have been used to fit the target reliability dependent safety factor. The resulting semi-probabilistic rule is comparable to the previously derived relations in OI2014_v3. Analyses show that there is no significant effect of differentiating the calibrated safety factor to the safety standard, geology and uplift/no uplift; possibly due to the limited number of cases. The preliminary consequence analysis shows overall agreement with previous assessments and relatively limited additional required berms.

Deltares

Title
Derivation of the semi-probabilistic safety assessment rule for inner slope stability

Client	Project	Reference	Pages
Rijkswaterstaat Water, Verkeer en Leefomgeving Locatie Lelystad	1220080-003	1220080-003-ZWS-0019	197

The calibration presented in this report showed that the determination of the relation between reliability index and required factor of safety was successful for 11 different dikes using the new, undrained material model. However, there are two main limitations to the performed calibration:

a) *Limited number of cases*: The amount of test cases is insufficient to provide well-founded safety factors; it cannot be determined if the derived safety factors are representative enough for the Netherlands and how safe the safety factors are. Neither it is possibly optimize the safety factors (e.g. by differentiating to region). Hence, it is recommended to consider more cases in the calibration.

b) *Limited influence of outside water level* leading to remarkable results and possibly a conservative set of safety factors. This limited influence of the water level can be due to the undrained material model or due to water pressures that are not incorporated probabilistically in the probabilistic slope stability analyses. It is recommended to first investigate the effects of the probabilistic modelling of water pressures. This could also result in smaller required safety factors. When the dependency of the water level on the safety factor and reliability is still limited when the uncertainty related to the water pressures is taken into account explicitly, it should be investigated whether proven strength can be incorporated in slope stability computations.

Another important finding is that the slope stability computations with Spencer did not results in stable output. Hence, only Uplift Van has been used for the calibration and it is recommended to thoroughly test the current implementation of Spencer before using it as the default WTI method.

Version	Date	Author	Initials	Review	Initials	Approval	Initials
1	Nov. 2015 concept	dr.ir. W. Kanning		dr.ir. Jongejan		ir. A. de Leeuw	
2	Dec. 2015	dr.ir.. Kanning		dr.ir. Jongejan		ir. A. de Leeuw	
3	Dec. 2015	dr.ir.. Kanning		dr.ir. Jongejan		ir. A. de Leeuw	

State
final

Deltares

Title
Derivation of the semi-probabilistic
safety assessment rule for inner slope stability

Client	Project	Reference	Pages
Rijkswaterstaat Water, Verkeer en Leefomgeving Locatie Lelystad	1220080-003	1220080-003-ZWS-0019	197

Samenvatting
In Nederland worden alle primaire waterkeringen periodiek getoetst aan de wettelijke veiligheidsnormen. In het kader van de nieuwe normen (gedefinieerd in termen van overstromingskansen) en het nieuwe wettelijk toetsinstrumentarium WTI2017 kan zowel volledig probabilistisch als semi-probabilistisch worden getoetst met partiële veiligheidsfactoren. Voor consistentie tussen beide methodes moeten semi-probabilistische toetsregels gekalibreerd worden om tot vergelijkbare resultaten in semi-probabilistische analyses te komen als in probabilistische analyses.

In dit rapport wordt de beoogde procedure voor de kalibratie van het semi-probabilistische toetsvoorschrift voor het faalmechanisme macrostabiliteit binnenwaarts (STBI) in het WTI-2017 beschreven en gedemonstreerd. De kalibratie behelst de volgende stappen: 1) het vaststellen van de doelbetrouwbaarheid van een doorsnede, 2) het vaststellen van het veiligheidsformat, 3) het vaststellen van de partiële veiligheidsfactoren en 4) het vergelijken van de resultaten met huidige voorschriften. De stabiliteitsberekeningen zijn gebaseerd op een ongedraineerd materiaalmodel voor slecht doorlatende materialen (veen en klei) en gedraineerd materiaalmodel voor zand. Uplift-Van is de gebruikte zoekmethode voor het kritieke schuifvlak. Effecten door overslag zijn niet beschouwd in deze kalibratie. De afgeleide veiligheidsfactoren zijn dan ook enkel geldig voor gevallen zonder overslag.

Voor de kalibratie van partiële veiligheidsfactoren zijn 11 dijkvakken beschouwd. Voor iedere dijk is de bermlengte gevarieerd om in de juiste range van betrouwbaarheid te komen. Dit resulteert een totaal van 33 geanalyseerde cases. Voor iedere case zijn de stabiliteitsfactor, betrouwbaarheidsindex en invloedcoëfficiënten berekend. Op basis van deze resultaten is het veiligheidsformat vastgesteld: de stabiliteitsfactor (bepaald met Uplift-Van) wordt berekend met karakteristieke (5%) waarden voor de sterkteparameters; verder is voorzien in een modelfactor (1.06 voor Uplift Van), de waterstand bij MHW en een betrouwbaarheidsindex-afhankelijke veiligheidsfactor (schadefactor). De afgeleide schadefactor (γ_n) is γ_n = 0.161 · $\beta_{T,cross}$ + 0.463, waarin $\beta_{T,cross}$ de vereiste betrouwbaarheid is.Een verschil met het huidige veiligheidsformat is de afwezigheid van materiaalfactoren. De onzekerheden ten aanzien van materiaalparameters wordt namelijk al voldoende verdisconteerd door het gebruik van karakteristieke waarden. Het veiligheidsformat is alleen geldig voor berekeningen met Uplift Van.

De bovengenoemde cases zijn gebruikt om de relatie tussen betrouwbaarheidsindex en schadefactor af te leiden. Het resulterende semi-probabilistische voorschrift vertoont geen grote verschillen met de huidige relaties die zijn afgeleid voor het OI2014_v3. Verschillende analyses hebben uitgewezen dat er geen reden is om verschillende relaties af te leiden voor verschillende veiligheidsnormen, uplift/geen uplift cases of voor verschillen in geologie, waarschijnlijk door het beperkte aantal cases. In termen van benodigde bermlengtes om te voldoen aan de norm, laat de voorlopige consequentieanalyse zien dat de resultaten dezelfde orde van grote vertonen in vergelijking met de voorgaande toetsingen.

Deltares

Title
Derivation of the semi-probabilistic
safety assessment rule for inner slope stability

Client	Project	Reference	Pages
Rijkswaterstaat Water, Verkeer en Leefomgeving Locatie Lelystad	1220080-003	1220080-003-ZWS-0019	197

De kalibratie in dit rapport laat zien dat de bepaling van de relaties tussen betrouwbaarheidsindex en benodigde stabiliteitsfactor succesvol gebruikt kan worden. Echter, er zijn twee beperkingen:

a) *Beperkt aantal cases*. Doordat slechts een beperkt aantal cases voor de kalibratie zijn gebruikt, kan niet worden bepaald of de afgeleide veiligheidsfactoren representatief zijn voor heel Nederland en in welke mate deze voldoende veilig zijn. Daarnaast is het niet mogelijk om de veiligheidsfactoren te optimaliseren (bijv. per regio) Het wordt aanbevolen om de kalibratie uit te breiden met meer cases.
b) *Een beperkte afhankelijkheid van de buitenwaterstand* leidt tot opmerkelijke resultaten en mogelijk een conservatieve set van veiligheidsfactoren. De beperkte invloed van de waterstand kan het gevolg zijn van het ongedraineerde materiaalmodel of omdat de waterspanning niet probabilistisch is meegenomen in de kalibratie. Het wordt aanbevolen om eerst verder te onderzoeken wat het effect is wanneer waterspanningen probabilistisch worden meegenomen. Dit leidt mogelijk ook tot lagere benodigde veiligheidsfactoren. Als de afhankelijkheid van de waterstand op de stabiliteitsfactor en betrouwbaarheid dan nog steeds beperkt is, kan bewezen sterkte mogelijk worden meegenomen in stabiliteitsberekeningen.

Een laatste bevinding is dat de glijvlakberekeningen met methode Spencer-Van der Meij niet heeft geleid tot stabiele resultaten. Om deze reden is de kalibratie alleen uitgevoerd met Uplift-Van. Een aanbeveling is om de huidige implementatie van de methode Spencer nader te onderzoeken, voordat deze wordt gebruikt als de standaard methode in het WTI.

Symbols (Latin)

Symbol	Definition	Unit
a	Fraction of the length that is sensitive to the failure under study	-
b	Length-effect factor for slope stability failure	m
c'	Effective soil cohesion	kN/m^2
f	Failure probability factor for the failure mechanisms	-
F_s	Factor of safety	-
$F_{s,des}$	Factor of safety computed for design values of input parameters	-
F_exc	Safety standard	yr^{-1}
$FoS_{char}(MHW)$	Factor of safety given MHW computed with design values of input parameters	-
d_w	Decimal height for the water level characterisation	m
h_{dec}	decimate height, water level difference that corresponds to a difference in exceedance frequency of a factor 10	m
IL	Intrusion length	m
L	Total length of the dike segment	m
L_3, L_4	Foreland and hinterland leakage lengths	m
m	Strength increase exponent	-
m_d	Model uncertainty	-
MHW_used	normative water level	m
M_R	Resisiting moment for macrostability limit equilibrium	kN.m
M_S	Driving moment for macrostability limit equilibrium	kN.m
OCR	Over consolidation ratio of the soil	-
$P(\cdot)$	Probability of an event	-
P_f	Probability of failure	yr^{-1}
P_{norm}	Maximum allowable probability of failure (safety standard)	yr^{-1}
P_T	Target failure probability: maximum allowable probability of flooding due to the series of events triggered by the instability of the inner slope that lead to flooding	yr^{-1}
$P_{T,cross}$	Cross-sectional target failure probability; the average cross-sectional probability of failure may not exceed $P_{T,cross}$	yr^{-1}
$P*_{cross}$	Calculated cross-section failure probability	yr^{-1}
POP	Pre-overburden pressure in the soil	kN/m^2
R	Resistance	-*
R_{char}	Characteristic value of stochastic resistance variable	-*
R_{des}	Design value of stochastic resistance variable	-*
S	Load or undrained shear strength ratio	-*
S_i	Subsoil Scenario i	-
S_{char}	Characteristic value of the load	-*
S_{des}	Design load	-*
s_u	Undrained shear strength	kN/m^2
$\tan(\varphi')$	Tangent of the effective friction angle of the soil	-
T	Return period that corresponds to the safety standard of a segment	yr
u	Standard normally distributed variable (mean μ=0 and standard deviation σ=1)	-
WL	Water level at a particular moment relative to NAP	m
X_i	Stochastic variable	-*

Symbol	Definition	Unit
$X_{d,i}$	Design value of the stochastic variable	-*
Z	Limit state function (Z=R-S)	-
Z_{II}	Linearized and normalized limit state function	-

* unit depends on the variable concerned

Symbols (Greek)

Symbol	Definition	Unit
α_i	Influence coefficient for stochastic variable X_i ($\sum\alpha_i^2$=1)	-
α_m	Influence coefficient for model uncertainty parameter	-
α_h	Influence coefficient for water level	-
α_R	Influence coefficient of the resistance in the limit state function	
α_S	Influence coefficient of the hydraulic load in the limit state function	-
β	Reliability index	-
β_{norm}	Reliability index that corresponds to the safety standard	-
β_T	Target reliabiltiy index: minimum allowable reliability index for flooding due to the series of events triggered by the instability of the inner slope that lead to flooding	-
β^*_{cross}	Calculated reliability index	
$\beta_{T,cross}$	Cross sectional reliability requirement (reliability index)	-
γ_d	β_T – invariant model factor	-
γ_m	β_T – invariant material factor	-
γ_n	β_T – dependent safety factor	-
γ^*_n	Calculated safety factor	
γ_R	Partial safety factor for stochastic resistance variable R	-
γ_S	Partial safety factor for stochastic load variable S	-
γ_{unsat}	Unsaturated volumetric unit weight	kN/m^3
γ_{sat}	Saturated volumetric unit weight	kN/m^3
τ	Ultimate shear stress	kN/m^2
$\Phi(\cdot)$	Standard normal distribution function	-
f	Maximum allowable contribution of the failure mode to the probability of flooding	-
μ	Mean value	-*
σ	Standard deviation	-*
σ'_{vy}	Effective vertical yield stress	kN/m^2
$\sigma'_{v,i}$	Effective vertical stress	kN/m^2
ψ	Dilatancy angle	deg

* unit depends on the variable concerned

Contents

1 Introduction **1**
1.1 The WTI project context and background on calibrations 1
1.2 Objectives and scope 2
1.2.1 Objective 2
1.2.2 Scope of the report 2
1.2.3 Software and data 2
1.2.4 Limitations 3
1.3 Approach 3
1.4 Timeline calibration 3
1.5 Outline of the report 4

2 Basic concepts **5**
2.1 Failure probabilities, reliability indices and influence coefficients 5
2.2 The relations between probabilistic and semi-probabilistic assessments 6

3 Slope stability **9**
3.1 Limit equilibrium models 9
3.1.1 Uplift-Van 9
3.1.2 Spencer 9
3.1.3 The WTI 2017 default 9
3.2 Shear strength 10
3.2.1 Mohr-Coulomb for drained analysis 10
3.2.2 Critical state soil mechanics model for undrained analysis 10
3.2.3 Slope stability computations in D-Geo Stability 10
3.3 List of input variables 11
3.4 Spatial averaging 12
3.5 Previously recommended safety factors 13
3.6 Limitations of the calibration 14

4 Calibration procedure **15**

5 Step 1: Establishing reliability requirement **17**
5.1 Target probabilities of flooding 17
5.2 Reliability requirement for slope stability in general 17
5.3 Reliability requirement for slope stability at cross-section level 18

6 Step 2: Establishing the safety format **21**
6.1 Establishing a test set 21
6.1.1 Considerations to establish a test set 21
6.1.2 Location of test set cases 21
6.1.3 Case descriptions and input data 22
6.2 Defining representative influence coefficients 23
6.3 Safety format: representative values and safety factors 25
6.4 The resulting safety format 27

7 Step 3: Establishing safety factors **29**
7.1 The calibration criterion 29

7.2 Calibrating the beta-dependent safety factor 29
7.2.1 Calibration procedure 29
7.2.2 Safety factor as function of the reliability 30

8 Calibration results 31
8.1 Test case results 31
8.1.1 Approach 31
8.1.2 Results of the computations 31
8.1.3 Results of the individual cases 32
8.2 Calibration of the safety factors 33
8.2.1 Approach 33
8.2.2 Fit on all, uncorrected, cases 34
8.2.3 Calibration fit 34
8.3 Differentiation to safety level 35
8.3.1 Beta-gamma relation for different safety levels 35
8.4 Differentiation safety factors: uplift and geology 36
8.4.1 Approach for differentiation to uplift 36
8.4.2 Comparison of the results (FoS and reliability) for uplift and non-uplift cases 38
8.4.3 Differentiation to riverine and marine deposits 39
8.5 Sensitivity analysis 40
8.5.1 Sensitivity for yield stress points 40
8.5.2 Sensitivity for traffic load 41
8.6 Spencer 42
8.7 Conclusions of the calibration 43

9 Semi-probabilistic assessment steps and comparison with other assessments 45
9.1 Inner slope stability semi-probabilistic assessment steps 45
9.2 Comparison with current methods and safety factors 47
9.2.1 Comparison with current safety factors 47
9.2.2 Comparison calibration with VNK and the WTI2006 47
9.3 Preliminary consequence analysis 48
9.4 Examples 49
9.4.1 Example of the proposed semi-probabilistic assessment procedure 49
9.4.2 Example of a semi-probabilistic assessment with SOS subsoil scenarios for dp_190 50

10 Discussion 53
10.1 Discussion on general calibration results 53
10.1.1 General 53
10.1.1 Limited number of cases 53
10.1.2 Limited influence of the water level and proven strength 53
10.1.3 Dealing with proven strength 55
10.2 Discussion on safety format 55
10.3 Proposed activities for 2016 56

11 Conclusions and recommendations 59
11.1 Conclusions 59
11.2 Recommendations 60
11.2.1 Recommendations for the short term (2016): 60
11.2.2 Recommendations for the medium term (2017 - 2019): 60
11.2.3 Recommendations for D-GeoStablility 60

References **63**

Appendices

A Appendix: Characteristic values, safety factors and design points

B Appendix: Probabilistic prototype macrostability

C Appendix: Input and output per test set member

D Appendix: Spatial averaging

E Appendix: The insensitivity to the water level

F Appendix: The influence of traffic loads

1 Introduction

1.1 The WTI project context and background on calibrations

The Dutch primary flood defences are periodically tested against statutory safety standards. These standards were, until recently, defined in terms of design loads. Then, policymakers decided to move towards safety standards defined in terms of maximum allowable probabilities of flooding. To facilitate such a move, a new set of instruments for assessing the safety of flood defences is currently being developed: the WTI 2017.

The WTI 2017 will include probabilistic as well as semi-probabilistic assessment procedures. The latter rest on a partial safety factor approach and allow engineers to evaluate the reliability of flood defences without having to resort to probability calculus. To ensure consistency between probabilistic and semi-probabilistic assessments, the currently used safety factors have to be (re)calibrated. Important aspects within the standard WTI 2017 calibration procedure concern the derivation of reliability requirements, the definition of design values on the basis of influence coefficients, and the handling of spatial correlations.

Generally speaking, the calibration procedure can be summarised in the following steps (based on Jongejan, 2013):

Step 1: Establish a reliability requirement for the cross-section level, which is based on the maximum allowable probability of flooding.

Step 2: Establish the safety format. This includes a study on the FORM influence coefficients (α) based on a wide variety of test data sets. Based on this, characteristic values and partial safety factors that are to be included or not in the semi-probabilistic assessment rule are chosen.

Step 3: Establish the safety factors. This step comprises:

a) the recommendation of reliability index β – invariant safety factors (based on results step 2),
b) generating “designs” that fulfil the semi-probabilistic assessment rule for a range of values of the so-called β – dependent safety factor,
c) assessment of the probability of failure of each “designed” test set member,
d) and application of calibration criteria to select the appropriate functional relationship of the β – dependent safety factor.

Step 4: Compare calibration results with present-day rules. Having finalized the theoretical exercise above, it is highly recommended in the fourth step to compare the calibrated semi-probabilistic assessment rules to the present-day rules, to explain potential differences, and to provide an indication of the consequences.

1.2 Objectives and scope

1.2.1 Objective

This report concerns the derivation of the semi-probabilistic assessment for the WTI 2017 and the respective safety factors' calibration regarding the inner slope stability failure mechanism for dikes in the Netherlands.

More specifically, the main objectives are:

- to determine the reliability requirement accounting for the failure probability budget assigned to slope stability and the length-effect (step 1 from the procedure above);
- to establish the safety format in terms of the envisaged characteristic values and partial factors to be applied (step 2 from the procedure above);
- to derive, based on the step 3 of the procedure above, the functional relationship of the β– dependent safety factor to be applied in a semi-probabilistic assessments of slope stability, as well as other possible safety factors.

1.2.2 Scope of the report

The calibration results concern D-Geo Stability (Deltares' slope stability software) computations carried out with the Uplift-Van method, using an undrained material model for the clay and peat layers, as well as drained material model for sand layers. Other variations to this, such as using Spencer's method, are presented in the sensitivity analysis. The calibration of safety factors covers the failure mechanism slope instability of the inner slope (STBI), slope instability of the outer slope is outside the scope of this report (STBU). Hence, when slope stability is mentioned in this report, it refers to the failure mechanism instability of the inner slope. Slope stability is referred to in the Netherlands as macrostability, which is why the kernel and prototype (used for reliability analysis) are called macrostability. In this report, when referring to safety factors, in fact partial safety factors are meant. When referring to factor of safety, the computed factor of safety using D-Geo Stability is meant.

Besides the calibration, this report discusses the following activities:

- study of the results of the calibration procedure;
- determination and analysis of the test set used for the calibration;
- comparison with the semi-probabilistic assessment rules of the WTI 2011.

Concerning the scope of this study, the following should be noted. While the steps described in Section 1.1 above comprise the entire calibration exercise, the present proof-of-concept study only covers steps 2-3 for a limited number of test cases.

1.2.3 Software and data

- The slope stability computations are made with the D-Geo Stability kernel, beta version of 01-10-2015;
- The waternet creator, version 01-10-2015, is used to determine the phreatic line and water pressures in the soil layers as a function of outside water level;
- the probabilistic calculations are made with a D-Geo Stability prototype implemented in `Python` using PYRE (https://github.com/hackl/pyre), see also Appendix B;
- The geometrical and hydraulic data used for the calibration mainly come from VNK2 databases, while the hydraulic database TMR2006 was used for the derivation of design water levels with Hydra-Ring. The undrained material parameters are provided by Cluster Macrostability.

1.2.4 Limitations

The calibration's goal is to derive a safety format and safety factors for slope stability. The proper functioning of the D-Geo Stability software was supposed to be tested by WTI Cluster Software. The representative test set was provided by WTI Cluster Slope Stability. Errors in both software and cases have been communicated with the Clusters but it was not the main focus of the calibration to test these in great detail. The main emphasis was to obtain consistent and stable output.

The following methods are not discussed in this report:

- Other slope stability methods than Uplift-Van and Spencer are outside the scope of this report. E.g. the method of Bishop, which is a special case of the Uplift Van method, is not explicitly used in the calibration.
- The effect of overflow/overtopping on the safety factors is not considered in the calibration. Jongejan (2015) provides an option on how to deal with overtopping in relation to slope stability. However, since a decision has not yet been made on how to deal with overtopping, this has been not incorporated in the calibration. Hence, the calibration is only valid for situations without overtopping. This is one part of the proposed approach in Jongejan (2015), the step that includes overflow/overtopping is recommended to be investigated.
- The resulting safety factors are not intended for drained shear strength parameters. Only the behaviour of sand layers that might be present in the calibration is modelled as drained behaviour, the behaviour of peat and clay layers are modelled as undrained.

1.3 Approach

To derive a semi-probabilistic safety assessment for inner side slope stability, the calibration approach by Jongejan (2013) has been used. A number of cases has first been used to establish the safety format. From probabilistic calculations, reliability indices and influencing parameters have been derived. These have been used to define the safety format, including safety factors, which should be appropriate, functional and easy to use. Based on this format, a relationship of the β – dependent safety factor has been derived. Two options are possible to derive safety factors: the first option is fitting the factor of safety based on computed values of β. This option is used in the calibration, since it is in line with the WTI2017 approach (see e.g. Jongenjan 2013). The second option is to use standardized influence coefficients of the most important parameters; this option has not been applied in this report. Finally, the potential for optimizing the safety factor – target reliability relation has been investigated, considering effects of e.g. geology and sub-mechanisms (e.g. uplift).

It must be noted that the whole process of choosing a safety format and deriving safety factors is referred to as calibration in this report.

1.4 Timeline calibration

The final 'frozen' version of the DGeo Stability kernel was provided at 01-10-2015. This left less than 2 months for the calibration that is presented in this report. The main consequence of this is that only a relatively limited amount of cases could be analysed. A total of 12 independent dikes have been analysed, of which 11 gave sufficient results to be incorporated in the calibration (Case dp43 did not results in consistent and reproducible output and was left aside). Based on these 11 dikes, a total of 33 cases have been manually adapted, reviewed and analysed by adding various berms lengths to the dikes. The implication of this relatively limited amount of cases is discussed in Chapter 10. The computations and reporting have been carried out by the authors of this report, with help from Maria Luisa Tacari from Deltares with the computation of several cases.

1.5 Outline of the report

The outline of this report follows the same approach as the other WTI calibration studies. Subsequent to this introduction, this report is structured as follows:

- Chapter 2 introduces the basic concepts and definitions of probabilistic and semi-probabilistic design;
- Chapter 3 provides concise descriptions of the computational models applied in the WTI 2017 for slope stability and the relevant input parameters;
- Chapter 4 discusses the procedure developed and envisaged for the final calibration;
- Chapter 5 further describes the first step of this procedure, *i.e.* the definition of reliability requirements;
- Chapter 6 discusses the second step, *i.e.* the establishment of the safety formats; Chapter 7 discusses the third and final step, *i.e.* the establishment of safety factors;
- Chapter 8 provides an overview of the results of the calibration;
- Chapter 9 a summary of the semi-probabilistic assessment steps and comparison with the present-day relations are given;
- Chapter 10 provides a discussion on the results
- Chapter 11 summarizes the most important findings and provides recommendations following from this study.

2 Basic concepts

This section provides a brief overview of the probabilistic context and link between the probabilistic and semi-probabilistic assessments of engineering structures in general. More detailed description of the probabilistic background can be found in standard textbooks.

2.1 Failure probabilities, reliability indices and influence coefficients

A flood defence will fail when the load (S) exceeds its resistance/strength (R). The resistance parameters of a flood defence are, in principle, deterministic. In practice, however, they are uncertain due to spatial variability, a limited number of measurements and measurement uncertainties. Also, the models used to predict critical combinations of parameter values (i.e., combinations that would lead to failure), might produce outcomes that are besides the (unknown) truth. Such model uncertainties also have to be taken into consideration in reliability analyses. This means that the resistance of a flood defence should be treated as a stochastic variable, just like the uncertain loads.

The probability of failure (P_f) equals the probability that load (S) exceeds resistance (R). Herein Z stands for the limit state function. Herein, Z is the limit state function.

$$P_f = P(R - S < 0) = P(Z < 0) \tag{2.1}$$

The First Order Reliability Method (FORM) (Rackwitz, 2001) is an efficient method to compute failure probabilities. It also known as a level II approach. In a FORM-analysis, the limit state function is normalized and linearized in the design point. The design point is the combination of parameter values with the highest probability density for which Z=0. The linearized and normalized limit state function (Z_{II}) resulting from a FORM-analysis has the following form:

$$Z_{II} = \beta - \sum_{i=1}^{n} \alpha_i u_i \tag{2.2}$$

Herein, β is the reliability index, α_i is the influence coefficient for stochastic variable X_i ($\sum \alpha_i^2$=1), and u_i is a standard normally distributed variable (a normal distribution with mean μ=0 and standard deviation σ=1), representing a normalized stochastic variable, involved in the limit state function.

An influence coefficient is a measure for the relative importance of the uncertainty related to a stochastic variable. The squared value of an influence coefficient corresponds to the fraction of the variance (σ^2) of the linearized and normalized limit state function that can be attributed to a stochastic variable.

Generally, a FORM-analysis yields a close approximation of the probability of failure:

$$P(Z_{II} < 0) \approx P(Z < 0) \tag{2.3}$$

Note that the failure probability estimate $P(Z_{II}<0)$ is equal to $P(Z<0)$ when the limit state function is linear and all stochastic variables are independent and normally distributed.

From equation (2.2) and the fact that the sum of the squares of the alpha values is equal to 1, it follows that:

$$P(Z_{II} < 0) = \Phi(-\beta) \tag{2.4}$$

Herein, $\Phi(\ )$ stands for the standard normal cumulative distribution function.

It also follows from equation (2.2) that the design point value ($X_{d,i}$) of a normally distributed stochastic variable X_i with a given mean value μ_i and standard deviation σ_i equals:

$$X_{d,i} = \mu_i + \alpha_i \cdot \beta \cdot \sigma_i \tag{2.5}$$

2.2 The relations between probabilistic and semi-probabilistic assessments

Semi-probabilistic and probabilistic safety assessments are closely related. Both rely on predefined safety standards, limit state functions, and the statistical properties of the stochastic variables that represent the uncertain load and strength parameters. The same uncertainties play a role in semi-probabilistic and probabilistic assessments. Yet a semi-probabilistic assessment rests on a number of simplifications and approximations, giving it the appearance of a deterministic procedure.

In probabilistic safety assessment on calculates the probability of exceeding the ultimate limit state, in which the load (S) and resistance (R) are compared. The evaluated probability of failure, $P(S>R)$, has to be smaller than a given maximum allowable ('target') value (P_T).

In semi-probabilistic assessment, one analyses the difference between the design values of load (S_{des}) and strength (R_{des}): S_{des} should not exceed R_{des}. Design values are defined in terms of representative values (e.g. characteristic values such as 5th or 95th percentiles – 5% or 95%) and (partial) safety factors. This use of terminology is consistent with the Eurocode EN 1990 (CEN, 2002). Readers should be aware that similar terms may have different definitions in other international standards.

It is recommended to calibrate the design values such that the condition $S_{des} \leq R_{des}$ is fulfilled. This implies that the probability of failure meets the reliability requirement: $P(S>R) \leq P_T$. The relationship between probabilistic and semi-probability safety assessments is illustrated in Figure 2.1.

The resistance is decreased by the ratio $1/\gamma_R$ and whereas the load is increased by γ_S [1]. The design values of normally distributed resistance and load variables are given in the following equations.

$$R_{des} = \mu_R - \alpha_R \cdot \beta_T \cdot \sigma_R = R_{char} / \gamma_R \text{ (resistance/strength parameter)} \tag{2.6}$$

$$S_{des} = \mu_S - \alpha_S \cdot \beta_T \cdot \sigma_S = S_{char} \cdot \gamma_S \quad \text{(load parameter)} \tag{2.7}$$

Herein, μ_R and μ_S are the expected values of R and S, α_R and α_S are the values of the FORM-influence coefficients for R and S, β_T the target reliability index, σ_R and σ_S its standard deviation

[1] *Notice that the partial factor γ_S is mentioned here for the sake of completeness in the description of the theoretical concept. In WTI-2017 this value is typically set equal to 1.0 so that the design water level equals the representative value.*

of R and S, R_{char} and S_{char} are the characteristic values of R and S (e.g. 5th percentile for strength parameters and 95th percentile for load parameters) and γ_R and γ_S are the (partial) safety factors.

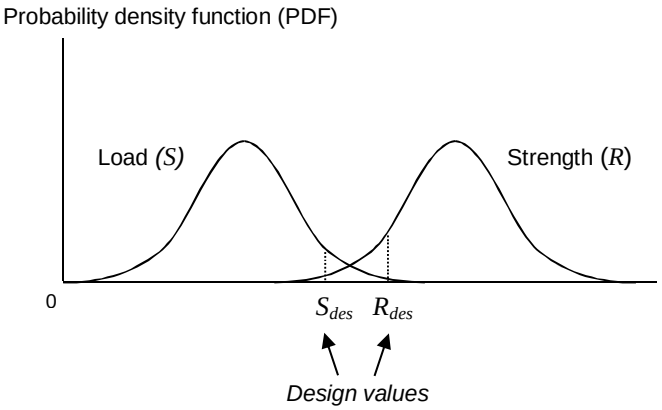

Figure 2.1. Probability density function of load (S) and strength (R), and the correspondent design values S_{des} and R_{des}.

In short, probabilistic and semi-probabilistic assessments *both* require:

- A model of the failure mechanism,
- The probability density functions (PDF) for all stochastic variables (based on statistical data and/or engineering judgment) and
- a reliability requirement ('target') reliability.

The essential differences between probabilistic and semi-probabilistic assessments are:

- In a probabilistic assessment, a failure mechanism model is fed with all possible parameter values and their probabilities (i.e. probability density functions),
- In a semi-probabilistic assessment, a failure mechanism model is fed with unique, 'sufficiently safe' values (i.e. design values). How safe 'sufficiently safe' is, depends ultimately on the reliability requirement and a calibration criterion.

As such, to ensure consistency between probabilistic and semi-probabilistic assessments, calibration exercises are indispensable. The equations for deriving the characteristic values of normally and log-normally distributed variables are given in Appendix A.

3 Slope stability

This section gives a brief overview of the limit equilibrium models and corresponding input, which are used in slope stability assessments. For more information about slope stability assessments, please refer to Van Duinen (2014a) and Van Deen and Van Duinen (2015).
The limit equilibrium models can be used in the macrostability kernel (Van der Meij, 2013), that is used to compute the slope stability FoS. For more and detailed information on limit equilibrium models, the reader is referred to the references (Bishop, 1955; Van, 2001; Spencer, 1967). Additionally, an overview of the basics of drained and undrained shear strength of soils is given. Different limit equilibrium models are available in D-Geo Stability. The D-Geo Stability kernel of 01-10-2015 has been used for calibrating safety factors.

3.1 Limit equilibrium models

Limit equilibrium models compare the driving moment M_S of a potential slip plane or surface with the resisting moment M_R to obtain the factor of safety F_s via eq.(3.1).

$$F_s = \frac{M_R}{M_S} \tag{3.1}$$

To calculate F_s, the following models are used in the calibration:

3.1.1 Uplift-Van

High pore pressures at the horizontal interface of weak layers with an underlying sand layer can cause reduction or even complete loss of shear resistance at this plane. This can yield an uplift failure mechanism. The Uplift-Van method assumes that the total slip plane is composed of a horizontal part bounded by two circular parts. The safety is determined using equilibrium of the horizontal forces acting on the compressed area between the active and passive slip circles. The method becomes equal to Bishop's method if the length of the horizontal part reduces to zero and the radius of the active and the passive circle coincide. In contrast to Bishop, Uplift-Van satisfies horizontal equilibrium between active, horizontal and passive parts; Spencer satisfies horizontal equilibrium between al segments (Van der Meij, 2013).

3.1.2 Spencer

The Spencer method is not constrained to any shape of slip plane and it can therefore be used to freely search the (in practice piecewise linear) slip plane with the smallest resistance. Like Uplift-Van, Spencer also satisfies moment, horizontal and vertical equilibrium (Van Duinen, 2014a). However, due to stability issues (see Section 8.6), Spencer has not been used here for the calibration of safety factors.

3.1.3 The WTI 2017 default

The anticipated default limit equilibrium model used in the WTI 2017 will be the Spencer model (Van Duinen, 2014a). Only if one of the validity criteria, as specified in the kernel (Van der Meij, 2013), is not met the computation switches to Uplift-Van. Bishop is not considered, as, in principle, Bishop circles can also be analysed with the Uplift-Van model. Because the Spencer implementation in the D-Geo Stability kernel (version 01-10-2015) does not always give stable output, only Uplift-Van has been used in the calibration.

3.2 Shear strength

3.2.1 Mohr-Coulomb for drained analysis

The Mohr-Coulomb model is used for modelling the drained shear strength of soils in the macrostability kernel. This is only applicable to possibly present sand layers. Herein the cohesion c' (0 for sand), the angle of dilatancy ψ (also 0) and the effective friction angle φ' are used to calculate the ultimate shear tress τ in relation to the vertical effective stress $\sigma'_{v,i}$, given in the equation below. A more detailed description is given in (Van der Meij, 2013).

$$\tau = c' + \sigma'_{v,i} \frac{\cos\psi \cdot \sin\varphi'}{1 - \sin\psi \cdot \sin\varphi'} \tag{3.2}$$

3.2.2 Critical state soil mechanics model for undrained analysis

Within the critical state soil mechanics (CSSM), the undrained shear strength model for the macrostability kernel is as follows, for more information see Van Deen and Van Duinen (2015):

$$s_u = \sigma'_{v,i} \cdot S \cdot OCR^{\,m} \quad \text{with} \quad OCR = \sigma'_{vy} / \sigma'_{v,i} \quad \text{and} \quad \sigma'_{vy} = \sigma'_{v,i} + POP \tag{3.3}$$

Herein, s_u is the undrained shear strength [kN/m^2], $\sigma'_{v,i}$ the in-situ effective vertical stress [kN/m^2], S the undrained shear strength ratio (normally consolidated) = $(s_u/\sigma'_{v,i})_{nc}$ [-], OCR the Over-Consolidation Ratio [-], m the strength increase exponent [-], σ'_{vy} the vertical yield stress [kN/m^2], and POP the pre-overburden pressure [kN/m^2]. The POP can be either a direct input per layer or an indirect input, deduced from a list a pre-consolidation stress measurements and X- and Z-coordinates. POP and $\sigma'_{v,i}$ are a function of the outside water level.
The undrained analysis is used for the calibration, with the exception of sand layers that are modelled as drained.

3.2.3 Slope stability computations in D-Geo Stability

The slope stability calculations are carried out with the software D-Geo Stability using a beta version as the WTI kernel. Herein, the low permeable layers are modelled by means of the undrained shear strength and the aquifer layers (or e.g. sand cores) are modelled as drained layers. The soil parameters are derived from expert judgement in combination with laboratory tests for both the undrained and the drained parameters. Additionally to S and m, the user has to define the yield stress points in each undrained layer. It is recommended to place at least one yield stress point in each undrained layer; if the vertical stresses change through e.g. a dike or berm, one should add additional yield stress points to consider these conditions. Each yield stress point has been derived for the calibration based on effective stress for daily water level conditions. Alternatively, one case use local measurements if available. If a value of the pre-overburden pressure (POP) is available, one can use the relation $\sigma'_{vy} = \sigma'_{v,i} + POP$ to estimate the value of the yield stress. In the cases presented in this report, we used expert judgment to adjust the yield stress values to realistic values, if necessary.

Inside the D-Geo Stability software, the Waternet creator is used for the generation of pore pressures. Note that the Waternet creator may give unrealistic values if not all required values are filled in and if wrong layers are defined as aquifer.

If there is a blanket layer of less than 4 meters and an uplift potential bigger than 1.2, the shear strength of the low permeable, undrained layers in this region has to be reduced to 0

due to uplift. Note that in the present version of D-Geo Stability (10/2015) one has to manually select strength reduction in case this happens.

Note also that one has to check carefully the boundary conditions of the search algorithm that is employed to find the realistic slip plane with the lowest factor of safety. In case of the Uplift-Van method, one should pay attention to the coarseness of the search grids and corresponding tangent lines. If necessary, one has to modify them to find the slip surface or other calculation options such as *minimal slice depth*, *zone area*, *number of slices*, etc. In case of the Spencer algorithm, one should check carefully the boundary conditions of the genetic algorithm. It is highly recommended to vary the default *automatic boundary conditions* to find the slip surface with the lowest safety factor.

Note that shallow slip surfaces might not lead to a slope stability failure. These shallow surfaces are excluded using an entry zone for the slip plan through the crest.

3.3 List of input variables

When using the macrostability kernel to model the mechanism, one needs the input variables given in Table 3.1. Also, this table provides information on which parameters are considered random variables and their default values (when applicable).

Table 3.1 Parameters for Slope stability analyses used in the macrostability kernel

Symbol	Unit	Description	Drained	Undrained	Distribution	Default	Used ranges in the calibration
γ_{unsat}	[kN/m^3]	unit weight of soil above phreatic level	x	x	Deterministic	*	
γ_{sat}	[kN/m^3]	unit weight of soil below phreatic level	x	x	Deterministic	*	
c'	[kN/m^2]	effective cohesion	x		Lognormal	*	
$\tan\varphi'$	[-]	effective friction angle	x		Lognormal	*	COV = 15 %
S	[-]	undrained shear strength ratio (nc)		x	Lognormal	*	COV = Silty clay: 10 % Peat: 10-15% Organic clay: 10-28% Dike material: 33 %
m	-	strength increase exponent		x	Lognormal	*	σ=0.03 -
σ'_{vy}	[kN/m^2]	vertical yield stress		x	Lognormal	*	σ=6 kN/m^2
L_i	[m]	leakage length	x	x	Deterministic	-	
IL	[m]	intrusion length	x	x	Deterministic	-	
WL	[m+NAP]	water level	x	x	Gumbel	**	

* Each parameter has to be specified for each layer. One can find suggestions on the variability and default values of the soil random variables in the 'Schematiseringshandleiding" (Van Deen and Van Duinen, 2015 and Van Duinen, 2014b) and Appendix C.

** The hydraulic properties have to be specified for the whole cross-section. The water level is assumed to follow a Gumbel distribution, which can be derived from the mean water level and the decimate height (see e.g. Schweckendiek, 2014).

An additional parameter to be considered is the model uncertainty. The model uncertainties arise from the theoretical approaches used to model the behaviour of structures or materials

and the simplifications associated with these approaches. Model uncertainties are uncertainties that arise due to the fact that models are imperfect representations of reality. Model uncertainties can be addressed using a variable (m_d) that represents the ratio of the predicted over the real response for the model used. The model uncertainty m_d is applied by dividing the factor of safety F_s by m_d, see eqn. 3.4. This means that the mean of a model uncertainty higher than 1 means on average the model is too optimistic and the computed factor of safety needs to be reduced. In the case of the slope stability failure mode, the model uncertainties for the different failure plane models described above are given in Table 3.2. These are based on Van Duinen (2015) and show a mean very close to 1. For the drained analysis (in case of sand), the model uncertainties have a mean of 0.95 and a standard deviation of 0.08 for both Spencer and Uplift-Van according to current state of practice.

Table 3.2 Model uncertainty for different limit equilibrium models for undrained shear strength computations

model	distribution type	mean value	standard deviation
Spencer	lognormal	1.008	0.035
Uplift-Van	lognormal	1.005	0.033

In a probabilistic analysis, the model uncertainty m_d is used together with the factor of safety F_s in the following limit state function (Z):

$$Z = F_s / m_d - 1 \tag{3.4}$$

In a semi-probabilistic analysis, the partial factor γ_d (model factor) is used to cover the model uncertainty , together with the factor of safety $F_{s,des}$ (calculated with design values of the input parameters) and other safety factors, in the following equation:

$$\frac{1}{\gamma_d \cdot \gamma_n} \cdot \frac{M_{R,d}}{M_{S,d}} = \frac{1}{\gamma_d \cdot \gamma_n} \cdot F_{s,des} \tag{3.5}$$

(3.6)

The following condition should be met

$$\frac{1}{\gamma_d \cdot \gamma_n} \cdot F_{s,des} > 1$$

Herein, Z is the limit state function, m_d is the model uncertainty, γ_d is the model safety factor, γ_n is the *schadefactor* (TAW, 1989) which is the so called β – dependent safety factor in this report.

3.4 Spatial averaging

Spatial averaging plays an important role because vertical fluctuations in shear strength properties have relatively small scales of fluctuation compared to the size of the failure plane. This results in partial averaging (only the vertical part) of uncertainty over the failure plane. This is important since it reduces the variance in shear strength properties. How much averaging occurs depends on the contribution of vertical fluctuations to the total variance in the data. This depends on whether the data is from a local of regional dataset. This calibration uses cases based on regional datasets. Partial averaging of shear strength properties, as well as the effect of the limited amount of samples, has been considered. This is further explained in Appendix D. Spatial averaging does not apply to the m-factor and the yield stress points according to the Cluster Macrostability.

3.5 Previously recommended safety factors

As a reference, previously recommended safety factors are presented in Table 3.3.It should be noted that safety factors are only relevant for the material model for which it is derived; and in in relation to the whole safety format. Hence, comparison of individual safety factors does not result in meaningful conclusions.

Table 3.3 Review of the safety factors for slope stability (studies, assessment and design).

		Source			
		Van der Meer et al. (2008) / TRWG addendum	Jongejan et al. (2012)	Jongejan et al. (2014)	OI2014 v3 (2015)
Purpose of document/study		Design, assessment	Test WTI calibration procedure	Preliminary comparison of CSSM and MC	Preliminary design
Safety factor	Description				
Material	γ_m				
γ_{unsat}	unit weight of soil above phreatic level	1.0	1.0	1.0	1.0
γ_{sat}	unit weight of soil below phreatic level	1.0	1.0	1.0	1.0
	Drained				
c'	effective cohesion	Clay: 1.25 Peat: 1.50 Sand: -	1.0 (all soil types)	-	-
tan(φ')	tangent of effective friction angle	Clay: 1.20 Peat: 1.25 Sand: 1.20	1.0 (all soil types)	-	-
	Undrained	-	-		
S	undrained shear strength ratio (NC)	-	-	1.03 – 1.17*	1.05 – 1.18 avg. 1.08
POP	pre overburden pressure	-	-	1.00 – 1.09*	1.00 – 1.13 avg. 1.08
Model	γ_d				
	Drained	B**: 1.0	1.03	-	LV & SP** No uplift: 0.95 Uplift: 1.05
	Undrained	-	-	LV: 1.03	LV**: 1.06 SP**: 1.07
β – dependent	*Schadefactor* $\gamma_n = \gamma_\beta$				
	Drained	1 + 0.13 ($\beta_{eis,dsn}$−4.0)	1 + 0.35 ($\beta_{eis,dsn}$−5.0)	-	-
	Undrained	-	-	1 + 0.18 ($\beta_{eis,dsn}$−4.8)	1 + 0.21 ($\beta_{eis,dsn}$−4.3)

* These values correspond to a relatively strict target reliability in combination with less pessimistic influence coefficients; other material factors, for other combinations, have also been presented in Jongejan et al. (2014).
** B = Bishop. The model factor varies, for *drukstaafmodel* between 0.9 and 1.0 and for *opdrukveiligheden* between 1.2 and 1.0.
** LV = LiftVan
** SP = Spencer-Van der Meij

3.6 Limitations of the calibration

Yield stress points
In the WTI2017, different methods are available for undrained slope stability computations (e.g. see Van Deen and Van Duinen, 2015). In the calibration, stability computations have been made using yield stress points (Van der Meij, 2013). The yield stresses can be calculated based on the effective stress in the yield stress point for the daily water level and the POP value (see Van Deen and Van Duinen, 2015 for more information). A combination of this procedure and expert judgment has been used for the calibration. An alternative method would be to determine the local yield stresses based on CPT's; this methods has been applied for only one case, since not sufficient CPT's were locally available. The uncertainty of the yield stress points has been estimated on the basis of available laboratory test data and expert judgement.

In a previous study (Jongejan et al., 2014), because of software limitations, the POP was the input parameter that had to be chosen, based on which the yield stresses were determined. The modelling framework used in the present study is a clear improvement since the POP should ideally not be treated as a fixed value.

Waternet creator
The waternet creator as of 01-10-2015 has been used for the calibration. This waternet creator defines the phreatic line inside a dike and piezometric level (PL) lines in the soil layers beneath the dike as function of the outside water level, assuming overtopping is absent. The resulting phreatic line is probably slightly conservative. The phreatic lines are treated as deterministic (no uncertainty) since there is no probabilistic version of the waternet creator.

Berm optimization
The berms that have been designed to increase the reliability of dike sections have not been optimized. The height of the berm is usually around one-third of the dike height. Optimizations of the berm dimensions and weight may lead to smaller berms. This is mainly of interest for the actual design of berms, but less relevant for the calibration of partial factors.

4 Calibration procedure

In this chapter, the following procedure is applied for calibrating the semi-probabilistic safety assessment rules for inner slope stability. The procedure is based on Jongejan (2013) and Jongejan et al. (2014).

Step 1: Establish the reliability requirement. This requirement is defined as a maximum allowable probability of failure for the failure mechanism under consideration for an entire segment (*normtraject*). The length-effect is also discussed in this step. This effect is taken into account in step 3(c), when deciding which safety factors may be considered sufficiently safe.

Step 2: Establish the safety format. This step comprises the following activities:

a) establish a test set that ideally covers a wide range of cases. The test set members concern existing or fictitious cross-sections of dikes;
b) calculate influence coefficients for each test set member, for a specific target failure probability or a range of values;
c) based on the outcomes of the previous activity and practical considerations, define representative values (characteristic values) and decide on the safety factors that are to be included in the semi-probabilistic assessment rule.

Step 3: Establish safety factors. This step comprises the following activities:

a) establish, on the basis of representative influence coefficients and a target reliability index, the values of all but one safety factor. Herein, these safety factors will be called β_T – invariant safety factors (β_T stands for the required, or target, reliability index);
b) for each test set member, determine the required stability berm so that $R_{des} = S_{des}$, for a range of values of the remaining β_T – dependent safety factor. When this condition is fulfilled, each (modified) test set member would just pass a semi-probabilistic assessment. Then calculate the probability of failure of each (modified) test set member. The objective of this step is to establish a relationship between the value of the β_T – dependent safety factor and the probability of failure (or reliability index), for each test set member;
c) apply a calibration criterion to select the appropriate value of the β_T – dependent safety factor. The calibration criterion provides a reference for deciding which design values are sufficiently safe. According to the criterion, the failure probability of a segment should be smaller than the target failure probability that applies to the segment (step 1).

Step 4: Compare calibration results with present-day rules. A 4th step is to compare the calibrated semi-probabilistic assessment rule with the present-day $\gamma - \beta$ relations. As a comparison, also the OI2014_v3 (2015) is used.

The following chapters give more detail on the steps stated above.

5 Step 1: Establishing reliability requirement

This chapter discusses the establishment of the reliability requirement that is needed for calibration purposes. It starts with a maximum allowable probability of flooding (section 5.1), from which the reliability requirement for slope stability is derived (section 5.2). The relationship between the reliability requirement for entire dike segments and cross-sectional failure probabilities is discussed section 5.3.

5.1 Target probabilities of flooding

The flood safety standards are defined in terms of target probabilities of flooding (DPV, 2015). These standards apply to dike segments (*normtraject*). A dike segment is a dike system or part thereof. Segments can be over 20 km long and are usually located in one water system. Segments may consist of numerous dike sections and/or hydraulic structures. For the calibration, a reliability requirement is needed that can be translated to a requirement for a cross-section. How this requirement is derived is outside the scope of the calibration.

5.2 Reliability requirement for slope stability in general

For calibrating a semi-probabilistic assessment rule for a particular failure mechanism, a reliability requirement for that failure mechanism is needed. Such a reliability requirement can be derived from a fault tree analysis. Each failure mechanism may lead to flooding, the fault tree's top event. The combined probabilities of the various failure mechanisms may not exceed the maximum allowable probability of flooding. To ensure this requirement is met, the maximum allowable failure probabilities for the failure mechanisms, their 'failure probability factors', should be defined in such a manner that their combined value does not exceed the maximum allowable probability of flooding. The maximum allowable contributions of the different failure mechanisms to the maximum allowable probability of flooding are shown in Table 5.1.

Table 5.1 Maximum allowable failure probabilities per failure mechanism, defined as a fraction of the maximum allowable probability of flooding - Jongejan (2013).

Type of flood defence	**Failure mechanism**	**Failure probability factor (*f*)**	
		Sandy coast	Other (dikes)
Dikes and structures	Overflow and wave overtopping	0	0.24
Dikes	Uplift and piping	0	0.24
	Macro instability of the inner slope	**0**	**0.04**
	Revetment failure and erosion	0	0.10
Structures	Non-closure	0	0.04
	Piping	0	0.02
	Structural failure	0	0.02
Dunes	-	0.70	0 or 0.10
Other	-	0.30	0.30 or 0.20
Total		1.00	1.00

The fractions in Table 5.1 are based on the expected importance of the different failure mechanisms if all dike systems were to meet their (assumed) safety standards. These estimates are based on calculations with PC-Ring and VNK2-data as well as a number of expert sessions with representatives of research institutes (TNO, Deltares, Delft University of Technology), engineering consultancies, water boards, and *Rijkswaterstaat*. For further

details about the maximum allowable failure probabilities per failure mechanism, the reader is referred to Jongejan (2013). It should be noted that the fractions of Table 5.1 are the basis of the calibration. However, the WTI also allows for a redistribution of fractions, as well as a full probabilistic analysis for more detailed assessments. This is outside the scope of this report.

The default failure probability factor f for the slope stability mechanism[2] is 0.04. This factor leads to maximum allowable failure probabilities (P_T) as shown in Table 5.2. The reliability requirements are also expressed in terms of reliability indices (β_T). It should be noted that the reliability requirements (P_T or β_T) in Table 5.2 apply to dike segments. These should not be confused with cross-sectional reliability requirements. Due to the length-effect, cross-sectional reliability requirements will have to be more stringent than reliability requirements for entire segments. It should be noted that in Table 5.2, requirements are shown for the anticipated, new safety standards .

Table 5.2 Reliability requirement for a range of safety standards – slope stability mechanism.

f [-]	P_{norm} [yr^{-1}]	Reliability requirement (entire dike segment)	
		$P_T = f.P_{norm}$ [yr^{-1}]	$\beta_T = -\Phi^{-1}(P_T)$ [yr^{-1}]
0.04	1/300	1.3E-04	3.65
	1/1,000	4.0E-05	3.94
	1/3,000	1.3E-05	4.20
	1/10,000	4.0E-06	4.47
	1/30,000	1.3E-06	4.69
	1/100,000	4.0E-07	4.94

5.3 Reliability requirement for slope stability at cross-section level

The difference between the reliability requirement for an entire segment and the reliability requirement for individual cross-sections will increase with decreasing spatial correlations and decrease with greater variability in cross-sectional reliabilities. The latter is because the failure probabilities of the weakest cross-sections will dominate the failure probability of the entire segment when the weakest cross-sections have relatively high probabilities of failure (Calle and Kanning, 2013).

In the case of the slope stability failure mechanism, the length-effect is characterised by the parameters a and b, and the relation between the reliability requirement for a dike cross-section and the reliability requirement for a dike segment is given as follows:

$$P_T = P_{T,cross}\left(1+\frac{a \cdot L}{b}\right) \tag{5.1}$$

and

$$P_T = f \cdot P_{norm} = \frac{f}{T} \tag{5.2}$$

[2] *The macrostability mechanism refers to the inner slope stability failure mechanism. From now on this terminology will be used in this report.*

where:

P_T	the target failure probability of a dike segment for a certain failure mechanism [yr^{-1}],
$P_{T,cross}$	the target failure probability of a dike cross-section for that mechanism [yr^{-1}],
T	the return period that corresponds to the safety standard of a segment [yr],
L	the total length of the segment [m],
a	the fraction of the length that is sensitive to the slope stability failure [-],
b	a measure for the intensity of the length effect within the length $a.L$ [m],
P_{norm}	the maximum allowable failure probability (safety standard) [yr^{-1}],
f	the budget for the failure mechanism under consideration [-].

The length-effect parameters a and b, can be interpreted as follows. The constant a may be interpreted as the percentage of dikes that contribute significant to the total failure probability for slope stability and b may be interpreted as the equivalent auto-correlation length of the performance (or limit state) function. LOR2 (TAW, 1989) states a = 0.033 and b = 50m, which is based on the analysis of a single dike ring. At present, there are no new insights on which to base alternative values, which is why the parameter values of a an b have been maintained. Table 5.3 shows the range of $\beta_{T,cross}$ for several segment lengths and values of T (=1/P_{norm}), a and b. It shows that the range of $\beta_{T,cross}$ is roughly between 4 and 6; this is the range the calibration focuses on. It also shows $\beta_{T,cross}$ is not very sensitive to variations in a and b. This means they do not play a major role in the calibration exercise. Hence, the factors a and b have not been studied further. This is also in line with the conclusion of a meeting between the WTI and ENW.

Table 5.3 Range of $\beta_{T,cross}$.

parameter	Variation 1	Variation 2	Variation 3	Variation 4
a	0.033	0.033	0.2	0.2
b	50	50	200	50
L (m)	5000	30000	5000	30000
f	0.04	0.04	0.04	0.04
T	300	30000	30000	30000
$P_{T,cross}$	3.1E-05	1.9E-08	6.7E-08	3.3E-09
$\beta_{T,cross}$	4.0	5.5	5.3	5.8

6 Step 2: Establishing the safety format

The safety format concerns the definition of representative values (characteristic values) and the types of safety factors that are to be included in the semi-probabilistic assessment rule. The safety format depends on the relative importance of the uncertainties related to the various random variables (see also section 2.2). To obtain insight into the relative importance of the uncertainties, probabilistic analyses are indispensable. Section 6.1 first discusses the test set for which probabilistic analyse were carried out. The calculated influence coefficients are discussed in section 6.2, which lie at the heart of the safety format that is detailed in section 6.3. Finally, a summary is provided in section 0.

6.1 Establishing a test set

6.1.1 Considerations to establish a test set

To obtain insight into the relative importance of the random variables, probabilistic analyses have been carried for a representative set of cases. The test set cases should reflect the variety of sub-soil conditions and loading conditions found throughout the Netherlands. The test set is composed of actual dikes from the VNK2-project and Delta Programma Veiligheid that are linked to specific locations. It must be noted that the VNK2 project focused on cases that were considered relatively unsafe; hence, there is a bias in the test set for unsafe dikes. The geometry and subsoil composition is mainly based on the VNK2-project data. The Cluster Macrostability provided undrained shear strength parameters. These are based on the default values that will be provided to WTI users, since there is very limited local data available and expert judgement. The hydraulic loads are based on known normative water levels and their exceedance frequencies, in combination with the local decimate height. These parameters were used to fit Gumbel distributions.

General specifications that apply to the selection are:

- The test cases are primary flood defences;
- Different water systems are covered by the test cases;
- Different geo-hydrological (with or without uplift) and (drained and undrained) soil conditions are covered;
- Different soil profiles and dike geometries are represented;
- Furthermore, the considered safety standards cover the entire range of the safety standards as defined in DPV (2015).

As mentioned in the previous chapters, the cases have been adapted with berms in order to reach the required reliability levels. The anticipated, new safety standards have been used for the cases. However, the new water level distributions (i.e. based GRADE) were not available. This is dealt with by keeping the Gumbel distributions based on the old MHW, and determining the new MHW based on the new safety standard. For case 43001007, this results in a MHW higher than the crest, which was dealt with by lowering the MHW.

6.1.2 Location of test set cases

The location of the test set members (cases) is shown in Figure 6.1. For further details about the test set, see Appendix C.

Figure 6.1 Test set members. In red all the cases that are used to derive the final calibrated safety factors, in orange the calculated cases that are not incorporated in the final safety factor due to insufficiently stable results.

6.1.3 Case descriptions and input data

The case descriptions and input data are shown in Table 6.1 and Table 6.2. The tables show there is a good coverage with respect to geology, uplift or not, safety standard (F_exc), decimate height and shear strength; given the small dataset. However, since these are only just 11 cases, not all combinations are covered. The default strength parameters for the WTI2017, on which most of the cases are based, are presented in Appendix C.1.4; these are derived from (Van Deen and Van Duinen, 2015). In all cases, a default traffic load of 13 kN/m^3 has been assumed, in accordance with the VTV2006. The traffic load might be removed for stability assessments in the WTI2017..More information about the cases is presented in Appendix C.

Table 6.1 Summary of the selected cases. F_exc is the safety standard, MHW_used is the normative water level and h_{dec} is the decimate height.

name	location	geology	uplift?	F_exc (yr^{-1})	MHW_used (m+NAP)	h_{dec} (m)
43001007	Waal near Gorkum	riverine	no	1/30000	6.5	0.57
dp_190	Lek near Streefkerk	transition	not without berm, yes with berm	1/2000*	3.4	0.20
41_W_237	Waal near Tiel	Riverine	no, though shear strength reduction	1/10000	12.8	0.73
Dp43	Ijssel near Deventer	Riverine	no, though shear strength reduction	1/3000	7.6	0.68
Dp_5_521	Ijssel near Zwolle	Riverine	yes/no	1/3000	6.9	0.69
dwp0	Oude Maas near Barendrecht	Marine	no	1/3000	3.0	0.27
41_W_270	Waal near Tiel	Riverine	yes/no	1/3000	12.6	0.73
41_M_28	Maas near Nijmegen	Riverine	yes	1/3000	13.4	0.73
DV13	Ijsselmeer near Den Oever	marine	no	1/30000	1.0	0.25
Wsno_0161	Westerschelde near Kruiningen	marine	no	1/10000	6.7	0.67
Dp92	Ijssel near Zutphen	riverine	shear strength reduction	1/10000	10.8	0.66

* This case is based on real data. The numerical value of the old safety standard (1/2000 per year) was used. The new norm for this dike is 1/30 000 per year.

Table 6.2 Soil parameters of the cases: mean value of Su-ratio [kN/m^2] or friction angle [degrees] (marked with)*

case	dike_1	dike_2	sub 1	sub_2	sub_3	...							sub_n	aquifer_1	aquifer_2
41_M_28	0.45		0.21	0.21	0.23									38.02*	
41_W_237	0.45	35*	0.21	0.21	0.23									34.58*	
41_W_270	0.45		0.21	0.19	0.24	0.45	0.19	0.45						34.58*	
43001007	0.35		0.15	0.27	0.37	0.27	0.15	0.24						30*	
Dp43	0.45	0.45	0.21	0.23	40*	40*								35.24*	35.24*
Dp92	0.3	0.3	0.3	35.24*										35.24*	35.24*
dp_190	0.35	0.35	0.26	0.26	0.3	0.37	0.3	0.3	0.3	0.37	0.24	0.31	0.24	35*	
Dp_5_521	0.45	0.45	0.21	0.21	0.23									35.24*	
DV13	0.45	36.79*	0.45	0.19	0.32									42.2*	
dwp0	0.22	36.77*	0.21	25.27*	0.21	0.32	0.21							36.77*	
wsno	0.22	38.02*	29.89*	0.21	0.21	0.32	0.21							34.26*	
dp_190	0.35	32*	0.37	32*	0.24	32*								32*	

6.2 Defining representative influence coefficients

The relative importance of the uncertainties related to random variables can be expressed in terms of FORM influence coefficients (see also section 2.1). An inspection of influence coefficients provides useful clues about appropriate representative values (quantiles) and/or the variables for which partial safety factors should be introduced. Influence coefficients can be obtained from FORM calculations. Figure 6.1 shows the squared influence coefficients for (groups of) random variables, for the considered cases.

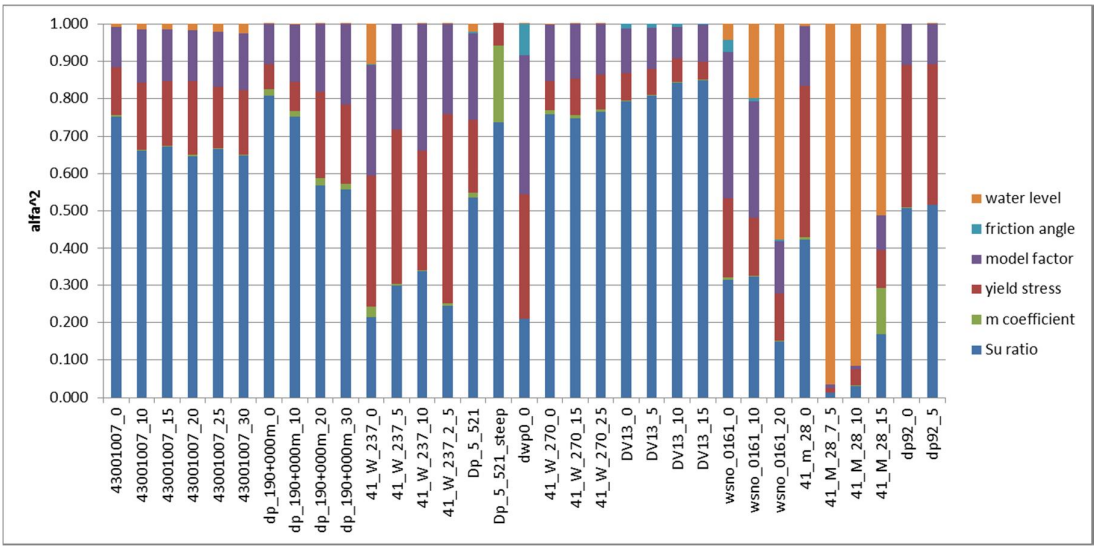

Figure 6.2 Squared FORM influence factors α^2 ("alfa^2") of the computed cases

From Figure 6.2 the uncertainty related to the hydraulic loading conditions (outside water level h) appears to be significantly less important than found in VNK2 and Jongejan et al. (2013) for drained stability analyses. In case of undrained behaviour, a smaller sensitivity is to be expected, which is further discussed in Appendix E. The yield stress and the undrained shear strength ratio (Su) appear to have the highest influence, together with the model uncertainty. There are two cases with a high influence of the water level. Case wsno_0161 has a high α_h due to the sand core, which results in drained behaviour. Case 41_M_28 is effected by uplift (for the cases with a berm) and relatively small failure planes, resulting in a high influence of the water level. There are other cases with uplift but these also have large failure planes, resulting in a relatively high contribution of undrained behaviour (most of the shear strength along the slip circle is mobilized outside the uplift zone) and thus a low influence of the water level. In most cases model uncertainty plays an important role, emphasizing that (imperfect) models play an important role.

The limited effect of the water level could be due to the (undrained) material model, the variance of input parameters or due to overly conservative (water pressure) schematizations. It has the following implications:

- In case the limited influence of the water level is due to the material model or uncertainty related to input parameters, performance observations (proven strength) would have a significant impact on reliabilities and required safety factors would be much lower.
- In case the limited effect influence is due to a conservative water pressure schematization in the probabilistic slope stability analyses, the derived safety factors in this calibration are likely to be conservative, but also the potential for proven strength would be much smaller.

The implications of the low influence of the water level are further discussed in Chapter 10. Either way, more research into the possible conservative water pressure schematization is highly recommended.

For the calibration, it was chosen not to investigate water pressure uncertainties and proven strength due to time constraints.

6.3 Safety format: representative values and safety factors

Representative values and safety factors should ideally be chosen on the basis of (target) reliability indices and influence coefficients, see section 2.2, to obtain an efficient format. On the other hand the safety format should be as simple as possible. Hence, a balance between simplicity and effectiveness is pursued. The following reasoning is followed to derive the safety format.

For pragmatic reasons, representative values should be defined as uniformly as possible. The consistent use of 5%-quantiles for strength parameters is preferable over the use of e.g. the 10%-quantile for variable X_1, the 25%-quantile for X_2, the 55%-quantile for a variable X_3 and so on. The use of the 5%-quantile as representative value is due to practical reasons (WTI2017 uniformity).

Second, within the WTI 2017, the strategy, for reasons of uniformity, is to select the load (i.e. water level on the water side) with an exceedance probability equal to the allowable probability of flooding (Jongejan, 2013). This ensures consistency across failure mechanisms in the WTI 2017 and facilitates comparisons between today's rules and $\gamma - \beta$ relations.

Third, representative values are normally defined as quantiles. Yet when it comes to the model uncertainty parameter, it seems practical to choose a representative value equal to 1. The design value of the model uncertainty parameter is then directly equal to the partial safety factor. Analysts would otherwise have to combine a representative value (quantile) for the model uncertainty parameter with a partial safety factor.

Finally, in theory, all design values should depend on reliability requirements. That would be impractical, however. A pragmatic solution is to define a β_T – invariant model factor and a separate β_T– dependent safety factor to account for the stringency of the safety standard and the remaining uncertainties. The β_T– dependent safety factor is to be applied to the ratio $M_{R,d}/M_{S,d}$ – eq.(3.5).

The result of a deterministic analysis is a factor of safety FoS. In a semi-probabilistic safety assessment, the input parameters are characteristic values (see Appendix A) or design values (if factored with a partial safety factor). Table 6.3 presents the current characteristic values (TRWG for drained, OI2014 for undrained). Note that in current practice with drained analysis only the cohesion and (tangent of the) friction angle are factored with partial safety factors (see e.g. TAW, 1989).

Table 6.3. Summary of the characteristic values for drained and undrained variables (based on TRWG and OI2014).

Symbol	Unit	Description	Drained	Undrained	Characteristic values
γ_{unsat}	[kN/m^3]	unit weight of soil above phreatic level	x	x	50 %
γ_{sat}	[kN/m^3]	unit weight of soil below phreatic level	x	x	50 %
$tan(\varphi')$	[-]	tangent of effective friction angle	x	x	5 %
S	[-]	undrained shear strength ratio (NC)		x	5 %
m	-	strength increase exponent		x	5 %
σ'_{vy}	[kN/m^2]	vertical yield stress		x	5 %
POP	[kN/m^2]	pre overburden pressure		x	-*
L_i	[m]	leakage length	x	x	-*
IL	[m]	intrusion length	x	x	-*
WL	[m+NAP]	water level	x	x	-*

* no characteristic values used: POP is not a variable in the calibration, it is used to determine the vertical yield stress. L, IL and WL are used as deterministic, conservative estimates in the water pressure schematization, how conservative is not known though.

It is proposed to keep the characteristic values from Table 6.3. Furthermore, it is proposed not to use partial safety factors for the drained and undrained variables (material factors), for the following reasons:

1) The influence coefficients and computational results (Figure 8.1) do not indicate an explicit need for safety factors; the uncertainty is mostly covered by the 95% quantiles.
2) It keeps the safety format simple
3) There are not enough cases available to differentiate between the various materials
4) The beta-dependent safety factor stays mostly above 1 in the required beta range (see Chapter 8 and Chapter 10).

This reasoning may change if there are more test cases available and a differentiation can be made between different soils (peat, clay).

The model uncertainty (see Table 3.2) is covered by a model factor (γ_d). Based on a squared influence coefficient of the model uncertainty of about 0.15 (Figure 6.2), a basic reliability index of about 4.3, and a representative value equal to 1.0 (see above), the model factor should correspond with a value with a cumulative probability equal to $\Phi(4.3 \cdot \sqrt{0.15}) = 0.95$. This is equal to the characteristic value. The resulting model factors are presented in Table 6.4 below.

Table 6.4 Model factor

model	distribution type	mean value	standard deviation	Model factor
Spencer	lognormal	1.008	0.035	1.07
Uplift-Van	lognormal	1.005	0.033	1.06

6.4 The resulting safety format

This section provides a summary of the safety format.

The criterion for slope stability is (see Chapter 3):

$$\frac{1}{\gamma_d \cdot \gamma_n} \cdot F_{s,des} > 1 \qquad (6.1)$$

The safety format for the slope stability mechanism is defined as follows:

1. The representative values of all random strength variables[3] are 5%-quantiles and 50% quantiles, see Table 6.3, apart from the model uncertainty parameter. This is in accordance with current assessment rules;
2. The representative value of the model uncertainty parameter is equal to one; The model safety factor (γ_d), is 1.06 for Uplift-Van and 1.07 for Spencer, see Table 3.2;
3. The representative value of the outside water level (design water level or MHW) is defined as the water level with an exceedance probability equal to the maximum allowable probability of flooding;
4. The material factors are equal to 1;
5. $F_{s,des}$ is computed with design values of the input parameters (representative values divided by partial safety factors)
6. A β_T – dependent safety factor γ_n is introduced to cover all other uncertainties. It is applied to $F_{s,des}$ together with γ_d see eqn. 6.1.

The γ_n factor is the only variable that needs calibration.

[3] *Increasing the values of these variables* ***decreases*** *the failure probability.*

7 Step 3: Establishing safety factors

This chapter discusses the derivation of partial safety factors for semi-probabilistic assessments of dikes with respect to the slope stability failure mechanism. Safety factors should be sufficiently safe but not unduly stringent. A calibration criterion is used to decide 'how safe is safe enough'. This criterion is introduced in section 7.1. Section 7.2 discusses how the safety factor has been calibrated.

7.1 The calibration criterion

According to the WTI 2017 calibration criterion, the failure probability of a dike segment should be smaller than the target failure probability that applies to this segment (*normtraject*). This criterion is fulfilled, with a sufficient accuracy, when the average of cross-sectional failure probabilities in the segment is smaller than the target failure probability for a dike cross-section in this segment.

When relating the cross-sectional reliabilities of individual test set members to reliability requirements/targets that apply to entire segments, the length-effect has to be accounted for. This was discussed in section 5.3.

7.2 Calibrating the beta-dependent safety factor

7.2.1 Calibration procedure

Overviews of the calibration procedure and how the software is used are presented Appendix B. The greater the value of the overall safety factor for the slope stability mechanism, the greater the required berm and the greater the reliability index. The required berm and corresponding reliability indices have been calculated for a range of berm lengths. The berm lengths have been adapted in such a way that the reliability indices are in the order 3.5 – 5.5 (see Section 5.3). In other words, the following algorithm has been applied to each case:

1. Select inputs:
   - a dike cross-section with geometry and input parameters for soil properties and geo-hydrological characterization,
   - the water level derived for an exceedance probability equal to the safety standard for the case under consideration (i.e. depending on the location of the cross-section and the envisaged new safety standard),
   - the β_T – invariant safety factors following from step 2 and 3 (if applicable) and
   - the recommended characteristic values (step 2) of all variables present in the limit state function(s) and model-uncertainty factor γ_d (Table 3.2),
2. Increase the safety of the cross-section by adding a stability berm.
3. Determine the factor of safety (FoS_char(MHW)) for the cross-section generated, based on characteristic values and given MHW, and perform a reliability analysis on the geometry at the cross-section level.
4. Repeat points 1 to 3 for different values of the safety factor.

For the overview of the calculated reliability indices (β_{cross}) as a function of FoS_char(MHW), please refer to chapter 8.

When a plot of FoS_char(MHW) – β_{cross} is composed, a study on possible clustering of the results is generally recommended (clustering per water system, safety standard, blanket thickness class) in order to optimize the safety format.

7.2.2 Safety factor as function of the reliability

The next step is to propose the $\gamma_n - \beta_{T,cross}$ relation in a functional form (typically a linear function). The functional form will have the following format:

$$\gamma_n = g(\beta_{T,cross}) = A \cdot \beta_{T,cross} + B \tag{7.1}$$

with

$$\beta_{T,cross} = -\Phi^{-1}\left(\frac{f/T}{1+\frac{a \cdot L}{b}}\right) \tag{7.2}$$

where:

A,B	are constants [-],
$\beta_{T,cross}$	cross-sectional reliability requirement (reliability index) [-],
f	is the budget for the failure mechanism under consideration [-].
T	is the return period that corresponds to the safety standard of a segment [yr],
L	is the total length of the segment [m],
a	is the fraction of the length that is sensitive to the failure under study [-],
b	is a measure for the intensity of the length effect within the length [m],

Equation 7.1 should represent the average values of the computed cross-sectional failure probabilities for the factors of safety. This probability is roughly equal to the 20%-quantile value of the calculated reliability indices based on modelled normal distributions. Both metrics may be used in calibration exercises to relate cross-sectional reliability requirements to the results of probabilistic analyses (see Jongejan, 2013). Considerable differences between these two metrics can result from e.g. the presence of outliers or a strong scatter.

For a given cross-sectional reliability requirement (as set and explained in chapter 5 – step 1), the values of the β_T – dependent safety factors can be obtained from the proposed $\gamma_n - \beta_{T,cross}$ relation.

The steps to perform a semi-probabilistic slope stability assessment of a dike cross-section are described in section 9.2.1.

8 Calibration results

This chapter presents the results of the calibration of the semi-probabilistic slope stability mechanism, i.e. it presents the achieved $\gamma_n - \beta_{T,cross}$ relation to be applied in the slope stability safety assessment. The results follow from step 3 of the calibration procedure, as described in the previous chapter. γ_n is the *required* factor of safety that follows from the calibration. FoS_char(MHW) is the factor or safety of a dike that is *computed* with characteristic input values.

8.1 Test case results

8.1.1 Approach

The cases that have been discussed Chapter 6 have been assessed probabilistically and semi-probabilistically. The first gives the reliability index, which is computed using the prototype (see Appendix A) and the inputs as discussed in Chapter 5 and 6. The second gives the factor of safety of the dike using design values of the input parameter according to the safety format, FoS_char(MHW). Combining these two outputs allows the calibration of the required safety factor γ_n. Berms have been added to obtain factors of safety in the required reliability index range. It should be noted that berm designs have not been optimized. Default values have been used for the density of soil material, the height is usually around 1/3 to 1/2 of the dike height.

8.1.2 Results of the computations

The results of the computations of the cases are shown in Figure 8.1. The figure shows the test cases including an added berm (all with the same symbol). The corresponding influence coefficients are shown in Figure 6.2.

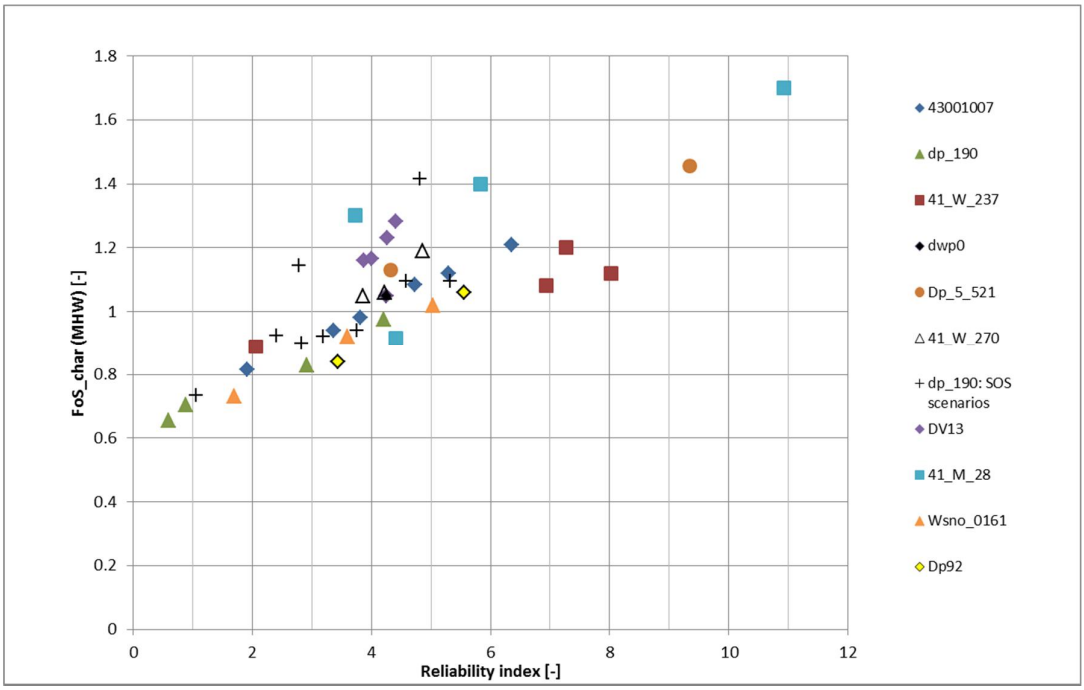

Figure 8.1 Test case results showing the computed FoS_char(MHW) and computed reliability indices of test set.

The output for all test cases can be consulted in Appendix D. The beta-gamma computations presented in Figure 8.1 are based on the input discussed in Chapter 6. This implies that cases with different safety standards (and hence design water levels with different exceedance probabilities) are shown in the figure.

The main conclusions from the figure are:

- Even though there is quite some scatter (changes in FoS of up to 0.4 for the same reliability level), there is a clear trend: a higher FoS_char(MHW) corresponds to a higher reliability index.
- The reliability index and FoS_char(MHW) mostly increase consistently with extra berm length. However, this is not the case for 41_W_270, which is likely due to the use of constant yield stress points even though the berm dimensions increase.

A more detailed discussion of the results is provided in the following sections.

8.1.3 Results of the individual cases

A small description and analysis of each cases is provided in Table 8.1. For more information about the individual cases, reference is made to Appendix B. A general observation is that the design point value of the water level is, for most cases, close to the median value (and thus much lower than MWH), which is consistent with the low α values shown in Figure 6.2. All cases (inputs, schematizations and outcomes) have been checked by the WTI Cluster Macrostability.

Table 8.1 Description and analysis of the cases

Case	Description and analysis
43001007	The slip planes in the cases with and without berm are large and deep. Consistent increase of FoS and reliability index with berm length. Based on 1D SOS subsoil model, adapted to 2D.
Dp_190	For the basic geometry, the FoS for characteristic values increases for WL>NAP +3,6m This is because the head level PL3 is very high, so there is a different normative slip plane. Due to low volumetric weights at the inner side, effective stresses are very low and consequently the normative slip circle exits in the ditch for berm lengths 20 and 30m.
41_W_237	This cross section shows quite a large increase of the reliability with increasing the berm length. However, it is not fully clear how to explain the reliability indices and influencing factors when comparing the results of the different berm length with each other.
DP43	Case does not provide satisfactory results. The results are very difficult to reproduce and showed strong dependencies of the user executing the probabilistic analysis. Therefore, this cross section was not incorporated in the calibration. Neither the automatic boundary conditions nor user defined boundary conditions could be used for reliable results using Spencer
Dp_5	Has a very strong levee body (Su ratio about 0.45) and thus a high reliability index. It is made steeper to reach the reliability range of interest
dwp0	Spencer and Uplift-Van give comparable results in reliability and safety factor using characteristic values.
41_W_270	The basic geometry results in a higher SF and higher beta than the 15 m berm. This is caused because the same yield stress points are used

	for the berm, however the berm height is increased. Therefore effective stresses and consequently shear stresses are different.
41_M_28	No berm, no uplift. Results in a relatively high FoS and low beta for this case. With berms, uplift and a high α of the water level. The design point of the water level is above the crest for the uplift cases. There is a drop in the FoS due to change from no-uplift to uplift and corresponding shear strength reduction. Hence, the change from no-uplift to uplift makes it very sensitive to the water level.
DV13	Very limited influence of the water level due to intrusion length
wsno_0161	Sand dike on clay, slip circle in the dike is mainly through drained material. High α of the water level
Dp_92	Consistent development of FoS for increasing water levels. In case of mean water level, critical slip circle through clay cover layer. For high water levels, uplift (NL: opbarsten) occurs. Then, the critical slip circle goes through the sand below the aquifer. Unless uplift occurs, there is little influence of the water level, because the slip plane is mainly in the (relatively strong) dike material.
SOS scenarios	High gamma and low beta for some sand dominated SOS scenarios.

Cases Dp43 (with and without berm), as well as cross section dwp0 with berm, did not give satisfactory results. This is probably due to the very high stability factors and thus very high reliability indices.

For case dp_190, both a base case with various berms and the different SOS scenarios have been analyzed to show the sensitivity of the results. The SOS scenarios have not been considered further to avoid over-representation of this dike in the calibration process. The SOS scenarios have been used to test the procedure to combine scenarios, see section 9.4.2.

Hence, all cases have been used for the calibration, except the SOS scenarios of case dp_190, case dp43 and some of the cases with berms that result in beta's higher than 6.5 (see Section 8.2.3).

8.2 Calibration of the safety factors

8.2.1 Approach

In accordance with the general WTI calibration procedure (Jongejan, 2013), the beta-gamma relation is fitted to the 20% quantiles of the betas, see Chapter 7. This roughly corresponds to a fit on the mean failure probability. The scatter has been dealt with as follows, in contrast to to e.g. piping where all the cases are on lines with constant gamma: first the relation between gamma and beta is established as:

$$\beta_{T,cross} = C \cdot \gamma_n + D \tag{8.1}$$

Next, a least square error fit is made. The slope of this line (C) is fixed. D is corrected by subtracting 0.84 times the error of the fit to fulfil the 20% beta fit criterion. The obtained beta-gamma relation is transformed into the required gamma-beta relation:

$$\gamma_n = A \cdot \beta_{T,cross} + B \tag{8.2}$$

8.2.2 Fit on all, uncorrected, cases

First, to obtain a first estimate on the order of magnitude of the beta-gamma relation, the above mentioned approach has been applied to all the cases. The mean fit, as well as the 95% confidence interval are shown in Figure 8.2. As a reference, also the OI2014_V3 relation has been plotted.

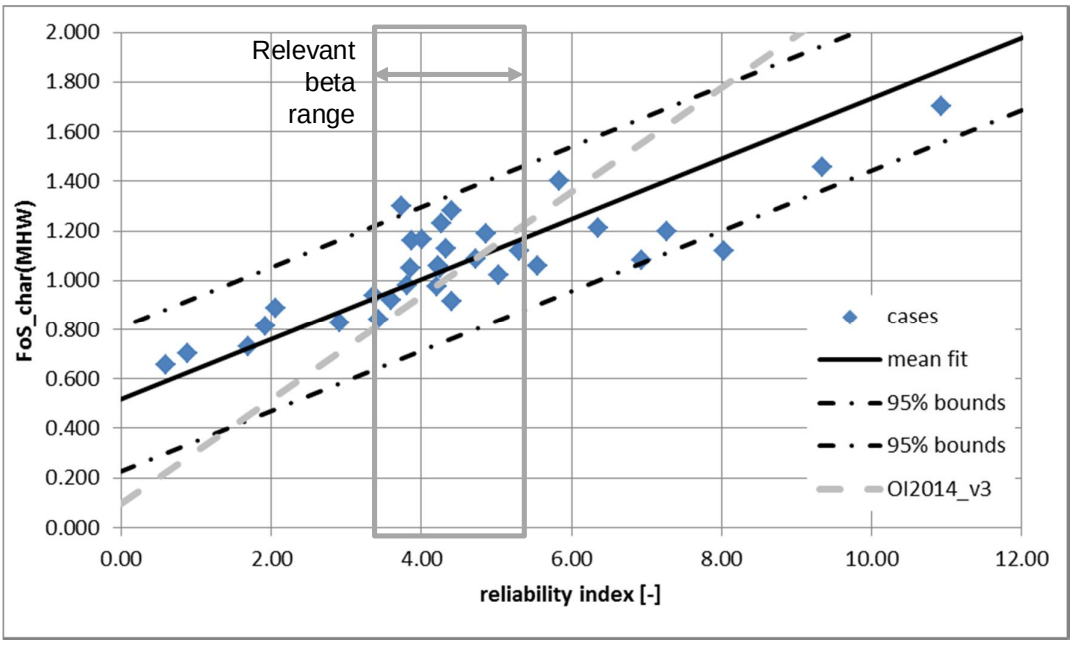

Figure 8.2 Fit on all the raw cases using the 20% beta quantile

8.2.3 Calibration fit

Two main modifications are applied in order to fit the final beta-gamma relation:

1) The raw computed safety factors (FoS_char(MHW)) are divided by the model safety factor, with a value of 1.06, according to the safety format
2) The cases with a high reliability, over 6.5, are removed from the data set since this is outside the applicable range and these pull the fit more downward (less conservative for higher beta's). Ideally, the fit would be made only on the cases in the required reliability range. However, there are not enough cases available in this range for a stable fit. If the cases with low beta (below 3.5) are removed, the fit becomes very sensitive to small variations. This again emphasizes the need for more cases.

As discussed in section 8.2.1, the 20% beta fit has been applied. The result is the proposed relation between gamma and beta, which is shown in Figure 8.3. This is referred to as the Calibration fit in both the figure and the remainder of the report.

As a reference the OI2014_v3 relation is plotted as well, which is based on representative α values. It should be noted that the slope of the lines is comparable; the main difference is the offset, but the OI2014_vs also includes material factors of about 1.08 (see Table 3.3) which largely makes up for the difference between the Beta-dependent safety factors. Hence, the relations do not differ that much, even though the approaches and the underlying computations (schematizations, models) are very different.

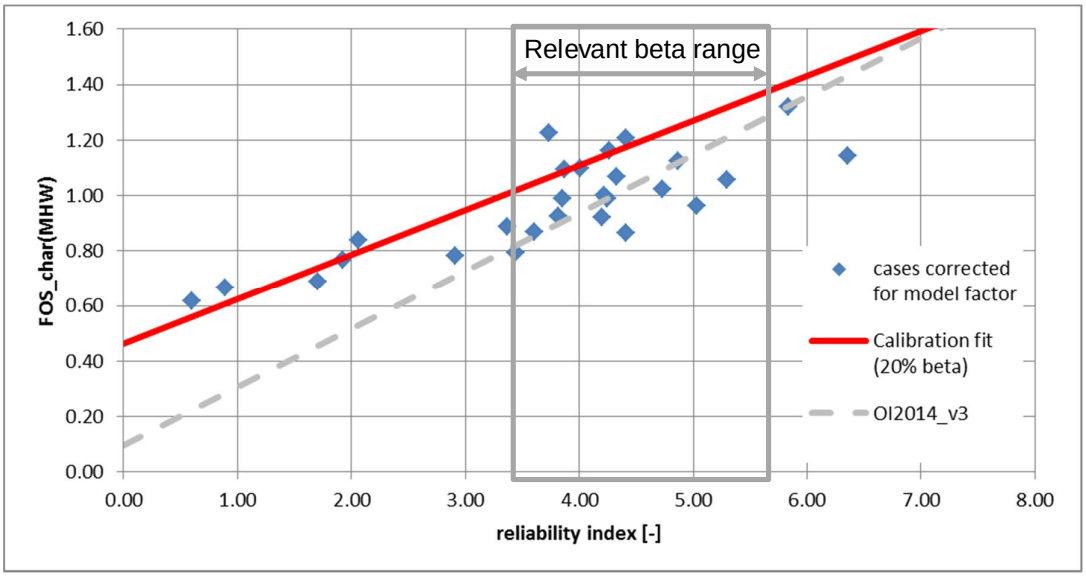

Figure 8.3 The final calibration fit

The equation corresponding to the calibration fit is:

$$\gamma_n = 0.161 \cdot \beta_{T,cross} + 0.463 \tag{8.3}$$

The equation has no lower bound (it is not limited by a lower bound of 1), which is relevant for dealing with low probability, high failure probability scenarios. Hence, scenarios with safety factors lower than one also result in representative failure probability.

8.3 Differentiation to safety level

Ideally, required γ_n values are derived for multiple safety standards. This is investigated in this section.

8.3.1 Beta-gamma relation for different safety levels

The different safety levels first affect the value of the normative water level (MHW). The higher the safety standard, the higher the MHW. The higher the MHW, the lower the safety factor, while the reliability index remains the same. This is implemented by computing the FoS_char(MHW) of all the cases for MHW's corresponding to the safety standards 1/100, 1/1000, 1/10 000 and 1/100 000. The result is shown in Figure 8.4. The figure shows a consistent decrease in FoS with increases safety standards, though the effect is small for the cases where there is a limited influence of the water level.

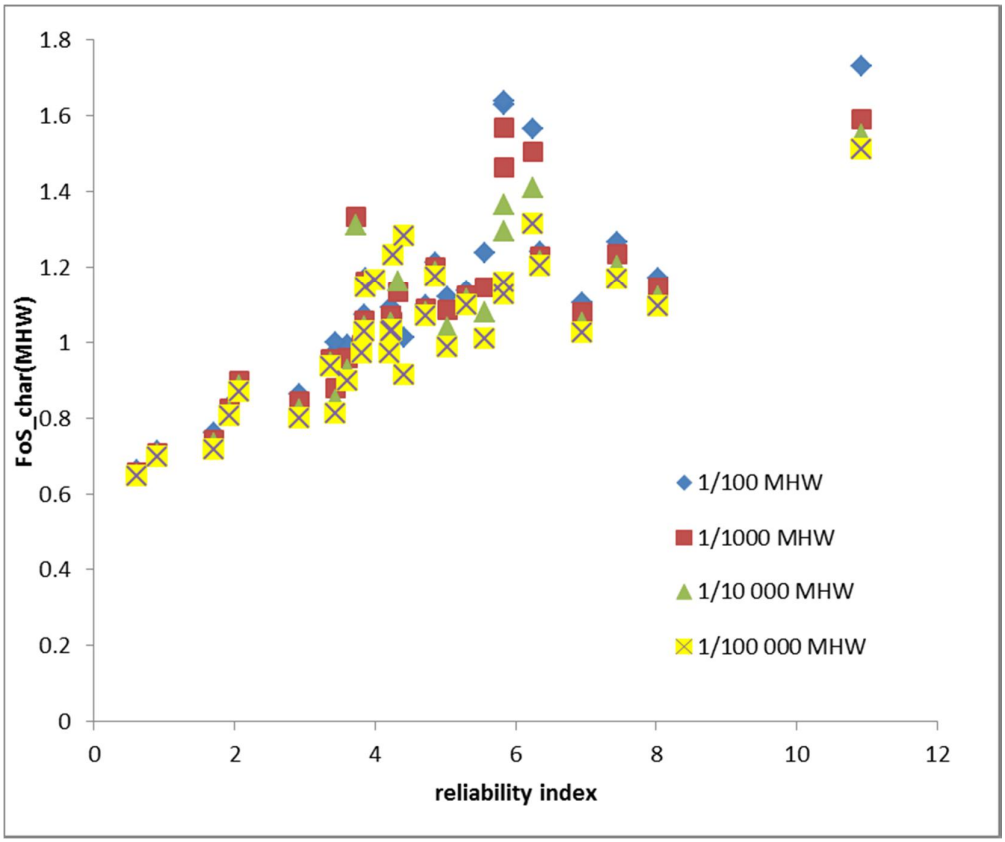

Figure 8.4. Influence of the safety level on the factor of safety.

Based on these results, it is concluded there are not enough cases to determine a significant difference of the required safety factors for the various safety standards. Hence, this differentiation will not be part of the safety format. Even though the different safety standards hardly have an effect on the required safety factor, the different safety standards still affect the target reliability as was discussed in Chapter 5.

8.4 Differentiation safety factors: uplift and geology

This section investigates whether there are differences if the results are differentiated to uplift and to geology.

8.4.1 Approach for differentiation to uplift

The results are divided into cases with and without uplift conditions. The cases with blanket rupture are in general cases with a relatively thin blanket layer; the cases with reduced shear strength by PL3 reduction (uplift, reduction of shear due to high pressures in the sand layer, which is called PL3) are cases with a thicker layer of weak soils with low weight. The different cases are described below and for each an example is given.

1 Blanket rupture (‘opbarsten)
2 Uplift: Reduced shear strength due to excess water pressures in sand aquifer (opdrijven)
3 No uplift

The main difference between 1 and 2 is that with blanket rupture (1), there is no shear strength present in passive zone due to rupture of the blanket; while with reduced shear

strength (2), the blanket does not rupture. Hence, there is still shear strength present in the passive zone of the blanket but not at the interface between blanket and aquifer.

Ad 1. Blanket rupture (Dutch: opbarsten)
If blanket layers of clay or peat are less thick than 4 m, these layers can lift up and rupture in case of overpressure in the aquifer below (head PL3). If the uplift potential is larger than 1.2 times the weight of the blanket, uplift occurs and the resisting shear strength is reduced to 0. This only takes place in the passive part of the slip plane.

For instance in case 41_M_28, uplift is a large problem. For a water level of NAP +11m, there is still a significant shear stress, whereas a water level of NAP +13m results in an uplift situation with shear stresses drop to 0, see Figure 8.5. For more information about the cases mentioned in this section, please refer to Appendix C.

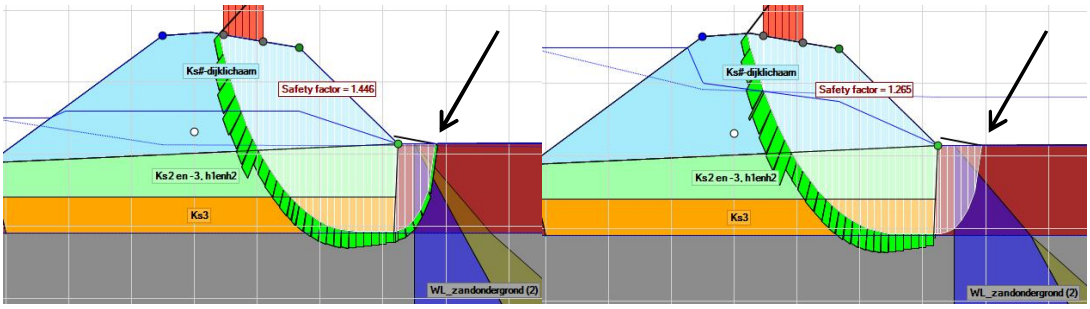

Figure 8.5 41_M_28 (Maas): Blanket rupture due to high PL3 head and blanket layer D<4m. The green planes show the mobilized shear strengths along the failure plane.

Ad 2. Uplift: Reduced shear strength due to excess water pressures in sand aquifer (Dutch: opdrijven)
In case the PL3 level is high, the pore water pressure below the blanket layer can be higher than the total stress, for instance in cases with a thick weak soil layer (e.g. peat with volumetric weights of 10-11 kN/m^3). The high head level in the deep sand might lead to calculated “negative effective stresses”. To prevent the model from doing so, the PL3 level is “adjusted to uplift”, so no negative effective stresses will be calculated. However, along the interface between blanket and aquifer, the effective stress is nearly 0 and therefore the shear strength is reduced significantly.

This is the case in dp_190: for a water level of NAP +2m, the PL3 does not lead to negative pore water pressures, whereas it is for a water level of NAP +4m, see Figure 8.6.

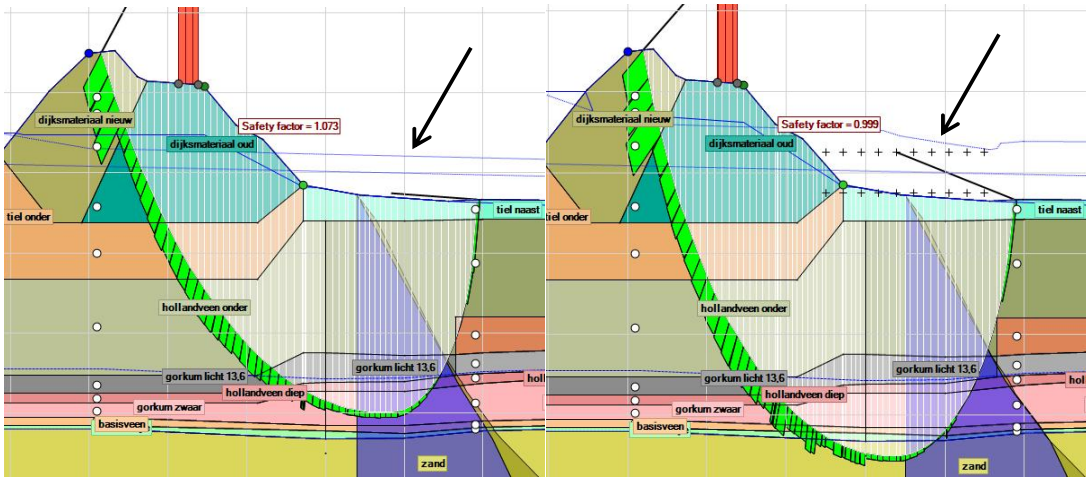

Figure 8.6 Dp_190 (Lekdijk): Uplift due to thick layers with low weight. The green planes show the mobilized shear strengths along the failure plane.

Ad 3. No Uplift

If the head in the aquifer is relatively low (or maybe has under pressure) and is closed by an impermeable layer, the increase of a water level has a negligible effect on the PL3 level. No uplift occurs and shear stress is not significantly reduced.

This is for instance the case in DV13. No uplift occurs and PL3 is not adjusted for uplift, see Figure 8.7.

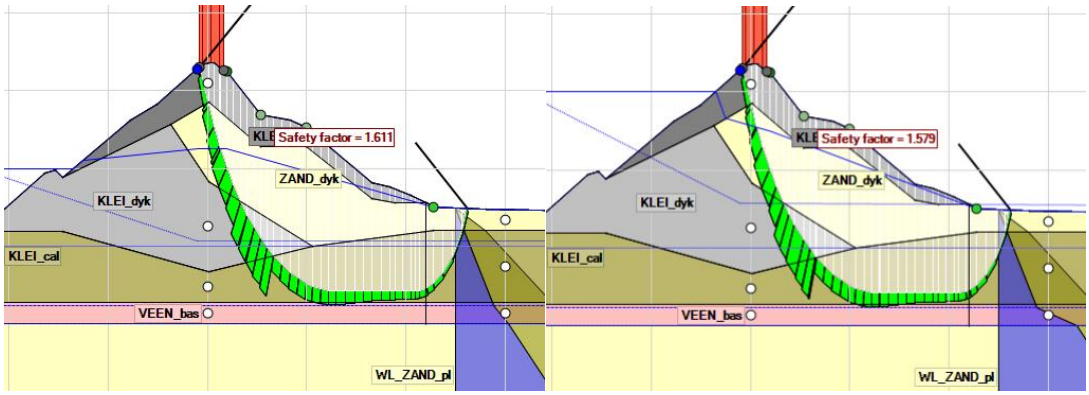

Figure 8.7 DV13 (Ijsselmeer) No uplift.

8.4.2 Comparison of the results (FoS and reliability) for uplift and non-uplift cases

For the different types of uplift, the results (FoS and reliability) have been separated. Whether a case shows blanket rupture, uplift or no uplift is determined for the water level in the design point and for the MHW level. This difference is made because the design point of the water level is often significantly lower than the water level for which uplift occurs. Hence, there may be a difference, see Figure 8.8 and Figure 8.9.

The difference between uplift, blanket rupture and no uplift is not significant and the amount of cases is limited. Hence, no differentiation is made in the beta-gamma relation based on uplift or no-uplift.

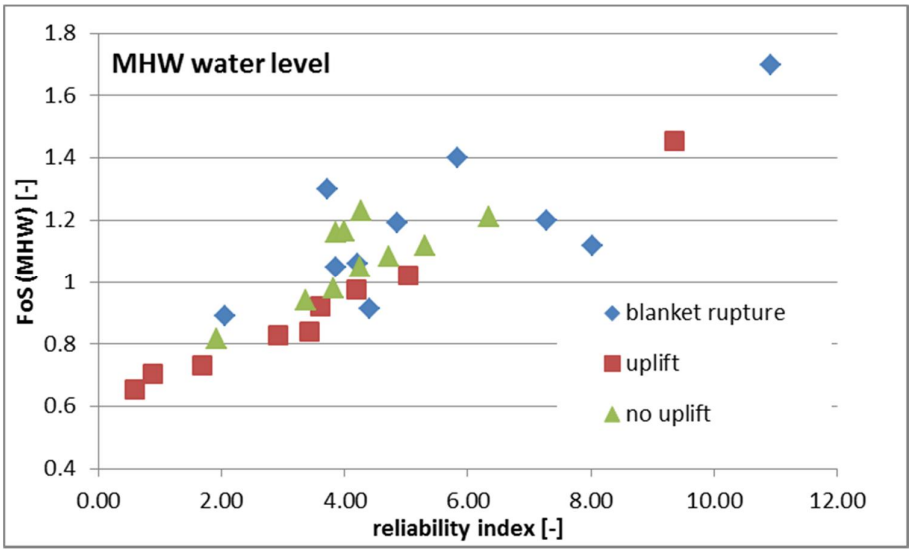

Figure 8.8 FoS versus reliably separated in uplift or non-uplift for the MHW water level.

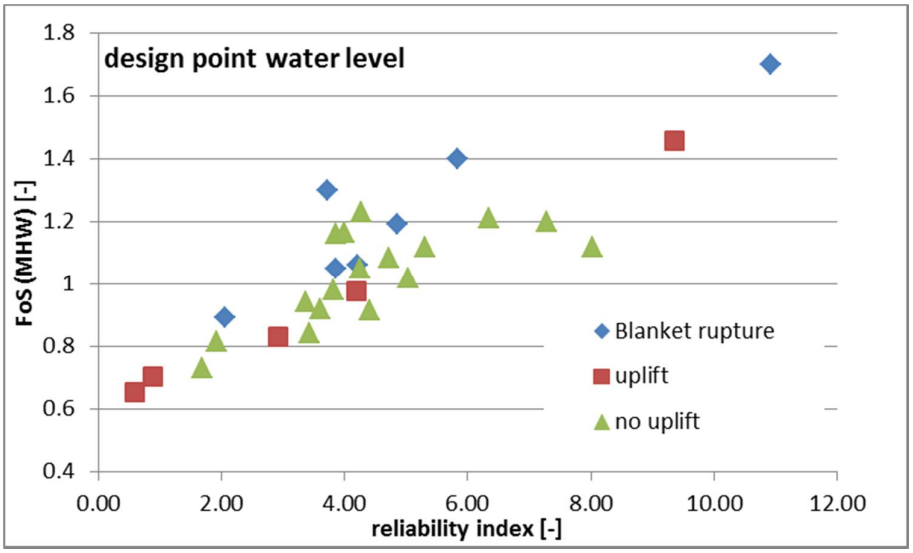

Figure 8.9 FoS versus reliably separated in uplift or non-uplift for the water level in the design point.

8.4.3 Differentiation to riverine and marine deposits

In Figure 8.11, the results for FoS and reliability are sorted to the geology. Broadly speaking, cases left of the line (Figure 8.10) have a marine geology, whereas cases west of the line have a river geology. From the results it is seen that the marine cases show both lower reliability as factor of safety. This could be related to thick layers of weak soil which are present in this area. In the area with river geology the clay layers are often less thick and more compressed (higher volumetric weights). Both sets show more or less the same trend. However, the number of cases is again not sufficient to draw conclusions.. For this reason there is no ground for calibrating multiple beta-gamma relations.

Figure 8.10 Separation in marine (west) and river (east) geology.

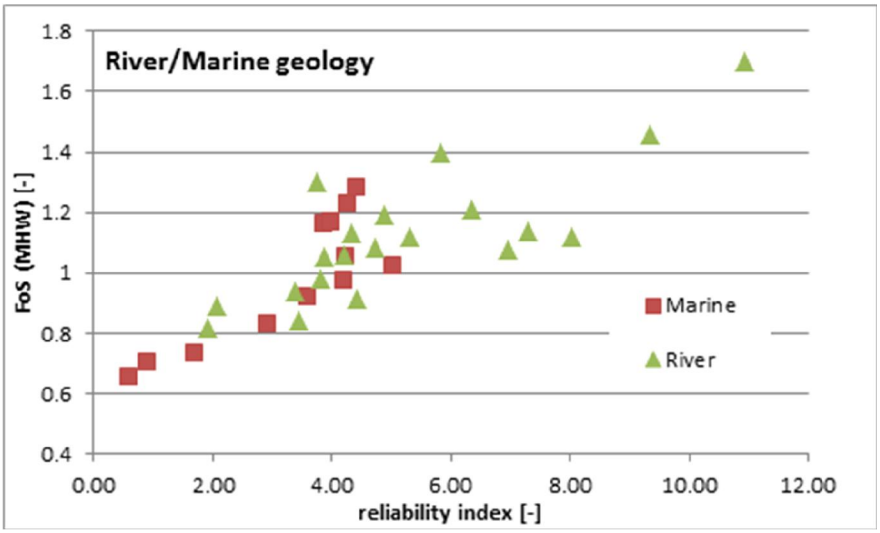

Figure 8.11 FoS versus reliably separated in cases with marine and river geology.

8.5 Sensitivity analysis

8.5.1 Sensitivity for yield stress points

The influence of the schematisation of the yield stress points on the reliability index has been investigated. To that end, a standard subsoil schematisation given in Figure 8.12 was varied. The yield stress at the toe of cross section 41_M_28_0 and 41_M_28_15 was increased from σ_{vy} = 3kN/m^2 to 16 kN/m^2. These cross sections have been evaluated using the probabilistic prototype and the results are given in Figure 8.13. One can clearly see in Figure 8.13 that a lower value of the yield stress at the toe of the cross section leads to lower reliability indices for given water levels. Only the absolute values of the conditional reliability indices, but not the basic S-shapes of the fragility are changed. This is valid also in case of an additional berm. Figure 8.13 shows for the 41_M_28 a slight increase of beta with the water level. This is not to be expected and likely due to a numerical error, which occur sometimes for very high

betas. This is not considered to be a major issue since it is far outside the required beta range.

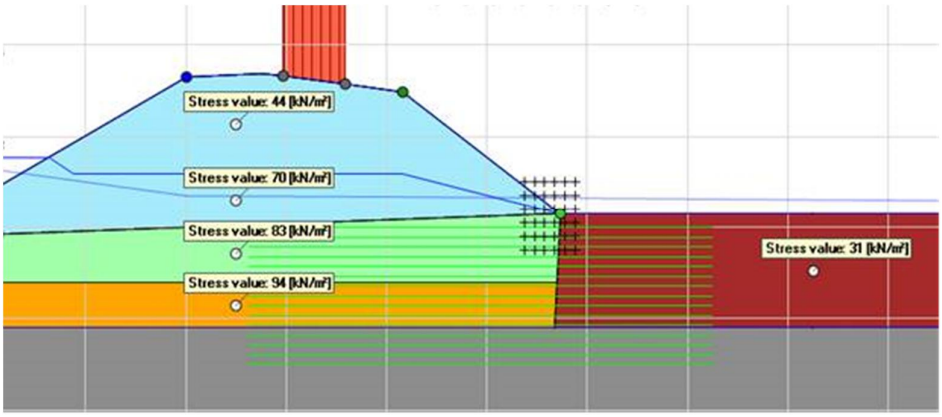

Figure 8.12 Standard schematisation of the subsoil for 41_M_28_0 .

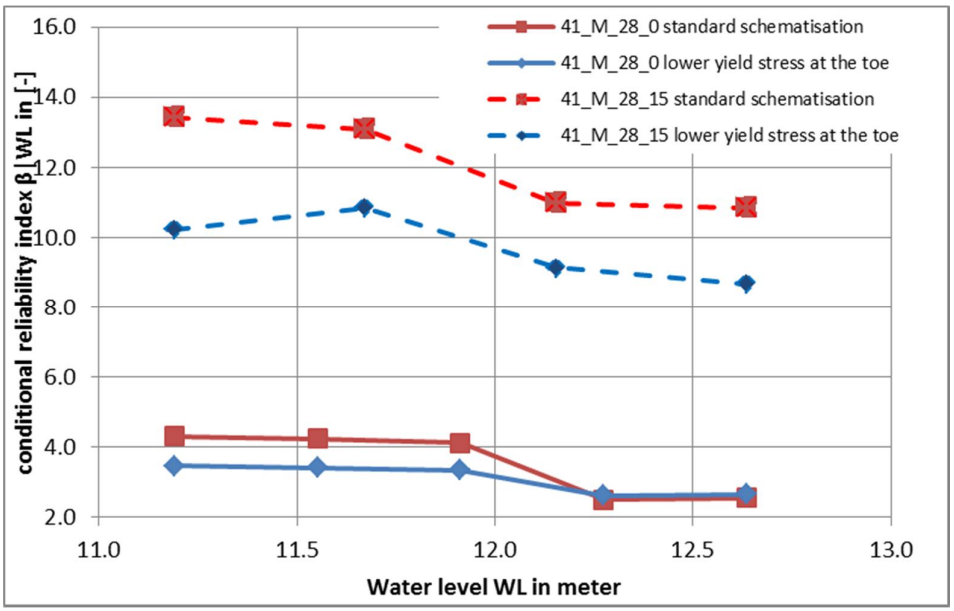

Figure 8.13 Fragility curves of cross sections 41_m_28_0 (solid lines) and 41_m_28_15 (dotted lines) using a standard schematisation of the subsoil (red lines) and a lower values of the yield stress at the toe of the cross sections (blue lines).

8.5.2 Sensitivity for traffic load

In all calibration calculations, an external traffic load is taken into account. A consequence analysis has been made for the deterministic and probabilistic calculations of two cross sections with and without traffic load since traffic load may not be incorporated in the WTI2017. The first involves a case with a small slip plane and the second involves a case with a large (deep) slip plane.

Both the cases with traffic load and without traffic load are depicted in the calibration graph, see Figure 8.14. It is clearly seen that ignoring the traffic load leads to an increase in both the Factor of Safety (characteristic values) and the reliability index. The increase of the dp92 FoS is relatively larger than the FoS increase of 43001007, relative to the reliability index. In

general the points are within the same range as the surrounding cases. More importantly, the shift in beta relates to a shift in gamma that is in the same angle as the calibration fit. Hence, the traffic load is not expect to influence the results of the calibration based on these two cases. Moreover, the influence coefficients are also nearly the same.

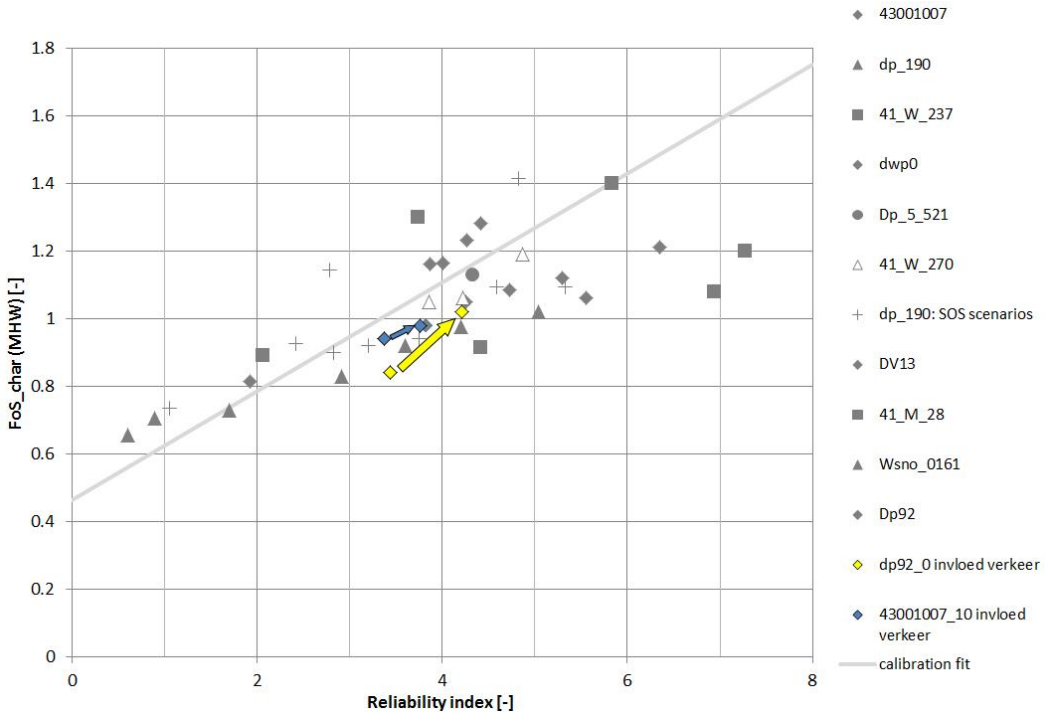

Figure 8.14 Calibration fit (grey) with the calibration points of two cross sections, with and without traffic load.

8.6 Spencer

The Spencer method to determine the minimal failure plane (see e.g. Van Duinen, 2014a) can be employed in the present version of the prototype. Uplift Van was the default method in the calibration. Most cases have also been evaluated with Spencer. This showed that it is challenging and time consuming to find the minimum slip plane with Spencer using the standard boundary conditions. As described in Appendix B, it is recommended to manually control the search process of the Spencer slip surface using D-Geo Stability. As shown in Figure 8.15 and Table 8.2, selected cases (43001007_20, 41_W_237_0/5/10 and dwp0) have been evaluated using the probabilistic prototype with Spencer in combination with standard boundary conditions. The results (reliability index and stability factor for a given MHW) are given in Figure 8.15 and show good agreement with respect to their reliability index as well in their squared alpha values for Spencer and Uplift-Van results. The other investigated cross sections (Dp43_ 1, Dp_5, 41_W_270_0) did not produce satisfying outcomes. The reason is that finding the Spencer slip surface with the genetic algorithm using an automatic selection gives unstable results. Manual manipulation proved to be time consuming and still is prone to errors. Due to time constraints, the Spencer method has not been used in the calibration process. Nonetheless, the Spencer computation with manual setting the boundary conditions, for the cases without errors, provides similar results as Uplift-Van, although setting the manual boundary conditions should be done with care.

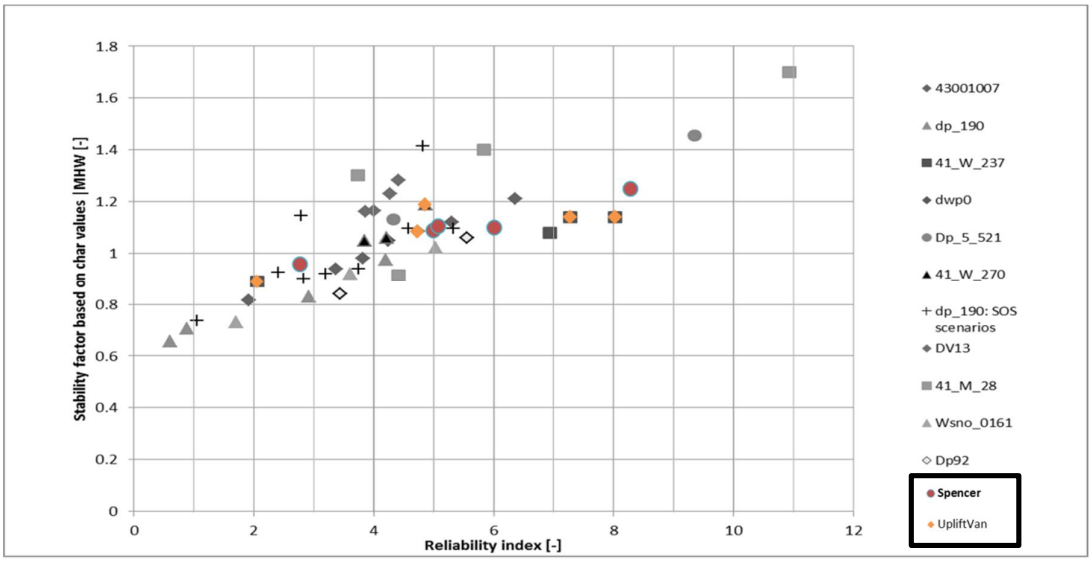

Figure 8.15. Comparison of the Spencer calculation results (red dots) with results of Uplift-Van (orange) with the test cases in grey.

Table 8.2 Comparison of Spencer and Uplift-Van

		43001007_20	41_W_237_0	41_W_237_5	41_W_237_10	dwp0_0
Uplift-Van	beta	4.73	2.06	8.03	7.28	4.86
	FOS_char (MHW)	1.09	0.89	1.14	1.14	1.19
Spencer	beta	5.00	2.78	6.01	8.28	5.07
	FOS_char (MHW)	1.09	0.96	1.10	1.25	1.11

If Spencer will be used as the preferred method in Hydra-ring/Ringtoets, it is suggested that it would be beneficial to improve the Spencer method. It would be good if this approach could be made more robust.

8.7 Conclusions of the calibration

The main conclusions of the calibrations are:

- The 20% beta fit has applied to the test cases and gives results that are in the same order as the OI2014v3 (taking into account the differences between material factors)
- There is no reason yet, based on the limited amount of cases, to differentiate between different safety standards
- The results of the calibration rest on a limited amount of cases, making it difficult to judge the robustness of the calibrated safety factors.
- There is no reason, based on the limited amount of cases, for differentiating between uplift/no uplift of marine/river conditions; this may change when more cases are available
- The automatic implementation of the Spencer algorithm did not produce sufficiently stable output for calibration purposes.

9 Semi-probabilistic assessment steps and comparison with other assessments

This chapter presents in the first section (section 9.1) how to carry out a semi-probabilistic assessment for the slope stability failure mechanism, including how to deal with sub-soil scenarios. In section 9.2.1, a comparison of the calibrated relations with the present-day ones, is made. Section 9.3 provides a preliminary consequence analysis. Two example computations with the new calibrated safety factors are presented in section 9.4.

9.1 Inner slope stability semi-probabilistic assessment steps

This section outlines the steps of a semi-probabilistic assessment of a dike cross-section regarding the slope stability mechanism, following Jongejan & Klerk (2015), see Figure 9.1. The assessment is carried out per sub-soil scenario, in the end, the combined results of the assessments per sub-soil scenario are combined to an overall result. It is assumed that the dike cross-section is situated in a dike segment (*normtraject*) with the safety standard of $1/T$ years and n is the number of sub-soil scenarios.

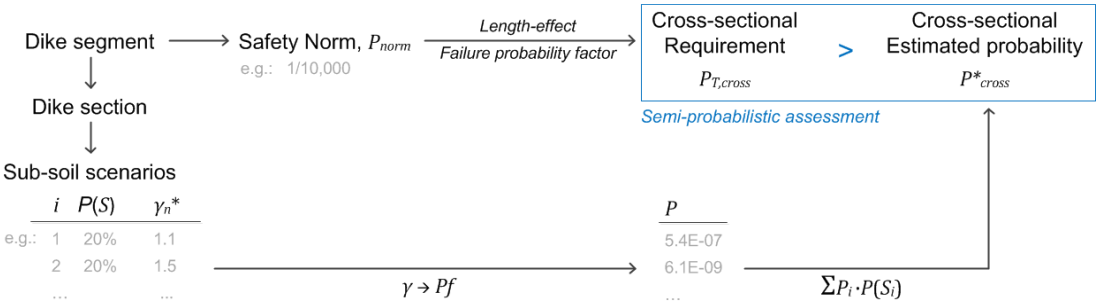

Figure 9.1 Schematised semi-probabilistic assessment for the slope stability mechanism in the WTI2017 (as in Jongejan & Klerk (2015)).

The goal is to compare the target safety with the occurring safety in terms of the reliability index or the probability of failure:

$$\beta^*_{cross} \geq \beta_{T,cross} \Leftrightarrow P^*_{cross} \leq P_{T,cross} \tag{9.1}$$

where $\beta_{T,cross}$ ($P_{T,cross} = \Phi(-\beta_{T,cross})$) is the target reliability index at the cross-section level and β^*_{cross} ($P^*_{cross} = \Phi(-\beta^*_{cross})$) the derived/estimated reliability index for the dike cross-section. Hence, in this section all variables with a "*" are computed values and variables with at "$_T$" is referring to target values. One should follow the steps below in the assessment.

1. Determine characteristic values of variables involved in the semi-probabilistic rule, as specified in Table 9.1, for each sub-soil scenario. Characteristic values of random variables are marked with index *char*. Derive the outside water level *with an exceedance probability equal to* the safety standard of the dike segment.

2. With the characteristic values and design water level, determine the β– dependent safety factors for each sub-soil scenario ($\gamma_{n,i}$* and $i = 1,\ldots, n$, where n = the number of subsoil scenarios considered):

$$\gamma_n^* = \frac{1}{\gamma_d} \cdot \frac{M_{R,d}}{M_{S,d}} = \frac{1}{\gamma_d} \cdot F_{s,des} \tag{9.2}$$

Where, γ_n^* is the assessed/occurring β– dependent safety factor for the cross-section, γ_d is the model safety factor, and $F_{s,des}$ the factor of safety (calculated with design values of the input parameters).

3. The calibrated $\gamma - \beta$ relation(s) may be used inversely to obtain a (safe) estimate of the conditional reliability index per sub-soil scenario. Accordingly, use the recommended rules to transform the occurring safety factors into reliability indices ($\beta_{n,i}$* and i = 1,…, n).

$$\beta_n^* = g^{-1}(\gamma_n^*) \tag{9.3}$$

where g(.) is the $\gamma - \beta$ relation, see Chapter 8

4. To reach an overall verdict, the results of assessments for slope stability for the different sub-soil scenarios have to be combined. Having the failure probabilities for each sub-soil scenario, calculate the total occurring failure probability P^*_{cross} and reliability index β^*_{cross} by:

$$P^*_{cross} = \sum_{i=1}^{n} P_i \cdot \mathrm{P}(S_i) \quad \text{and} \quad \beta^*_{cross} = -\Phi^{-1}\left(P^*_{cross}\right) \tag{9.4}$$

where $\mathrm{P}(S_i)$ is the probability of sub-soil scenario i and $\sum_{i=1}^{n} \mathrm{P}(S_i) = 1$. P^*_{cross} is a conservative (safe) estimate of the cross-sectional probability of failure.

5. To assess the cross-section, based on the safety standard T and the length-effect parameters for the slope stability failure mechanism, determine the target failure probability (or reliability index) of the dike cross-section by using:

$$P_{T,cross} = \frac{f / T}{\left(1 + \frac{a \cdot L}{b}\right)} \quad \text{and} \quad \beta_{T,cross} = -\Phi^{-1}\left(P_{T,cross}\right) \tag{9.5}$$

where L is the total length of the segment [m], a is a fraction of the length that is sensitive to slope stability [-], b is a measure for the intensity of the length-effect within the part of the segment that is sensitive to slope stability (the length of independent, equivalent dike sections) [m] and f is the slope stability failure probability factor (default value equal to 0.04).

6. The considered dike cross-section complies to the safety standard regarding the slope stability failure mechanism if it fulfils eqn. (9.1).

Steps 1 to 4 refer to the estimation of the failure probability, whereas Step 5 refers to the derivation of the target failure probability. In the last step (Step 6), both failure probabilities (or reliability indices) are compared.

9.2 Comparison with current methods and safety factors

9.2.1 Comparison with current safety factors

The currently applied safety format applies to undrained analyses and can therefore only be compared to the OI2014_v3, see Section 3.5. The differences in the safety format as compared to the current assessments are discussed in Chapter 7 and in Section 3.5. The main differences are:

1 The value of the material factor which is 1 in this calibration and around 1.08 in the OI2014v3.
2 Beta-dependent overall safety factor which ranges between 1.0 and 1.3 in this calibration. This is a bit higher than OI2014_v3.

The model factor for Uplift Van is1.06 according to both the calibration and the OI2014v3.The net result of these differences is a semi-probabilistic rule that is broadly similar. For high beta's the calibration results in a beta dependent safety factor that is 0.1 higher than in OI2014v3 (which is compensated mostly by a material factor of 1.08 in the OI2014v3), see Figure 8.3. For lower beta's, the difference is 0.2, and the calibration thus results in more conservative safety factors. It is not possible though to draw firm conclusions on what this would mean for required berms since there are difference in the undrained shear strength computation between the two methods. It must be noted though that the safety factors only make sense in relation to the safety format.

9.2.2 Comparison calibration with VNK and the WTI2006

In this section, assessments based on the calibrated rule (β calibration) are compared to the results of VNK2 studies (results are obtained from Jongejan et al., 2012) and to the last assessment using the WTI2006 (IVW 2006). The results are shown in Table 9.1.

Table 9.1 Review of the safety factors, reliability indices and assessment achieved in other studies.

Cross-section id:	Cross-section name:	β cali-bration	FoS * drained	β * drained	β ** drained	β ** undrained	WTI 2006***
43001003	43001007	1.92	-	-	-	-	No assessment
16003028	dp_190	0.6	-	-	-	-	Not ok
41003039	41_W_237	2.06	1.09	5.5	4.5	4.0	Not ok
52002014	Dp43	-	1.45	5.8	-	-	Ok
52003005	Dp_5_521	9.35	1.46	4.9	4.6	0.0	Ok
17003020	dwp0	4.25	1.26	5.8	5.7	5.7	Ok
41003037	41_W_270	4.22	1.21	7.1	4.3	1.9	Not ok
41003002	41_M_28	4.41	1.49	6.8	5.9	5.4	Ok
12002008	DV13	3.87	1.39	6.2	10.5	9.0	Not ok
31001003	Wsno_0161	1.7	0.82	4.0	3.8	2.2	No assessment
52001005	Dp92	3.44	1.50	5.7	-	-	Ok

* Jongejan et al. (2012)
** Jongejan et al. (2014)
*** IVW (2006)

It should be noted that a comparison cannot be done unambiguously since different schematizations and material models are used. Even though the calibration rests on

undrained analyses while VNK2 and the WTI2006 results are based on drained computations, the general trends are similar. Dikes deemed unsafe with the WT2006 correspond on average to a low reliability index, with the exceptions of 41_W_270 and DV13. However, the amount of cases is limited and the material model and schematizations are different, which combined do not allow for firm conclusions.

9.3 Preliminary consequence analysis

This section provides an overview of the results of a preliminary consequence analysis of the calibrated semi-probabilistic rule by analysing the required berms to comply with two target reliabilities (3.5 and 5.5). This is done by plotting the target reliability index against the berm lengths, see Figure 9.2.This allows an estimation of how much berm would be needed to comply to a target reliability of 3.5 and 5.5.

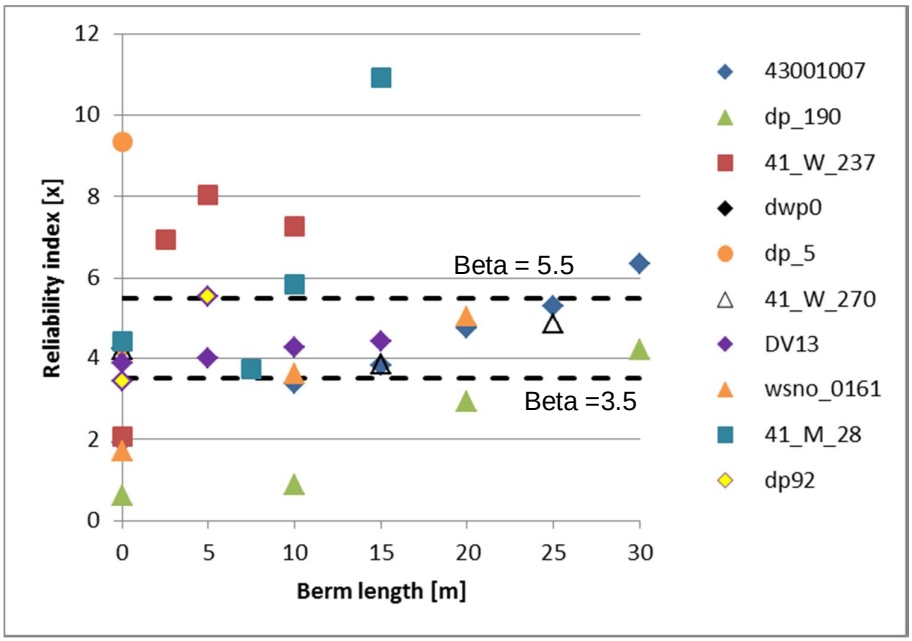

Figure 9.2 Berm length versus reliability index for the test cases

The required berms are summarized in Table 9.2. The results of the last official safety assessment for slope stability, the LRT3 (IVW,2006) are presented in the final column. The first interesting observation is that the dikes that need reinforcement based on the calibration analysis were mostly assessed unsafe and the other way around. It must be noted that dp_190 is a very weak dike which is currently in the improvement process. The average required berm length is 6 meter for the low target reliability and 17 meter for higher target. However, this is mainly due to dikes that were already assessed unsafe. The required reinforcement, based on a not-optimized berm and soil investigation, for dikes that complied in the LRT3 is very limited. Again, it is not possible to draw firm conclusions since different schematizations and different material models are used. Hence, a more elaborate consequence analysis is recommended.

Table 9.2 Required berm length to comply with two target reliabilities.

cases	Required berm length [m]		LRT3 assessment
	Target reliability = 3.5	Target reliability = 5,5	
43001007	12	27	no assessment
dp_190	30	40	does not comply
41_W_237	3	3	does not comply
Dp_5_521	0	0	comply
dwp0	0	5	comply
41_W_270	0	> 30	does not comply
41_M_28	0	10	comply
DV13	0	40	does not comply
Wsno_0161	10	25	no assessment
Dp92	2	5	comply
average	6	17	

9.4 Examples

9.4.1 Example of the proposed semi-probabilistic assessment procedure

The first step of the semi-probabilistic safety assessment is the determination of the maximum allowable probability of failure. According to the Safety Norms [ref1], the safety standard for this particular dike section is 1/3000, so:

$$P_{norm} = 1/3000 \tag{9.6}$$

For dikes, the standard failure budget (ω) for inner slope stability is equal to 0,04. The length of this segment is 24,4 km (based on Bijlage Werkgetallen nHWBP versie 1.2 oktober 2014). For slope stability, the default values are used: a = 0.033 and b = 50m. Therefore:

$$N = 1 + \frac{a \cdot L_{segment}}{b} = 1 + \frac{0.033 \cdot 24500}{50} = 17.2 \tag{9.7}$$

And consequently:

$$P_{T,cross} = \frac{P_{norm} \cdot \omega}{N} = \frac{1/3000 \cdot 0.04}{17.2} = 7.8 \cdot 10^{-7} \tag{9.8}$$

The required reliability for this maximum probability of failure is:

$$\beta_{T,cross} = \Phi\left(1 - P_{T,cross}\right) = 4.80 \tag{9.9}$$

For inner slope stability, this required reliability is translated into a beta-dependent factor of safety using the calibrated relation. This is visualized in Figure 9.3

$$\gamma_{n,required} = 0.161 \cdot \beta_{T,cross} + 0.463 = 1.24 \quad (9.10)$$

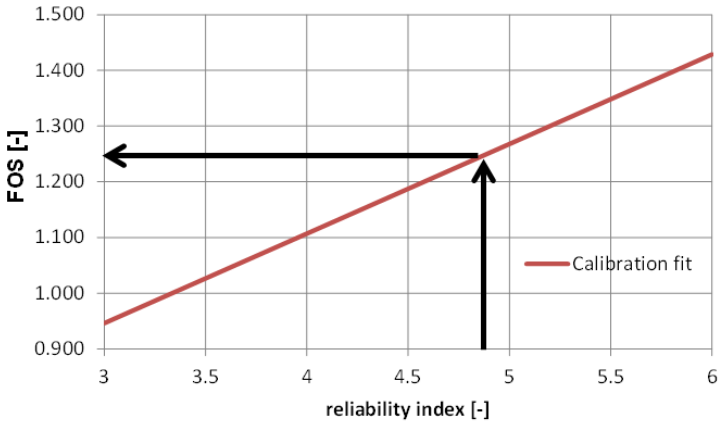

Figure 9.3 Derivation of the required factor of safety, given a target reliability.

The next step is to calculate the factor of safety of the cross section at the selected dike section. For all strength parameters of the materials, characteristic values are used. The design water level is a water level with an exceedance frequency equal to the safety norm. Hypothetically, an Uplift-Van calculation result in a factor of safety γ^*= 1.30. This has to be divided by the model factor for Uplift-Van: 1.06.

$$\gamma^*_{n,char} = 1.30 / 1.06 = 1.22 \quad (9.11)$$

The assessment is made by comparing the calculated factor of safety with the required factor of safety.

$$\begin{aligned} &if \quad \gamma^*_{n,char} > \gamma_{n,required} \quad \text{assessment fulfilled} \\ &1.22 < 1.24 \quad \text{assessment not fulfilled} \end{aligned} \quad (9.12)$$

In this hypothetical example, as small safety deficient (0.02) is found. This could be dealt with e.g. by an improved schematization based on local data in order to increase the computed factor or safety ($\gamma^*_{n,char}$) to the target ($\gamma_{n,required}$).

9.4.2 Example of a semi-probabilistic assessment with SOS subsoil scenarios for dp_190

For a specific cross section, dp_190, the different subsoil scenarios have been determined. Then, the slope stability calculations per scenario have been described and after that, the reliabilities per scenario have been combined and compared to the target reliability. For dp_190, 9 SOS (stochastisch ondergrond model) scenarios have been built. These are 1D soil profiles. Each subsoil scenario has a probability of $P(S_i)$. The sum of all probabilities $\Sigma P(S_i)$ is equal to 1. Each subsoil scenario has been analysed with default strength parameters (based on Van Deen and Van Duinen, 2015). For characteristic soil parameters and the model factor for Uplift-Van, this resulted in a FoS for each scenario, see Table 9.3.

Table 9.3 Probability of occurrence of a subsoil scenario and FoS for characteristic values and MHW

Subsoil scenario	$P(S_i)$	FoS_{char}
1	6%	0.87
2	9%	0.69
3	15%	1.03
4	15%	0.85
5	5%	0.87
6	15%	1.33
7	5%	1.08
8	15%	1.03
9	15%	0.89

Using the calibrated beta-gamma relation (γ_n = 0.161 * β + 0.463), the reliability and probability of failure ($P_{f,scen,i} = 1-\Phi(\beta_i)$) has been calculated. For the 9 scenarios, the results are shown in Table 9.4.

Table 9.4 Probability of failure given a subsoil scenario, calculated semi-probabilistically from beta-gamma relation

Subsoil scenario	$\beta_{scen,i}$	$P_{f,scen,i}$
1	2.87	2.06E-03
2	1.69	4.56E-02
3	3.93	4.33E-05
4	2.71	3.32E-03
5	2.84	2.27E-03
6	5.91	1.68E-09
7	4.24	1.14E-05
8	3.93	4.33E-05
9	2.96	1.52E-03

Using the schematization theory, the sub-soil scenarios need to be summed in the following manner: $\Sigma P_{f,scen,i} \cdot (S_i)$. For the 9 scenarios, this resulted in a probability of failure of 9.4E-03 per year, which is equal to β = 2.35. Besides semi-probabilistically calculations, the cross sections have also been analysed probabilistically. This results in a probability of failure per scenario, see Table 9.5. The results are also depicted in Figure 9.4.

Table 9.5 Reliability and probability of failure given a subsoil scenario, calculated probabilistically.

Subsoil scenario	β_{prob}	$P_{f,prob}$
1	2.42	7.85E-03
2	1.05	1.46E-01
3	4.58	2.29E-06
4	2.83	2.33E-03
5	3.20	6.94E-04
6	4.82	7.13E-07
7	2.79	2.67E-03
8	5.33	5.04E-08
9	3.75	8.74E-05

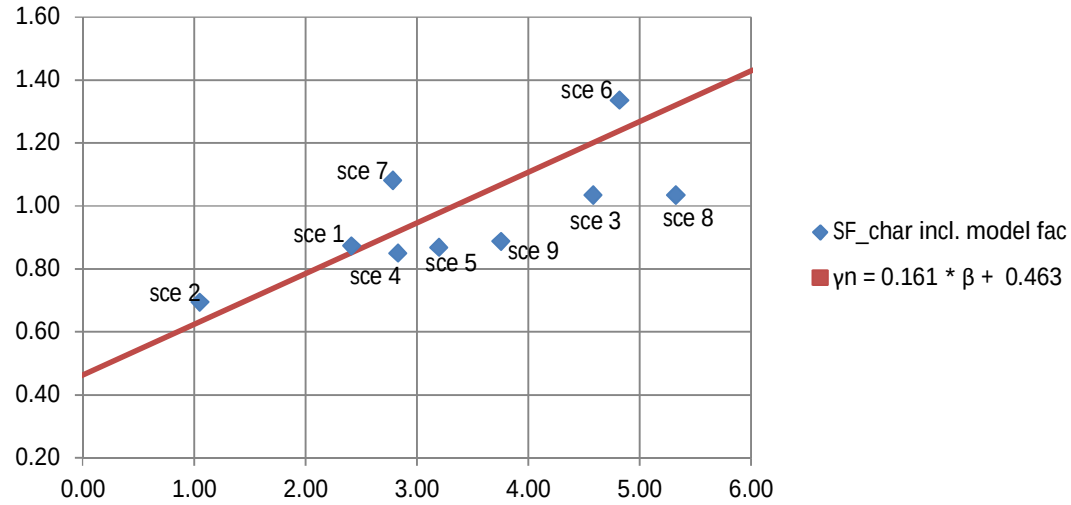

Figure 9.4 Reliability (probabilistic calculation) and characteristic Factor of Safety for 9 sub-soil scenarios. The red line describes the beta-gamma relation obtained from the calibration.

Summing these probabilities according to the schematization theory $\Sigma P_{f,prob,i} \cdot (S_i)$ results in a probability of failure of 1.4E-02 per year, which is equal to β = 2.19. This value van be compared to the combination of semi-probabilistic computation, this is show in Table 9.6.

Table 9.6 Comparison of the reliability and probability of failure of the combination of subsoil scenarios.

	β	**P_f**
Combined sub-soil scenarios semi probabilistic	2.35	9.4E-03
Combined sub-soil scenarios full probabilistic	2.19	1.4E-02

It is remarkable that the combined probability of failure for the semi probabilistic check is lower than the full probabilistic check. However, the final probabilities of failure are in the same order, in fact, the difference is only a factor 1,5, see Table 9.6. The calibration fit is based on 20% of the beta, which complies to a fit on a mean of the probability of failure. This implies that roughly half of the points will result in relatively high beta-value from the gamma-beta relation. Particularly sce2 in this example is accidentally at the 'favourable' side of the calibration fit. Since it has the lowest FoS and consequently beta, it contributes most to the combination of scenarios. This explains the higher reliability in the semi probabilistic assessment using the beta-gamma relation. The example illustrates how to obtain and interpret the results of semi-probabilistic analyses when calculating with different SOS scenarios.

10 Discussion

10.1 Discussion on general calibration results

10.1.1 General

The calibration presented in this report showed that the applied methodology can be used to derive a relation between reliability index and safety factor. However, there are two main limitations to the performed calibration:

a) Limited number of cases
b) Limited influence of outside water level leading to remarkable results and possibly a conservative set of safety factors

These limitations are further elaborated in the subsequent sections.

More specific findings of the calibration are:

- the prototype probabilistic model was successfully applied to perform reliability computations using the WTI kernel of D-Geo Stability.
- the relation between required safety factor and target reliability is comparable to the OI2014v3: the beta-dependent factor is higher, but no material factors are applied. The net result is a semi-probabilistic rule that is broadly similar.
- The required berms to obtain commonly found target reliabilities are relatively small, especially given the fact that the test cases mainly consisted of relatively weak dikes.

10.1.1 Limited number of cases

One of the two main limitations of the study is the limited number of cases. This has the following implications:

- It is not sure if the test set is fully representative for the Netherlands. I.e. whether there is enough variation in the cases to cover a sufficiently wide range of soils (peat, clay, sand), shear strength ranges, thick and thin layer, uplift and no uplift. The cases were selected to cover a wide variety of circumstances, yet it is likely that set of cases is not fully representative.
- In the test set, there are not many uplift cases with small slip circles. There is currently one case in the test set, besides the sandy dike, in which the water level has a high influence due to uplift. It is recommended to study additional cases in which uplift is relevant

Hence, the analysis of more cases is recommended to validate the current beta-gamma relation and possibly find optimization of this relation of e.g. materials or uplift/no uplift. These should ideally be based on field data.

10.1.2 Limited influence of the water level and proven strength

The safety factor (and reliability) based on the undrained shear strength computations is not changing as much with the outside water level as used to be the case for drained computations. This results in much lower α values for the water (α_h) level and lower design point values for the water level. This result i requires further investigation.

The following differences have been observed:

1 No uplift or blanket rupture: in these cases, the water level has a very low influence.
2 Blanket rupture (or uplift) with small slip circle: in these cases, the water level has a high influence
3 Blanket rupture (or uplift) with large slip circle: in these cases, the water level has a relatively limited influence since a large part of the mobilized shear strength is outside of the zone that ruptures.

Possible reasons for the limited influence of the water level

There are three possible explanationsfor the limited influence of the water level.

1. Material model: The low influence of the water level (i.e. low values of α_h) can be explained by the undrained material model; especially for situations with no blanket rupture or uplift. This is further discussed in Appendix E and Section 8.4.1. This material model inherently incorporates a limited effect of the shear strength on changes in the effective stress, especially for decreasing effective stresses that occur during high water situations. A comparative study with a drained computation (Appendix E) shows indeed that, keeping all inputs equal except the material model, drained computations result in a much higher influence of the water level. The choice for undrained computations in the WTI2017 had already been made before the start of the calibration. The factor that determines the sensitivity to the water level is the *m* factor. This factor is based on literature and not much is to be expected on the short term from further study into the *m*-value.

2. Water pressures. The water pressures have been calculated with the Waternet Creator. It uses a deterministic and conservative default method according to TAW (2004). Taking into account the uncertainties in the water pressures probabilistically may have significant implications. A higher influence of the water level is expected. For example, the current implementation of the Waternet Creator uses a high Dupuit water level in the dike for daily conditions. The effect of this is that there is only an effect on the phreatic line if the outside water level is higher than this Dupuit level. Making this Dupuit level a random variable may thus lead to a higher influence of the water level. Rozing (2015) provides guidance of how to deal with water pressure uncertainties.

It is recommended to investigate the effects of water pressure uncertainties in the short term. Expected effects are a higher influence of the water level and a higher reliability. The water pressure schematization influences both the probabilistic and semi-probabilistic calculations. It is proposed to keep the conservative Waternet defaults for the semi-probabilistic computations and the computed stability factor would remain the same. When taking the uncertainty related to water pressures into account in the probabilistic computations, the relatively importance (influence factors) of the uncertainty related to the other variables must decrease. This would probably result in higher reliabilities and lower required safety factors. *Hence, the current calibration that excludes water level uncertainties could be conservative.* If the effect of water level uncertainties is significant, this should be incorporated in the calibration. It is proposed to keep the water pressures for the semi-probabilistic computation the same for the calibration (based on TAW, 2004) since the Waternet Creator gives a conservative approach; and only change the probabilistic computation of the water pressures.

3. Uncertainty related to material properties. When the uncertainties related to the material properties are relatively important, the sensitivity to the uncertain water level diminishes. The uncertainty could be somewhat reduced by using actual data rather than default values. Still, this uncertainty is expected to remain relatively large and difficult to reduce.

Possible implications of proven strength

In case of a low effect of the outside water level on the safety factor and reliability, there is high potential to lower probabilities of failure by taking proven strength into account (performance observations). This is especially the case in case of blanket rupture dominated cases with a relatively small slip circle. A preliminary first estimate of proven strength, using very simplistic methods, is presented in Appendix E. The decrease in failure probability can be several orders of magnitude. However, the actual effect is case specific. If the outside water level appears to have more influence due to a probabilistic incorporation of the water pressure, the effects of proven strength become less pronounced and may even disappear.

10.1.3 Dealing with proven strength

The following options may be considered to deal with proven strength:

- Not incorporating proven strength at all. This would likely result in the under-estimation of the reliability of levees and unnecessary assessing dikes unsafe; it is therefore not recommended.
- Incorporate in the calibration. This is not recommended since the Markermeerdijk experience shows that it is time consuming and location dependent to incorporate proven strength. It would also be necessary to devise criteria for distinguishing between cases where proven strength would have large to small effects on reliabilities.
- Incorporate proven strength in the advanced assessment, or “Toets op Maat” (TOM).

This last option is recommended for now given the present state of knowledge and understanding. However, it would be worthwhile to investigate for which cases lowering the safety factors might be justified and for which cases a “proven strength analysis” within the context of the TOM would be most effective.

Incorporating proven strength in the TOM should come with certain conditions to deal with the scarcity of specialists. One option is to prioritize cases for which proven strength is expected to result in significant reductions in failure probabilities (this could also be done within the context of the HWBP prioritization process). Based on the calibration results, these mainly seem to be no-uplift cases. However, with a probabilistic incorporation of water pressures, more cases may show uplift conditions. Additional analyses may be used to devise an efficient filter or prioritization method.

10.2 Discussion on safety format

The safety format is determined from test case results. Uncertainties are mainly covered by characteristic values of material parameters, a model factor and a beta-dependent safety factor. This is done in order to provide a balance between simplicity and effectiveness. No material factors are currently used in the calibration, the main reasons for this are: a) most uncertainty seems effectively covered using characteristic values (this is supported by the α values that are not dominant for the Su ratio for all cases); b) the beta-dependent safety factor might otherwise become smaller than 1 for low beta’s; c) there are not enough cases available to differentiate between different soil materials. Additional cases may show that a distinction between clay and peat could be efficient, though reasons a) and b) might still hold. Incorporating material factors would change the safety format as well as the derived safety factors. Also, a model factor for Spencer could be added to the safety format in cases that are assessed with Spencer. It must be noted that the design point value of the water level is often much lower than MHW; however, MHW will still be used in accordance with other failure mechanisms.

10.3 Proposed activities for 2016

The following activities are proposed until August 2016:

A. Study more cases to validate the currently proposed safety factors
B. Incorporate water pressure uncertainties and the effects of overflow/overtopping
C. Develop a protocol on dealing with proven strength
D. Decide on an intermediate set of safety factors

A. More cases to validate currently derived safety factors
As discussed in Section 10.1, more cases are needed to calibrate the currently derived safety factors. At least 15 additional cases should be studied that should be representative for the Netherlands. Cases with blanket rupture or uplift cases with relative small failure planes seem under-represented at present. Sand dikes but mainly regular dikes with various combinations of weak clay, strong clay, peat etc. should be added to the dataset. These cases should ideally be based on actual, site specific data.

B. Incorporate water pressure uncertainties and effects of overflow/overtopping
Water pressure uncertainties can roughly be divided in 3 groups: uncertainty in the location of the phreatic line for high water conditions, uncertainty in the location of the daily Dupuit water level in the dike and uncertainty in the water pressures in the aquifer below the dike and the intrusion length. The current Waternet creator uses default values to model the water pressures. These defaults are conservative and should be transformed into random variables that reflect the uncertainty in the water pressures. The expected effects are a higher influence of the water level and a higher reliability. If the effects of incorporating water pressure uncertainties are significant, they should be incorporated in the calibration.

Activities A and B can be carried out independently. If activity B shows a high influence on the reliability, water pressure uncertainties should be modelled explicitly in the calibration. This would involve a re-analysis of both the cases from this report and the new 2016 cases.

The effects of overflow/overtopping have not been considered in the calibration yet. A way to incorporate effects of overflow/overtopping is proposed in Jongejan (2015). The proposed procedure is expected to be ready for practical application/field tests in March 2016. The possible consequences on the required safety factors should be investigated.

C. *Develop a protocol for dealing with proven strength.* This would include a procedure or set of criteria for identifying the dikes where proven strength ought to be considered. This also depends on the outcomes of activity B. A protocol should be developed that balances the effort and time of the assessment with HWBP information needs (carrying out proven strength analyses for all dikes during one assessment round might be too time-consuming). See also the discussion in Section 10.1.3. Furthermore, this activity should reassess if there is a subset of cases where proven strength could be incorporated in the safety factors.

D. Decide on an intermediate set of safety factors. A decision on an intermediate set of safety factors should be made when more cases are going to be analysed to validate the currently derived safety factors (Activity A). This intermediate set might be changed based on the findings of activity A.
There are two main options:

1. Use the calibrated set of this report. The main advantage is that this set is based on the WTI2017 models y. The main disadvantage is that the set is based on a limited amount of cases and that the set will probably change if more cases or water pressure uncertainties are considered. It is expected that the current set results in a conservative safety assessment (i.e. a relative large percentage of dikes that will be

qualified as ‘insufficient’) since e.g. water pressure uncertainties have not yet been incorporated.

2. Keep the OI2014_v3 safety factors for the time being and change to a new calibrated sets once activities A and B are carried out. This results in a semi-probabilistic assessment rule that is largely similar the calibrated rule. A disadvantage is that it is less founded on the WTI2017 slope stability computation . An advantage, however, is that users would be confronted with fewer changes in safety factors, as activities A to C may lead to further changes to the calibrated rule in 2016.

In case there will be no validation of the current set of safety factors (activity A), it is recommended to use the currently derived set.

11 Conclusions and recommendations

This chapter provides general conclusions and recommendations. For more detailed discussion on the calibration results and possible implications, please refer to Chapter 10.

11.1 Conclusions

This section provides general conclusions from the calibration.

Conclusions with respect to the analyzed test cases

- The amount of test cases is insufficient to provide well-founded safety factors. Hence, more test cases should be considered to validate the findings.
- A set of cases that covers a variety in geography, geometry and materials has been analyzed successfully using the new undrained shear strength modeling.
- Most test cases provided stable and consistent results for the factor of safety and the reliability index. A couple of cases gave counter-intuitive results (e.g. a slight increase in the factor of safety with a decrease in the outside water level), which might be due to computational inaccuracies. Furthermore, the results are sensitive to the yield stress points, which should be determined with care.
- The factor of safety and reliability index are relatively insensitive to the outside water level using undrained computations, especially for cases without uplift.
- The cases do not include overtopping, the calibration is therefore only valid for an assessment without overtopping.

Conclusions with respect to the safety format:

- The cases provided a basis for deriving a safety format, which balances simplicity and accuracy.
- The safety format entails the use of characteristic values without partial factors for most input parameters. There is one beta dependent safety factor, which has been calibrated.
- All uncertainty related to material properties is covered by characteristic values in (shear strength and other) parameters. This explains the absence of material factors (or material factors equal to 1.0) in the calibrated semi-probabilistic assessment rule.
- The safety format and safety factors only apply to computations with Uplift Van since Spencer did not result in stable output.

Conclusions with respect to the calibrated safety factors

- The derived range of safety factors is close to current safety factors (OI2014v3)
- The berms that are needed for the test set members to reach appropriate safety levels (when ignoring past performance) seem reasonable.

Conclusions with respect to implementation of the results

- For the undrained material model, the stability factors and reliability indices are much less sensitive to variations in the outside water level than for a drained material model, especially for cases without blanket rupture or uplift. This implies that considering proven strength in undrained slope stability analyses for cases without blanket rupture or uplift may strongly influence the outcomes of safety assessments.

11.2 Recommendations

11.2.1 Recommendations for the short term (2016):

- *More test cases*: it is recommended to validate the findings in this report by analysing more test cases.
- *Explain counter-intuitive outcomes*: Not all results of the test case computations can be fully explained (see Section 8.1). It is recommended to further look into these cases.
- *Additional validation of the probabilistic prototype*: a so-called prototype (Appendix B) has been used to compute the reliability of cross-sections. The prototype has been tested with simple methods due to unavailability of alternative models and due to time constraints. However, an overall validation using e.g. importance sampling or directional sampling should be possible using the Probabilistic Toolkit. This should include work on a search algorithm for the Uplift-Van and Spencer methods, in which default boundary conditions can be used to find the slip surface with the minimum safety factor. Especially the incorporation of the water level statistics (Gumbel distribution) should be validated to support the proper functioning of the prototype. Another improvement would be to include a computation around the design point of the water level. The additional validation of the prototype would mainly affect the probabilistic assessment; improvements in Uplift Van or Spencer would affect the semi-probabilistic analysis as well.
- *Consequence analysis*: it is recommended to carry out a consequence analysis to obtain insight in the required dike reinforcements as a result of slope stability assessments based on the new, calibrated safety factors.
- *Proven strength*, mainly for not-uplift cases: as discussed in Chapter 10, it is recommended develop criteria for identifying the cases in which there is a limited influence of the water level. For these cases, proven strength may result in much higher reliabilities. It is recommended to further investigate proven strength and apply it to several cases to determine the possible effects.
- Incorporate water *pressure uncertainties*: uncertainties in water pressures are important but these cannot be modelled explicitly yet. It is recommended to investigate how water pressure uncertainties may be incorporated in the semi-probabilistic and probabilistic assessment.
- *Overtopping.* It is recommended to investigate how the effects of overtopping should be incorporated in the slope stability assessment. Jongejan (2015) provides guidance on how to approach this topic.

11.2.2 Recommendations for the medium term (2017 - 2019):

- Validate if computations with *local shear strength data* change the calibration outcomes: the current study mainly rests on default undrained parameters due to a lack of local data.
- Validate if the values of a and b in the determination of the *target reliability* need adaptation once more experience is obtained with the WTI2017; default values of a and b are still used for this report.

11.2.3 Recommendations for D-GeoStablility

- If there is a blanket layer of less than 4 meters and an uplift potential bigger than 1.2, the shear strength of the low permeable, undrained layers in this region has to be reduced due to the loss of strength. Note that in the present beta version of D-Geo Stability (10/2015) one has to manually select strength reduction in case this happens. This should be made very clear in Ringtoets manuals.

- The Spencer algorithm using automatic boundary conditions does not always give stable and reasonable output. This algorithm should be tested rigorously before being implemented as the default in Ringtoets.

References

Bishop, A. W. (1955). The Use of the Slip Circle in the Stability Analysis of Earth Slopes, Geotechnique, Vol. 5, pp. 7-17.

Calle, E. and W. Kanning, 2013. WTI: Effecten ruimtelijke variabiliteit op geotechnische sterkte van waterkeringen. Deltates: 1207805-004-ZWS-005.

DPV (2015). Synthesedocument deelprogramma veiligheid - achtergrondrapport bij deltaprogramma 2015. Tech. rep., Dutch Ministry of Infrastructure and the Environment.

Deen, J. v. and A. v. Duinen (2015). Schematiseringshandeling Macrostabiliteit. Deltares 1220083-003.

Deltares (2015). D-GEO STABILITY. Slope stability software for soft soil engineering: User Manual. Version: 15.1. Revision: 00. Pub. Deltares.

Duinen, A. v. (2014a). Programma WTI 2017 – onderzoek en ontwikkeling landelijk toetsinstrumentarium – Modelonzekerheidsfaktoren Spencer – Van der Meij, Deltares: 1207808-001.

Duinen, A. v. (2014b). Memo on the variability of random variables used in Hydra- Ring, Memo, 1209434-012-GEO-0005, 22 Augustus 2014.

Duinen, A. v. (2015) . Modelonzekerheidsfactoren Spencer-Van der Meij model en ongedraineerde schuifsterkte. Programma WTI 2017, cluster Stabiliteit. Deltares: 1207808-001

ENW (2007) Expertise Netwerk Waterkeren, Addendum bij het Technisch Rapport Waterkerende Grondconstructies, Ministerie van Verkeer & Waterstaat, Den Haag, juli 2007.

Huber, M.H. (2015). Update probabilistic prototype macrostability. Deltares report 1220080-003-ZWS-0006.

IVW - Inspectie Verkeer en Waterstaat (2006). Primaire waterkeringen getoetst - Landelijke Rapportage Toetsing 2006.

Jongejan, R. B., Calle, E., Vrouwenvelder, A (2011). Kalibratie van semi-probabilistische toetsvoorschriften: Algemeen gedeelte. Deltares: 1204145-001.

Jongejan, R. B. (2012). Kalibratie semi-probabilistisch toetsvoorschrift voor macrostabiliteit binnenwaarts Deltares: 120606-606-ZWS-0004.

Jongejan, R.B. (2013). Kalibratie van semi-probabilistische toetsvoorschriften: Algemeen gedeelte. Deltares: 1207803-003.

Jongejan, R.B. , Duinen, A. v., Kuiper, B., Vastenburg, E. (2014) WTI 2017 Beoordeling macrostabiliteit met ongedraineerd materiaalmodel - probabilistische analyse en voorlopige veiligheidsfactoren, Deltares: 1207808-001.

Jongejan, R., Klerk, W. J. (2015). Functional design semi-probabilistic assessments Ringtoets, Deltares: 1209431-008-ZWS-0009.

Jongejan, R. (2015). Voorstel t.a.v. beoordeling macrostabiliteit incl. golfoverslag. Memo Kennisplatform Risicoanalyse, 10-09-2015.

Kruse, G. (2015). WTI 2017: Handleiding lokaal schematiseren met WTI-SOS, Deltares: 1209432-004.

Meij, R. v.d. (2013). WTI 2017 Failure mechanisms – Macrostability kernel, Deltares: 1207814-007.

OI2014v3 (2015). Handreiking ontwerpen met overstromingskansen, Veiligheidsfactoren en belastingen bij nieuwe overstromingsnormen. Report Concept vs. 2.5, Rijkswaterstaat Water, Verkeer en Leefomgeving.

Rackwitz, R. (2001). Reliability analysis – a review and some perspectives. Structural Safety, vol. 23, no. 4: 365-395.

Rozing (2015). Schematisering waterspanningen in WTI 2017 (Ringtoets), Deltares Report 1209434-012-GEO-0002

RWS (2013). Achtergrondrapport Ontwerpinstrumentarium 2014. Rijkswaterstaat.

Schweckendiek, T. (2014). On reducing piping uncertainties – a Bayesian decision approach, PhD Thesis, Delft University of Technology.

Spencer, E. (1967). A method of analysis of the stability of embankments assuming parallel interslice forces, Geotechnique (17), No 1, pp. 11-26.

TAW (1989). Leidraad voor het ontwerpen van rivierdijken deel 2 benedenrivierengebied.

TAW (2004). Technisch Rapport Waterspanningen bij dijken.

Van der Meer, M. T., Kapinga, H. S. O., Calle, E. (2008) Achtergrond materiaalfactoren rivierdijken, Fugro, Obdrachtnummer 1207-0055-000.

Van, M. A. (2001). New approach for uplift induced slope failure. XVth International Conference on Soil Mechanics and Geotechnical Engineering, Istanbul. 2285-2288.

Vastenburg, E., Zwan, I.v.d.(2013): Handleiding DAM 1.0 - Deel C - Functioneel ontwerp DAM 1.0, Deltares: 1207094-000.

A Appendix: Characteristic values, safety factors and design points

The following equations allow the determination of characteristic values, safety factors and design points for normally and log-normally distributed random variables.

A.1 Variables with Normal distribution

A.1.1 Characteristic value

If a random variable is normally distributed with mean μ and standard deviation σ, then the characteristic value of this variable, based on the 5%-quantile, is equal to:

$$\text{characteristic value} = \mu - 1.65\sigma \tag{A.1}$$

and, based on the 95%-quantile, it is equal to:

$$\text{characteristic value} = \mu + 1.65\sigma \tag{A.2}$$

A.1.2 Safety factors

In case of a normally distributed strength variable R with mean μ and standard deviation σ, the safety factor, based on the 5%-quantile, the reliability index $\beta_{cross\text{-}section}$ and the representative α-value, is derived as follows:

$$\gamma_R = \frac{\mu - 1.65 \cdot \sigma}{\mu - \beta_{\text{cross-section}} \cdot \alpha \cdot \sigma} \tag{A.3}$$

In case of a normally distributed load variable S with mean μ and standard deviation σ, the safety factor, based on the 95%-quantile, the reliability index $\beta_{cross\text{-}section}$ and the representative α-value, is derived as follows:

$$\gamma_S = \frac{\mu - \beta_{\text{cross-section}} \cdot \alpha \cdot \sigma}{\mu + 1.65 \cdot \sigma} \tag{A.4}$$

A.1.3 Design point

In case of a normally distributed random variable with mean μ and standard deviation σ, the design point based on the reliability index $\beta_{cross\text{-}section}$ and the representative α-value, is derived as follows:

$$\text{design point} = \mu - \beta_{\text{cross-section}} \cdot \alpha \cdot \sigma \tag{A.6}$$

A.2 Variables with Log-normal distribution

A.2.1 Characteristic value

If a random variable is log-normally distributed with mean μ and standard deviation σ, then the characteristic value of this variables, based on the 5%-quantile, is derived as follows:

$$\sigma_M^2 = \ln\left[1+\left(\frac{\sigma}{\mu}\right)^2\right] \quad \text{(A.7)}$$

$$\mu_M = \ln\mu - \frac{1}{2}\cdot\sigma_M^2 \quad \text{(A.8)}$$

$$\text{characteristic value} = \exp(\mu_M - 1.65\cdot\sigma_M) \quad \text{(A.9)}$$

and, based on the 95%-quantile, it is equal to:

$$\text{characteristic value} = \exp(\mu_M + 1.65\cdot\sigma_M) \quad \text{(A.10)}$$

A.2.2 Safety factor

In case of a log-normally distributed strength variable R with the coefficient of variation cov, the safety factor, based on the 5%-quantile, the reliability index $\beta_{cross\text{-}section}$ and the representative α-value, is derived as follows:

$$\gamma_R = \exp\left[(-1.65+\beta_{\text{cross-section}}\cdot\alpha)\cdot\sqrt{\ln(1+\text{cov}^2)}\right] \quad \text{(A.11)}$$

In case of a log-normally distributed load variable S with the coefficient of variation cov, the safety factor, based on the 95%-quantile, the reliability index $\beta_{cross\text{-}section}$ and the representative α-value, is derived as follows:

$$\gamma_S = \exp\left[(-1.65-\beta_{\text{cross-section}}\cdot\alpha)\cdot\sqrt{\ln(1+\text{cov}^2)}\right] \quad \text{(A.12)}$$

In case of a log-normally distributed load variable S with the coefficient of variation cov, the safety factor, based on the 99%-quantile, is derived as follows:

$$\gamma_S = \exp\left[(-2.32-\beta_{\text{cross-section}}\cdot\alpha)\cdot\sqrt{\ln(1+\text{cov}^2)}\right] \quad \text{(A.13)}$$

The coefficient of variation is defined as $\text{cov} = \sigma/\mu$.

A.2.3 Design point

In case of a log-normally distributed random variable with mean μ and standard deviation σ, the design point corresponding to the reliability index $\beta_{cross\text{-}section}$ and the representative α-value, is derived as follows:

$$\sigma_M^2 = \ln\left[1+\left(\frac{\sigma}{\mu}\right)^2\right] \tag{A.14}$$

$$\mu_M = \ln\mu - \frac{1}{2}\cdot\sigma_M^2 \tag{A.15}$$

$$\text{design point} = \exp(\mu_M - \beta_{\text{cross-section}}\cdot\alpha\cdot\sigma_M) \tag{A.16}$$

B Appendix: Probabilistic prototype macrostability

This appendix gives a summary of the workflow of the macrostability probabilistic prototype. This workflow is further elaborated in Huber (2015). The prototype is based on FORM calculations and is developed as a probabilistic test environment, using programming language `Python` which links the macrostability kernel with the probabilistic libraries PYRE (https://github.com/hackl/pyre).

B.1 Workflow

Standard reliability approaches like FORM are efficient and fast means for the calculation of the reliability of complex systems. However, FORM can be sensitive in case of strong discontinuities or singularities of the limit state equation. In case of slope stability problems, these discontinuities can be caused by nonlinear material behaviour, pore pressure distributions, which change with the water table and other nonlinearities like the reduction of the uplift potential in the present version of the D-Geo Stability software (10/2015)This formulates the need for a robust and efficient probabilistic calculation method, which can be used to calculate the reliability of a slope stability problem.

As such, the prototype does not consider WL directly as a random variable; instead, a conditional probability of failure $p_{f,i}|WL_i$ is calculated, which is used to construct the metamodel at a later stage of the workflow as presented in the following figures:

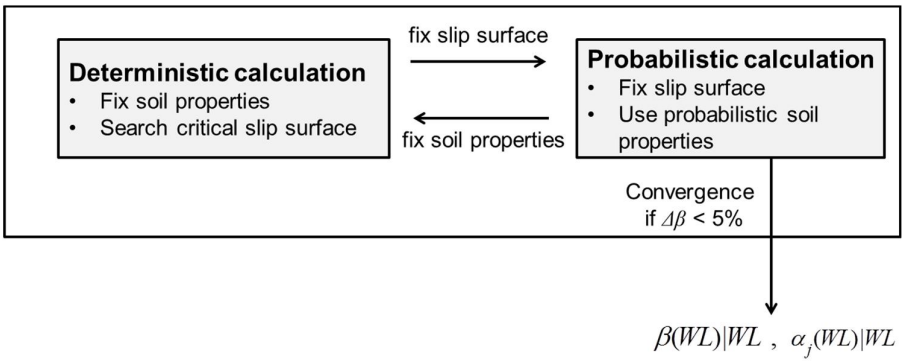

Figure B.1 Calculation scheme of the conditional reliability index $\beta(WL) \mid WL$ and of the conditional sensitivity factor $\alpha(WL)|WL$ for different water levels.

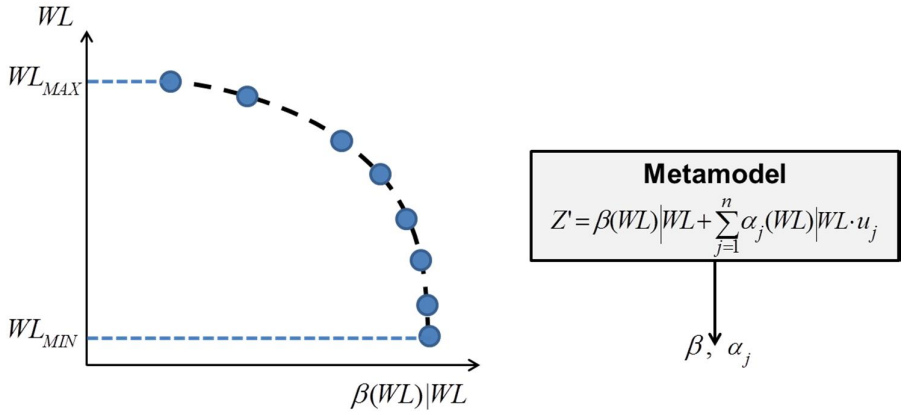

Figure B.2 Using the conditional reliability index $\beta(WL) \mid WL$ and the $\alpha(WL) \mid WL$ to construct the metamodel.

The workflow for the calculation of the reliability index and of the influencing factors, with the macro prototype, comprises of the following steps:

1 At first we introduce the **random variables** by defining their distribution functions, their corresponding mean values and standard deviations;

2 The characteristic values of the soil strength properties (95th percentiles) are used within the macrostability kernel for the calculation of the critical slip surface for a given water level WL_i. Herein, one can use the Bishop, Uplift-Van or Spencer models (drained or undrained approach). This **slip surface is fixed** for the reliability analysis. This fixed slip surface is checked in step 5 ;

3 **Reliability analyses** are performed using FORM and the macrostability kernel; within this the limit state equation Z as in eq.(B.1) is used:

$$Z = F_S / m_d - 1 \qquad \text{(B.1)}$$

Herein F_s is the factor of safety [-] and m_d the model factor [-];

4 After each reliability analysis, one **check**s automatically if the **slip surface** is resulting in the minimum stability factor and in the minimum reliability index. (for a given design point). For this reason, one has to use the values of the design point[4] for a given WL_i within an additional stability calculation and extract the critical slip surface from it. This slip surface is fixed and used for a reliability evaluation;

This loop (two previous steps) is repeated until the change of the reliability index is less than a given threshold of 5 %.

5 The steps 1 to 4 are repeated for different water levels between the lowest water level WL_{min} and the maximum waterlevel WL_{max}. WL_{min} is the lowest point of the surface at the river side and WL_{max} is the height of the dike crest.

At this point, the following is known for different water levels:

[4] *The design point is represents the combination of parameters, at which the slope is most likely to fail.*

– conditional probability of failure $p_{f,i}|WL_i$,
– the corresponding reliability index $\beta|WL_i$ and
– the vector of influence coefficients $\alpha_i|WL_i$

These results are used for the construction of a **metamodel** Z', which is used to create a limit state function as in eq.(B.2).

$$Z' = \beta|WL(WL) - \sum_{i=1}^{n} \alpha_i|WL(WL) \cdot u_i \quad \text{(B.2)}$$

This metamodel Z' is used for the evaluation of the probability of failure. Within this, the conditional reliability index $\beta|WL_i$ and the influence coefficients $\alpha_i|WL_i$ are linearly interpolated between the calculated reliability indices $\beta|WL_i$ and influence coefficients $\alpha_i|WL_i$. Note that the waterlevel WL_i is assumed to be between WL_{max} and WL_{min}.

6 Finally, one has to **check** if the design-point of the waterlevel is between WL_{max} and WL_{min}; if the design point is smaller WL_{min} the results of WL_{min} are taken as result; if it is bigger than WL_{max} an error message is given. Ideally, another computation with the design point of the water level, and points around it. This should ensure that the inaccuracy of the interpolation cannot become an important factor. Due to time constrains this has not been implemented yet.

B.2 Output

The probabilistic prototype has the following output:

- Results conditional to (a selection of) specific water levels
  probability of failure $p_f(WL)$
  reliability index $\beta(WL)$
  vector of influence coefficients $\boldsymbol{\alpha}(WL)$
  design point (WL)

- Results independent of the water level (including integration over water level domain)
  probability of failure p_f
  reliability index β
  vector of influence coefficients $\boldsymbol{\alpha}$
  design point

- Plots of the metamodel (reliability vs. water level)

B.3 Limitations

The macrostability calculation using the fixed slip circles based on 5%-quantiles of the resistance parameters is an approximation of the actual slip surface in the FORM design point. The approximation is improved by checking the slip surface after the reliability analysis, by using the design point values for the input properties, and by iterating towards the relevant (design point) slip surface, along which the slope fails.

The phreatic line is generated by using the Waternet creator. The input variables of the waternet creator are estimated in order to get conservative results. Note that no explicit uncertainties of the phreatic line are considered due to time constraints.

Due to the computation time of the macrostability analyses, one cannot apply a Monte Carlo analysis to check the results of the proposed approach. In the case studies in the appendix we compared these approximate results with results of FORM analyses, in which the soil properties and the water level is treated as a random variable and by using the fixed slip circle approach at the same time. The results show good agreement for the investigated cases.

Furthermore, the user has to carefully select the boundary conditions for the Macrostability calculations consisting of the following points:

- Manual selection of the slip surface using the Uplift-Van and Spencer approach. No stable results could be obtained using automatic boundary conditions with the present version of D-Geo Stability (10/2015).
- It is recommended to search for the slip surface using Uplift-Van or Spencer iteratively by changing the search settings for the slip surface in a smart way to get the one with the lowest factor of safety.

B.4 Validation of the prototype

The probabilistic computations of the prototype (PM) have been validated withs computation with the Probabilistic Toolkit (PT) for a simplified case given in Table B.1

The main differences between the PM and the PT are:

1) The PM uses a fixed slip circle approach to in the iterative calculation of the reliability. This approach is not used in the PT, which is using a not fixed slip circle in the FORM calculations.
2) The PM employs a metamodel using a fragility curve (Resistance) and water level distribution (Load) to calculate the reliability of the cross section.
3) One cannot prevent wrong or unrealistic slip surfaces in the PT.

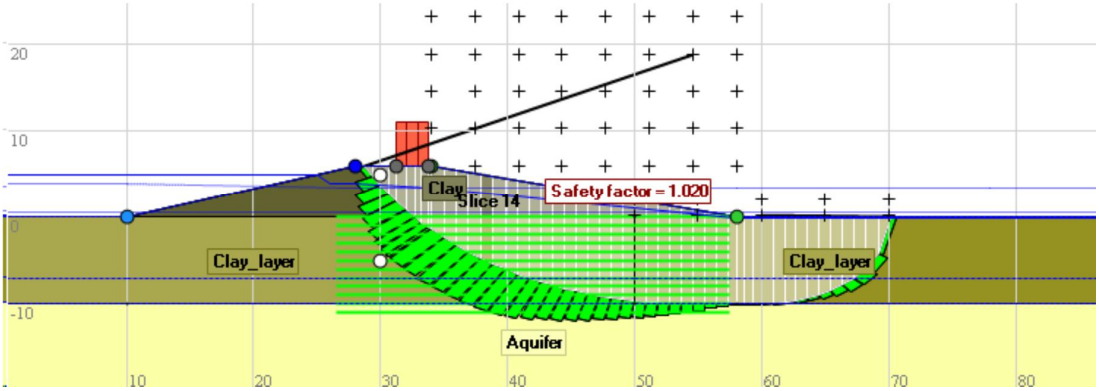

Figure B.3 Simplified case for validation Toolkit

The results of the PT and the PM are given in Table B.1. The resulting reliability index is nearly the same and also the squared alpha values are nearly the same. It can be concluded from this simplified example that both approaches offer more or less the same results. However, it has to be pointed out that this cannot be generalized to all possible cases. Generally speaking, it can be difficult to find the reliability index using FORM in case of a discontinuous limit state function. Factors like the distribution of the pore pressure, which changes for different water levels or the reduction of the uplift potential in D-Geo Stability can hinder FORM in finding a slip surface. This can be overcome by the proposed methodology.

Table B.1 Comparison Probabilistic Toolkit and Prototype

	Probabilistic Toolkit	**Prototype**
α^2		
CuPc	0.61	0.66
m	0.00	0.00
Yield stress	0.27	0.21
cohesion	0	0
friction	0	0
Model_fac	0.10	0.10
WL	0.02	0.02
Beta	**1.89**	**1.86**

C Appendix: Input and output per test set member

C.1 Introduction

C.1.1 Clarification output cases

In the next sections, the input and output presented and discussed. First, the input in terms of location (geographical, VNK, PC-Ring ID) and stratification of the cross section is discussed. Then, the material properties and schematization of the piezometric levels together with the water level distribution are summed up. This is followed by a description of the applied (traffic) load and schematization/derivation of yield stress points. Finally, other remarks are presented concerning the slip circle search method, strength reduction by uplift and (the number of cases with added) stability berms.

Deterministic calculations have been made for each cross section as part of a sanity check. It has been checked whether:

- The FoS decreases monotonously with increasing water level.
- The FoS is lower when it is calculated for characteristic values than for mean values.
- The FoS is higher for cases with a larger berm.

In case one of the checks fails, a remark is placed and it is explained why the anomaly occurs. They are mainly caused by differences in pore water pressure schematizations or different normative slip planes (for instance due to uplift). Discretization problems (for example with yield stress points) play a role in this.

After the deterministic calculations, the probabilistic calculations are described. First, the diagram for reliability conditional water level (β|WL) versus water level (WL) is shown. Below the graphs, the probability density function (pdf) and cumulative density function (cdf) for the water level distribution is shown.

Hereafter, the cumulative influence coefficients conditional the water level are shown in graphs. Most of the graphs show a fluent tendency, however in some cases, the graphs show some jumps. Some of these jumps are the result of minor numerical inaccuracies (anomalies in the order of 0,01 in alpha), changes in trends are usually caused by a different slip plane and accompanying problems. As this happens quite often, indivual cases are not pointed out at the graphs. In the end, a picture of the final slip circle in the design point is shown.

C.1.2 Yield stress points

A yield stress point is a point in the geometry for which the yield stress is defined in D-GeoStability. Each yield stress point therefore has an X-coordinate, Z-coordinate and a value for yield stress. The yield stress σ_y is defined as the in situ stress plus the pre-overburden pressure POP both at daily conditions. The calculations are made with explicit values of the yield stress point, using values for POP in the order of 10-20 to 50 kPa, dependent on the deposit. The used values are chosen on latest insights of field and lab tests of cases investigated in SBW and WTI. Mean values and real deviations are used in this calibration. The values of yield stress are fixed among calculations with different water levels, so the POP varies dependent on the outer water level. See also Van Deen and Van Duinen, 2015 for more information about yield stress points.

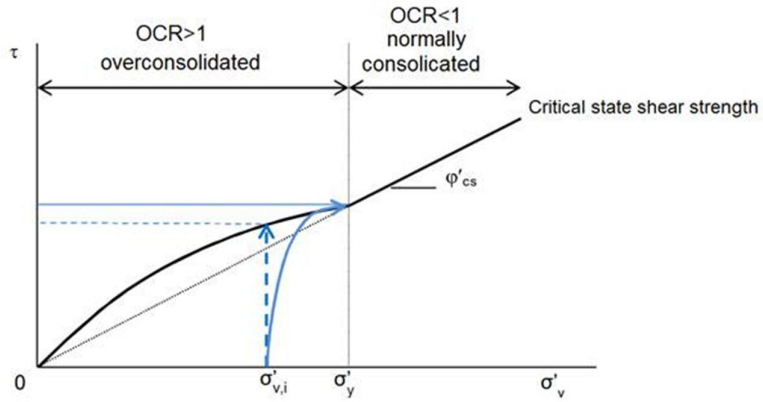

Figure C.1 Yield stress points

C.1.3 POP values

As described in the previous section, POP values need to be used to determine the yield stress points. The used POP values used to determine the yield stress points for the cases are shown in Table C.1 and are based on default estimates.

Table C.1 Default POP values

soil type	POP below dike				POP next to dike			
	μ [-]	σ [-]	char value [-]	CoV [-]	μ [-]	σ [-]	char value [-]	CoV [-]
veen mineraalarm	19.0	8.0	11.4	0.42	19.0	8.0	11.4	0.42
veen	21.0	3.5	17.7	0.17	21.0	3.5	17.7	0.17
veen kleiig	17.0	6.0	11.3	0.35	24.0	5.0	19.3	0.21
klei organisch (komklei)	17.0	6.0	11.3	0.35	24.0	5.0	19.3	0.21
klei met plantenresten (ondiep)	31.0	9.0	22.5	0.29	31.0	10.0	21.5	0.32
klei met plantenresten (diep)	16.0	4.5	11.7	0.28	16.0	5.5	10.8	0.34
klei zwaar (rivier ondiep)	38.0	11.0	27.6	0.29	34.0	10.0	24.5	0.29
klei zwaar (rivier diep)	17.0	6.0	11.3	0.35	24.0	5.0	19.3	0.21
klei zwaar (marien ondiep)	31.0	9.0	22.5	0.29	31.0	10.0	21.5	0.32
klei zwaar (marien diep)	16.0	4.5	11.7	0.28	16.0	5.5	10.8	0.34
klei zandig (rivier ondiep)	38.0	11.0	27.6	0.29	34.0	10.0	24.5	0.29
klei zandig (rivier diep)	17.0	6.0	11.3	0.35	24.0	5.0	19.3	0.21
klei zandig (marien ondiep)	31.0	9.0	22.5	0.29	31.0	10.0	21.5	0.32
klei zandig (marien diep)	16.0	4.5	11.7	0.28	16.0	5.5	10.8	0.34
dijksmateriaal klei	30.0	10.0	20.5	0.33	NA	NA	NA	NA

C.1.4 Default shear strength parameters

The default shear strength parameters for the WTI2017 are presented in Table C.2. These were used to determine most of the cases (except for case cp_190, which is based on local measurements).

Table C.2 Default shear strength parameters

	su-ratio <u>below</u> dike				**su-ratio <u>next to</u> dike**				**strength increase exponent m**			
	μ [-]	**σ [-]**	**char value [-]**	**CoV[-]**	**μ [-]**	**σ [-]**	**char value [-]**	**CoV[-]**	**μ [-]**	**σ [-]**	**char value [-]**	**CoV[-]**
veen mineraalarm	0.36	0.03	0.33	0.08	0.36	0.03	0.33	0.08	0.89	0.03	0.86	0.03
veen kleiig	0.33	0.08	0.25	0.24	0.33	0.08	0.25	0.24	0.89	0.02	0.87	0.02
klei organisch (komklei)	0.29	0.06	0.23	0.21	0.29	0.06	0.23	0.21	0.93	0.04	0.89	0.04
klei met plantenresten	0.29	0.09	0.20	0.31	0.29	0.09	0.20	0.31	0.93	0.04	0.89	0.04
klei zwaar (rivier)	0.25	0.02	0.23	0.08	0.25	0.02	0.23	0.08	0.93	0.02	0.91	0.02
klei zwaar (marien)	0.26	0.02	0.24	0.08	0.26	0.02	0.24	0.08	0.93	0.02	0.91	0.02
klei zandig (rivier)	0.23	0.02	0.21	0.09	0.15	0.02	0.13	0.13	0.92	0.03	0.89	0.03
klei zandig (marien)	0.23	0.02	0.21	0.09	0.15	0.02	0.13	0.13	0.92	0.03	0.89	0.03
dijksmateriaal klei	0.25	0.03	0.22	0.12	n.v.t.	n.v.t.	n.v.t.	n.v.t.	0.92	0.03	0.89	0.03

C.2 43001007

This section describes the steps and decisions made in setting up and performing deterministic and probabilistic calculations for slip failure of the inner slope for a specific cross section. Furthermore it summarizes the results for this case.

C.2.1 Setup

Location and geometry

The location of this cross section (VNK: 43.TG365.TG378, PC-Ring ID 43001007) is at the Waal, near Vuren. The surfaceline is taken from AHN.

Stratification

The stratification of the subsoil is the 1D-subsoil schematization from WTI-SOS with the highest probability. Particularly, this is Segment_43002_1D1 with a probability of occurrence of 49%. Only the first sand layer (aquifer) P_Rg_zg is taken into account, since the second deep sand layer will not contribute to critical slip planes. The 1D soil profile is split in three horizontal sections at 2/3 of the slope: respectively besides, below and besides the dike. This can be seen in Figure C.1 below.

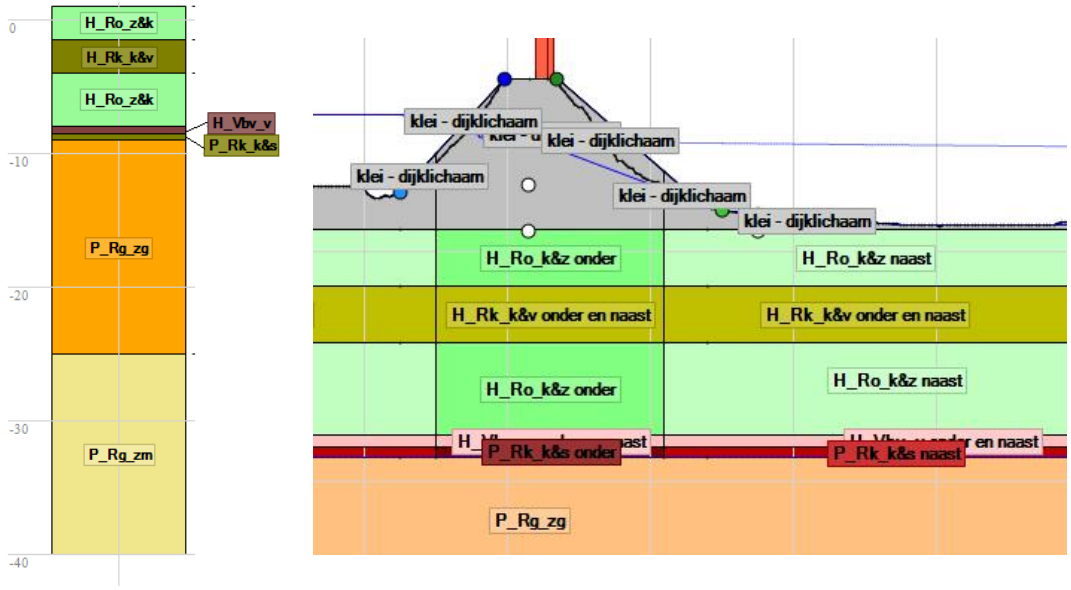

Figure C.2 Schematization

Material properties

Material properties for the soil types are taken from the WTI-SOS database. The distribution parameters for the random soil types are summed in the next table. This dataset already includes averaging from regional to local data and includes averaging along the slip plane.

The POP value for dijksmateriaal has a mean value of 30 kPa and a standard deviation of 10 kPa. For all the other materials, the POP is 25 kPa, standard deviation 7 kPa, according to the WTI-SOS database.

Table C.3 Material parameters

SOS-name	Soil type	deposit	Vol. weight	Su below		Su besides		Strength increase exp.	
				μ	σ	μ	σ		
H_aa_ht	Dijksmateriaal klei	Antropogeen	16 - 19	0.35	0.12	-	-	0.92	0.03
H_Ro_k&z	overwegend klei	Echteld	16 - 18	0.24	0.02	0.15	0.02	0.92	0.03
H_Rk_k&v	klei organisch (komklei)	Echteld	12 - 14	0.27	0.06	0.27	0.06	0.93	0.04
H_Vbv_v	veen mineraalarm	Nieuwkoop	10 - 11	0.37	0.05	0.37	0.05	0.89	0.03
P_Rk_k&s	klei zandig (rivier)	Kreftenheye	17 - 19	0.24	0.02	0.15	0.02	0.92	0.03
P_Rg_zg	zand	Pleistoceen	18 - 20	-	-	-	-	-	-

Waternet

The creation of phreatic lines is done by the Waternet Creator in D-Geo Stability, according to the following options.

Table C.4 Waternet Creator parameters

Option	Value
Creation method:	Create Waternet
Dike/soil material	Clay dike on clay
PL1 line creation method	Ringtoets WTI 2017

Since the MHW according to the new safety standards for this cross section is higher than the crest level, the MHW and water level distribution is “transposed” to a plausible value: 1,0 m below the crest. The decimate height and exceedance frequency are taken from the PC-Ring database:
h_{dec} = 0,565 m
$1/F_{exc}$ = 1/30000
MHW = 6,5 m

The average high outside water level GHW is taken as the water level at mean discharge for the river, NAP +1,23 m. The minimum phreatic line in the dike body is defined by the Dupuit water level: NAP +3,02 m. The polder water level is assumed to be at the inner toe of the dike.

For the PL3 and PL2 schematization, the leakage length is used. In this case back calculated from WTI Piping calculations. λ_{out} 465 m and λ_{polder} 1432 m.

The intrusion length is determined according to Schoofs en Van Duinen (2006). Based on the stratification and the duration of high water, the intrusion length is found to be 7,5 m. However, this length is larger than half the impermeable layer thickness; therefore this intrusion length is not realistic anymore. The intrusion length is taken as 0, so the phreatic line will be interpolated from PL3 to PL1.

Traffic load

A uniform load of 13kN/m2 over a width of 2,5 m is applied as temporary load for traffic in emergency situations.

Yield stress points

The yield stress points are defined at some “strategic” places. Since the POP values are the same for all sub-soil layers and is only different for dijksmateriaal, only 4 points are chosen.

Two points under the crest and two points under the toe. One in the dijksmateriaal-layer and one in the layer below. The yield stress value is defined at daily water level by the next equation $\sigma_y = \sigma'_{v,i} + POP$

Note 1: the yield stress points (white balls) are below the daily water level.
Note 2: the yield stress is dependent to the value of the POP. The vertical effective stress is not taken into account as stochastic parameter, but the POP is. Therefore, the standard deviation of the yield stress points is equal to the standard deviation of the POP (as fixed value, not as variation coefficient). Since the probabilistic prototype can yet only deal with a fixed standard deviation for yield stress, the value of 6 kPa is used for all yield stress points. Eventually, this may be checked in terms of influence coefficients.

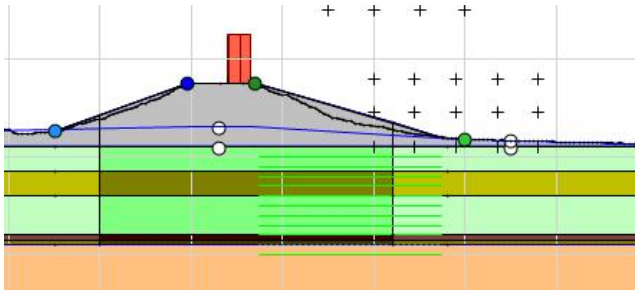

Figure C.3 Schematization yield stresses

Other information

Slip circle search method is Uplift-Van. The grid is predefined; the option “move grid” is checked. For the final design point it will be checked whether the critical slip circle is valid (centre point of active and passive circle not at the edge of the grid).

Uplift is not possible since the cover layer is thicker than 4 m.

Stability berms

In order to reach reliability numbers which are in the range of interest, stability berms are added. The material is the general “dijksmateriaal”. The berm length (measured as the total berm top width) is 0 for the basic geometry, 10, 15, 20, 25 and and 30 m.

C.2.2 Probabilistic prototype

Deterministic sanity check Automatic critical slip surface definition

Mean values

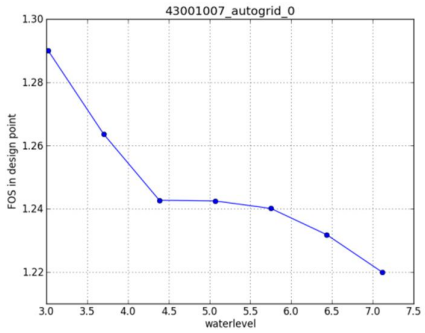

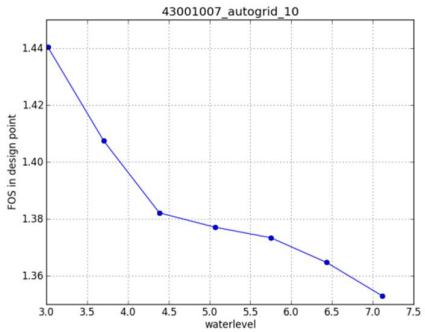

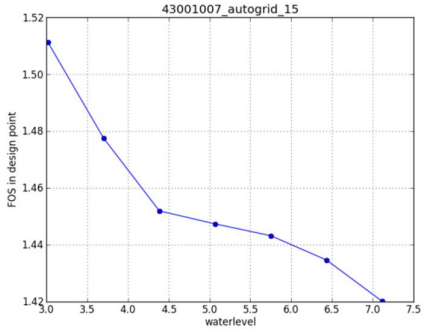

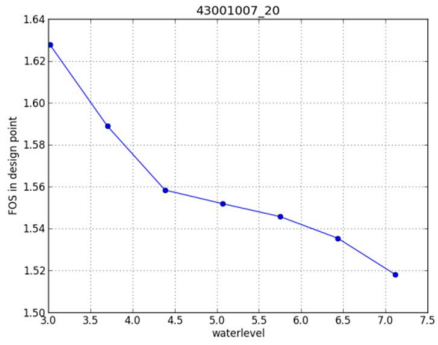

Characteristic values

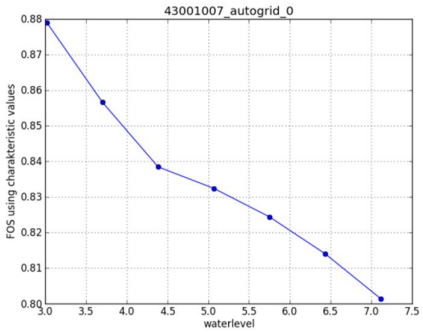

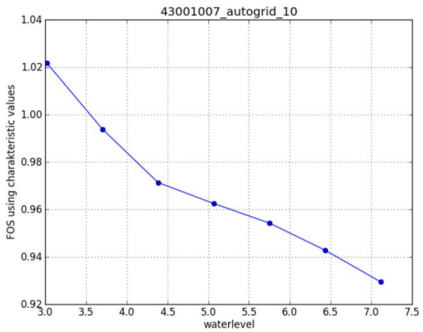

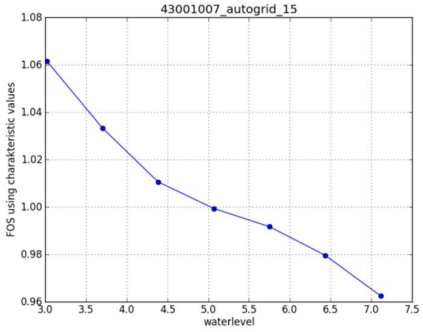

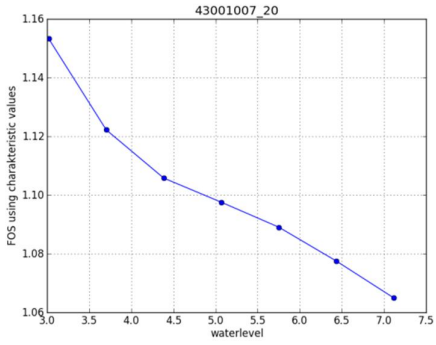

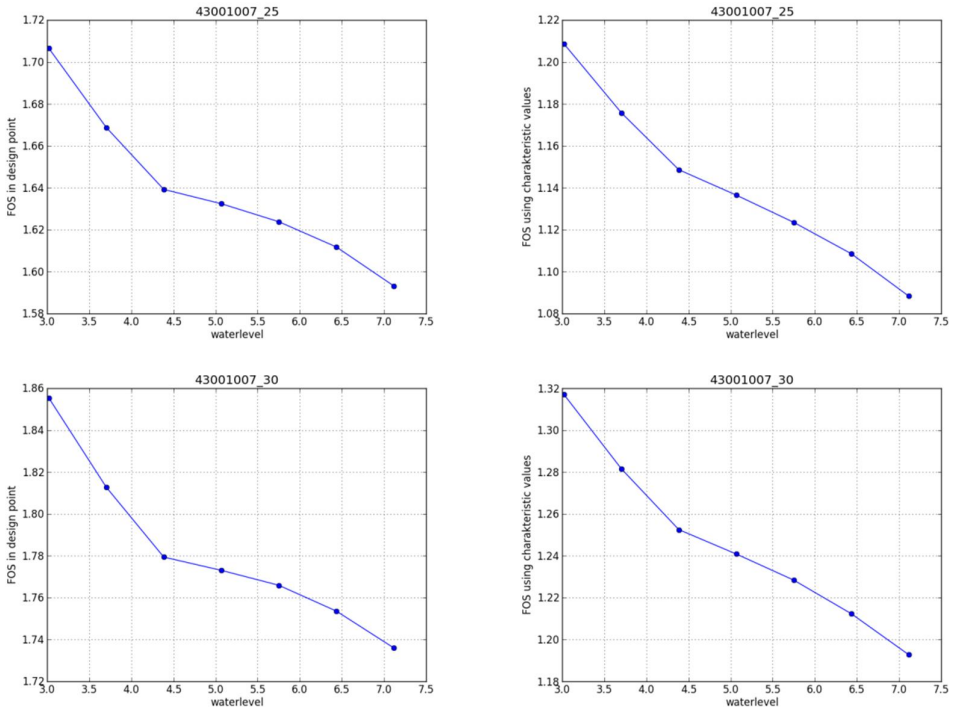

Figure C.4 Output case 43001007

Probabilistic fragility curve (Max_beta_interation_inner_loop = 0.05)
It should be noted that case 43001007_20 shows a small increase in reliability index, likely due to numerical inaccuracies.

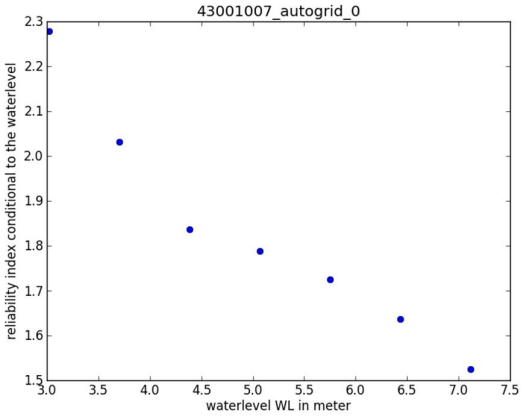

	dp	alpha^2
beta final	1.92	
SF char	0.815	
CuPc		0.752
m		0.003
yieldstress		0.128
cohesion		0.000
fric angle		0.000
model fac	1.026	0.109
water level	4.11	0.007

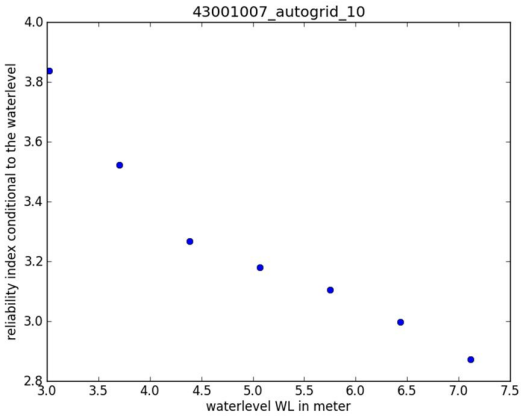

	dp	alpha^2
beta final	3.37	
SF char	0.940	
CuPc		0.661
m		0.004
yieldstress		0.179
cohesion		0.000
fric angle		0.000
model fac	1.048	0.142
water level	4.19	0.015

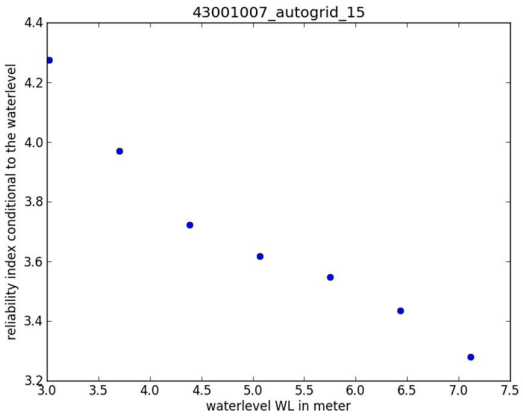

	dp	alpha^2
beta final	3.82	
SF char	0.980	
CuPc		0.672
m		0.004
yieldstress		0.172
cohesion		0.000
fric angle		0.000
model fac	1.053	0.138
water level	4.21	0.014

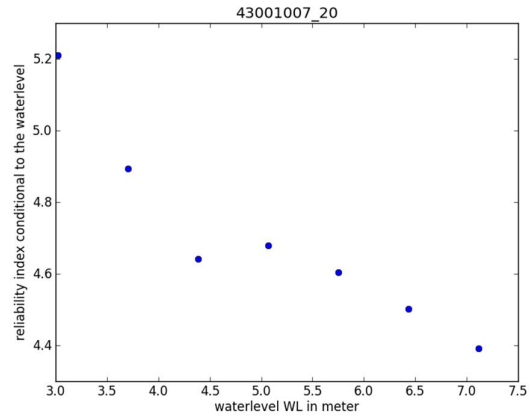

	dp	alpha^2
beta final	4.73	
SF char	1.085	
CuPc		0.647
m		0.003
yieldstress		0.198
cohesion		0.000
fric angle		0.000
model fac	1.064	0.136
water level	4.26	0.017

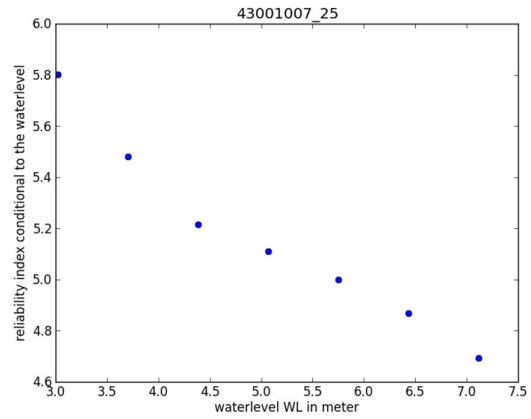

	dp	alpha^2
beta final	5.30	
SF char	1.120	
CuPc		0.665
m		0.003
yieldstress		0.164
cohesion		0.000
fric angle		0.000
model fac	1.074	0.147
water level	4.32	0.021

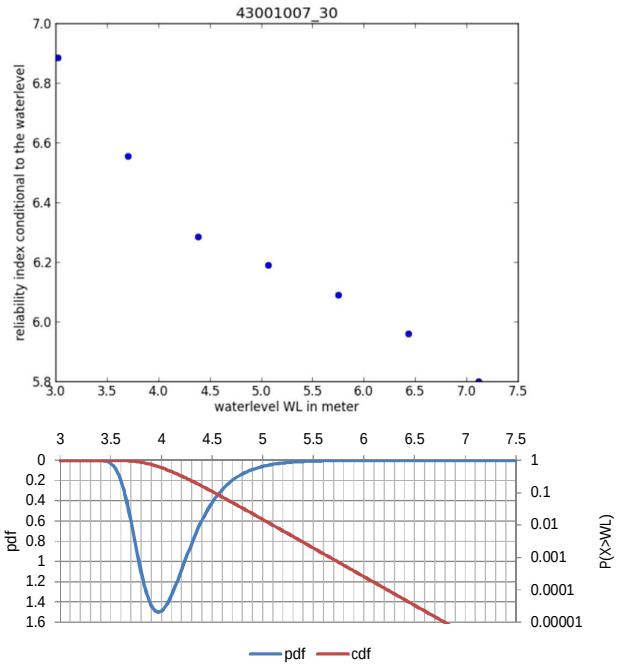

	dp	alpha^2
beta final	6.35	
SF char	1.210	
CuPc		0.648
m		0.003
yieldstress		0.172
cohesion		0.000
fric angle		0.000
model fac	1.090	0.152
water level	4.38	0.025

Figure C.5 Output case 43001007

Cumulative alpha values conditional to the water level

Basic geometry

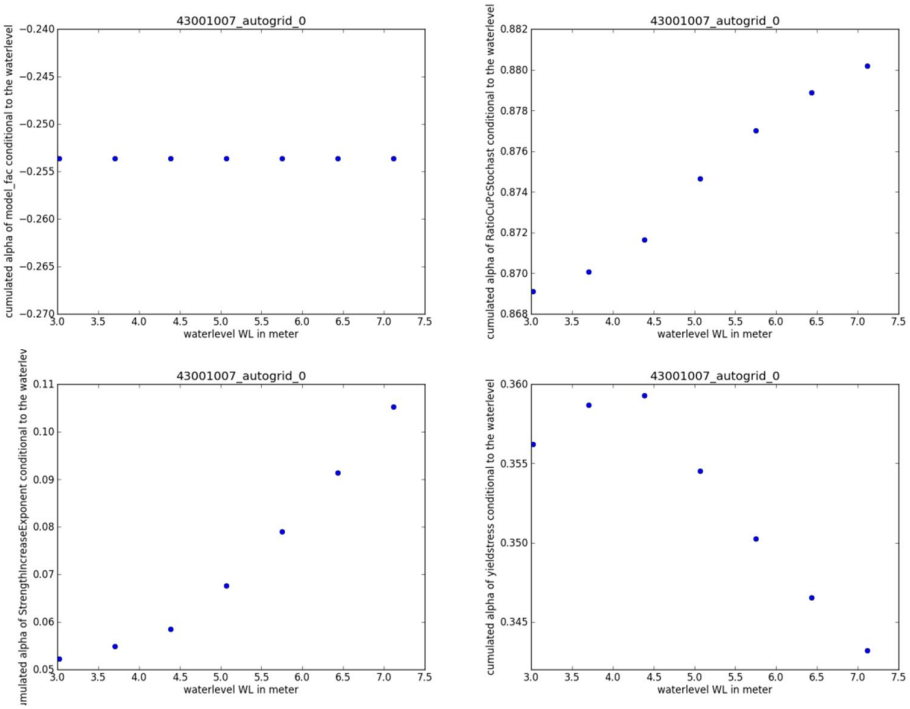

Basic geometry + 10m berm

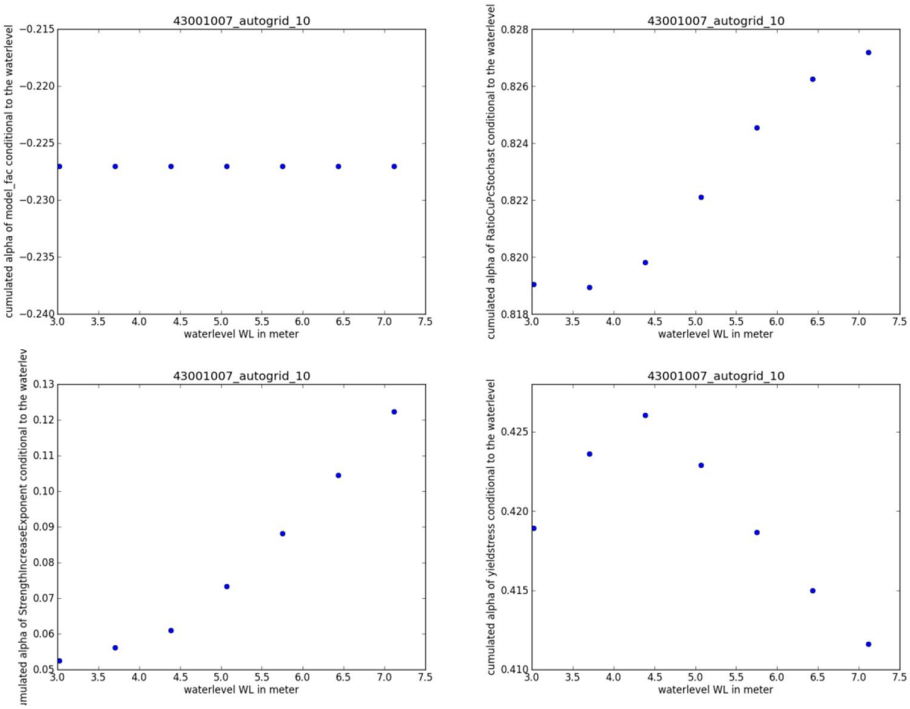

Figure C.6 Output case 43001007

Basic geometry + 15m berm

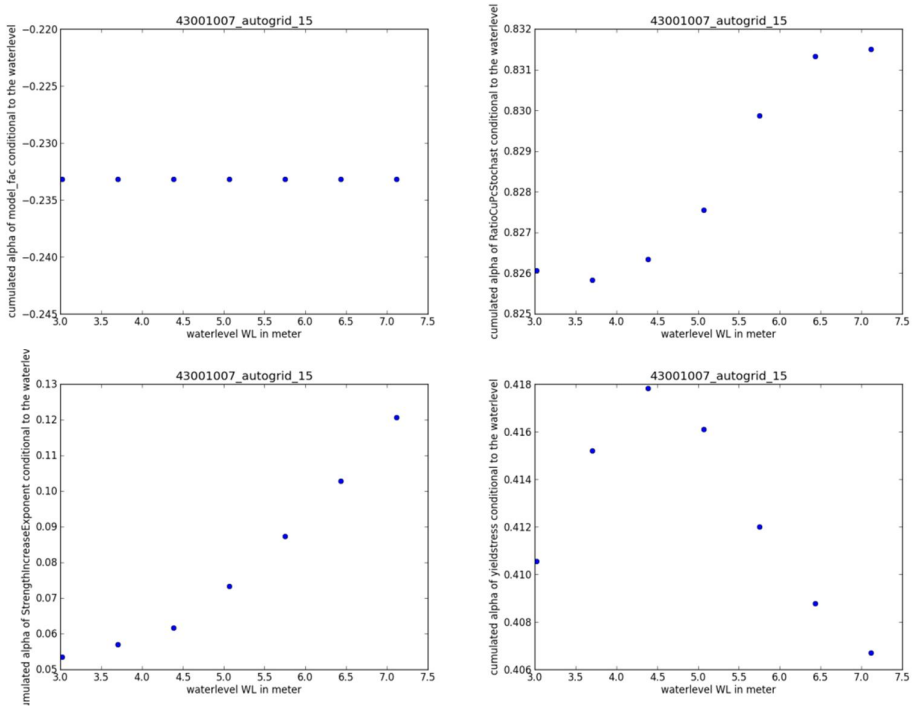

Figure C.7 Output case 43001007

Basic geometry + 20m berm

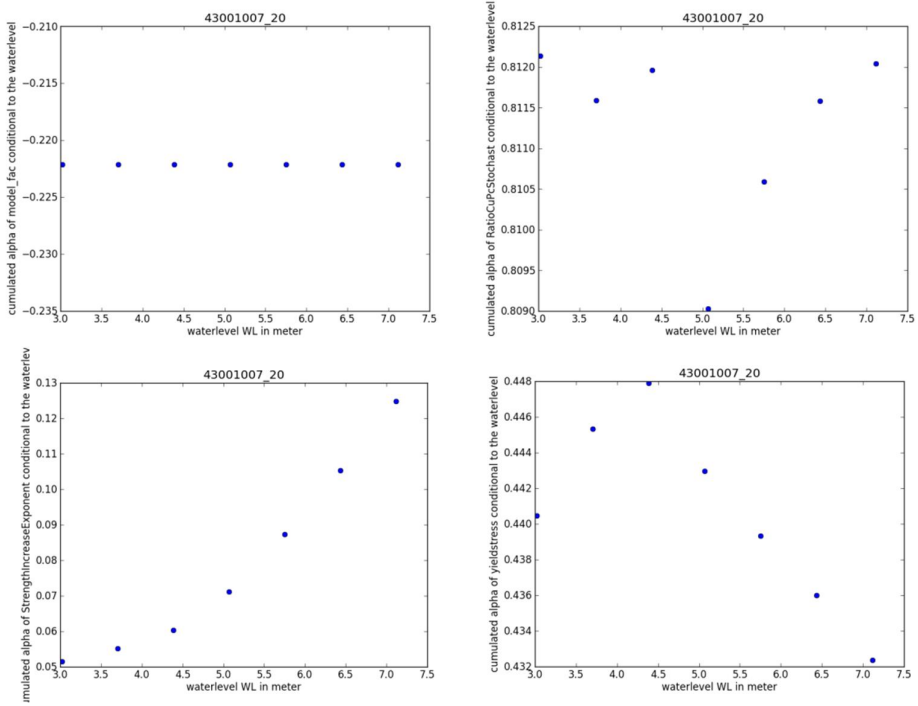

Figure C.8 Output case 43001007

Basic geometry + 25m berm

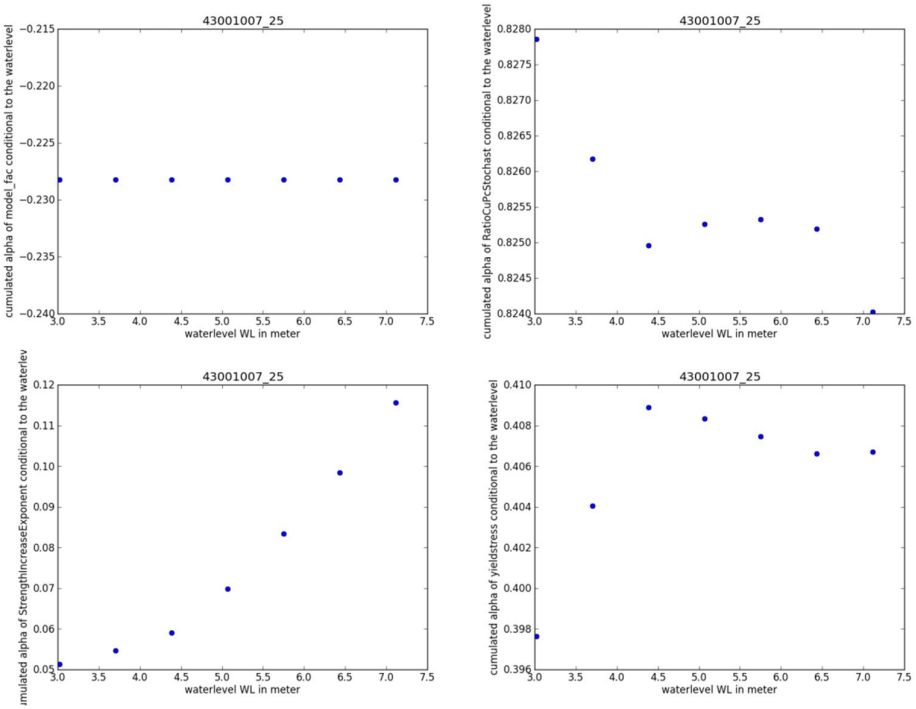

Figure C.9 Output case 43001007

Basic geometry + 30m berm

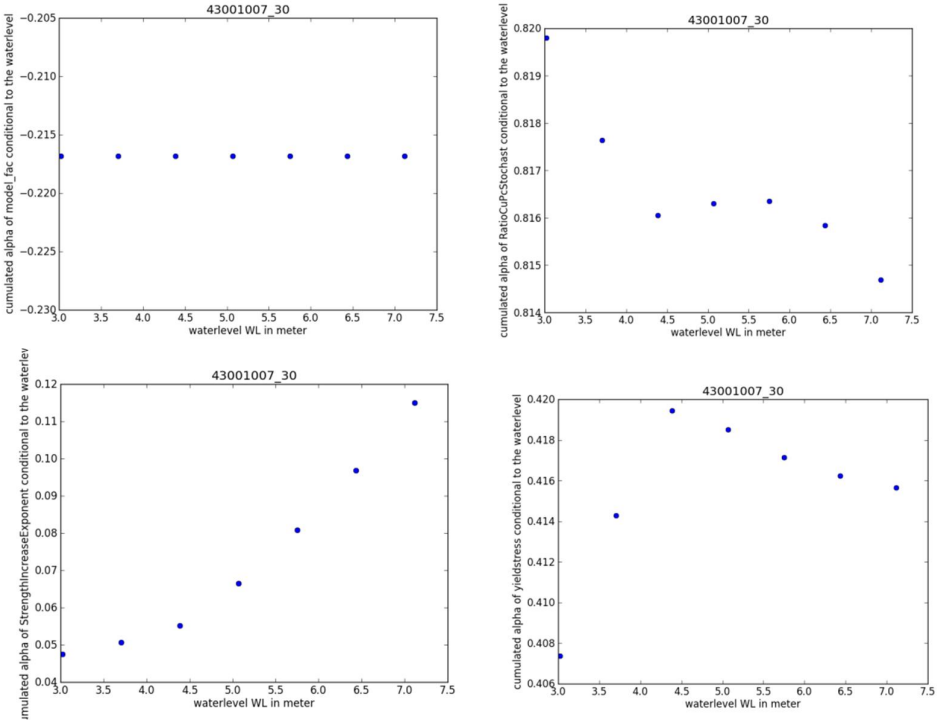

Figure C.10 Output case 43001007

Slip circle in design point

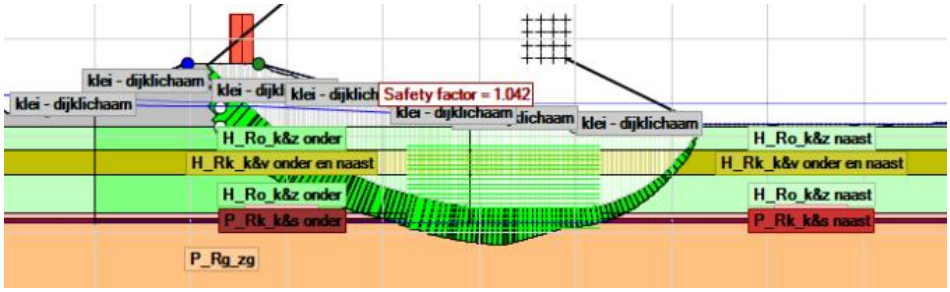

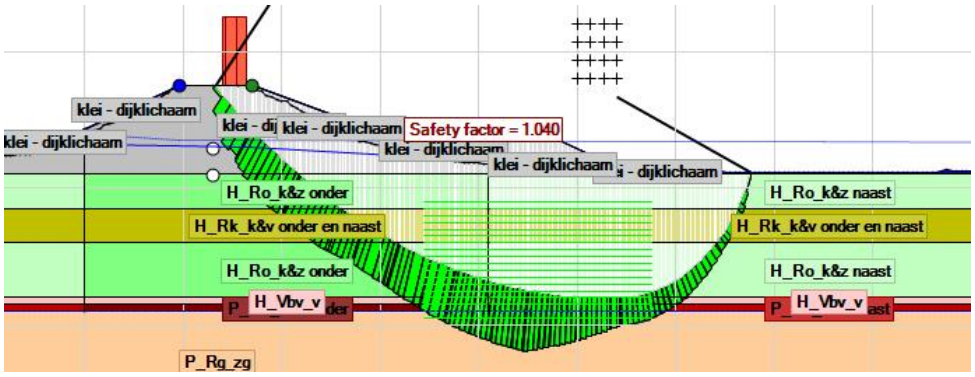

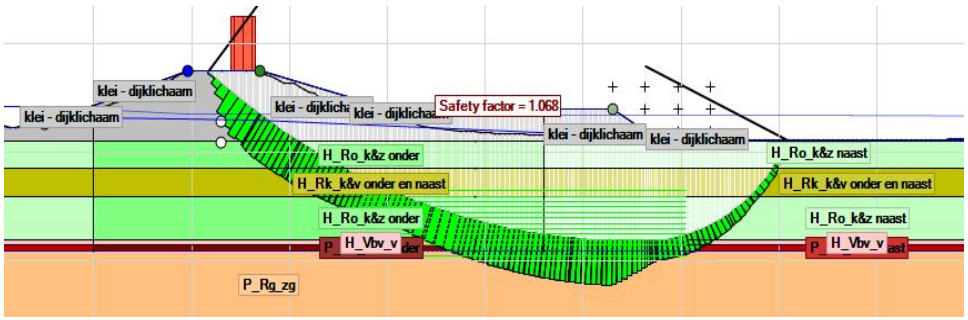

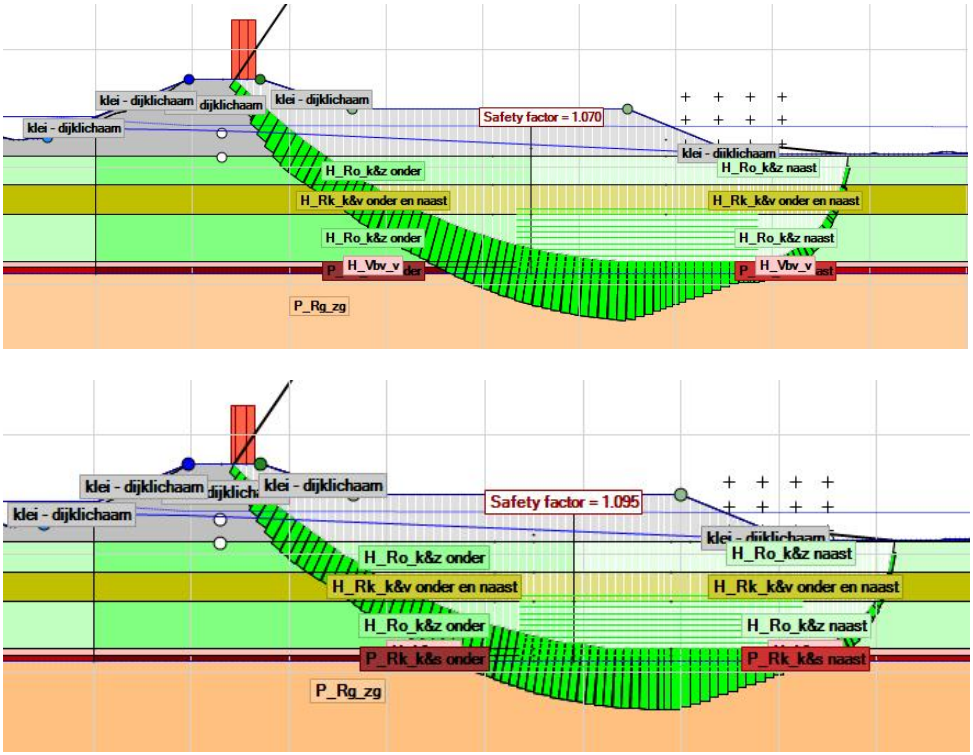

Figure C.11 Slip circle in the design point

C.3 Dp_190

This section describes the steps and decisions made in setting up and performing deterministic and probabilistic calculations for slip failure of the inner slope for a specific cross section. Furthermore it summarizes the results for this case.

C.3.1 Setup

Location and geometry

The location of this cross section (VNK: 16.AW190.198, PC-Ring ID 16003028) is at the Lek, near Streefkerk. The surfaceline and stratification is from a calculation made for a specific study. The data gathered (soil investigation, laboratory tests, CPTs) during this specific investigation a couple of years ago were used. A figure of the stratification is shown below.

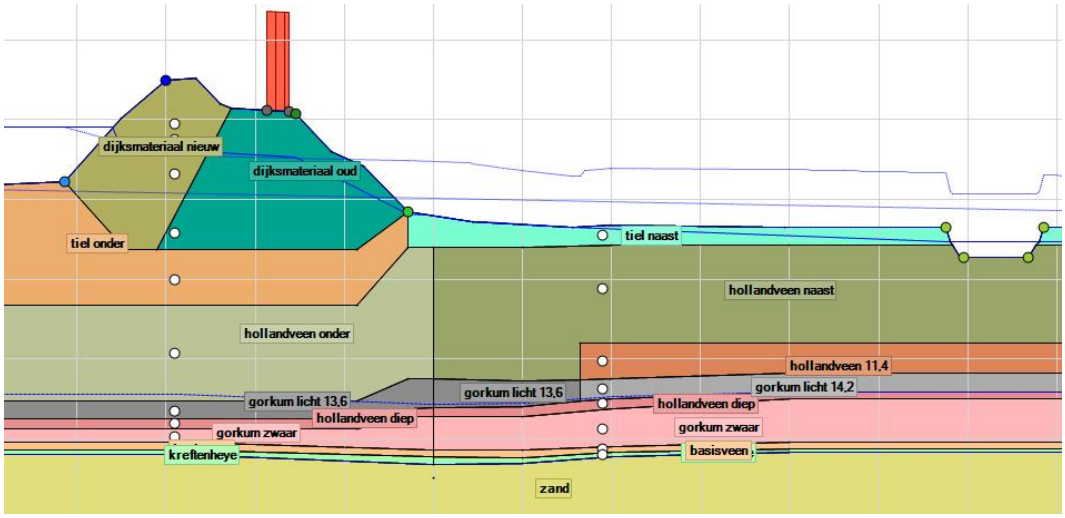

Figure C.12 Schematization

Material properties

Table C.5 Material parameters

Soil type	Vol. weight			Su ratio		Strength increase exp.	
		μ	σ	μ	σ	μ	σ
zand	20/18	35	5.25				
kreftenheye	18/18			0.24	0.10	0.9	0.02
basisveen	11/11			0.31	0.01	0.9	0.02
gorkum zwaar	15.6/15.6			0.24	0.01	0.9	0.02
hollandveen diep	10/10			0.37	0.07	0.9	0.02
gorkum licht 13,6	13.6/13.6			0.3	0.04	0.9	0.02
gorkum licht 14,2	14.2/142			0.3	0.04	0.9	0.02
hollandveen onder	11.8/11.8			0.3	0.07	0.9	0.02
hollandveen naast	10.2/10.2			0.37	0.07	0.9	0.02
hollandveen 171,4	11.4/11.4			0.3	0.07	0.9	0.02
tiel onder	14/14			0.26	0.11	0.9	0.02
tiel naast	15.6/15.6			0.26	0.11	0.9	0.02
dijksmateriaal oud	18/18			0.35	0.06	0.9	0.02
dijksmateriaal nieuw	19.3/19.3			0.35	0.06	0.9	0.02

Waternet

The creation of phreatic lines is done by D-Geo Stability, according to the following options.

Table C.6 Waternet Creator parameters

Option	Value
Creation method:	Create Waternet
Dike/soil material	Clay dike on clay
PL1 line creation method	Ringtoets WTI 2017

The decimate height and exceedance frequency are taken from the old available data from the sti file.
h_{dec} = 0,20 m
$1/F_{exc}$ = 1/2000
MHW = 3,4 m

The average high outside water level GHW is taken as the water level at mean discharge for the river, taken from the original sti file NAP +0,5 m. The minimum phreatic line in the dike body is defined by the Dupuit water level: NAP +0,69 m. The polder water level is NAP -2,1m. For the PL3 and PL2 schematization, the leakage length is used. In this case taken as λ_{out} 760 m and λ_{polder} 1440 m. The intrusion length is 3,0m.

Traffic load

A uniform load of 13kN/m2 over a width of 2,5 m is applied as temporary load for traffic in emergency situations.

Yield stress points

Yield stresses are defined along two vertical lines where CPT measurement are located. Yield stresses are derived from an empirical relation from q_c.

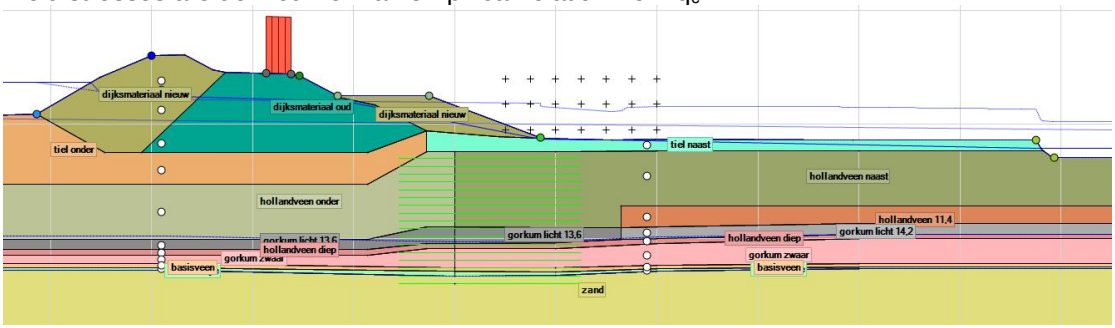

Figure C.13 Schematization yield stresses

Other information

Slip circle search method is Uplift-Van. The grid is predefined; the option “move grid” is checked. For the final design point it will be checked whether the critical slip circle is valid (centre point of active and passive circle not at the edge of the grid).

Stability berms

In order to reach reliability numbers which are in the range of interest, stability berms are added. The material is the general “dijksmateriaal nieuw”. The berm length (measured as the total berm top width) is 0 for the basic geometry, 10, 20 and 30 m.

C.3.2 Probabilistic prototype results

Dp_190_0 shows non-monotonous behaviour, likely due to the very low reliability index.

Deterministic sanity check with automatic critical slip surface definition

Mean values | Characteristic values

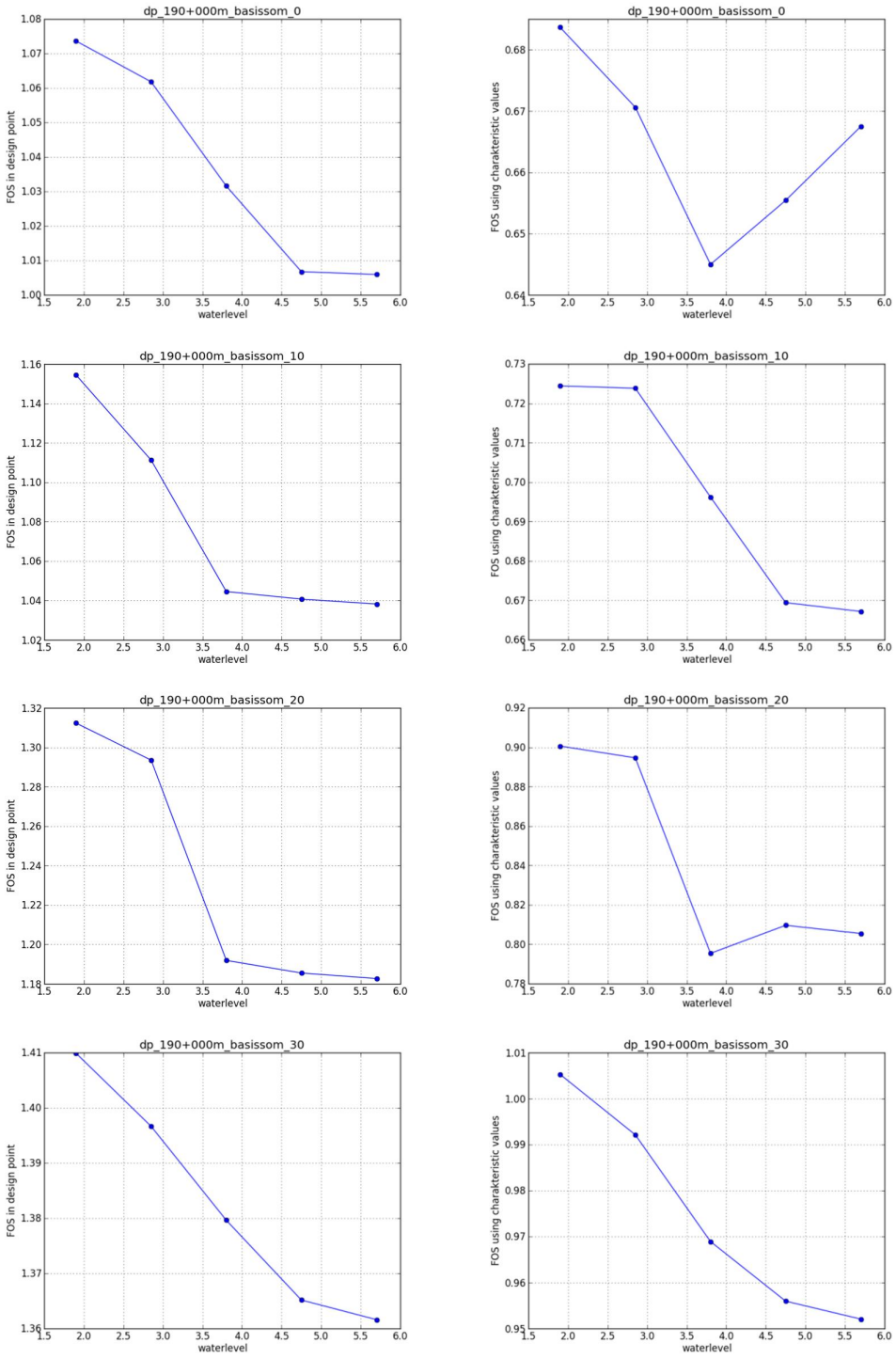

Figure C.14 Output case dp_190

Probabilistic fragility curve (Max_beta_interation_inner_loop = 0.05)
Automatic critical slip surface definition

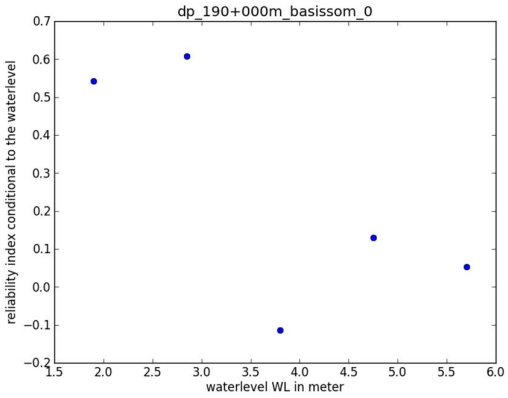

	dp	alpha^2
beta final	0.60	
SF char	0.655	
CuPc		0.808
m		0.017
yieldstress		0.066
cohesion		0.000
fric angle		0.000
model fac	1.012	0.108
water level	2.77	0.000

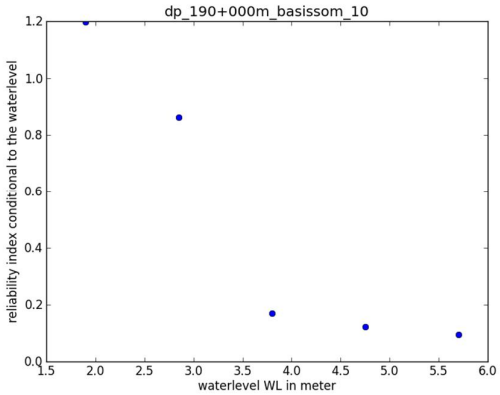

	dp	alpha^2
beta final	0.89	
SF char	0.705	
CuPc		0.753
m		0.014
yieldstress		0.077
cohesion		0.000
fric angle		0.000
model fac	1.017	0.154
water level	2.78	0.002

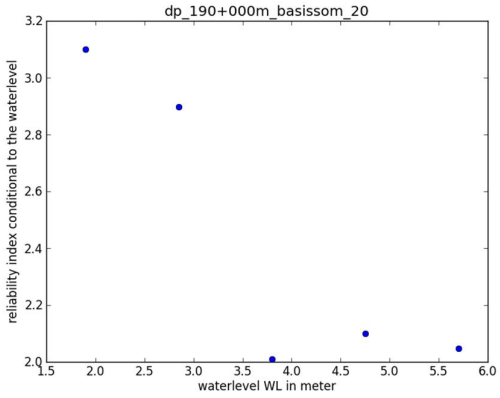

	dp	alpha^2
beta final	2.91	
SF char	0.830	
CuPc		0.569
m		0.019
yieldstress		0.231
cohesion		0.000
fric angle		0.000
model fac	1.047	0.181
water level	2.78	0.000

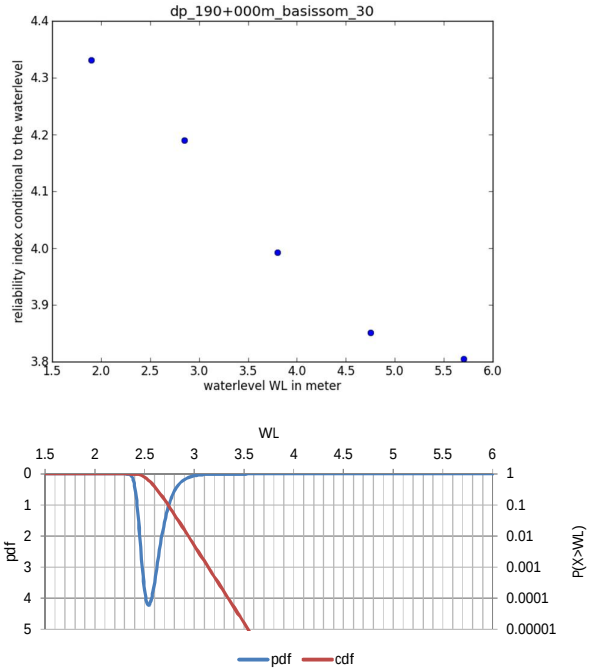

	dp	alpha^2
beta final	4.20	
SF char	0.975	
CuPc		0.558
m		0.015
yieldstress		0.211
cohesion		0.000
fric angle		0.000
model fac	1.072	0.216
water level	2.78	0.000

Figure C.15 Output case dp_190

Cumulative alpha values conditional to the water level

Basic geometry

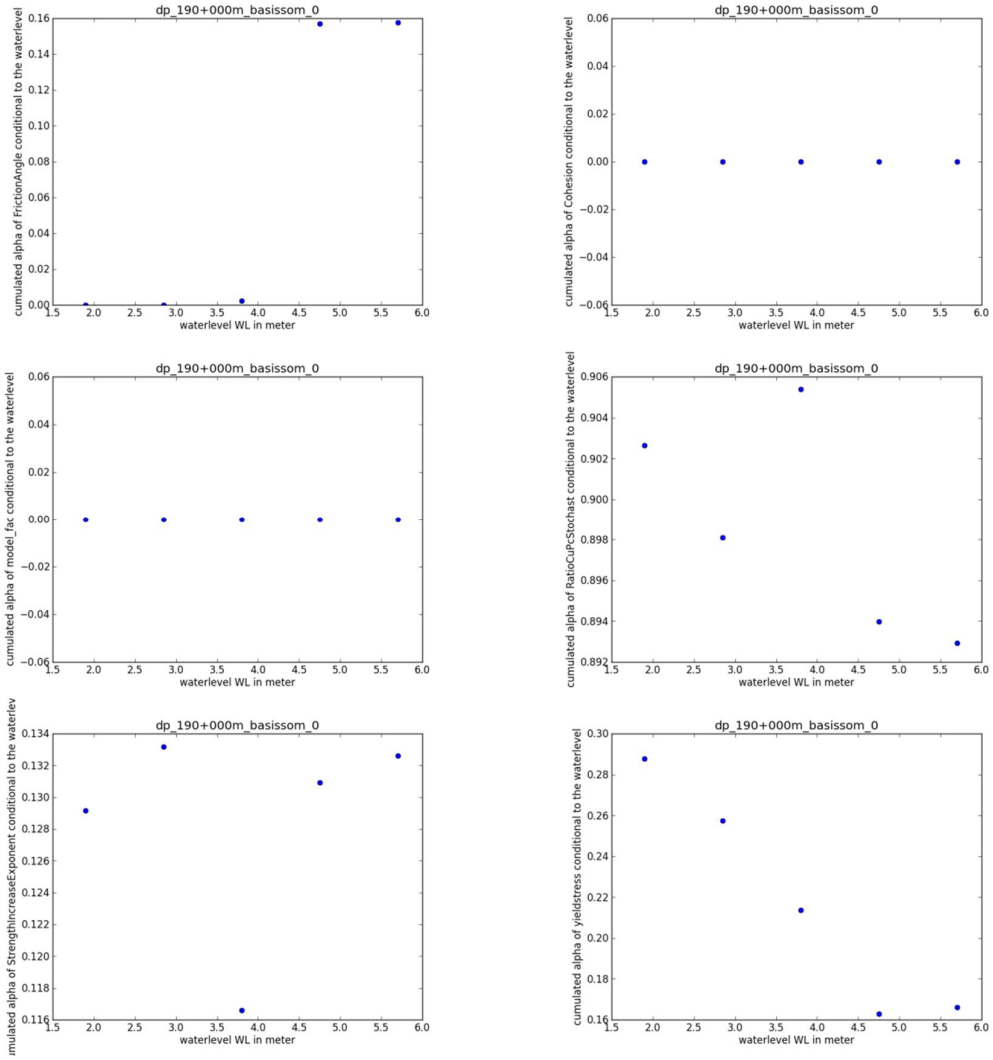

Figure C.16 Output case dp_190

Basic geometry + 10m berm

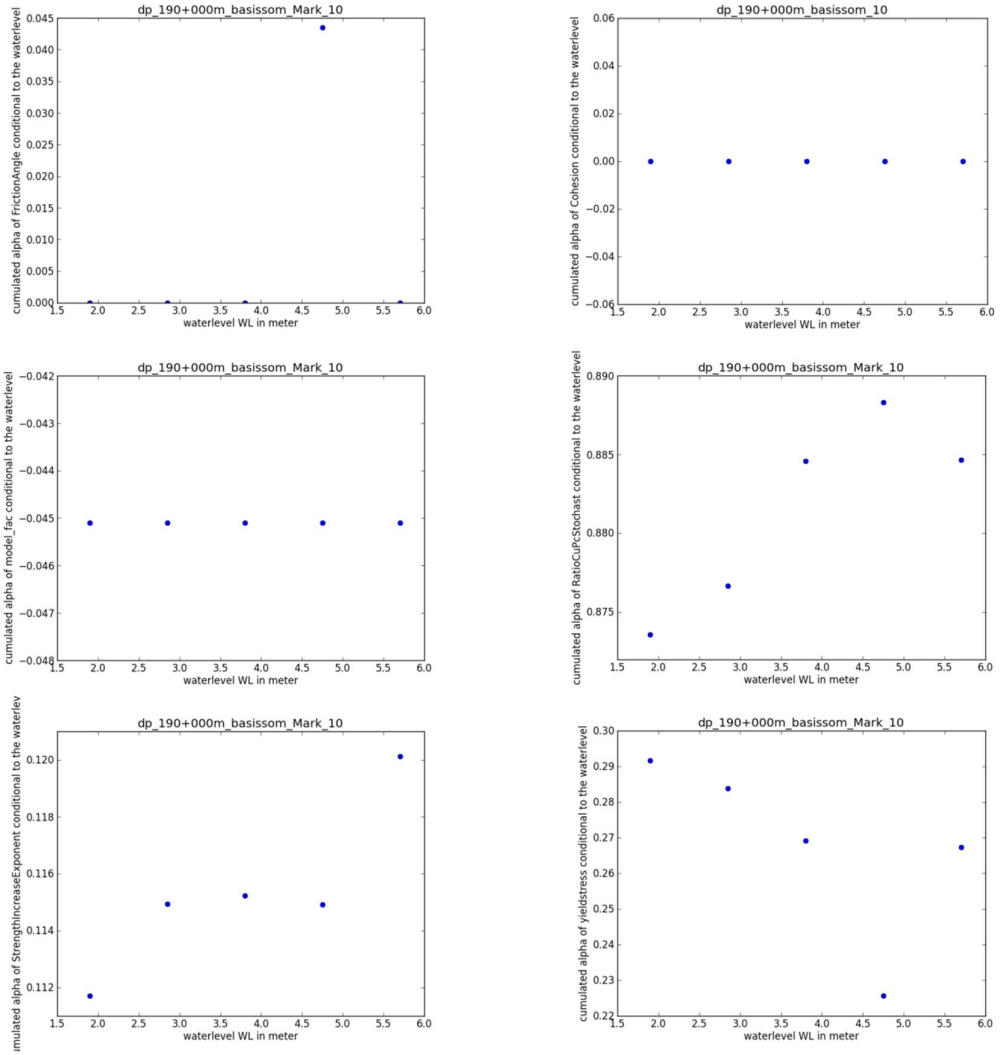

Figure C.17 Output case dp_190

Basic geometry + 20m berm

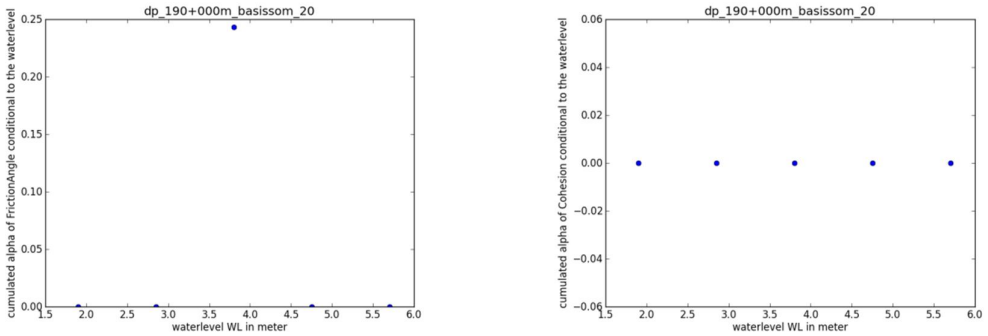

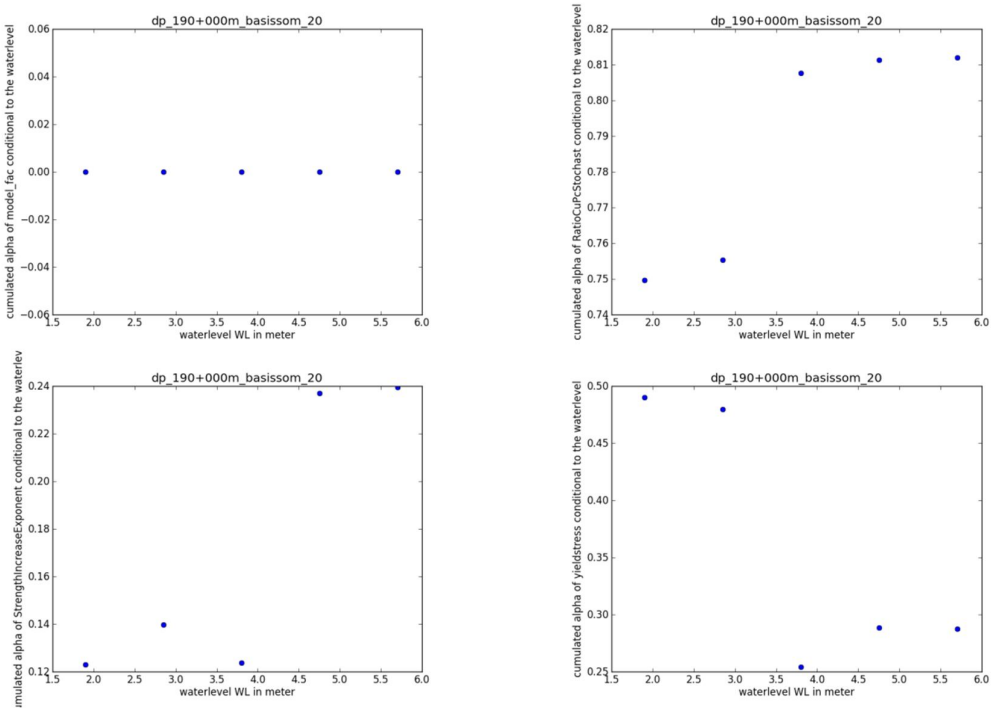

Figure C.18 Output case dp_190

Basic geometry + 30m berm

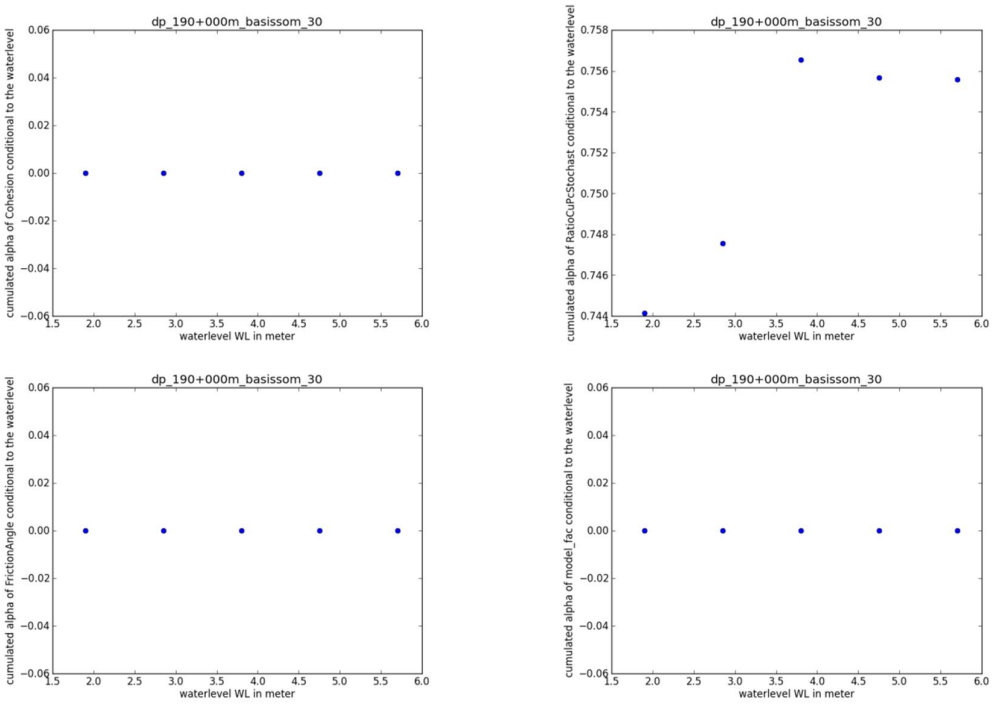

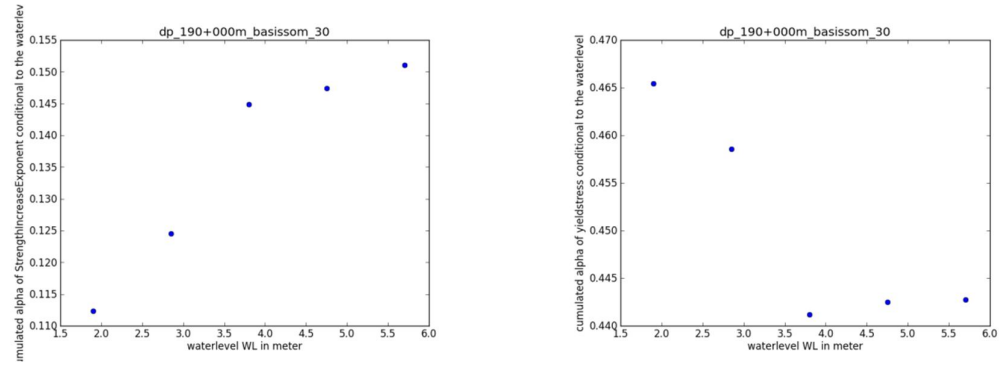

Figure C.19 Output case dp_190

Slip circles in the design point

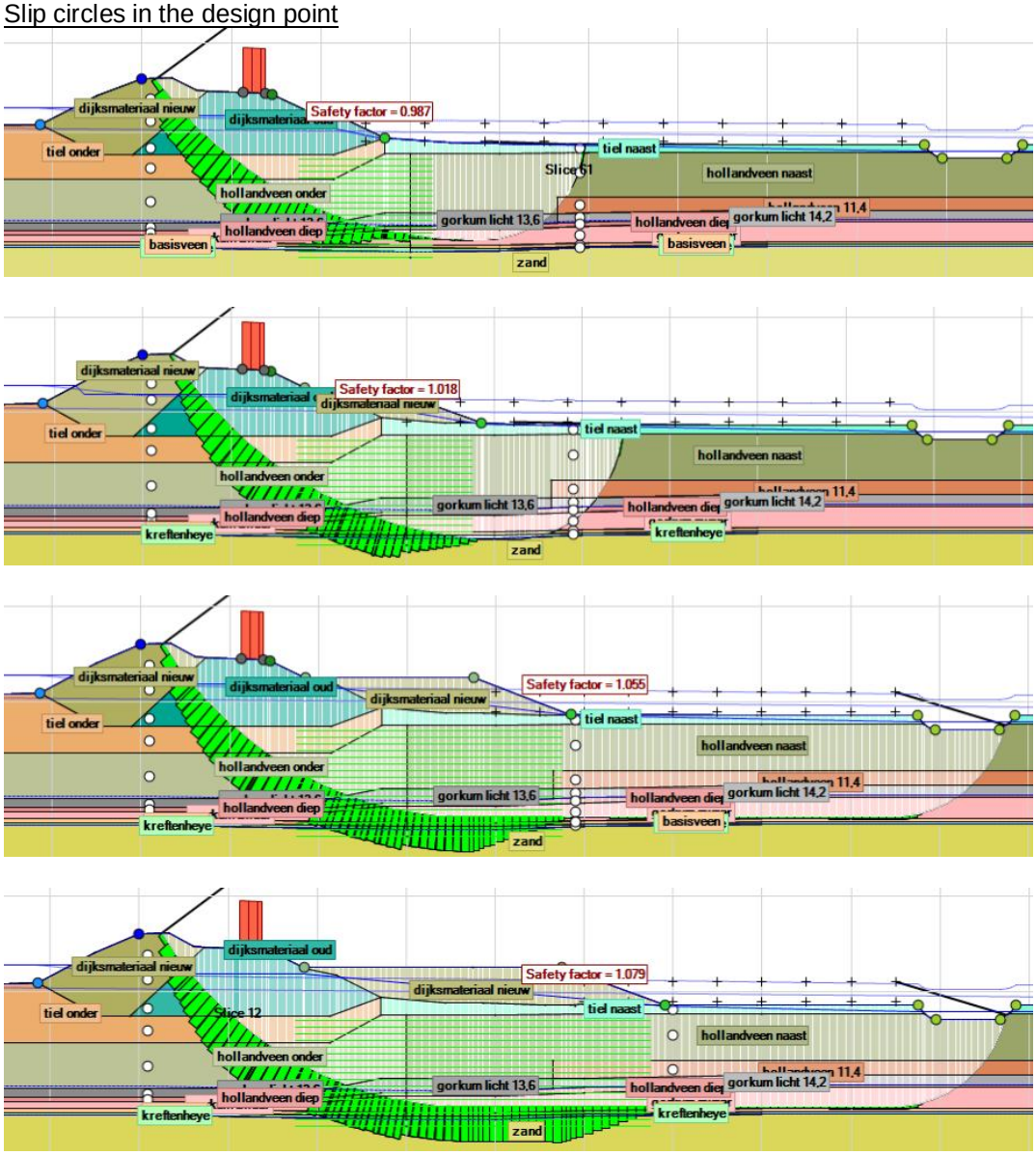

Figure C.20 Slip circle in the design point

C.4 41_W_237

This appendix describes the steps and decisions made in setting up and performing probabilistic calculations for slip failure of the inner slope for a specific cross section. Furthermore it summarizes the intermediate results for this case.

C.4.1 Setup

Location and geometry

The cross section (VNK: 41_Waal_Dp237_0_Mean_sce_1, PC-Ring ID 41003039) is part of dike ring 41. The surface line is taken form AHN.

Material properties

This cross section was used in the VNK-2 calibration and in the preliminary undrained macro stability calibration, see Table C.5

TableC.7 Material parameters

	unit weight						
Name	saturated	unsaturated		cohesion	friction angle	strength increase exponent	Su/Pc
	kN/m^3	kN/m^3		kN/m^2	degree	-	-
WL_zandondergrond	19	17	drained	0	34.58		
achter dijk - Ks2	15.6	15.6	undrained			0.9	0.23
voor dijk - Ks2	16.3	16.3	undrained			0.9	0.21
onder dijk - Ks2	16.6	16.6	undrained			0.9	0.21
dijklichaam	19.1	19.1	undrained			0.9	0.45
dijksmateriaal_klei	17	17	drained	1	35		

The creation of phreatic lines is done in D-Geo Stability, using the following options.

TableC.8 Material parameters

Option	Value
Creation method:	Create Waternet
Dike/soil material	Clay dike on clay
PL1 line creation method	Ringtoets WTI 2017

MHW, decimate height h_{dec} and exceedance frequency $1/F_{exc}$ are taken from the PC-Ring database:

MHW = 12.791 m
h_{dec}= 0.729 m
$1/F_{exc}$ = 1/10000

The average high outside water level GHW is taken as the water level at mean discharge for the river, NAP +5.37 m. The minimum phreatic line in the dike body is defined by the Dupuit water level: NAP +10.53 m. The polder water level is assumed to be at the inner toe of the dike.

For the PL3 and PL2 schematization, the leakage length is used. In this case back calculated from WTI Piping calculations. λ_{out} =112.92 m and λ_{polder} =1184.32 m.

The intrusion length is determined according to Schoofs en Van Duinen (2006). Based on the stratification and the duration of high water, the intrusion length is found to be 7,5 m. However, this length is larger than half the impermeable layer thickness; therefore this intrusion length is not realistic anymore. The intrusion length is taken as 0, so the phreatic line will be interpolated from PL3 to PL1.

Traffic load

A uniform load of 13kN/m^2 over a width of 2,5 m is applied as temporary load for traffic in emergency situations.

Yield stress points

The yield stress points are defined at some “strategic” places. Since the POP values are the same for all sub-soil layers and is only different for dijksmateriaal, only 5 points are chosen. Two points under the crest and two points under the toe. One in the dijksmateriaal-layer and one in the layer below. The yield stress value is defined at daily water level by the next equation $\sigma_y = \sigma'_{v,i} + POP$

Note 1: the yield stress points (white balls) are below the daily water level.
Note 2: the yield stress is dependent to the value of the POP. The vertical effective stress is not taken into account as stochastic parameter, but the POP is. Therefore, the standard deviation of the yield stress points is equal to the standard deviation of the POP (as fixed value, not as variation coefficient). Since the probabilistic prototype can yet only deal with a fixed standard deviation for yield stress, the value of 6 kPa is used for all yield stress points.

no berm *10 m berm*

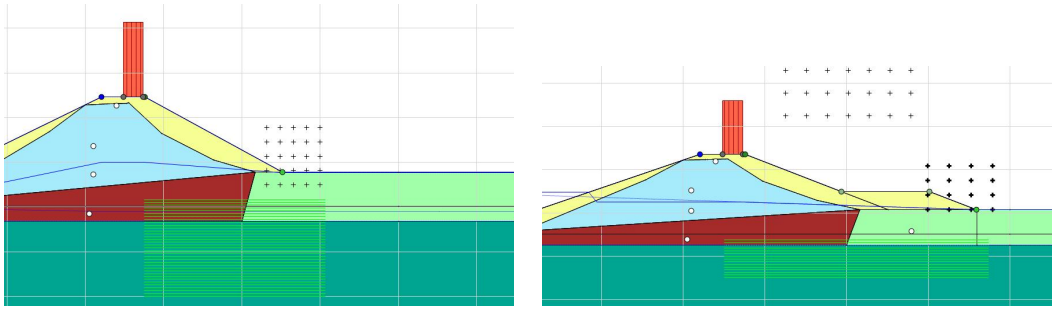

Figure C.21 Schematization yield stress

Other information

Slip circle search method is Uplift-Van. The grid is predefined; the option “move grid” is checked. For the final design point it will be checked whether the critical slip circle is valid (centre point of active and passive circle not at the edge of the grid).

No reduction of c-phi in case uplift potential n < 1,199
Full reduction of c-phi in case uplift potential n > 1,200

Stability berms

In order to reach reliability numbers which are in the range of interest, stability berms are added. The material is the general “dijksmateriaal”. The berm length (measured as the total berm top width) is 0 for the basic geometry, 10 m and 20 m.

C.4.2 Probabilistic prototype

deterministic sanity check

The critical slip plane has to be selected manually to be sure that the results are correct. This is done using mean values and characteristic values. It must be noted that ite_3 shows a slight increase of FoS with water level. However, this is only a very limited increase (1.553 to 1.559 and can be attributed to numerical approximations.

With mean values

Basic geometry

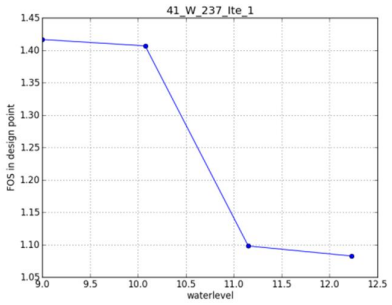

with characteristic values

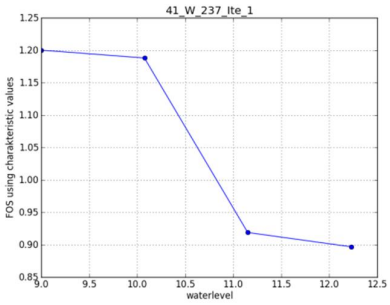

Basic geometry + 5 m berm

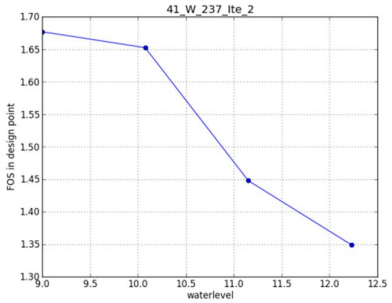

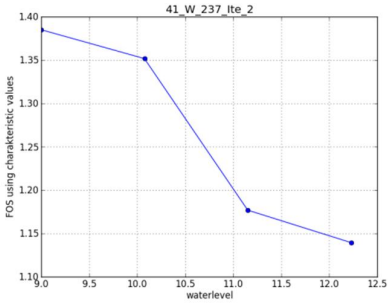

Basic geometry + 10 m berm

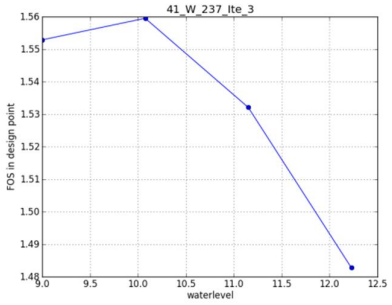

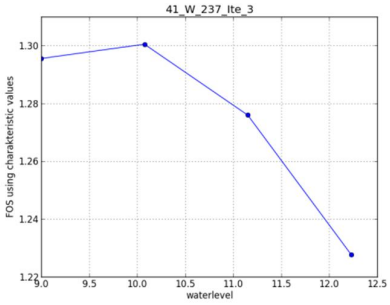

Figure C.22 Output case 41_W_237

Probabilistic fragility curve + metamodel results
Max_beta_interation_inner_loop = 0.05

Basic geometry + no berm

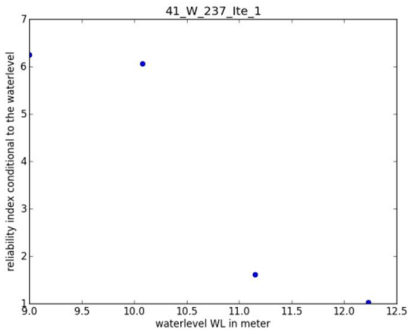

Stochast	dp	alpha	alpha^2
CuPc		0.462	0.213
m		0.172	0.030
yieldstress		0.592	0.351
cohesion		0.000	0.000
friction angle		0.047	0.002
model fac	1.03	5.45E-01	0.297
water level	11.16	0.327	0.107

beta	**2.06E+00**
gamma_characteristic = FOS_char(MHW)	0.89

Basic geometry + 5 m berm

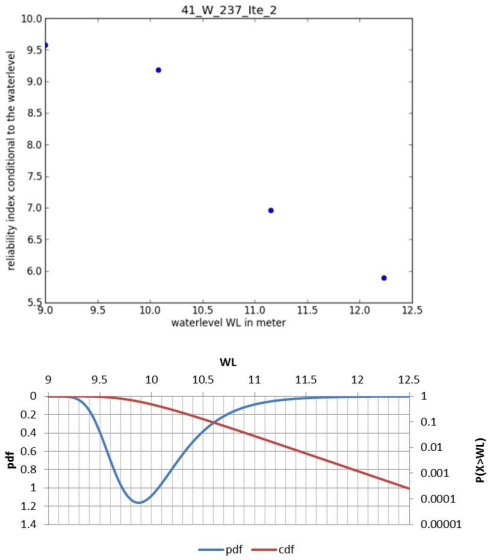

Stochast	dp	alpha	alpha^2
CuPc		0.214	0.046
m		0.112	0.013
yieldstress		0.200	0.040
cohesion		0.000	0.000
friction angle		0.244	0.060
model fac	1.05	2.38E-01	0.056
water level	10.00	0.886	0.785

beta	**5.50E+00**
gamma_characteristic = FOS_char(MHW)	1.14
FOS_char(DP)	1.35

Figure C.23 Output case 41_W_237

Basic geometry + 10 m berm

Stochast	dp	alpha	alpha^2
CuPc		0.582	0.339
m		0.051	0.003
yieldstress		0.565	0.320
cohesion		0.000	0.000
friction angle		0.000	0.000
model fac	1.15	5.82E-01	0.338
water level	10.01	0.016	0.000

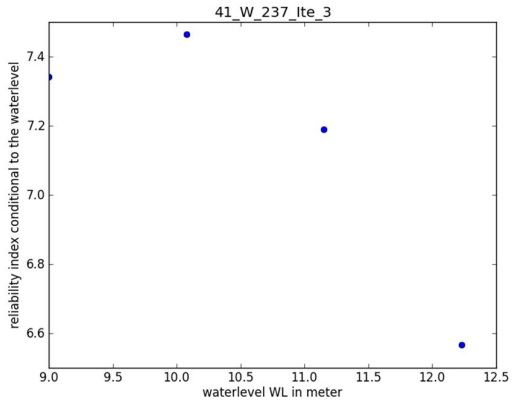

beta	7.45E+00
gamma_characteristic = FOS_char(MHW)	1.14
FOS_char(DP)	1.275

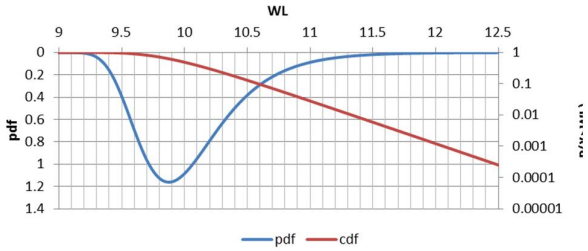

Figure C.24 Output case 41_W_237

Metamodel results

Basic geometry + no berm

CuPc

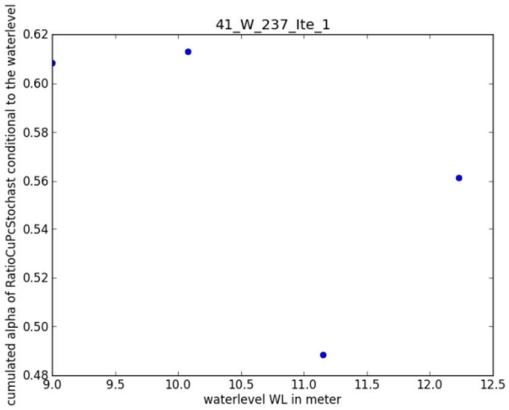

m

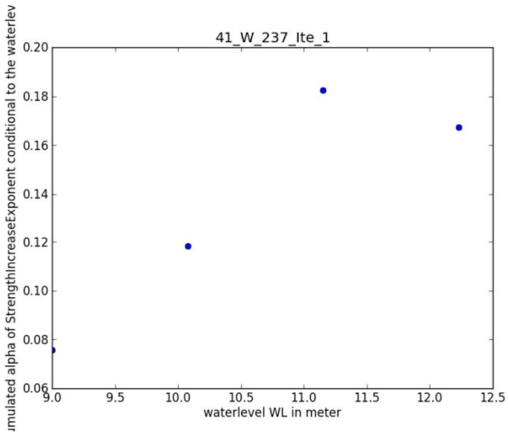

yield stresss

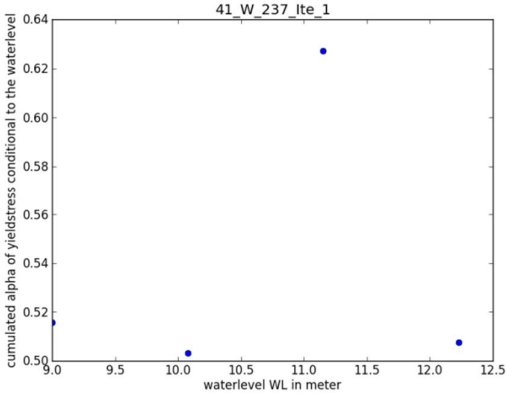

model factor

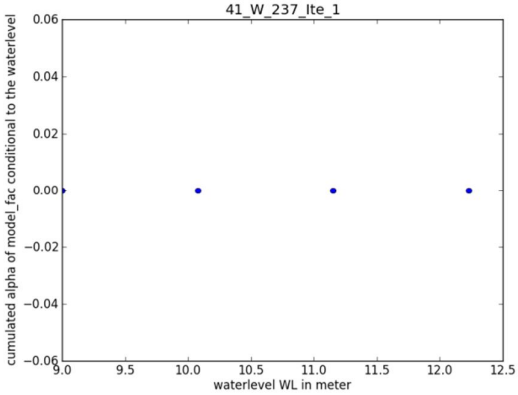

friction angle

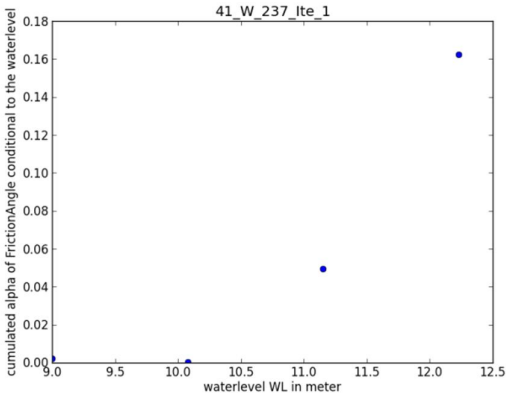

Figure C.25 Output case 41_W_237

5 m berm

CuPc

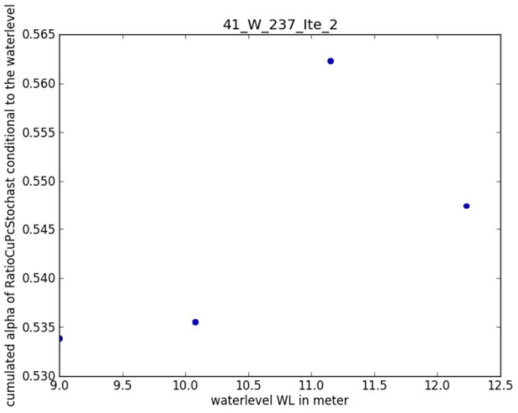

m

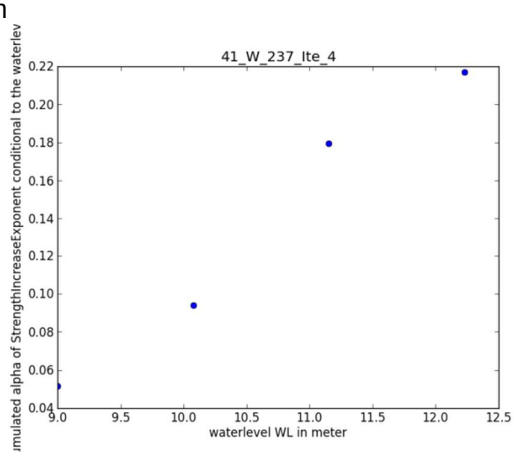

yield stress

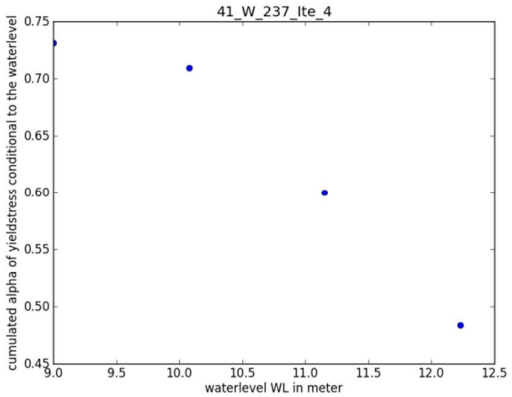

model factor

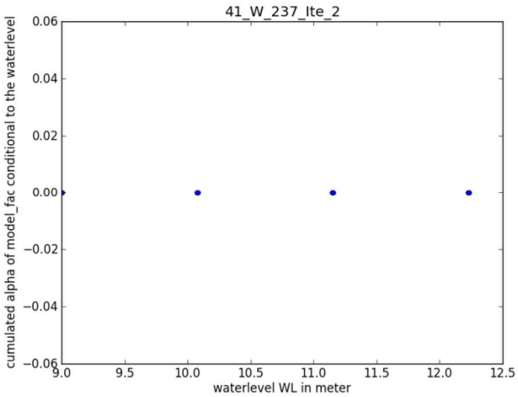

friction angle

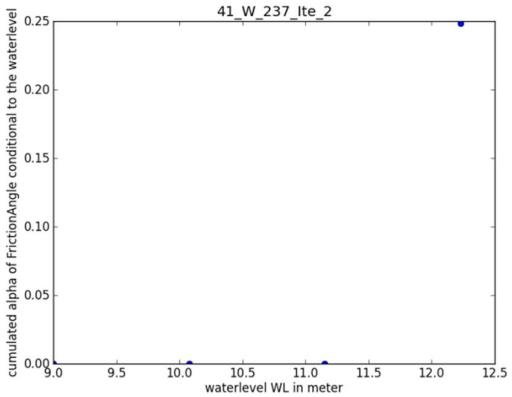

Figure C.26 Output case 41_W_237

10 m berm

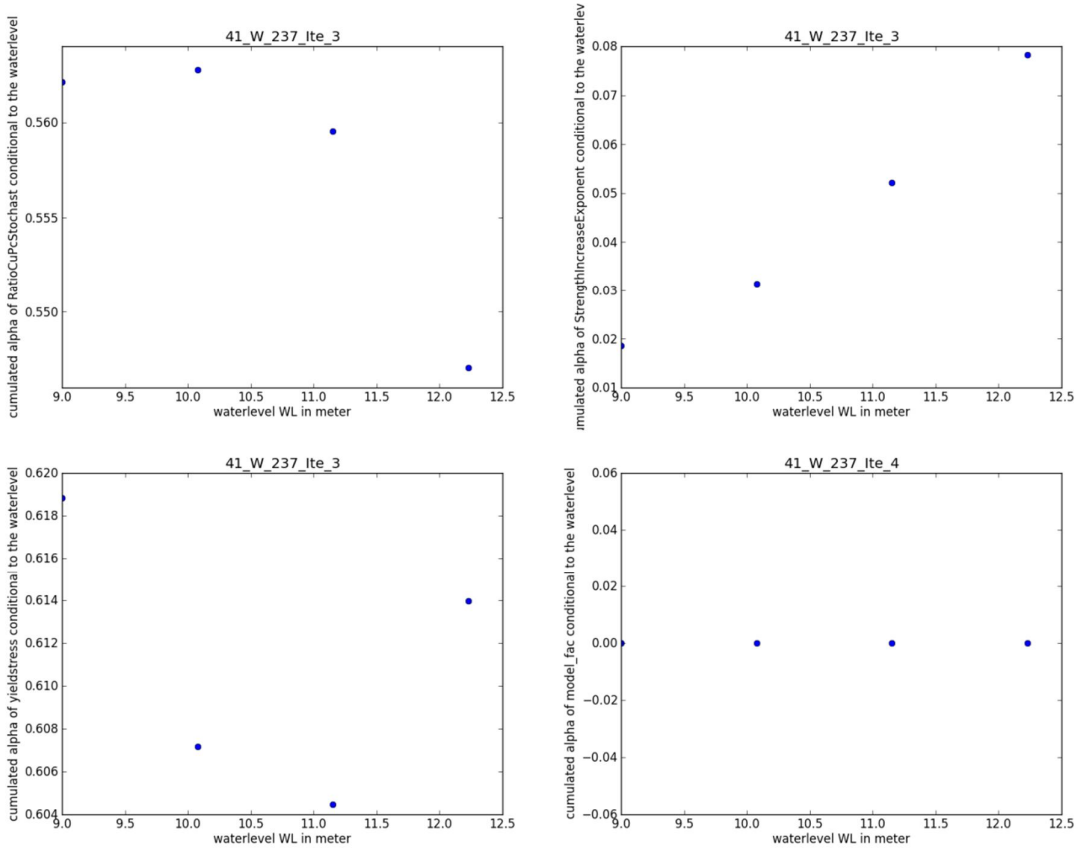

friction angle

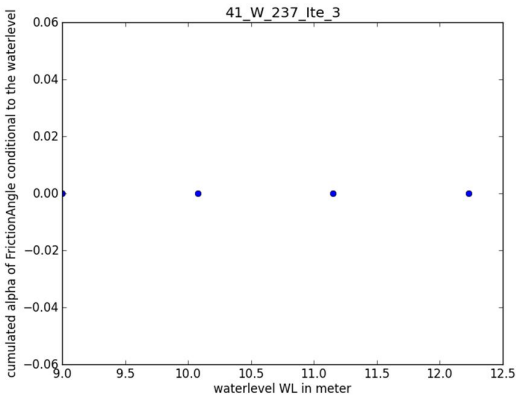

Figure C.27 Output case 41_W_237

Slip surface in the design point

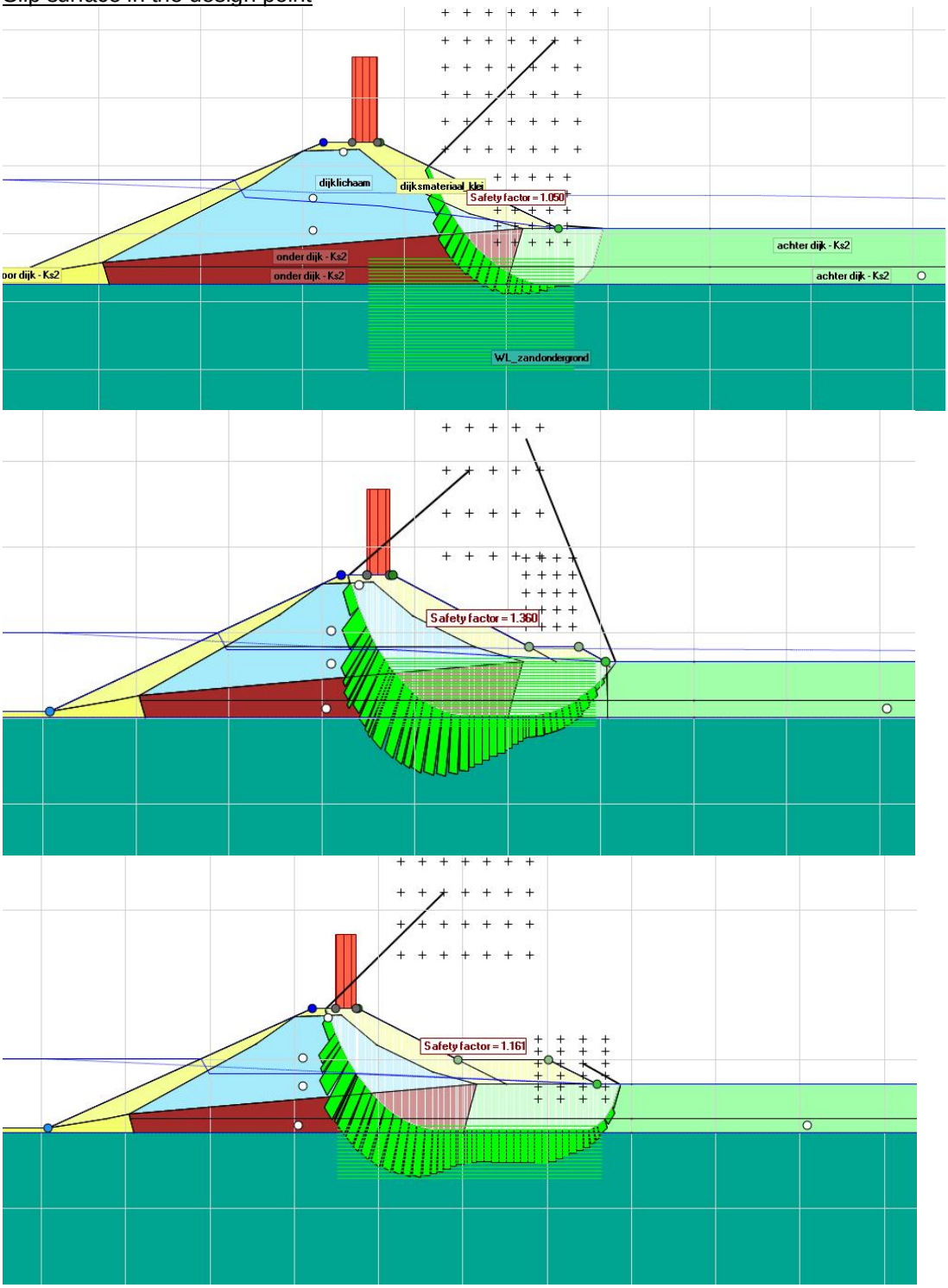

Figure C.28 Slip circle in design point

C.5 DP43

This appendix describes the steps and decisions made in setting up and performing probabilistic calculations for slip failure of the inner slope for a specific cross section. Furthermore it summarizes the intermediate results for this case.

C.5.1 Setup

Location and geometry

The cross section (VNK: Dp435_Matanse_Scherpenhof_001_Mean_sce_1, PC-Ring ID 52002014) is part of dike ring 52. The surface line is taken form AHN.

Material properties

This cross section was used in the VNK-2 calibration and in the preliminary undrained macrostability calibration.

TableC.9 Material parameters

	unit weight						
Name	saturated	unsaturated		cohesion	friction angle	strength increase exponent	Su/Pc
	kN/m^3	kN/m^3		kN/m^2	degree	-	-
WL_4 zand (2) (1)	20	18	drained	0	35.24		
Eemformatie	15.5	15.2	undrained			0.9	0.23
2b klei zandig (2)	19	18.7	undrained			0.9	0.45
2c klei halfgerijpt (1)	17.4	17.3	undrained			0.9	0.21
1 klei dijk (2)	20.2	19.9	drained			0.9	0.45
dijksmateriaal_klei	17	17	undrained	0	35		
bermmateriaal_klei	17	17	undrained	0	35		

The creation of phreatic lines is done in D-Geo Stability, using the following options.

TableC.10 Material parameters

Option	**Value**
Creation method:	Create Waternet
Dike/soil material	Clay dike on clay
PL1 line creation method	Ringtoets WTI 2017

MHW, decimate height h_{dec} and exceedance frequency $1/F_{exc}$ are taken from the PC-Ring database:

MHW = 7.617 m
h_{dec} = 0.680 m
$1/F_{exc}$ = 1/3000

The average high outside water level GHW is taken as the water level at mean discharge for the river, NAP +2.5 m. The minimum phreatic line in the dike body is defined by the Dupuit water level: NAP +5.80 m. The polder water level is assumed to be at the inner toe of the dike.

For the PL3 and PL2 schematization, the leakage length is used. In this case back calculated from the WTI Piping calculations. λ_{out} =526.7 m and λ_{polder} =1542.0 m.

The intrusion length is determined according to Schoofs en Van Duinen (2006). Based on the stratification and the duration of high water, the intrusion length is found to be 7,5 m. However, this length is larger than half the impermeable layer thickness; therefore this intrusion length is not realistic anymore. The intrusion length is taken as 0, so the phreatic line will be interpolated from PL3 to PL1.

Traffic load
A uniform load of 13kN/m^2 over a width of 2,5 m is applied as temporary load for traffic in emergency situations.

Yield stress points
The yield stress points are defined at some “strategic” places. Since the POP values are the same for all sub-soil layers and is only different for dijksmateriaal, only 5 points are chosen. Two points under the crest and two points under the toe. One in the dijksmateriaal-layer and one in the layer below. The yield stress value is defined at daily water level by the next equation $\sigma_y = \sigma'_{v,i} + POP$

Note 1: the yield stress points (white balls) are below the daily water level.
Note 2: the yield stress is dependent to the value of the POP. The vertical effective stress is not taken into account as stochastic parameter, but the POP is. Therefore, the standard deviation of the yield stress points is equal to the standard deviation of the POP (as fixed value, not as variation coefficient). Since the probabilistic prototype can yet only deal with a fixed standard deviation for yield stress, the value of 6 kPa is used for all yield stress points.

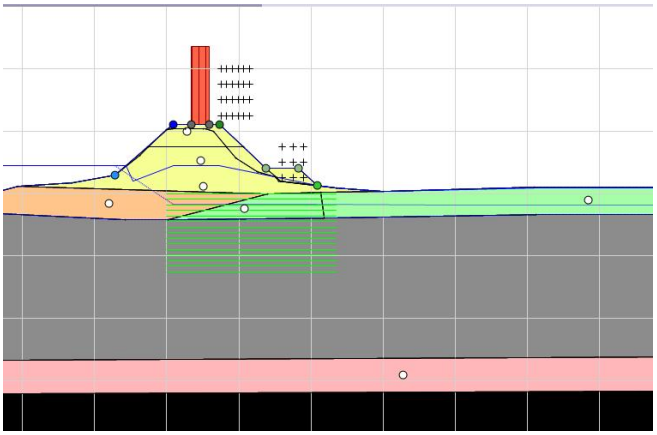

Figure C.29 Schematization no berm

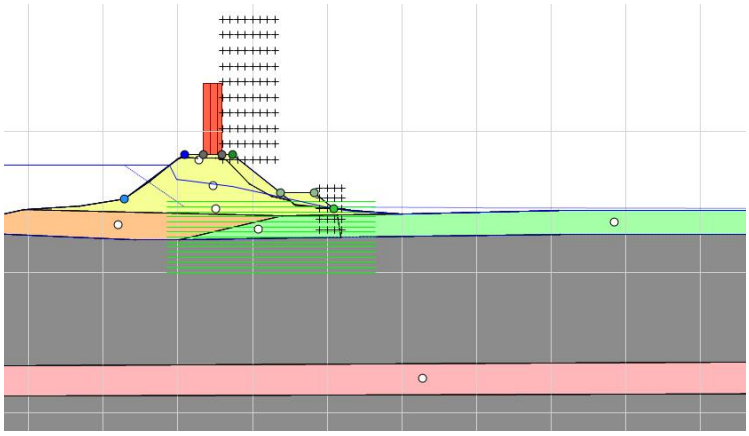

Figure C.30 Schematization 5m berm

Other information
Slip circle search method is Uplift-Van. The grid is predefined; the option “move grid” is checked. For the final design point it will be checked whether the critical slip circle is valid (centre point of active and passive circle not at the edge of the grid).

No reduction of c-phi in case uplift potential n < 1,199
Full reduction of c-phi in case uplift potential n > 1,200

Stability berms
In order to reach reliability numbers which are in the range of interest, stability berms are added. The material is the general “dijksmateriaal”. The berm length (measured as the total berm top width) is 0 for the basic geometry, and 5 m.

C.5.2 Probabilistic prototype

deterministic sanity check

The critical slip plane has to be selected manually to be sure that the results are correct. This is done using mean values and characteristic values. It must be noted that the basic geometry shows an increase of FoS with water level. This is one of the reason this case is not used in the calibration.

With mean values

Basic geometry

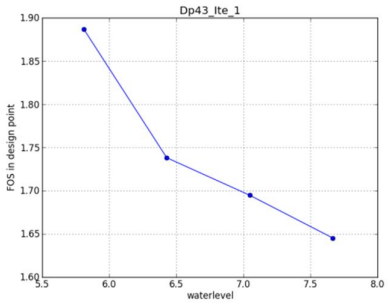

with characteristic values

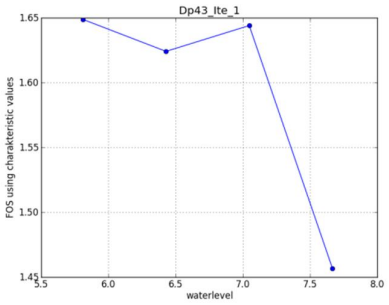

Basic geometry + 5 m berm

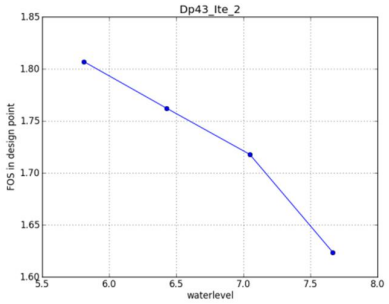

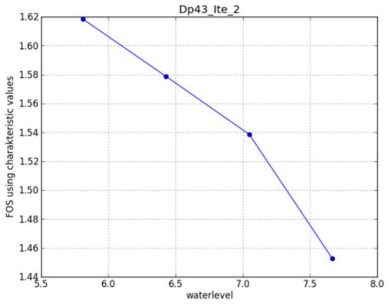

Figure C.31 Output case DP43

Probabilistic fragility curve + metamodel results
Max_beta_interation_inner_loop = 0.05

Basic geometry + no berm

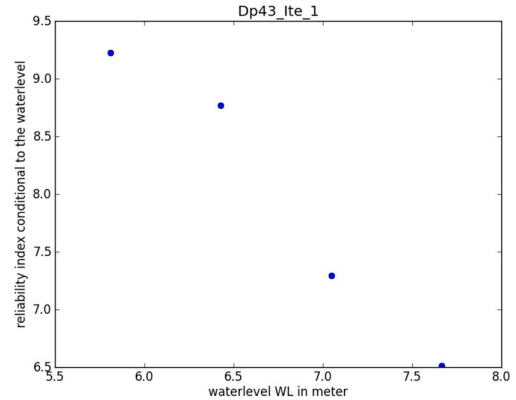

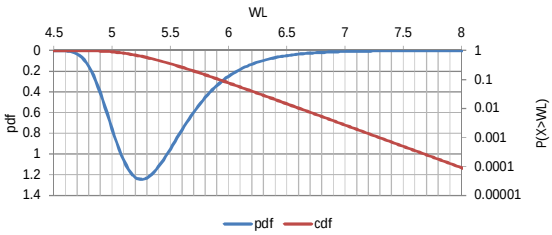

Stochast	dp	alpha	alpha^2
CuPc		0.622	0.386
m		0.001	0.000
yieldstress		0.558	0.311
cohesion		0.000	0.000
friction angle		0.011	0.000
model fac	1.08E+00	3.69E-01	0.136
water level	4.799	-0.407	0.166

beta	**5.84**
gamma_characteristic = FOS_char(MHW)	1.65
FOS_char(DP)	>>1.9

Basic geometry + 5 m berm

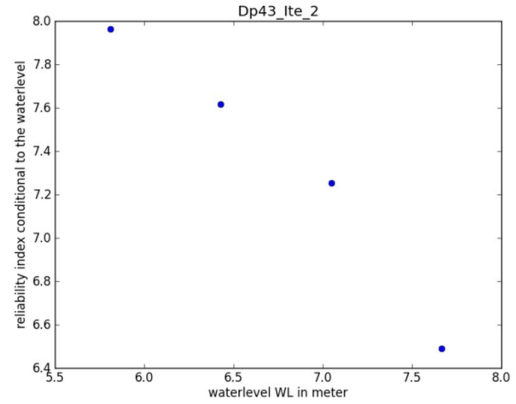

Stochast	dp	alpha	alpha^2
CuPc		0.377	0.142
m		0.002	0.000
yieldstress		0.026	0.001
cohesion		0.000	0.000
friction angle		0.005	0.000
model fac	1.05E+00	1.95E-01	0.038
water level	10.764	0.905	0.819

beta	**6.25**
gamma_characteristic = FOS_char(MHW)	1.45
FOS_char(DP)	

Figure C.32 Output case DP43

Metamodel results

Basic geometry + no berm

CuPc

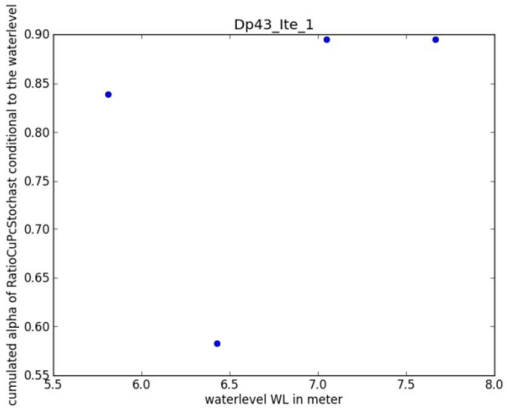

m

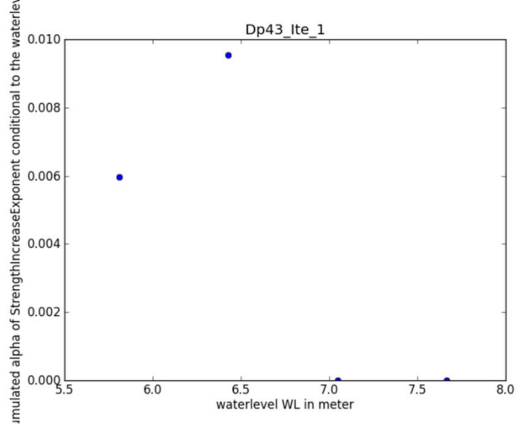

yield stresss

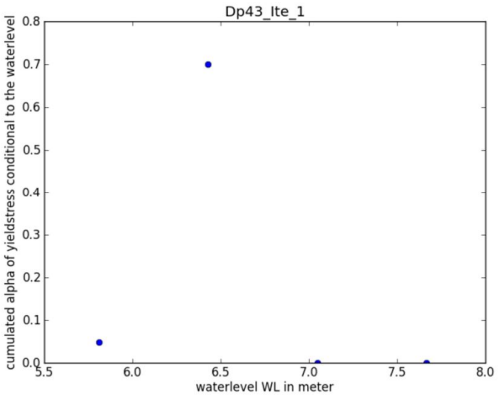

model factor

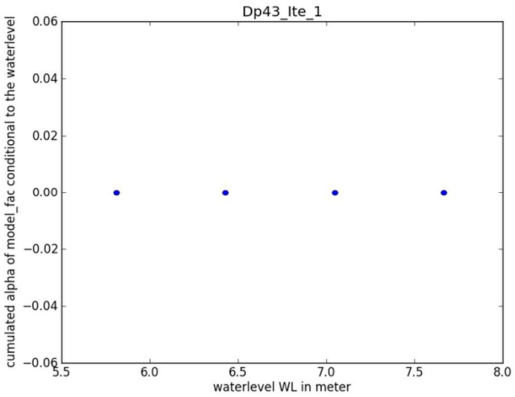

friction angle

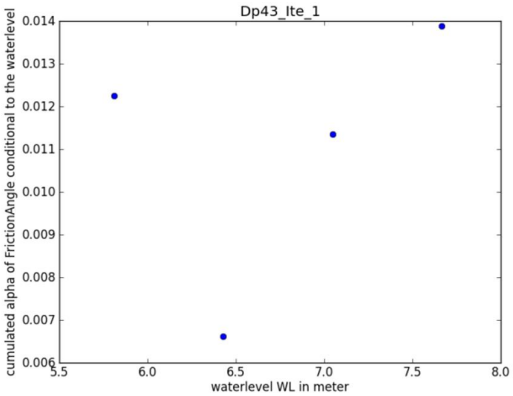

Figure C.33 Output case DP43

Slip surface in the design point

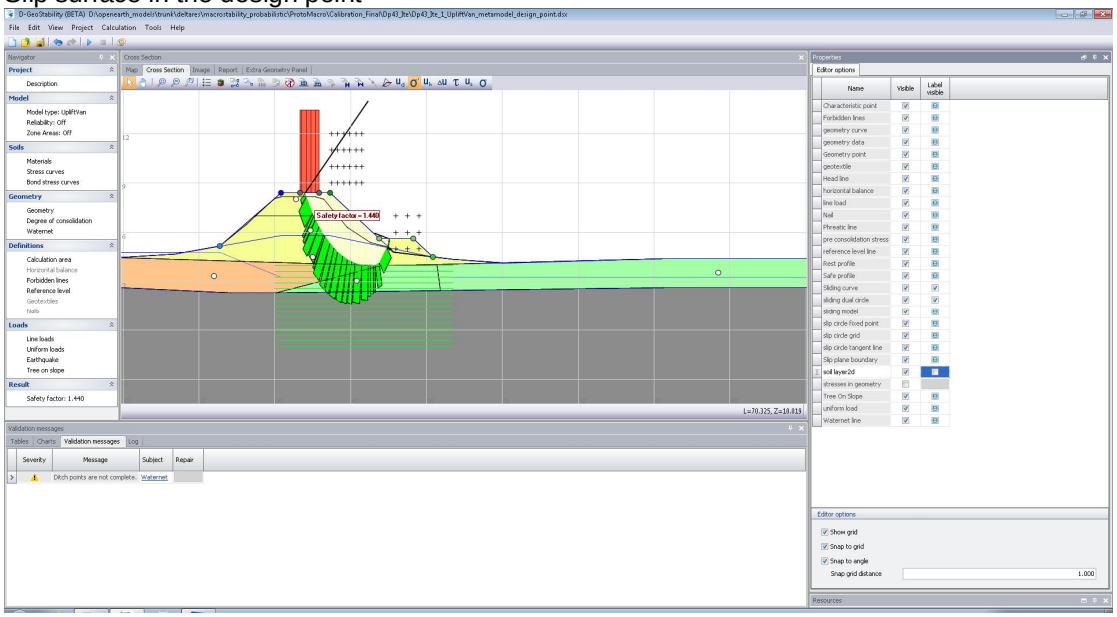

Figure C.34 Slip circle in design point

5 m berm

CuPc

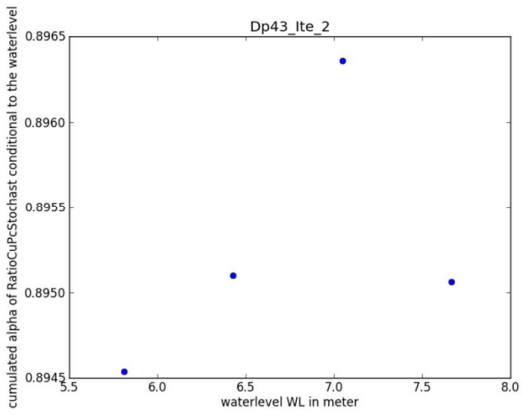

m

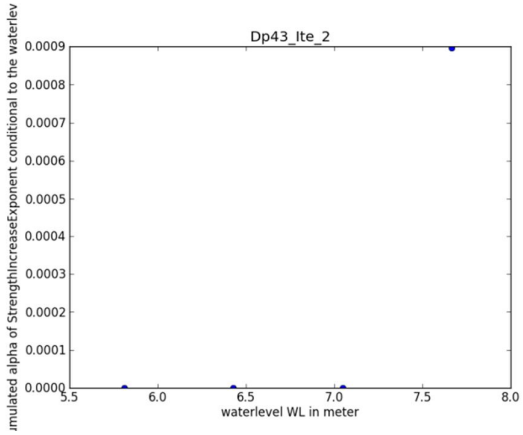

yield stress

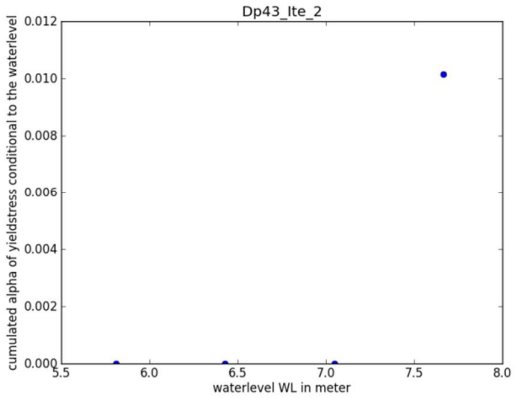

model factor

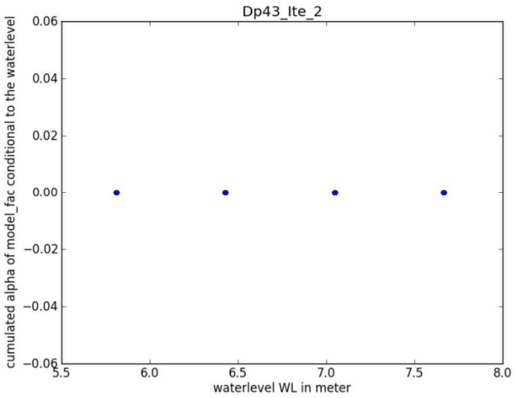

friction angle

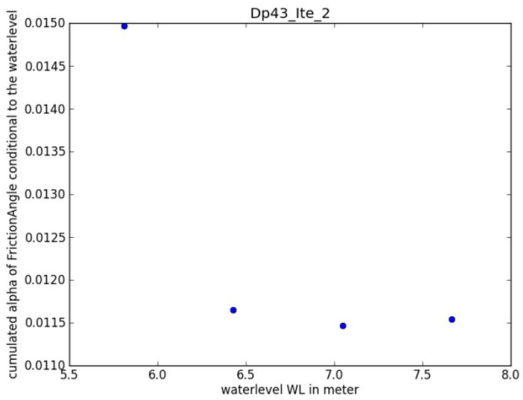

Figure C.35 Output case DP43

C.6 Dp_5

This appendix describes the steps and decisions made in setting up and performing probabilistic calculations for slip failure of the inner slope for a specific cross section. Furthermore it summarizes the intermediate results for this case.

C.6.1 Setup

Location and geometry

The location of this cross section (VNK: Dp_521_Epe_Veessen_001_Mean_sce_1, PC-Ring ID 52003005) is at Veessen.

Stratification

The stratification of the subsoil schematization from the VNK-2 project. There is a separation between soils below and besides the dike.

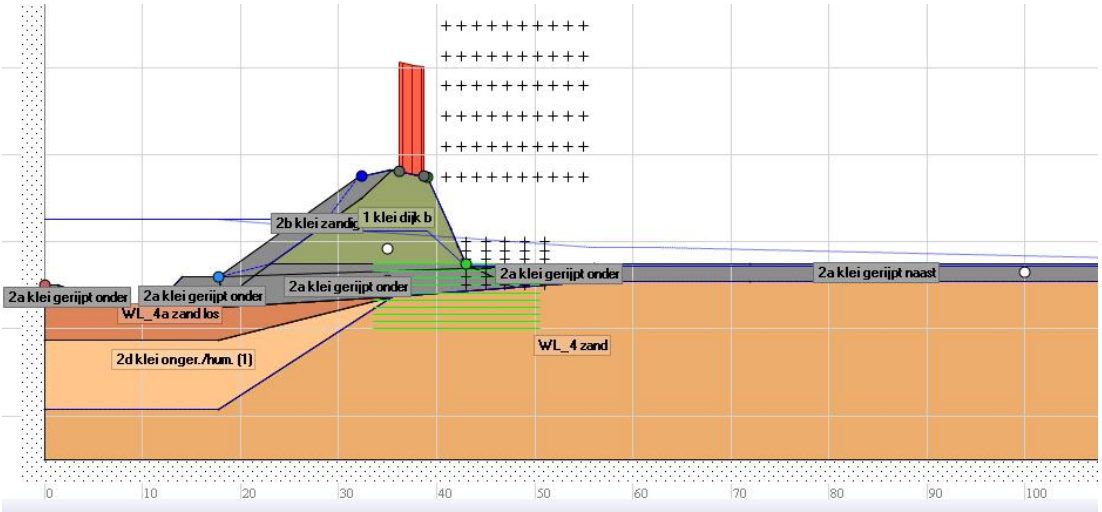

Figure C.36 Schematization

Material properties

Material properties for the soil types are taken from the original schematization (river undrained parameters). The distribution parameters for the random soil types are summed in the next table. This dataset already includes averaging from regional to local data and includes averaging along the slip plane.

The POP value for materials below the dike have a mean value indicated in the table below; the standard deviation is 6 kPa, according to the WTI-SOS database.

Table C.11 Material properties

Soil type	Vol. weight	Friction angle		Su-ratio		Strength increase exp.		POP
2a klei gerijpt naast	18.9			0.45	0.03	0.90	0.03	0.0
2a klei gerijpt onder	18.9			0.45	0.03	0.90	0.03	0.0
2b klei zandig	19.0			0.21	0.03	0.90	0.03	0.0
2d klei onger./hum. (1)	15.5			0.21	0.03	0.90	0.03	10.49
dijksmateriaal_klei	17.0			0.45	0.03	0.90	0.03	0.0

WL_4 zand	20.0			0.23	0.03	0.90	0.03	0.0
WL_4a zand los	19.0	35.0	1.75					
2a klei gerijpt naast	18.9	35.2	2.4					
2a klei gerijpt onder	18.9	35.2	2.4					

Waternet

The creation of phreatic lines is done by D-Geo Stability, according to the following options.

Table C.12 Waternet Creator options

Option	Value
Creation method:	Create Waternet
Dike/soil material	Clay dike on clay
PL1 line creation method	Ringtoets WTI 2017

Since the MHW according to the new safety standards for this cross section is higher than the crest level, the MHW and water level distribution is “transposed” to a plausible value: 1,0 m below the crest. The decimate height and exceedance frequency are taken from the PC-Ring database:
h_{dec} = 0,694 m
$1/F_{exc}$ = 1/3000
MHW = NAP +6.931 m

The average high outside water level GHW is taken as the water level at mean discharge for the river, NAP +2.05 m. The minimum phreatic line in the dike body is defined by the Dupuit water level: NAP +4.75 m. The polder water level is assumed to be at the inner toe of the dike.

For the PL3 and PL2 schematization, the leakage length is used. In this case back calculated from the WTI Piping calculations. λ_{out} =298 m and λ_{polder} =1509 m.

The intrusion length is determined according to Schoofs en Van Duinen (2006). Based on the stratification and the duration of high water, the intrusion length is found to be 7,5 m. However, this length is larger than half the impermeable layer thickness; therefore this intrusion length is not realistic anymore. The intrusion length is taken as 0, so the phreatic line will be interpolated from PL3 to PL1.

Traffic load

A uniform load of 13kN/m2 over a width of 2,5 m is applied as temporary load for traffic in emergency situations.

Yield stress points

The yield stress points are defined in each layer. The yield stress value is defined at daily water level by the next equation $\sigma_y = \sigma'_{v,i} + POP$. The used POP value is based on expert knowledge.

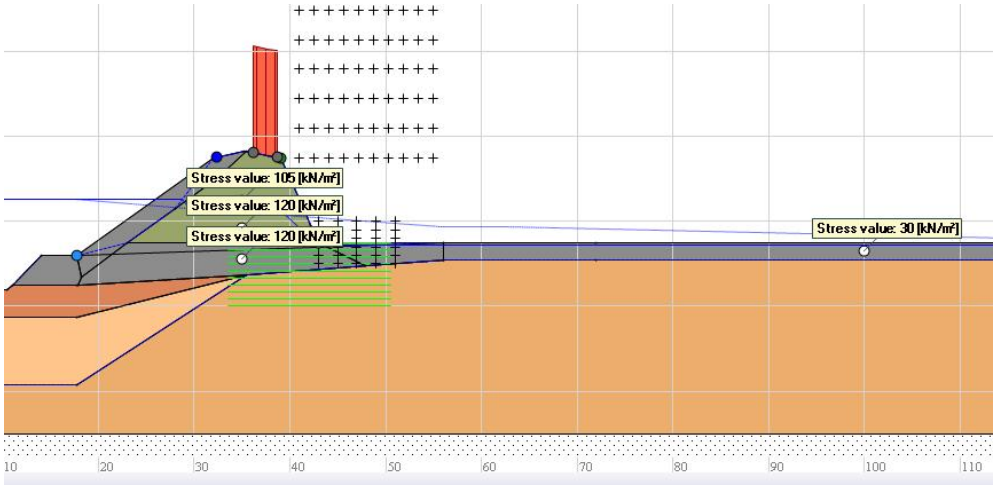

Figure C.37 Schematization yield stress

Other information

Slip circle search method is Uplift-Van. The grid is predefined; the option “move grid” is checked. For the final design point it will be checked whether the critical slip circle is valid (centre point of active and passive circle not at the edge of the grid).

The blanket layer is less thick than 4 metre, so uplift can occur; therefore the shear strength has to be reduced for uplift conditions:
No reduction of c-phi in case uplift potential n < 1,199
Full reduction of c-phi in case uplift potential n > 1,200

C.6.2 Probabilistic prototype

Deterministic sanity check

Mean values

Berm = 0 m

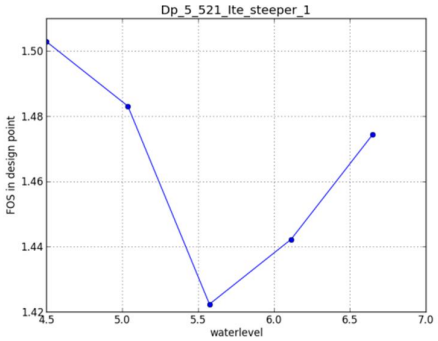

Characteristic values

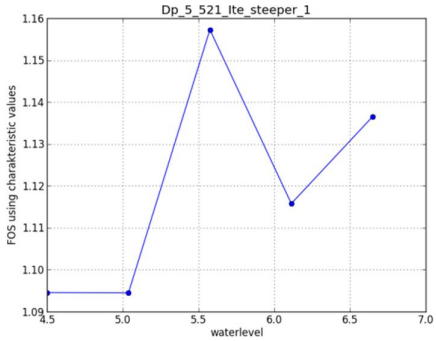

Figure C.38 Output case Dp_5

Probabilistic fragility curve (Max_beta_interation_inner_loop = 0.05)

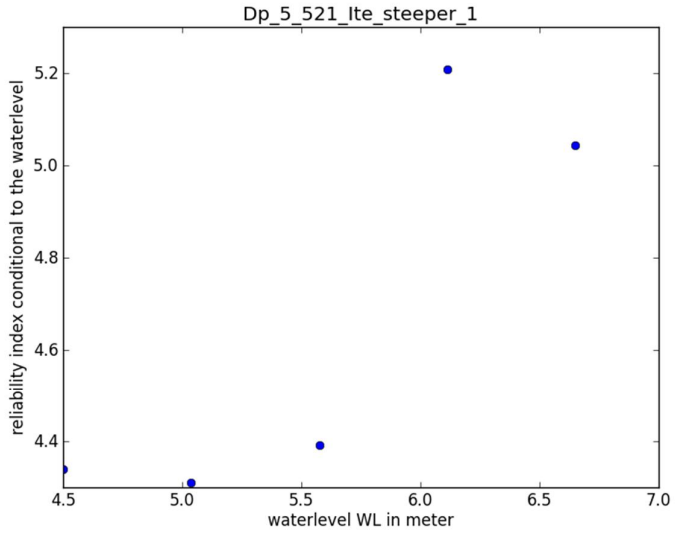

	dp	alpha 2
beta final	4.33	
SF char	1.13	
CuPc		0.73
m		0.20
yieldstress		0.48
cohesion		0.00
fric angle		0.04
model fac	1.07	0.43
water level	4.68	0.02

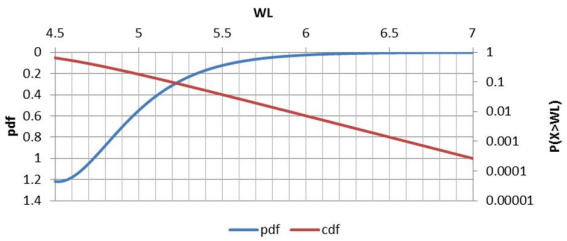

Figure C.39 Output case Dp_5

Note that the deterministic sanity checks show a very low influence of the water level on the stability factor. These relation should be smooth and decreasing. Additionally, note that the fragility curve of the conditional reliability indices vs water levels show an increase of the

reliability with the water level, which is hard to belief. This should be investigated, although it is expected not to result in a very large change in the total beta and gamma for this case.

Cumulative alpha values conditional to the water level

Basic geometry

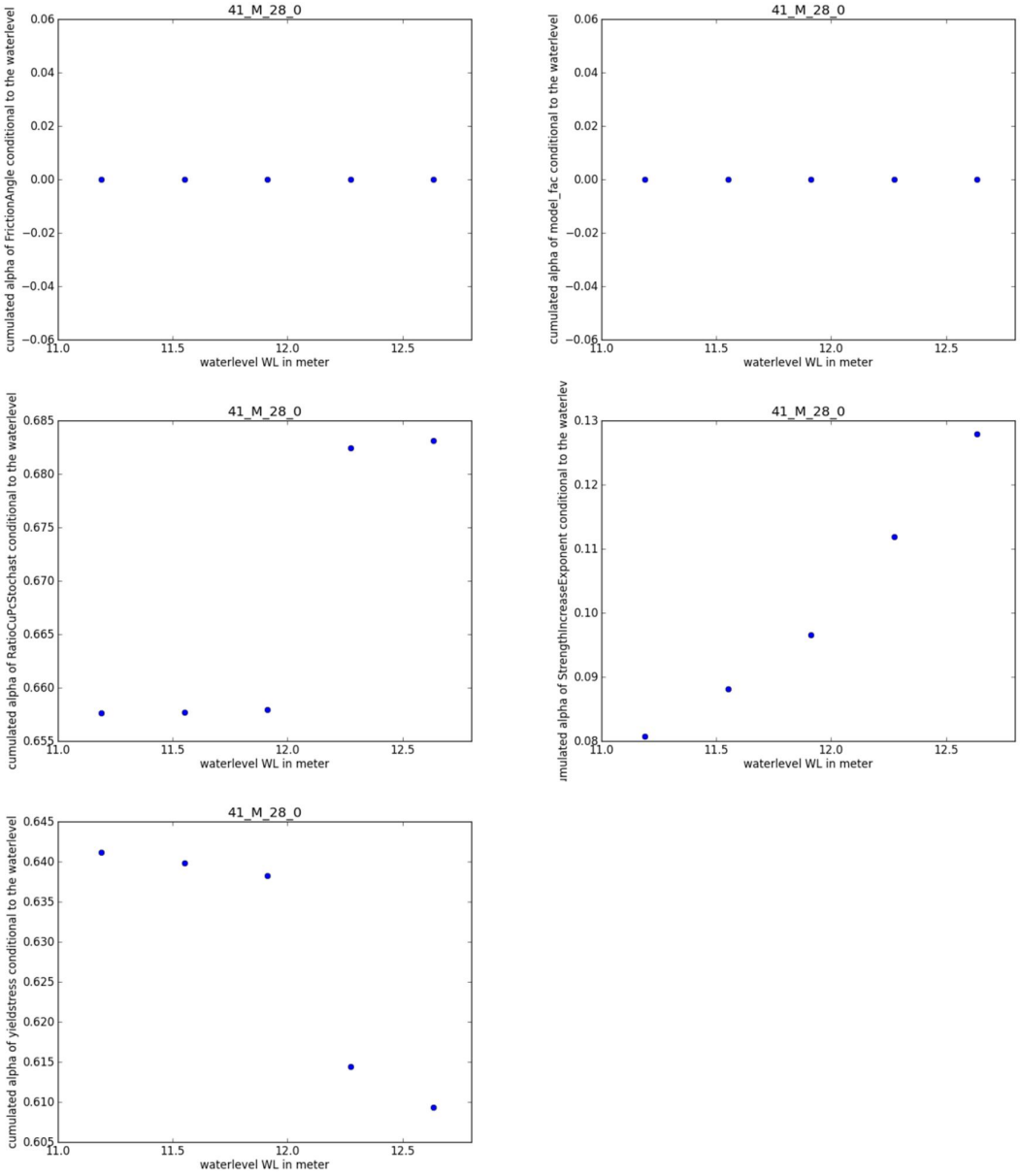

Figure C.40 Output case Dp_5

Basic geometry + 7.5 m berm

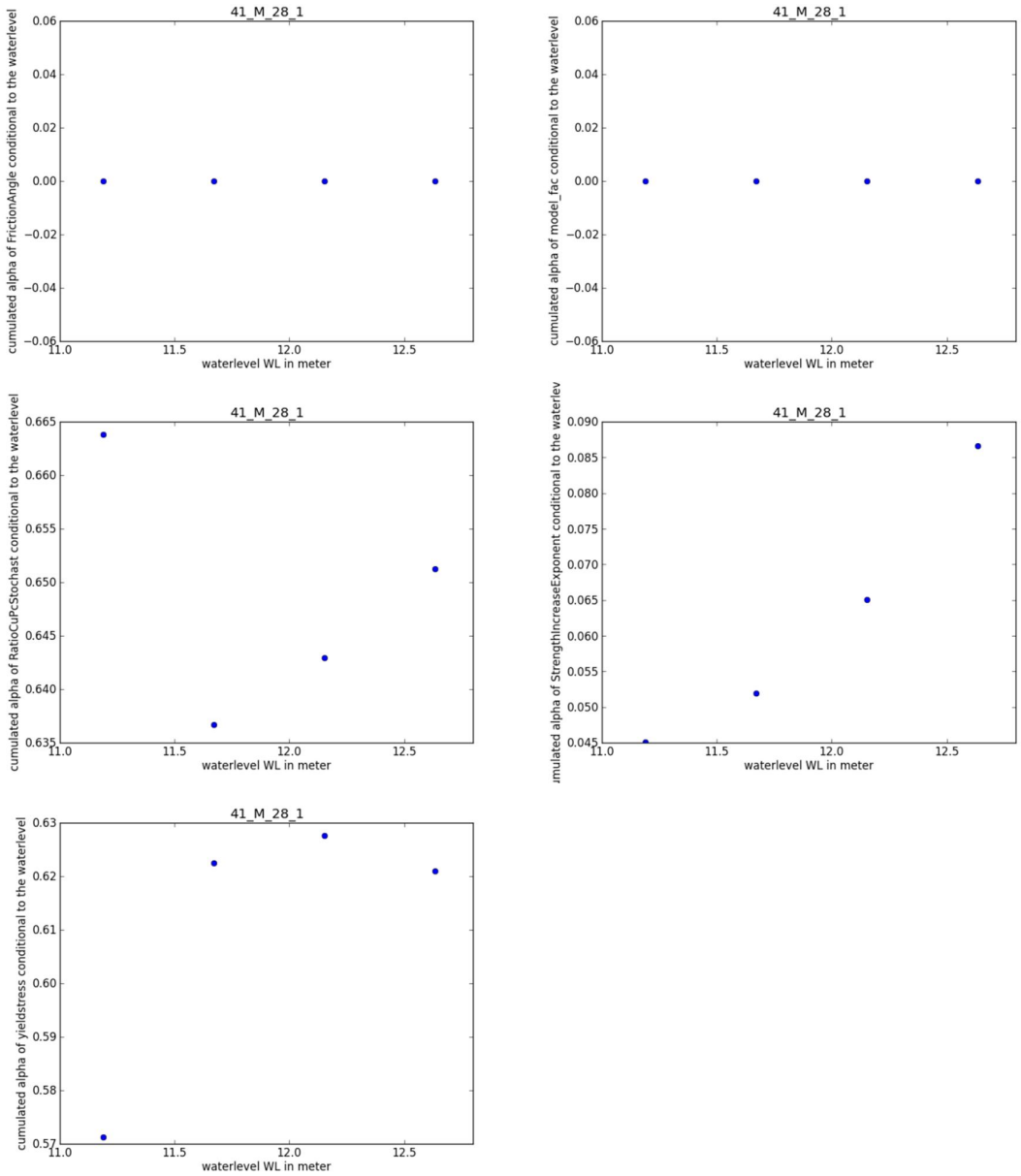

Figure C.41 Output case Dp_5

Basic geometry + 15 m berm

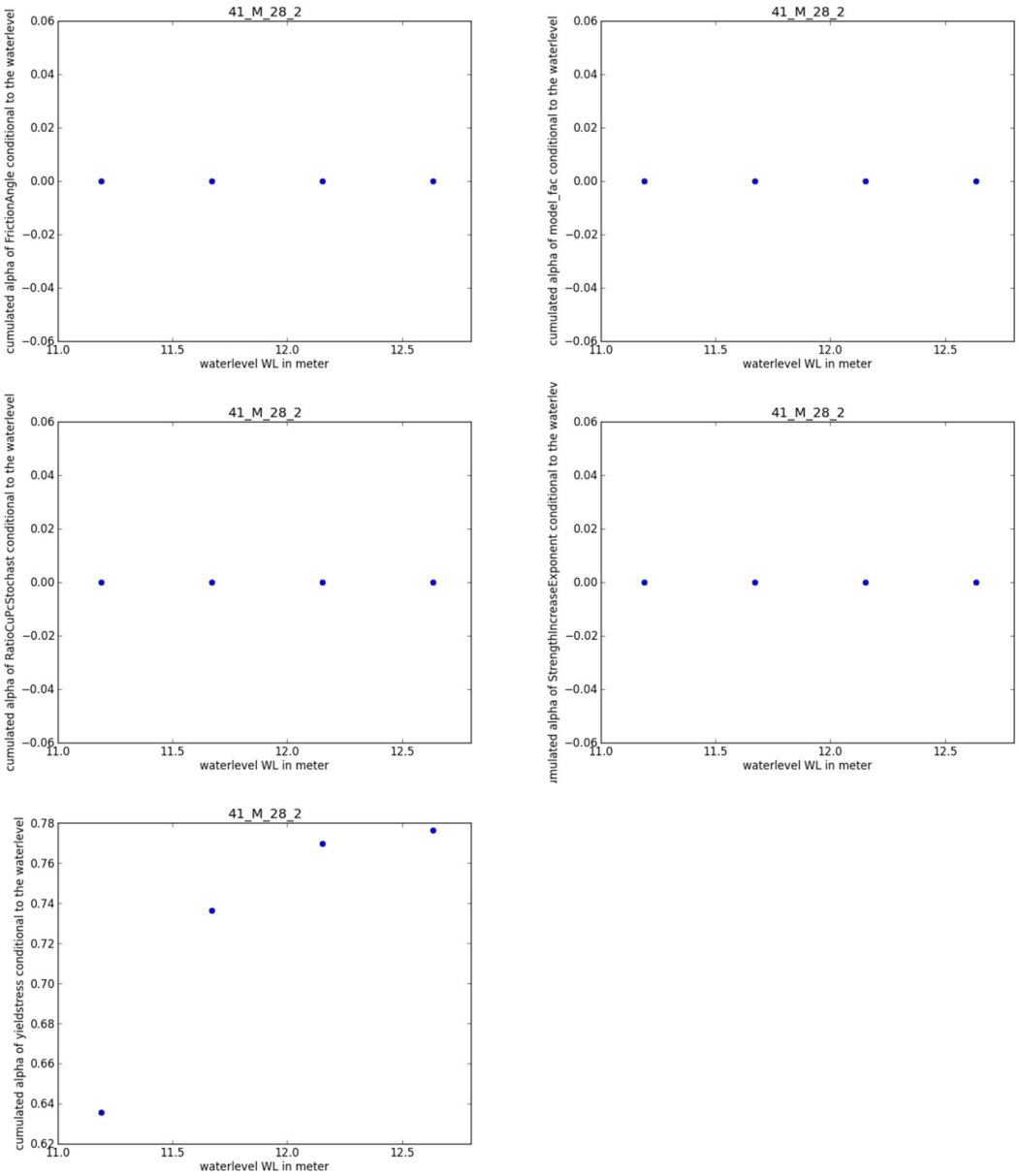

Figure C.42 Output case Dp_5

Slip circle in design point

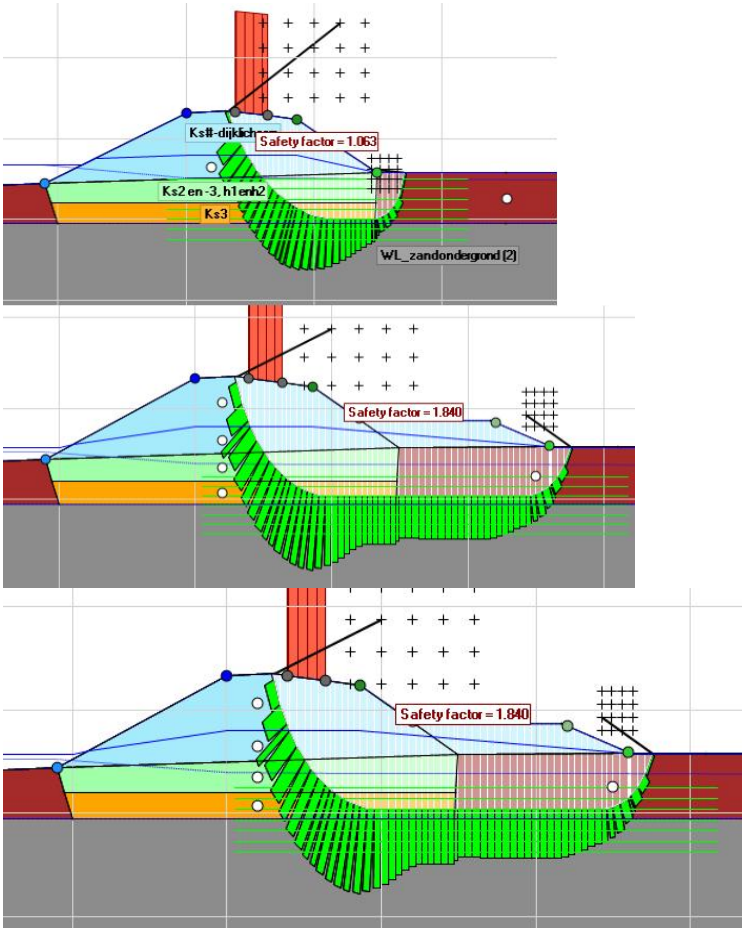

Figure C.43 Slip circle in design point

C.7 dwp0

This appendix describes the steps and decisions made in setting up and performing probabilistic calculations for slip failure of the inner slope for a specific cross section. Furthermore it summarizes the intermediate results for this case.

C.7.1 Setup

Location and geometry

The cross section (VNK: dwp090_5, PC-Ring ID 17003020) is part of dike ring 17. The surface line is taken form AHN.

Material properties

This cross section was used in the VNK-2 calibration and in the preliminary undrained macrostability calibration.

Table C.13 Material properties

	unit weight						
Name	saturated	unsaturated		cohesion	friction angle	strength increase exponent	Su/Pc
	kN/m^3	kN/m^3		kN/m^2	degree	-	-
WL_pleistoceen zand (1)	20	18	drained	0	36.77		
al -p - kreftenheye	18	18	undrained			0.9	0.21
Hollandveen (2)	11	11	undrained			0.9	0.32
Gorkum Licht (1)	17	17	undrained			0.9	0.21
Zand van Duinkerke	18	18	drained	2.41	25.27		
OB (1)	16.5	16.5	undrained			0.9	0.22
Klei van Duinkerke	16.5	16.5	undrained			0.9	0.21
OA (1)	20	17	drained	0	36.77		
dijksmateriaal_klei	17	17	drained	0	35		

The creation of phreatic lines is done in D-Geo Stability, using the following options.

Table C.14 Material properties

Option	Value
Creation method:	Create Waternet
Dike/soil material	Clay dike on clay
PL1 line creation method	Ringtoets WTI 2017

MHW, decimate height h_{dec} and exceedance frequency $1/F_{exc}$ are taken from the PC-Ring database:

MHW = 3.0 m
h_{dec}= 0.274 m
$1/F_{exc}$ = 1/30000

The average high outside water level GHW is taken as the water level at mean discharge for the river, NAP +0 m. The minimum phreatic line in the dike body is defined by the Dupuit

water level: NAP +1.246 m. The polder water level is assumed to be at the inner toe of the dike.

For the PL3 and PL2 schematization, the leakage length is used. In this case back calculated from the WTI Piping calculations. λ_{out} =857.59 m and λ_{polder} =2571.25 m.

The intrusion length is determined according to Schoofs en Van Duinen (2006). Based on the stratification and the duration of high water, the intrusion length is found to be 7,5 m. However, this length is larger than half the impermeable layer thickness; therefore this intrusion length is not realistic anymore. The intrusion length is taken as 0, so the phreatic line will be interpolated from PL3 to PL1.

Traffic load
A uniform load of 13kN/m^2 over a width of 2,5 m is applied as temporary load for traffic in emergency situations.

Yield stress points
The yield stress points are defined at some “strategic” places. Since the POP values are the same for all sub-soil layers and is only different for dijksmateriaal, only 5 points are chosen. Two points under the crest and two points under the toe. One in the dijksmateriaal-layer and one in the layer below. The yield stress value is defined at daily water level by the next equation $\sigma_y = \sigma'_{v,i} + POP$

Note 1: the yield stress points (white balls) are below the daily water level.
Note 2: the yield stress is dependent to the value of the POP. The vertical effective stress is not taken into account as stochastic parameter, but the POP is. Therefore, the standard deviation of the yield stress points is equal to the standard deviation of the POP (as fixed value, not as variation coefficient). Since the probabilistic prototype can yet only deal with a fixed standard deviation for yield stress, the value of 6 kPa is used for all yield stress points.

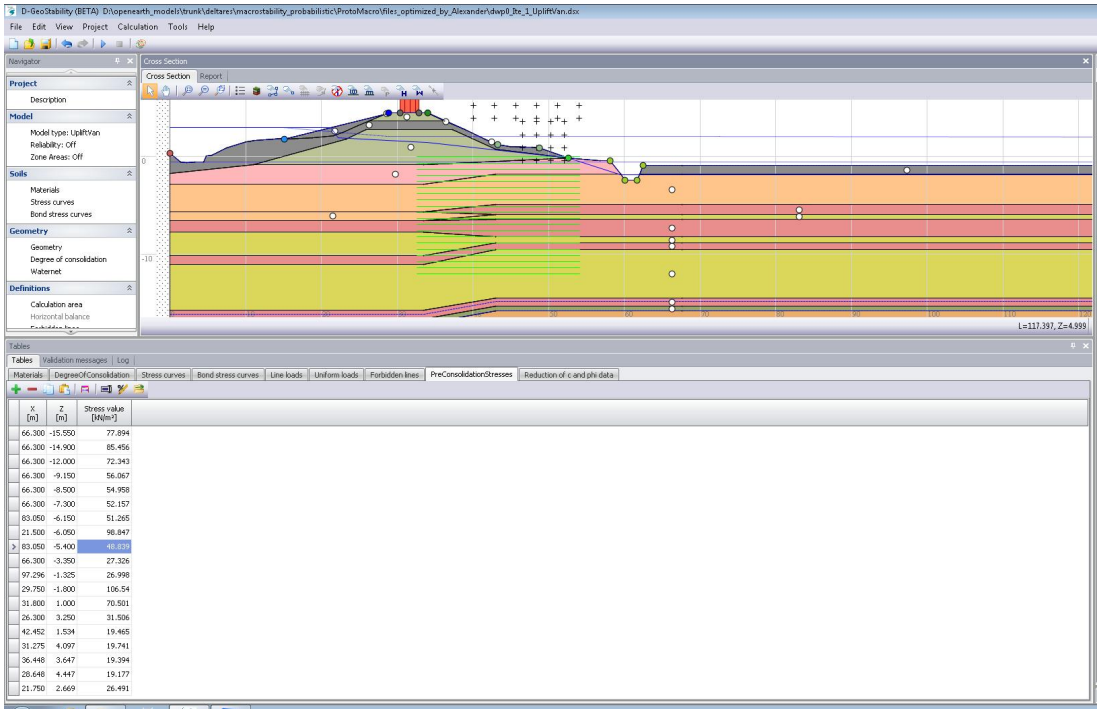

Figure C.44 Schematization of yield stress

Other information

Slip circle search method is Uplift-Van. The grid is predefined; the option “move grid” is checked. For the final design point it will be checked whether the critical slip circle is valid (centre point of active and passive circle not at the edge of the grid).

No reduction of c-phi in case uplift potential n < 1,199
Full reduction of c-phi in case uplift potential n > 1,200

C.7.2 Probabilistic prototype

deterministic sanity check

The critical slip plane has to be selected manually to be sure that the results are correct. This is done using mean values and characteristic values.

With mean values

Basic geometry

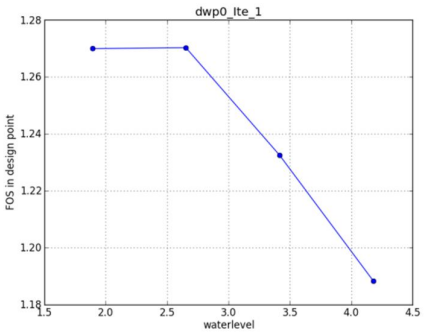

with characteristic values

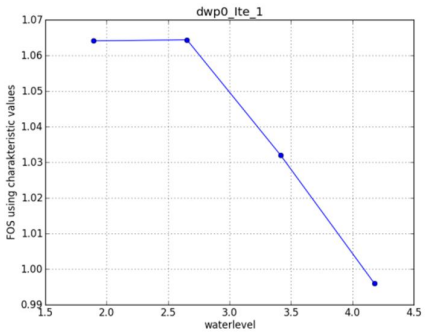

Figure C.45 Output case dwp0

Probabilistic fragility curve + metamodel results

Max_beta_interation_inner_loop = 0.05

Basic geometry + no berm

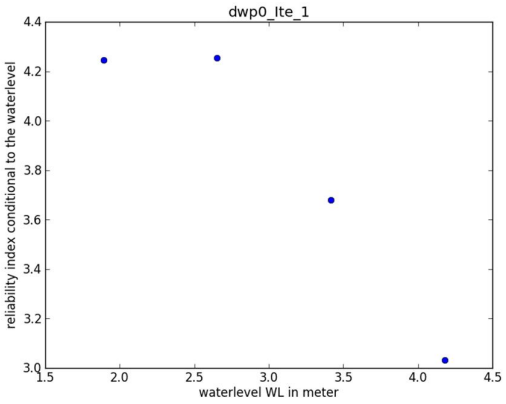

Stochast	dp	alpha	alpha^2
CuPc		0.459	0.210
m		0.010	0.000
yieldstress		0.579	0.335
cohesion		0.000	0.000
friction angle		0.288	0.083
model fac	1.09	6.10E-01	0.372
water level	2.086	-0.001	0.000

beta	**4.25**
gamma_characteristic = FOS_char(MHW)	1.05
FOS_char(DP)	1.06

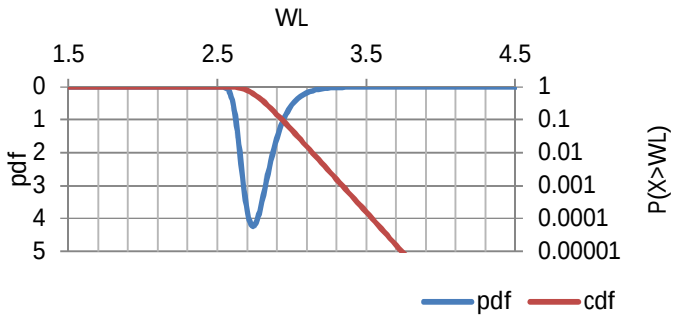

Figure C.46 Output case dwp0

Metamodel results

Basic geometry + no berm

CuPc

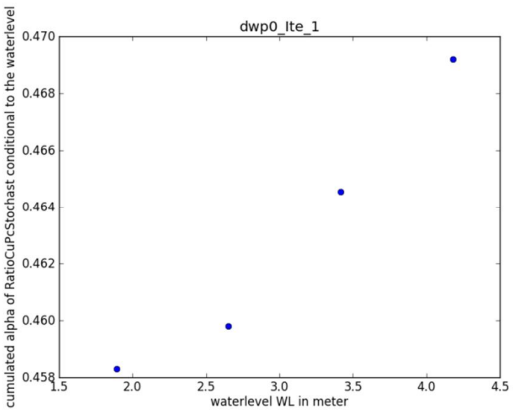

m

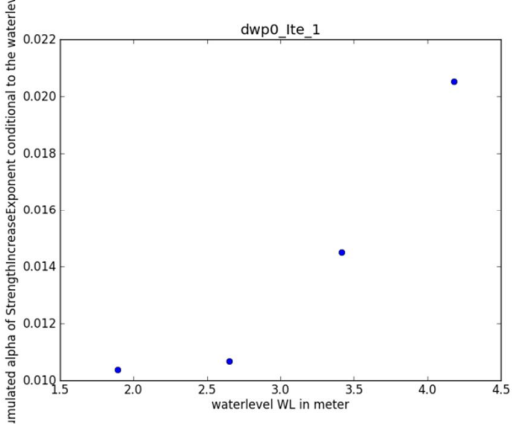

yield stress

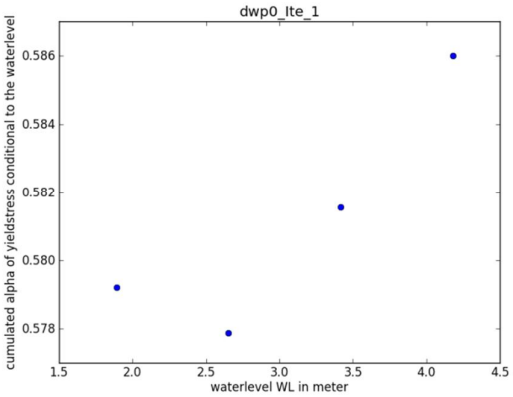

model factor

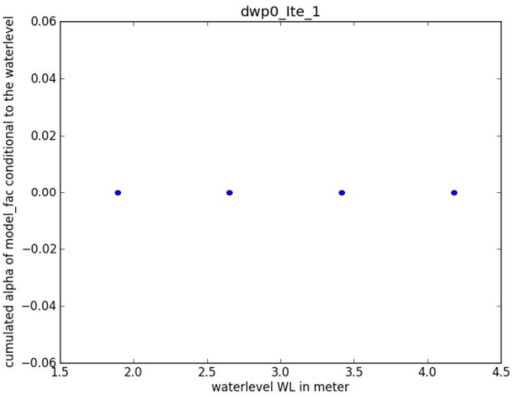

friction angle

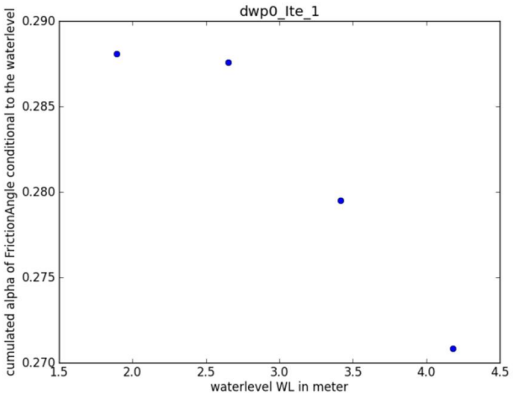

Figure C.47 Output case dwp0

Slip surface in the design point

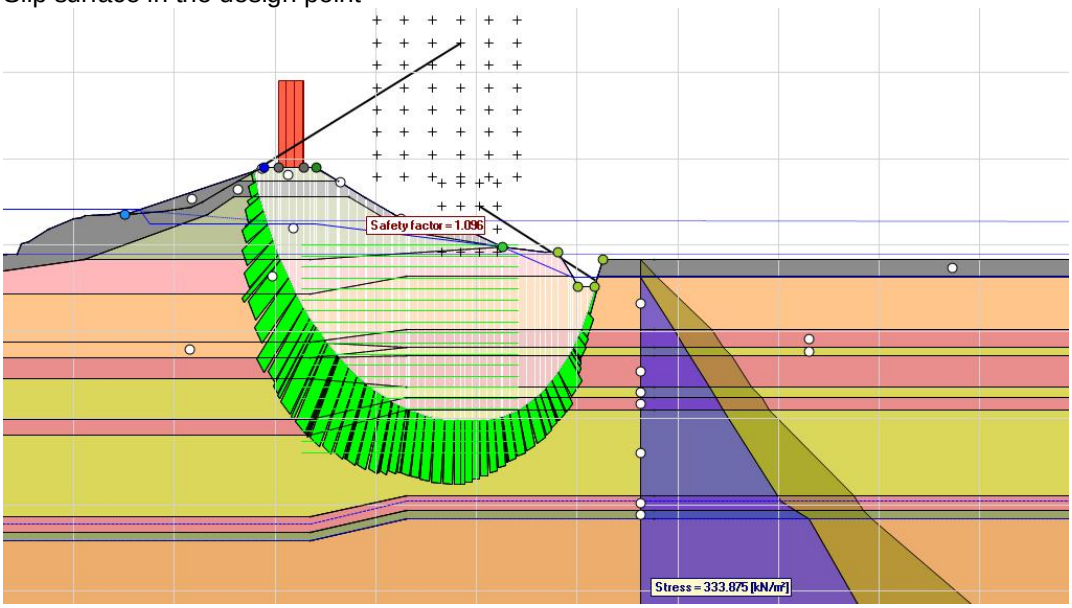

Figure C.48 Slip circle in design point

C.8 41_W_270

This appendix describes the steps and decisions made in setting up and performing probabilistic calculations for slip failure of the inner slope for a specific cross section. Furthermore it summarizes the intermediate results for this case.

C.8.1 Setup

Location and geometry

The location of this cross section (VNK: 41_Waal_Dp270, PC-Ring ID 41003037) is at the Waal, near Tiel.

Stratification

The stratification of the subsoil schematization from the VNK-2 project. There is a separation between soils below and besides the dike.

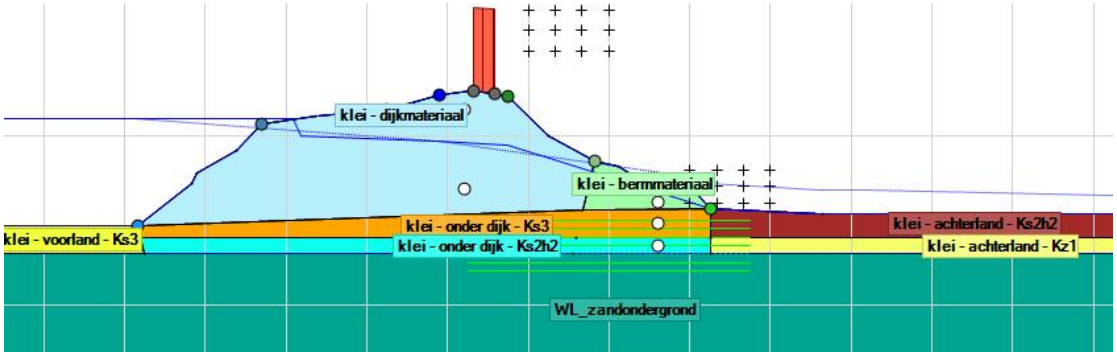

Figure C.49 Schematization

Material properties

Material properties for the soil types are taken from the original schematization (river undrained parameters). The distribution parameters for the random soil types are summed in the next table. This dataset already includes averaging from regional to local data and includes averaging along the slip plane.

The POP value for materials below the dike have a mean value of 50 kPa. All other materials, have a POP of 20 kPa. The standard deviation is 6 kPa, according to the WTI-SOS database.

Table C.15 Material properties

Soil type	Vol. weight	Friction angle		Su-ratio		Strength increase exp.	
		μ	σ	μ	σ	μ	σ
dijksmateriaal_klei	17/17			0.22	0.02	0.90	0.02
klei - achterland - Ks2h2	13.6/13.6			0.19	0.05	0.90	0.02
klei - achterland - Kz1	18.6/18.6			0.45	0.03	0.90	0.02
klei - bermmateriaal	19/19			0.45	0.03	0.90	0.02
klei - dijkmateriaal	19.1/19.1			0.45	0.03	0.90	0.02
klei - onder dijk - Ks2h2	13.6/13.6			0.19	0.05	0.90	0.02
klei - onder dijk - Ks3	17.6/17.6			0.21	0.01	0.90	0.02
klei - voorland - Ks3	15.9/15.9			0.24	0.01	0.90	0.02
WL_zandondergrond	17/17	34.6	2.4				

Waternet
The creation of phreatic lines is done by D-Geo Stability, according to the following options.

Table C.16 Waternet Creation options

Option	Value
Creation method:	Create Waternet
Dike/soil material	Clay dike on clay
PL1 line creation method	Ringtoets WTI 2017

Since the MHW according to the new safety standards for this cross section is higher than the crest level, the MHW and water level distribution is “transposed” to a plausible value: 1,0 m below the crest. The decimate height and exceedance frequency are taken from the PC-Ring database:
h_{dec} = 0,727 m
$1/F_{exc}$ = 1/10000
MHW = NAP +12,57m (this MHW is higher than the actual crest level, so the old MHW is taken: NAP +12,06m)

The average high outside water level GHW is taken as the water level at mean discharge for the river, NAP +4.50 m. The minimum phreatic line in the dike body is defined by the Dupuit water level: NAP +8,37 m. The polder water level is assumed to be at the inner toe of the dike.

For the PL3 and PL2 schematization, the leakage length is used. In this case back calculated from the WTI Piping calculations. λ_{out} 232 m and λ_{polder} 901 m.

The intrusion length is determined according to Schoofs en Van Duinen (2006). Based on the stratification and the duration of high water, the intrusion length is found to be 7,5 m. However, this length is larger than half the impermeable layer thickness; therefore this intrusion length is not realistic anymore. The intrusion length is taken as 0, so the phreatic line will be interpolated from PL3 to PL1.

To prevent peculiarities with higher phreatic lines in case of stability berms (because normally the PL1-line is interpolated linearly between the inner crest line and the inner toe), the PL1 offset below the start of the landside shoulder is set to 0,10m.

Traffic load
A uniform load of 13kN/m2 over a width of 2,5 m is applied as temporary load for traffic in emergency situations.

Yield stress points
The yield stress points are defined in each layer. The yield stress value is defined at daily water level by the next equation $\sigma_y = \sigma'_{v,i} + POP$. The used POP value is based on expert knowledge.

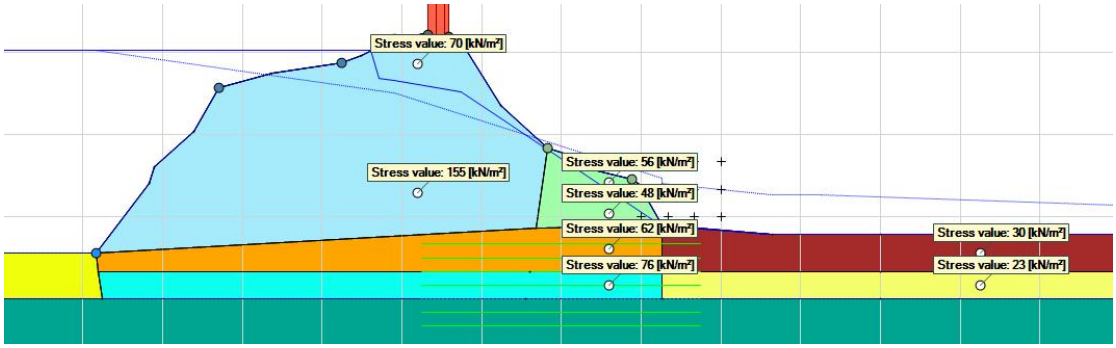

Figure C.50 Schematization of yield stress

Other information

Slip circle search method is Uplift-Van. The grid is predefined; the option “move grid” is checked. For the final design point it will be checked whether the critical slip circle is valid (centre point of active and passive circle not at the edge of the grid).

The blanket layer is less thick than 4 metre, so uplift can occur; therefore the shear strength has to be reduced for uplift conditions:
No reduction of c-phi in case uplift potential n < 1,199
Full reduction of c-phi in case uplift potential n > 1,200

Stability berms

In order to reach reliability numbers which are in the range of interest, stability berms are added. The material is the general “bermateriaal”. The berm length (measured as the total berm top width) is 0 for the basic geometry, 15 m and 25 m.

C.8.2 Probabilistic prototype

Deterministic sanity check Automatic critical slip surface definition and checked manually

Mean values | Characteristic values

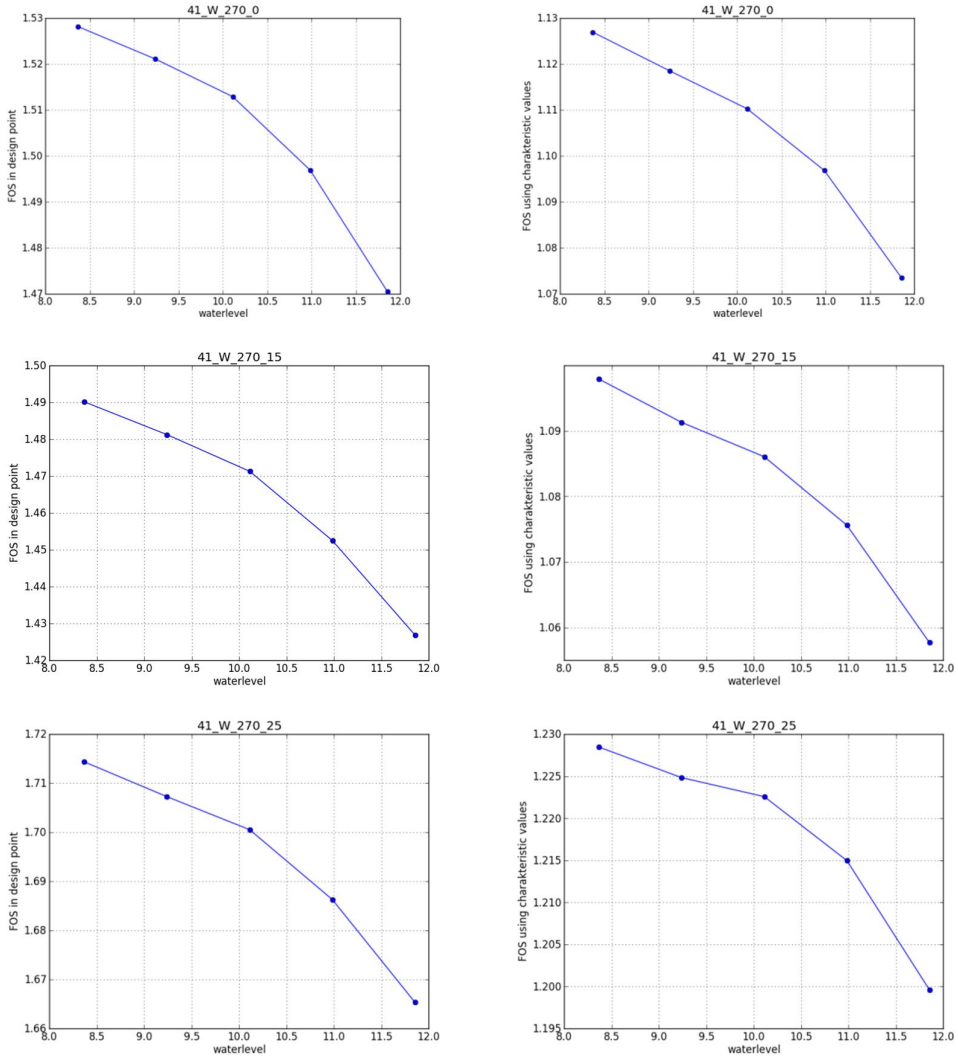

Figure C.50 Output case 41_W_270

Probabilistic fragility curve (Max_beta_interation_inner_loop = 0.05)

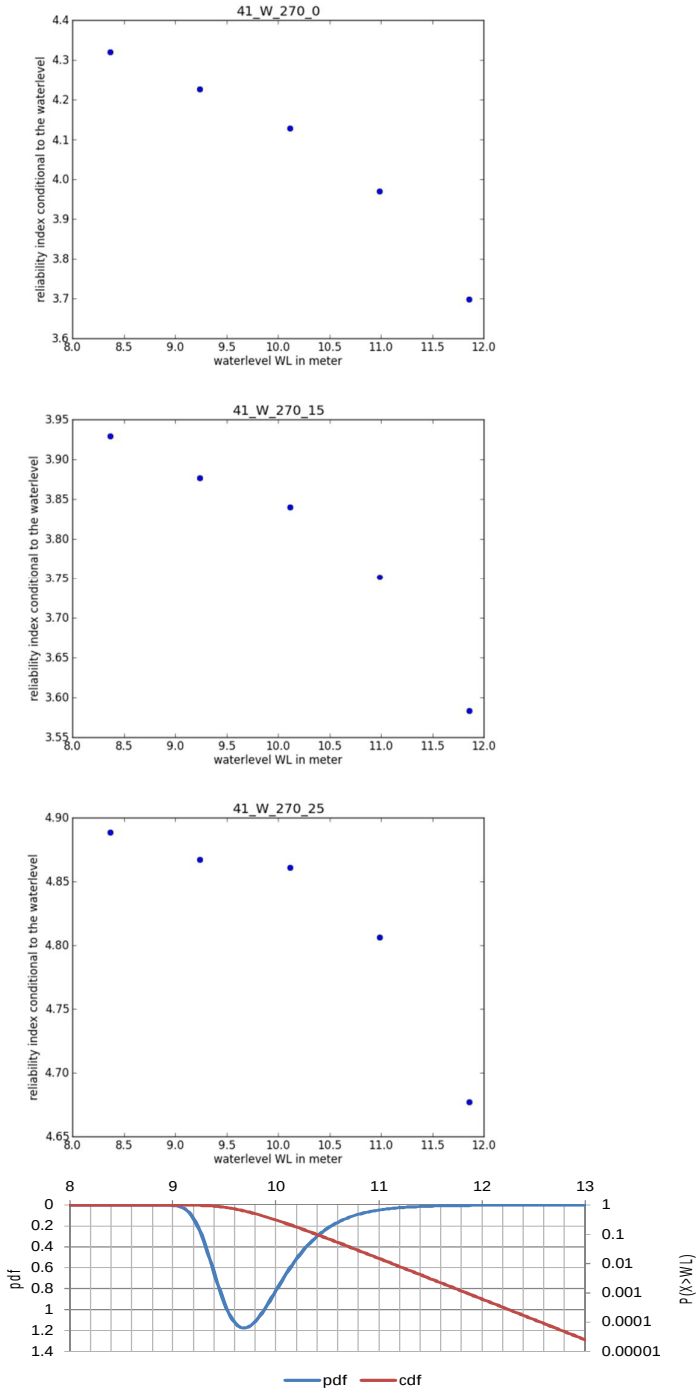

	dp	alpha^2
beta final	4.22	
SF char	1.060	
CuPc		0.759
m		0.011
yieldstress		0.077
cohesion		0.000
fric angle		0.000
model fac	1.062	0.152
water level	9.84	0.001

	dp	alpha^2
beta final	3.85	
SF char	1.050	
CuPc		0.749
m		0.008
yieldstress		0.097
cohesion		0.000
fric angle		0.000
model fac	1.056	0.147
water level	9.82	0.000

	dp	alpha^2
beta final	4.86	
SF char	1.190	
CuPc		0.765
m		0.007
yieldstress		0.093
cohesion		0.000
fric angle		0.000
model fac	1.067	0.135
water level	9.80	0.000

Figure C.51 Output case 41_W_270

It is remarked that the reliability for the 15 metre berm is lower than the basic case. The reason is that in the cases +15 and +25 metre berm a higher berm is schematized. This influences the effective stresses, OCR, and shear strength beneath the berm, in particular at the level of the horizontal part of the slip circle.

Cumulative alpha values conditional to the water level

Basic geometry

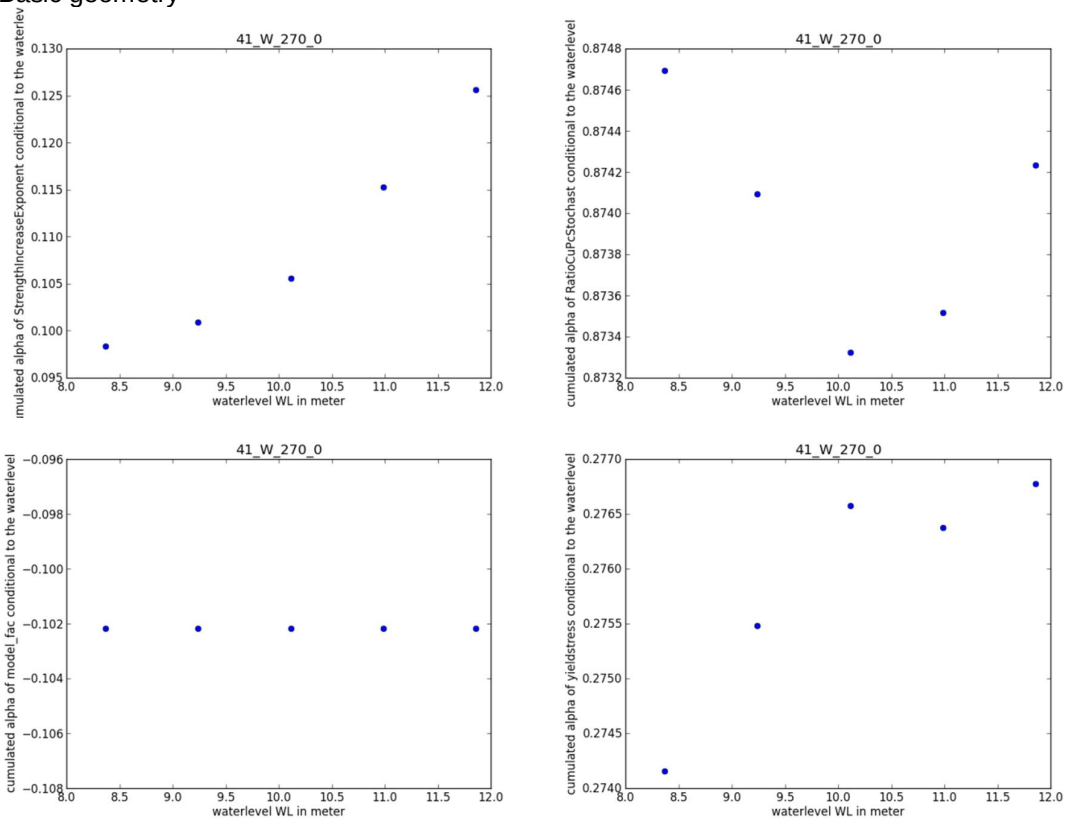

Figure C.52 Output case 41_W_270

Basic geometry + 15m berm

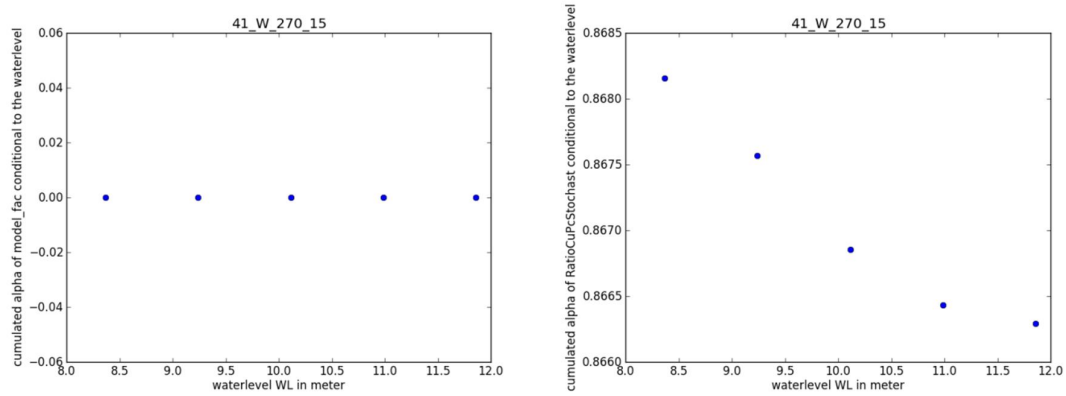

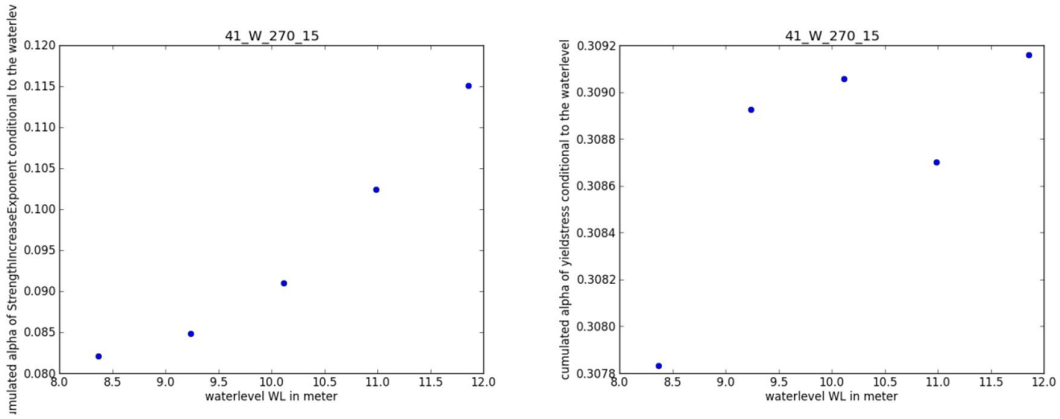

Figure C.53 Output case 41_W_270

Basic geometry + 25m berm

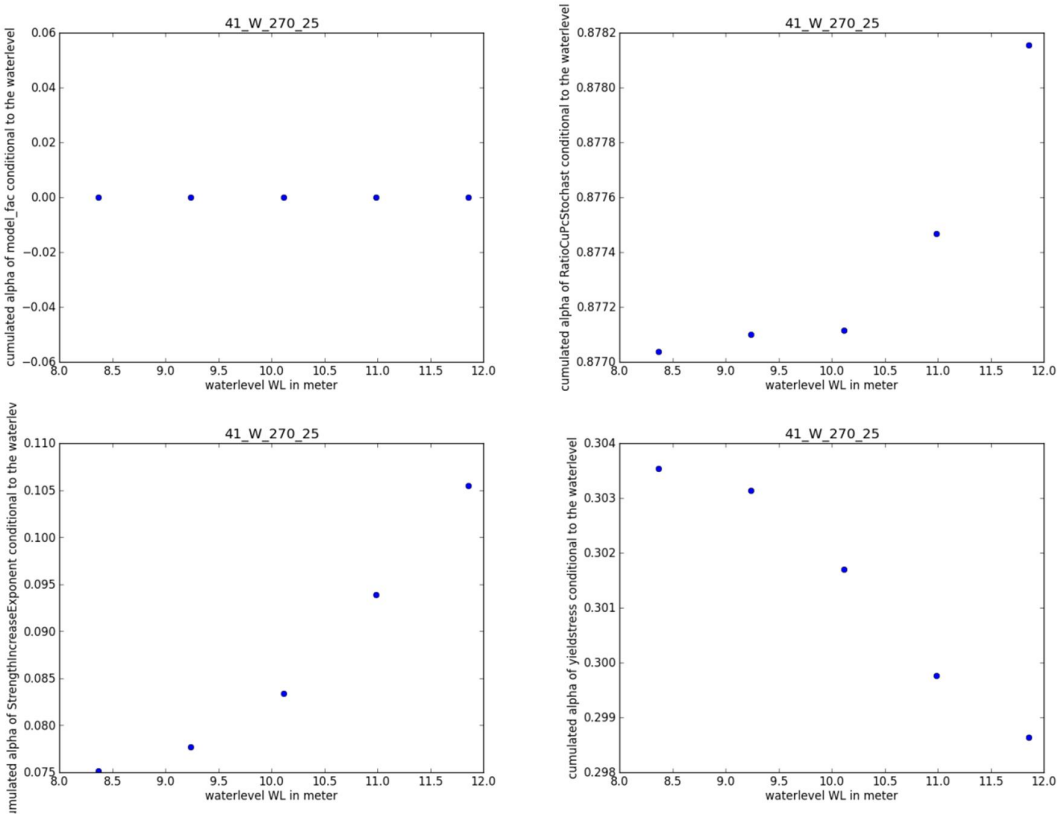

Figure C.54 Output case 41_W_270

Slip circle in design point

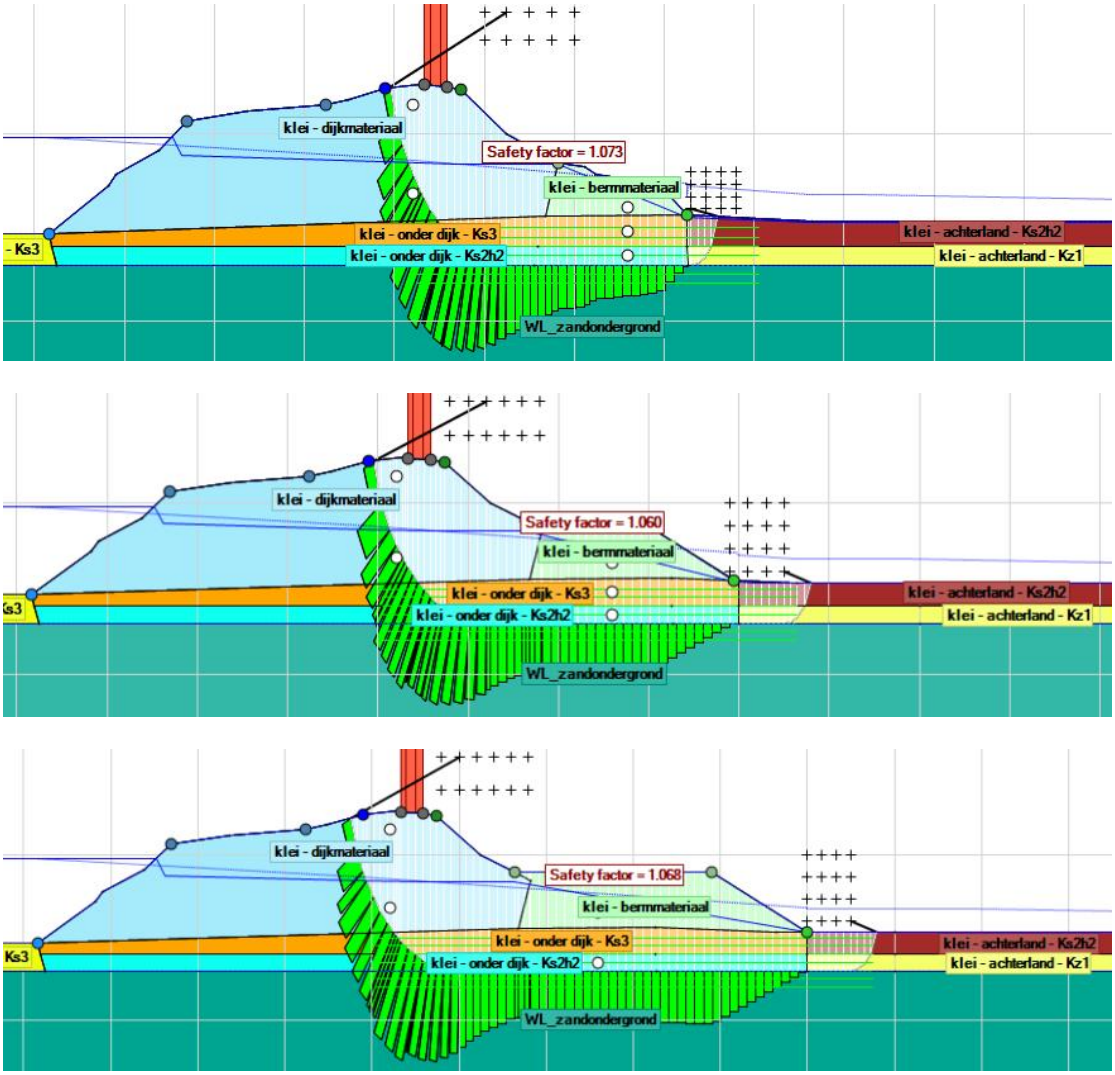

Figure C.55 Slip circle in design point

C.9 41_M_28

This appendix describes the steps and decisions made in setting up and performing probabilistic calculations for slip failure of the inner slope for a specific cross section. Furthermore it summarizes the intermediate results for this case.

C.9.1 Setup

Location and geometry

The location of this cross section (VNK: 41_Maas_Hm28_83_Mean_sce_1, PC-Ring ID 41003002) is at the Maas.

Stratification

The stratification of the subsoil schematization from the VNK-2 project. There is a separation between soils below and besides the dike.

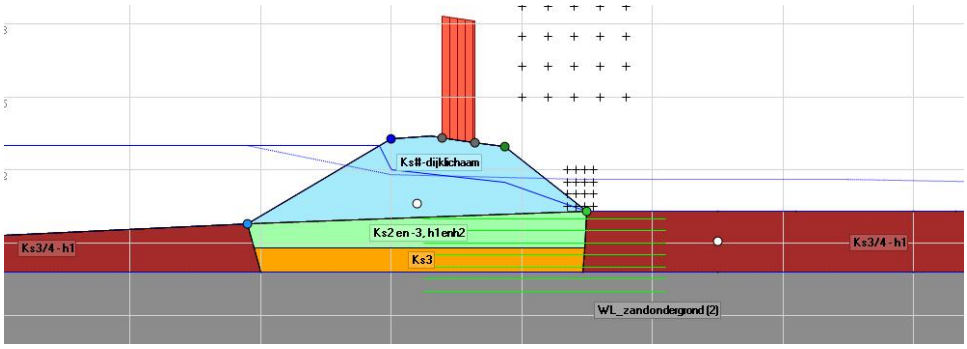

Figure C.56 Schematization

Material properties

Material properties for the soil types are taken from the original schematization (river undrained parameters). The distribution parameters for the random soil types are summed in the next table. This dataset already includes averaging from regional to local data and includes averaging along the slip plane.

The POP value for materials below the dike have a mean value indicated in the table below; the standard deviation is 6 kPa, according to the WTI-SOS database.

Table C.17 Material parameters

Soil type	Vol. weight	Friction angle		Su-ratio		Strength increase exp.		POP
		μ	σ	μ	σ	μ	σ	
WL_zandondergrond (2)	20/20	20	38.02	2.47				
Ks3/4 - h1	15/15				0.9	0.02	0.23	15
Ks3	18.5/18.5				0.9	0.02	0.21	30
Ks2 en -3, h1enh2	17/17				0.9	0.02	0.21	30
Ks#-dijklichaam	18/18				0.9	0.02	0.45	30

Waternet

The creation of phreatic lines is done by D-Geo Stability, according to the following options.

Table C.18 Waternet Creation options

Option	Value
Creation method:	Create Waternet
Dike/soil material	Clay dike on clay
PL1 line creation method	Ringtoets WTI 2017

Since the MHW according to the new safety standards for this cross section is higher than the crest level, the MHW and water level distribution is “transposed” to a plausible value: 1,0 m below the crest. The decimate height and exceedance frequency are taken from the PC-Ring database:
h_{dec} = 0,728 m
$1/F_{exc}$ = 1/10000
MHW = NAP +13.405m

The average high outside water level GHW is taken as the water level at mean discharge for the river, NAP +7.7 m. The minimum phreatic line in the dike body is defined by the Dupuit water level: NAP +11.19 m. The polder water level is assumed to be at the inner toe of the dike.

For the PL3 and PL2 schematization, the leakage length is used. In this case back calculated from the WTI Piping calculations. λ_{out} 272 m and λ_{polder} 992 m.

The intrusion length is determined according to Schoofs en Van Duinen (2006). Based on the stratification and the duration of high water, the intrusion length is found to be 7,5 m. However, this length is larger than half the impermeable layer thickness; therefore this intrusion length is not realistic anymore. The intrusion length is taken as 0, so the phreatic line will be interpolated from PL3 to PL1.

Traffic load

A uniform load of 13kN/m2 over a width of 2,5 m is applied as temporary load for traffic in emergency situations.

Yield stress points

The yield stress points are defined in each layer. The yield stress value is defined at daily water level by the next equation $\sigma_y = \sigma'_{v,i} + POP$. The used POP value is based on expert knowledge.

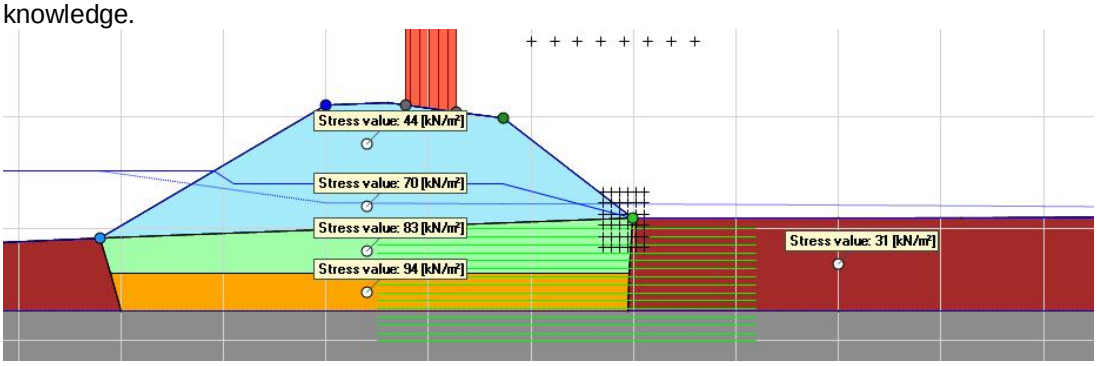

Figure C.57 Schematization of yield stress

Other information

Slip circle search method is Uplift-Van. The grid is predefined; the option “move grid” is checked. For the final design point it will be checked whether the critical slip circle is valid (centre point of active and passive circle not at the edge of the grid).

The blanket layer is less thick than 4 metre, so uplift can occur; therefore the shear strength has to be reduced for uplift conditions:
No reduction of c-phi in case uplift potential n < 1,199
Full reduction of c-phi in case uplift potential n > 1,200

Stability berms

In order to reach reliability numbers which are in the range of interest, stability berms are added. The material is the general “bermmateriaal”. The berm length (measured as the total berm top width) is 0 for the basic geometry, 7 m and 15 m.

C.9.2 Probabilistic prototype

Deterministic sanity check Automatic critical slip surface definition and checked manually

Mean values

Berm = 0 m

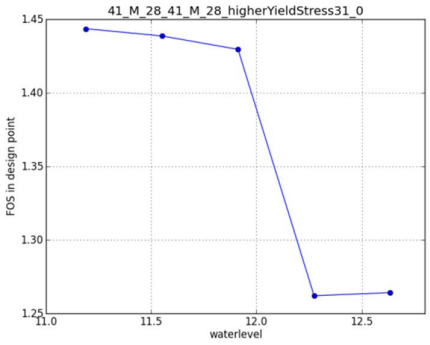

Characteristic values

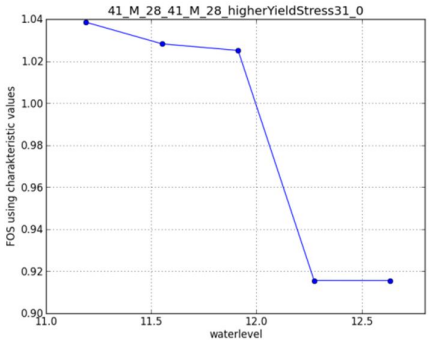

Figure C.58 Output case 41_M_28

Berm = 7.5 m

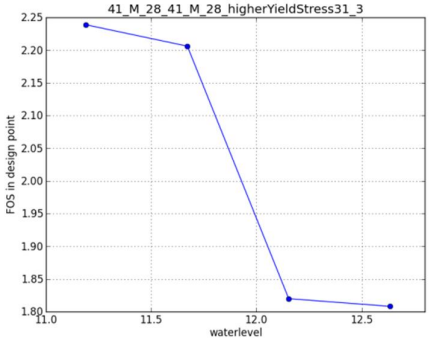

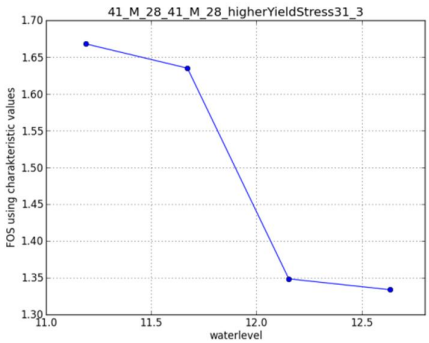

Figure C.59 Output case 41_M_28

Berm = 10 m

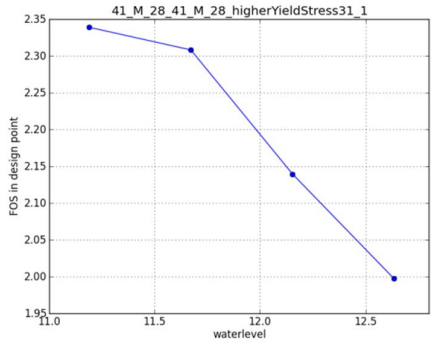

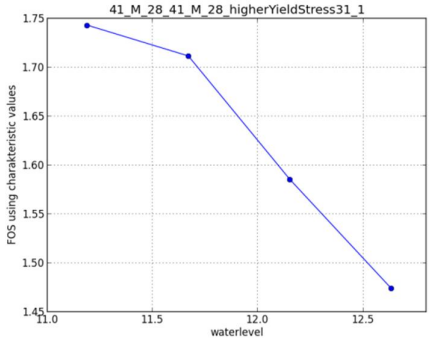

Figure C.60 Output case 41_M_28

Berm = 15 m

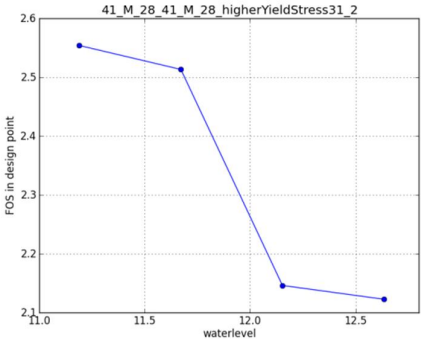

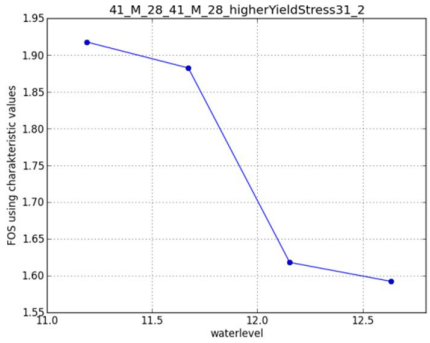

Figure C.61 Output case 41_M_28

Probabilistic fragility curve (Max_beta_interation_inner_loop = 0.05)

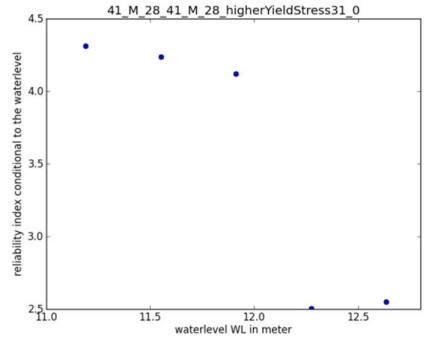

	dp	alpha^2
beta final	4.41	
SF char	0.915	
CuPc		0.43
m		0.01
yieldstress		0.41
cohesion		0.00
fric angle		0.00
model fac	1.05	0.15
water level	10.71	0.00

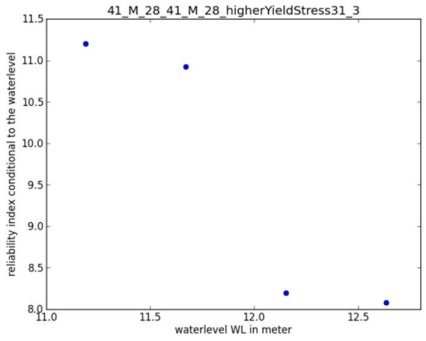

	dp	alpha^2
beta final	3.774	
SF char	1.3	
CuPc		0.01
m		0.00
yieldstress		0.01
cohesion		0.00
fric angle		0.00
model fac	1.11	0.01
water level	12.14	0.97

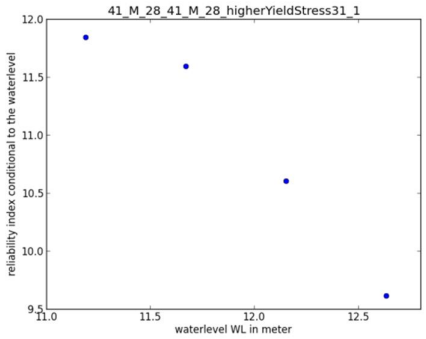

	dp	alpha^2
beta final	5.84E+00	
SF char	1.4	
CuPc		0.03
m		0.00
yieldstress		0.04
cohesion		0.00
fric angle		0.00
model fac	1.03	0.01
water level	16.29	0.92

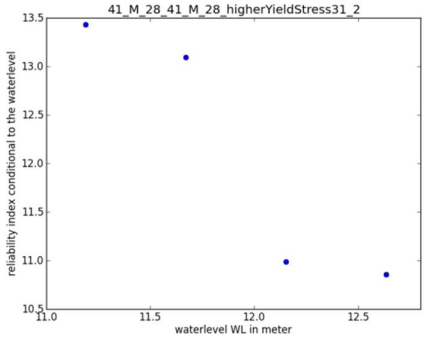

	dp	alpha^2
beta final	10.9	
SF char	1.7	
CuPc		0.17
m		0.12
yieldstress		0.10
cohesion		0.00
fric angle		0.00
model fac	1.12	0.09
water level	21.11	0.51

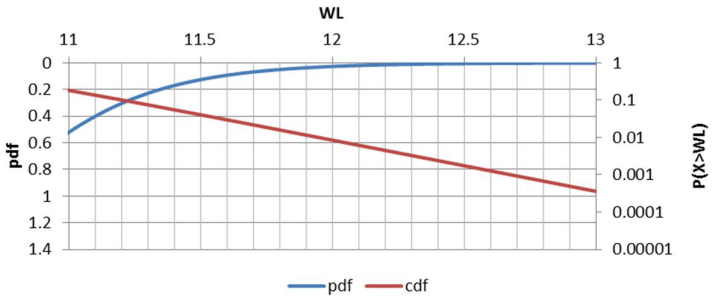

Figure C.62 Output case 41_M_28

Cumulative alpha values conditional to the water level

Basic geometry

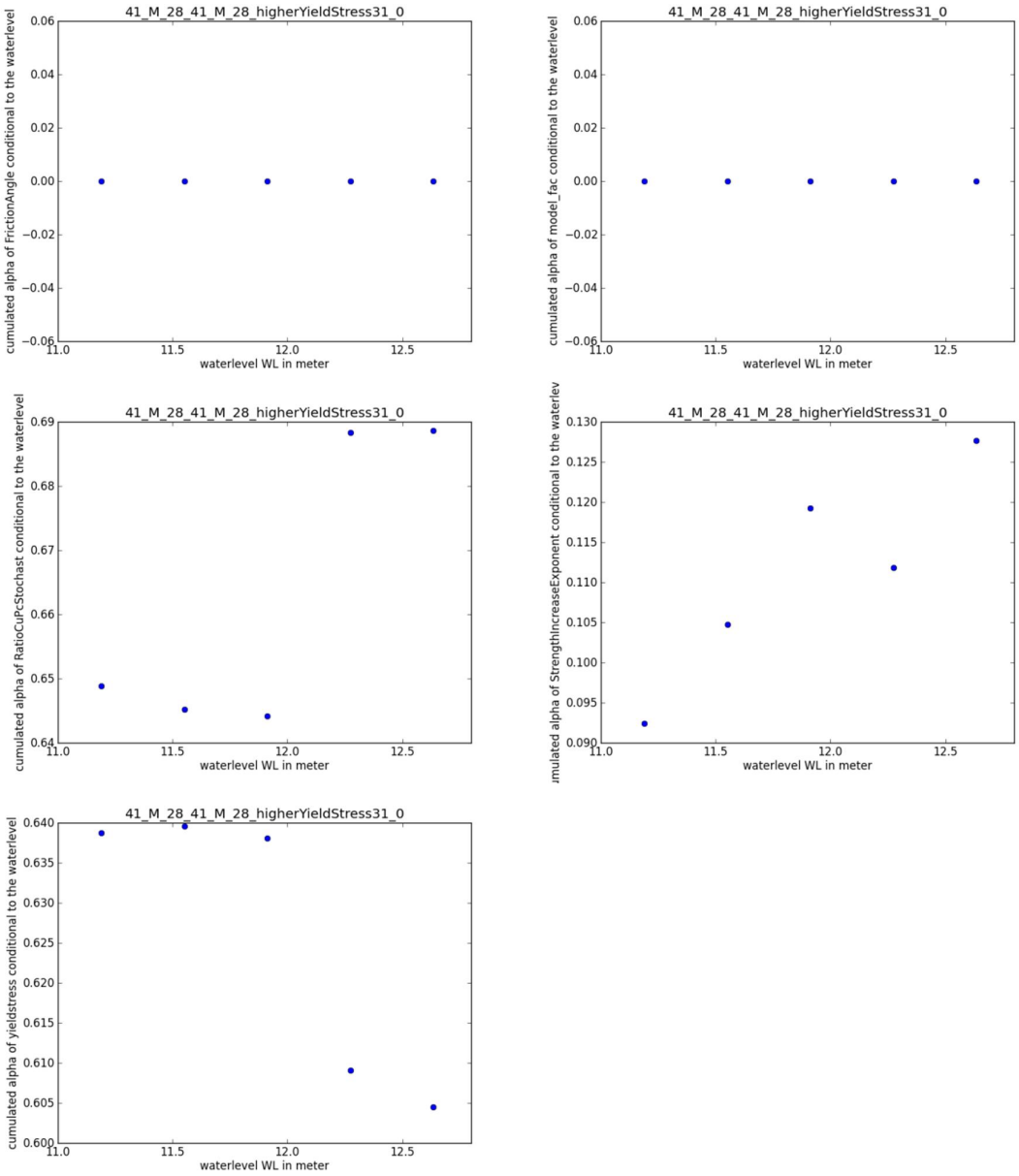

Figure C.63 Output case 41_M_28

Basic geometry + 7.5 m berm

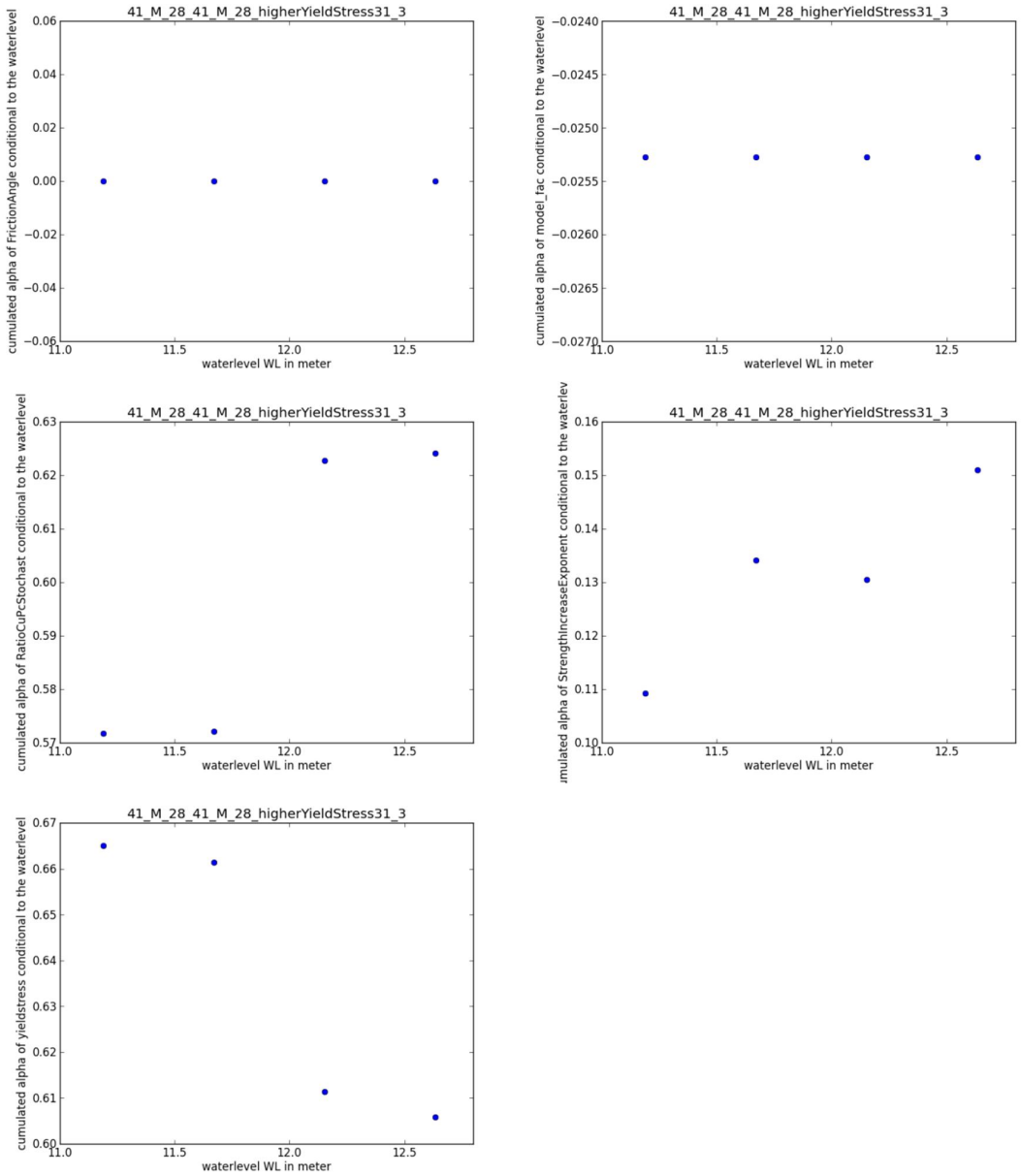

Figure C.64 Output case 41_M_28

Basic geometry + 10 m berm

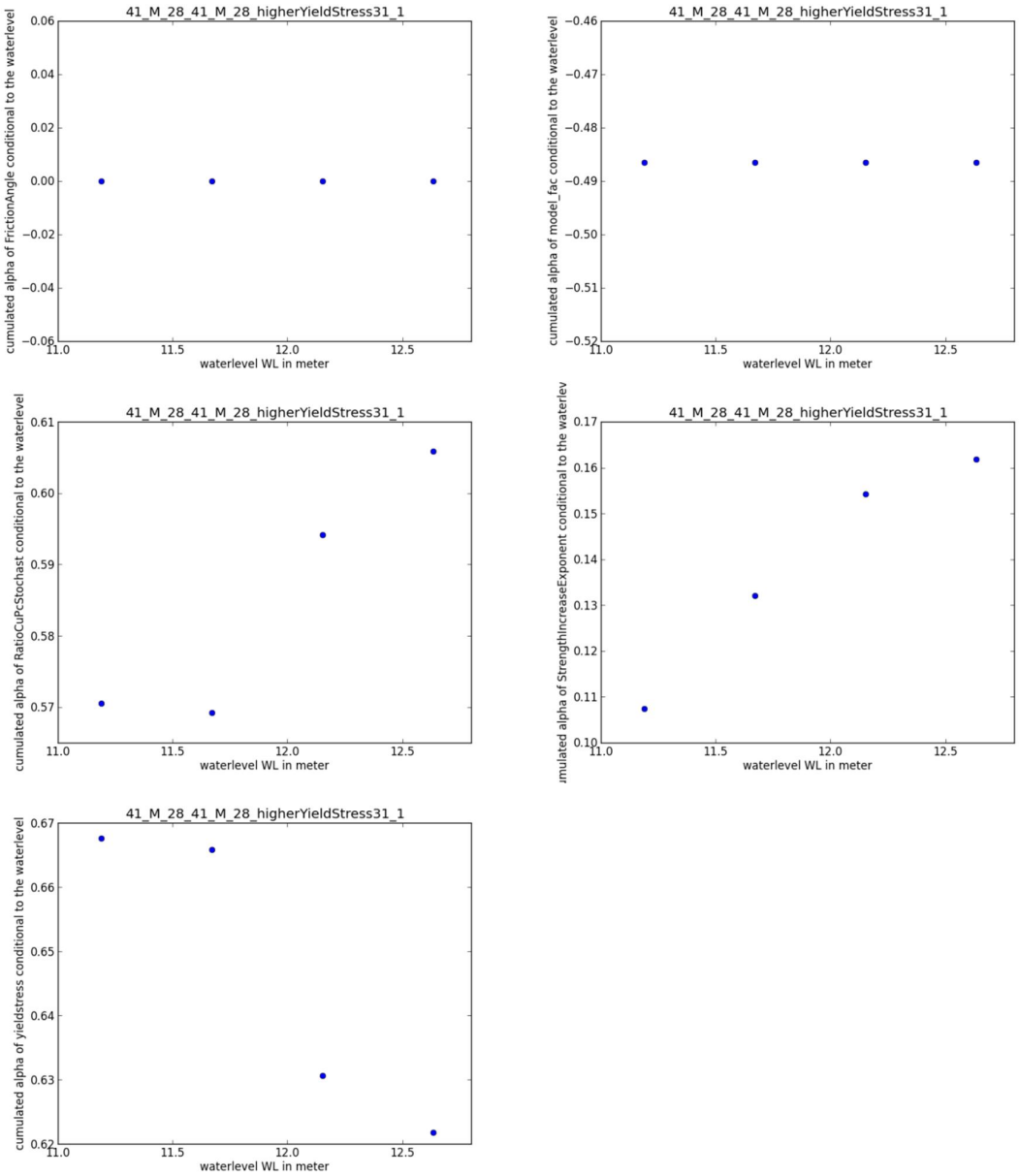

Figure C.65 Output case 41_M_28

Basic geometry + 15 m berm

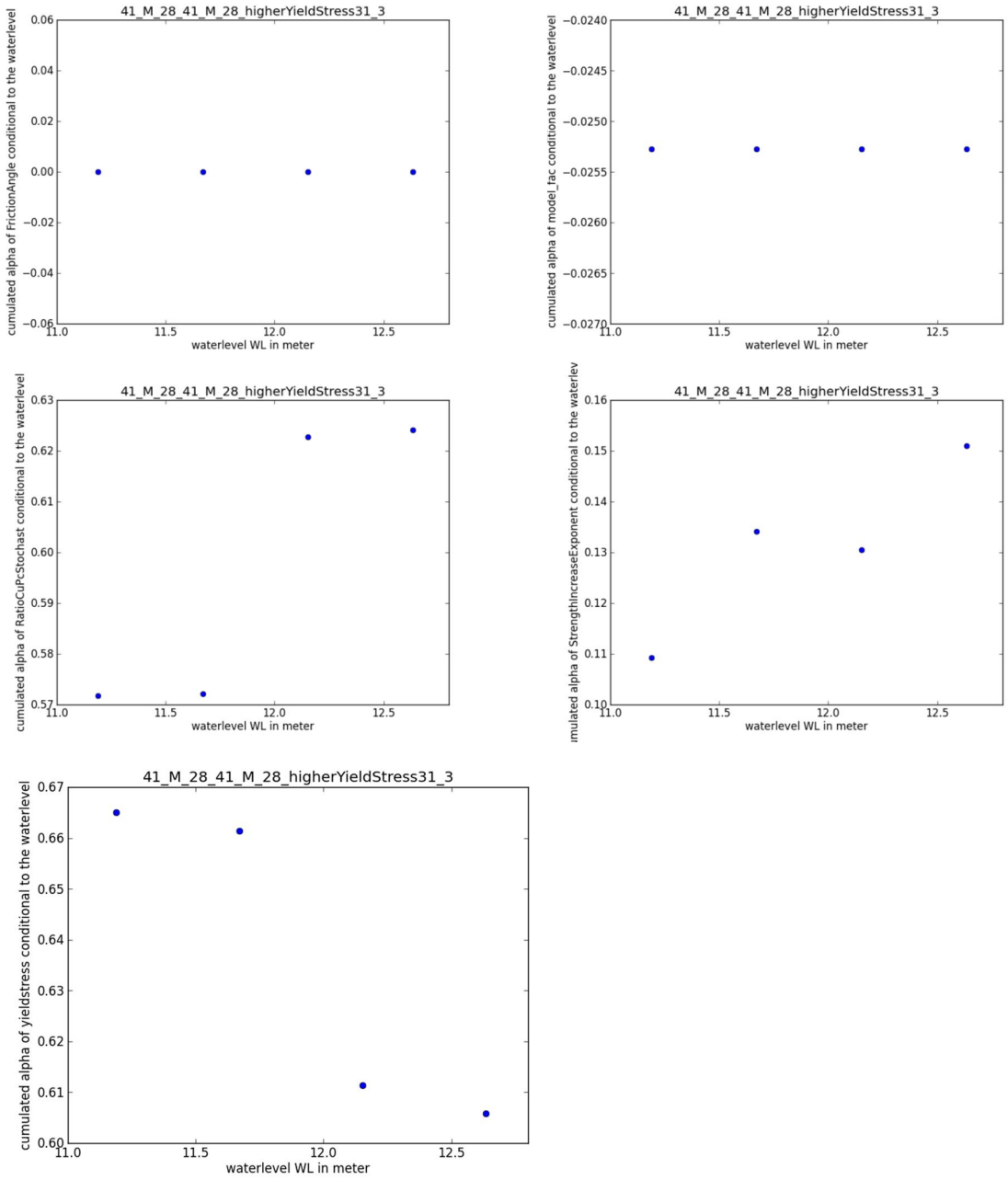

Figure C.66 Output case 41_M_28

Slip circle in design point

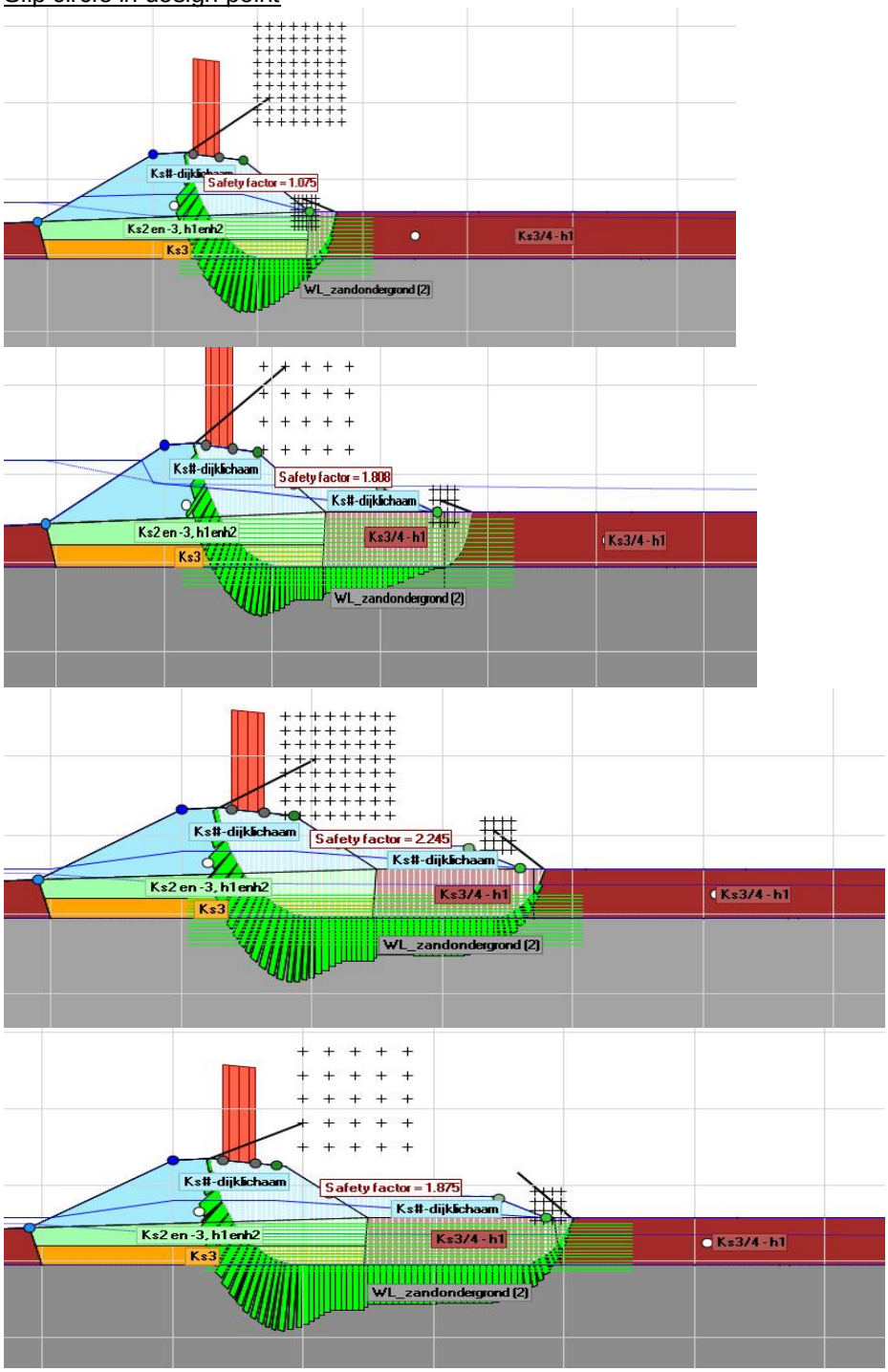

Figure C.67 Slip circle in design point

C.10 DV13

This appendix describes the steps and decisions made in setting up and performing probabilistic calculations for slip failure of the inner slope for a specific cross section. Furthermore it summarizes the intermediate results for this case.

C.10.1 Setup

Location and geometry

The location of this cross section (VNK: DV13_DP14_5_Bishop_RF_110519_Mean_sce_1, PC-Ring ID 12002008) is at the Maas.

Stratification

The stratification of the subsoil schematization from the VNK-2 project. There is a separation between soils below and besides the dike.

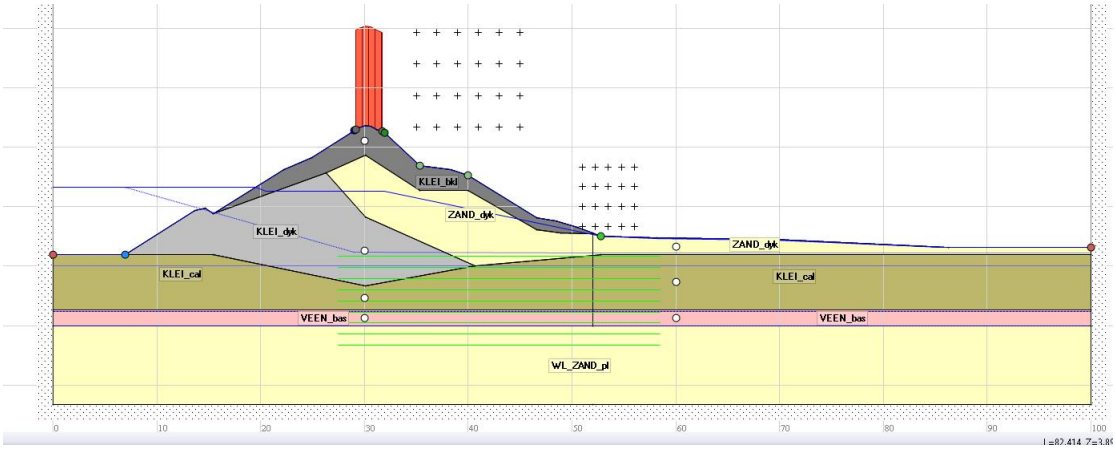

Figure C.68 Schematization

Material properties

Material properties for the soil types are taken from the original schematization (marine undrained parameters). The distribution parameters for the random soil types are summed in the next table. This dataset already includes averaging from regional to local data and includes averaging along the slip plane.

The POP value for materials below the dike have a mean value indicated in the table below; the standard deviation is 6 kPa, according to the WTI-SOS database.

Table C.19 Material parameters

Soil type	Vol. weight	Friction angle		Su-ratio		Strength increase exp.		POP
		μ	σ	μ	σ	μ	σ	
ZAND_dyk	20/20	36.8	2.4					
WL_ZAND_pl	20/20	42.2	2.5					
KLEI_bkl	20/20			0.45	0.03	0.9	0.02	0
KLEI_dyk	21/21			0.45	0.03	0.9	0.02	0
KLEI_cal	14/14			0.19	0.05	0.9	0.02	11.2
VEEN_bas	10.5/10.5			0.32	0.02	0.9	0.02	10.32

Waternet

The creation of phreatic lines is done by D-Geo Stability, according to the following options.

Table C.20 Waternet Creation options

Option	Value
Creation method:	Create Waternet
Dike/soil material	Clay dike on clay
PL1 line creation method	Ringtoets WTI 2017

Since the MHW according to the new safety standards for this cross section is higher than the crest level, the MHW and water level distribution is “transposed” to a plausible value: 1,0 m below the crest. The decimate height and exceedance frequency are taken from the PC-Ring database:
h_{dec} = 0,253 m
$1/F_{exc}$ = 1/3000
MHW = NAP +0.982 m

The average high outside water level GHW is taken as the water level at mean discharge for the river, NAP +-0.20 m. The minimum phreatic line in the dike body is defined by the Dupuit water level: NAP +0.046 m. The polder water level is assumed to be at the inner toe of the dike.

For the PL3 and PL2 schematization, the leakage length is used. In this case back calculated from the WTI Piping calculations. λ_{out} 167 m and λ_{polder} 590 m.

The intrusion length is determined according to Schoofs en Van Duinen (2006). Based on the stratification and the duration of high water, the intrusion length is found to be 7,5 m. However, this length is larger than half the impermeable layer thickness; therefore this intrusion length is not realistic anymore. The intrusion length is taken as 0, so the phreatic line will be interpolated from PL3 to PL1.

Traffic load

A uniform load of 13kN/m2 over a width of 2,5 m is applied as temporary load for traffic in emergency situations.

Yield stress points

The yield stress points are defined in each layer. The yield stress value is defined at daily water level by the next equation $\sigma_y = \sigma'_{v,i} + POP$. The used POP value is based on expert knowledge.

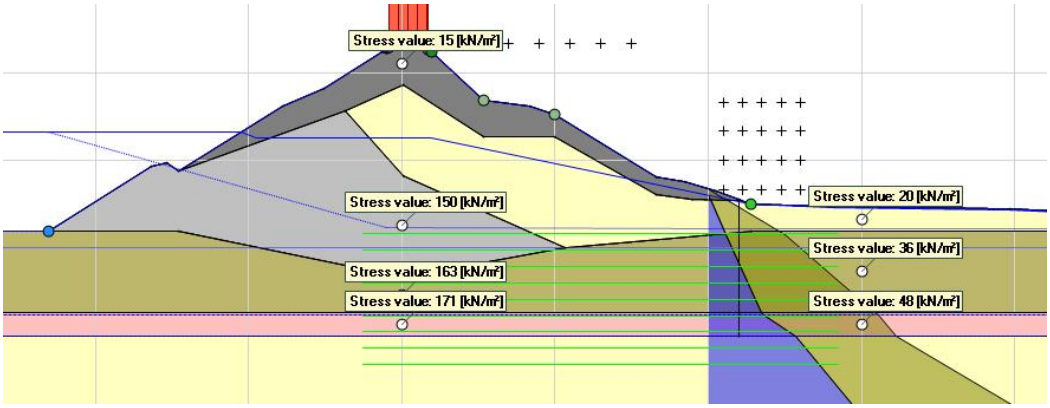

Figure C.69 Schematization of yield stress

Other information

Slip circle search method is Uplift-Van. The grid is predefined; the option “move grid” is checked. For the final design point it will be checked whether the critical slip circle is valid (centre point of active and passive circle not at the edge of the grid).

The blanket layer is less thick than 4 metre, so uplift can occur; therefore the shear strength has to be reduced for uplift conditions:
No reduction of c-phi in case uplift potential n < 1,199
Full reduction of c-phi in case uplift potential n > 1,200

Stability berms

In order to reach reliability numbers which are in the range of interest, stability berms are added. The material is the general “bermmateriaal”. The berm length (measured as the total berm top width) is 0 for the basic geometry and 5 m.

C.10.2 Probabilistic prototype

Deterministic sanity check Automatic critical slip surface definition and checked manually

Mean values

Berm = 0 m

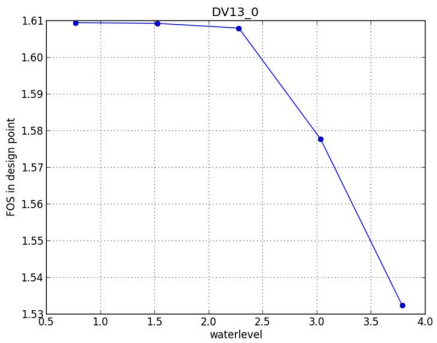

Berm = 5 m

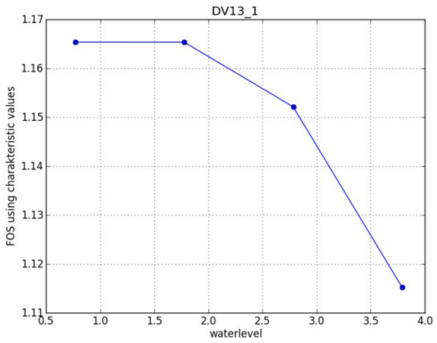

Berm = 10 m

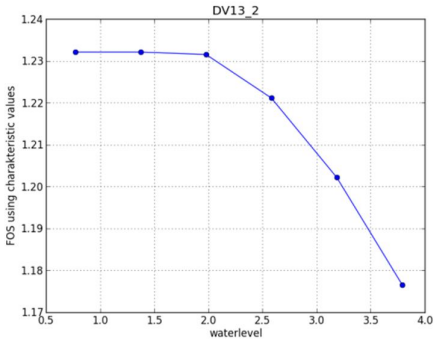

Characteristic values

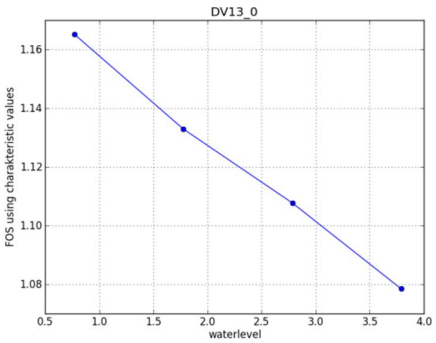

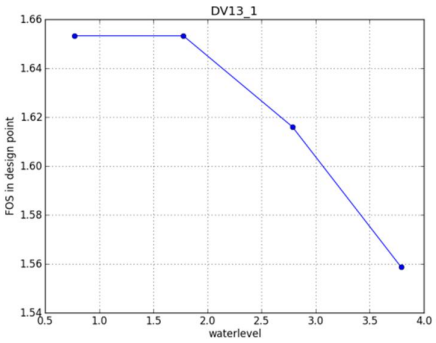

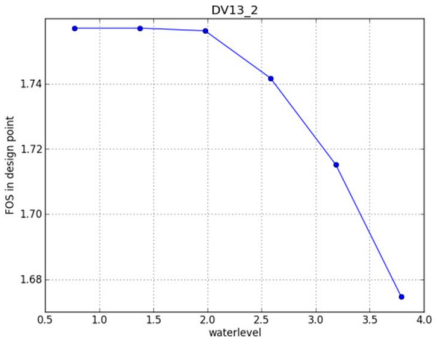

Berm = 15 m

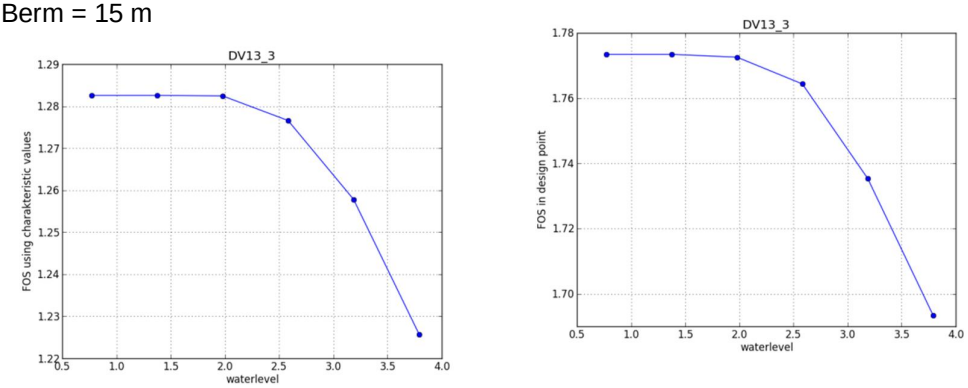

Figure C.70 Output case DV13

Probabilistic fragility curve (Max_beta_interation_inner_loop = 0.05)

Berm= 0 m

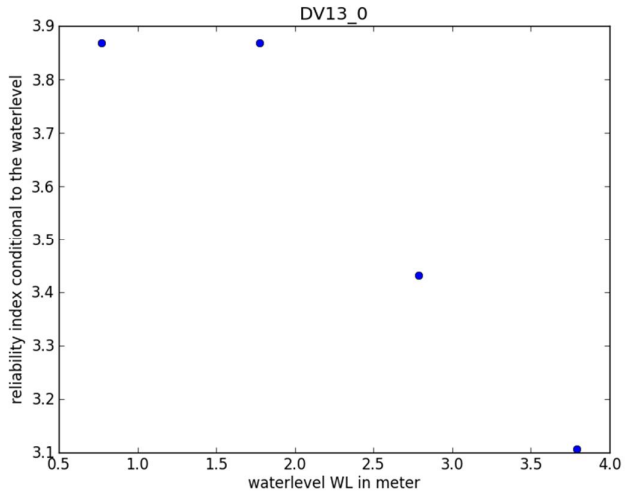

	dp	alpha^2
beta final	3.87	
SF char	1.161	
CuPc		0.79
m		0.00
yieldstress		0.07
cohesion		0.00
fric angle		0.01
model fac	1.05	0.12
water level	1.04	0.00

Berm= 5 m

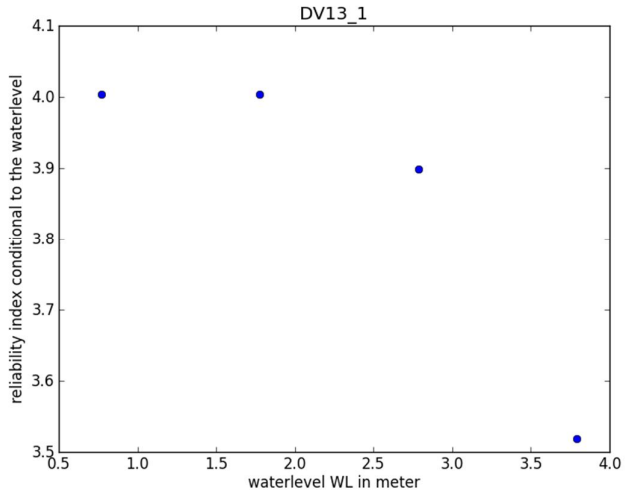

	dp	alpha^2
beta final	4.00	
SF char	1.165	
CuPc		0.81
m		0.00
yieldstress		0.07
cohesion		0.00
fric angle		0.01
model fac	1.05	0.11
water level	1.04	0.00

Berm= 10 m

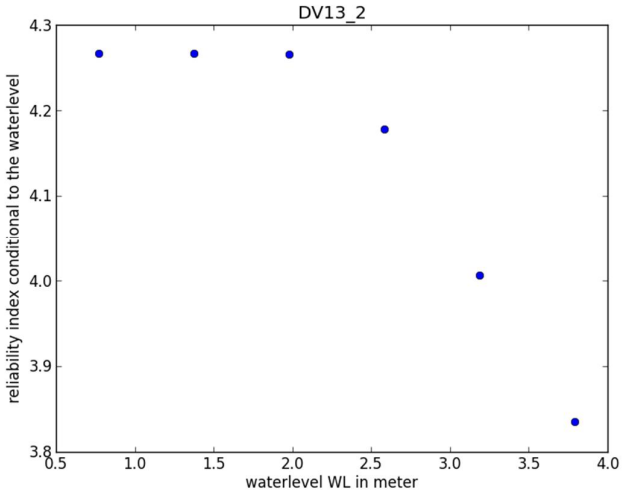

	dp	alpha^2
beta final	4.27	
SF char	1.231	
CuPc		0.84
m		0.00
yieldstress		0.06
cohesion		0.00
fric angle		0.01
model fac	1.04	0.09
water level	1.04	0.00

Berm= 15 m

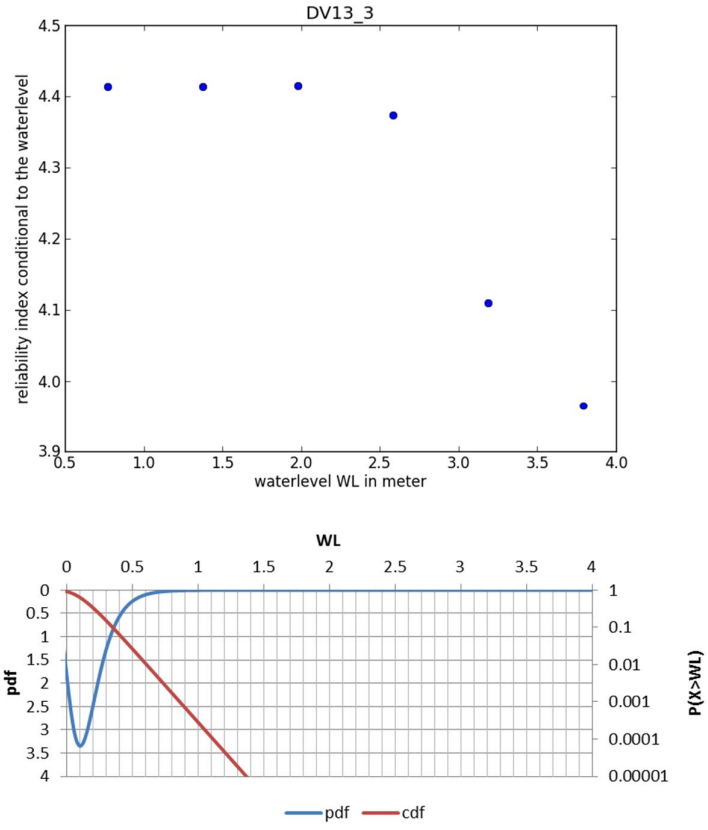

	dp	alpha^2
beta final	4.41	
SF char	1.231	
CuPc		0.85
m		0.00
yieldstress		0.05
cohesion		0.00
fric angle		0.00
model fac	1.04	0.10
water level	1.05	0.00

Figure C.71 Output case DV13

Cumulative alpha values conditional to the water level

Basic geometry

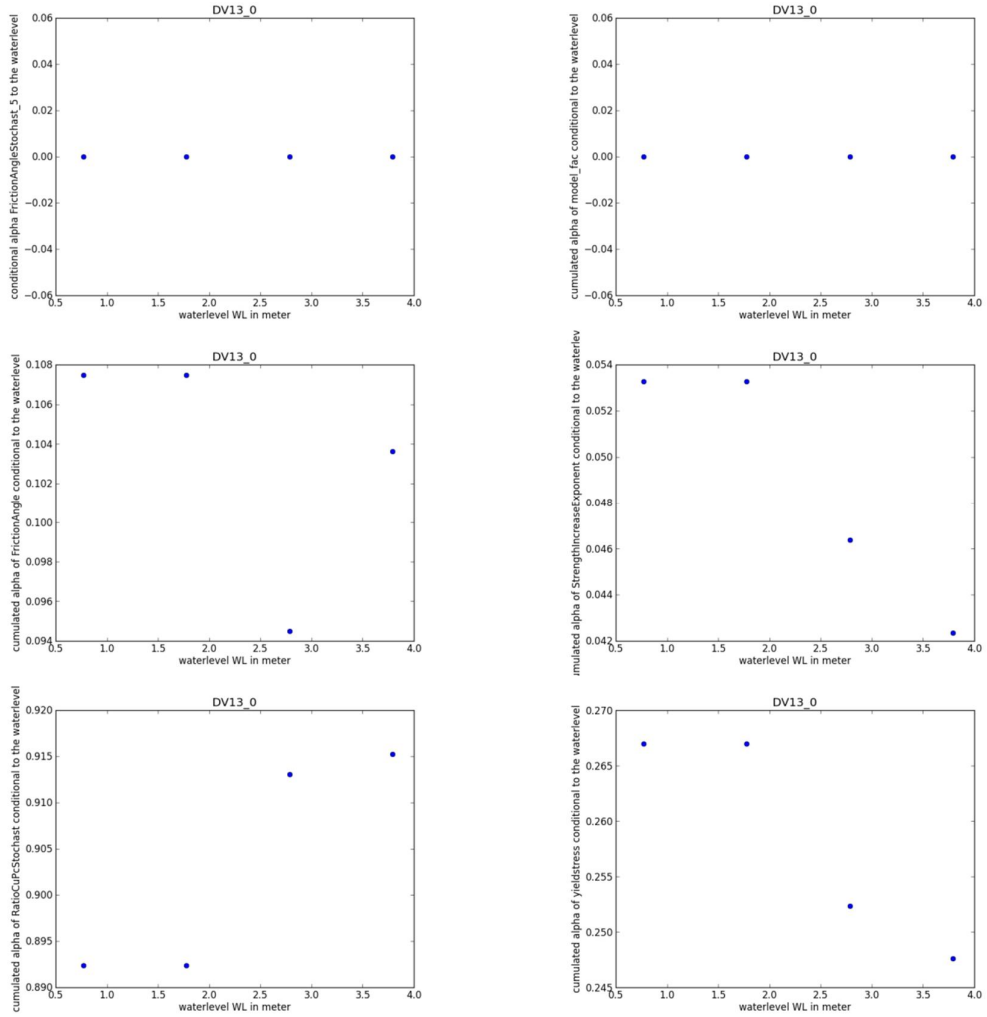

Figure C.72 Output case DV13

Basic geometry + 5 m berm

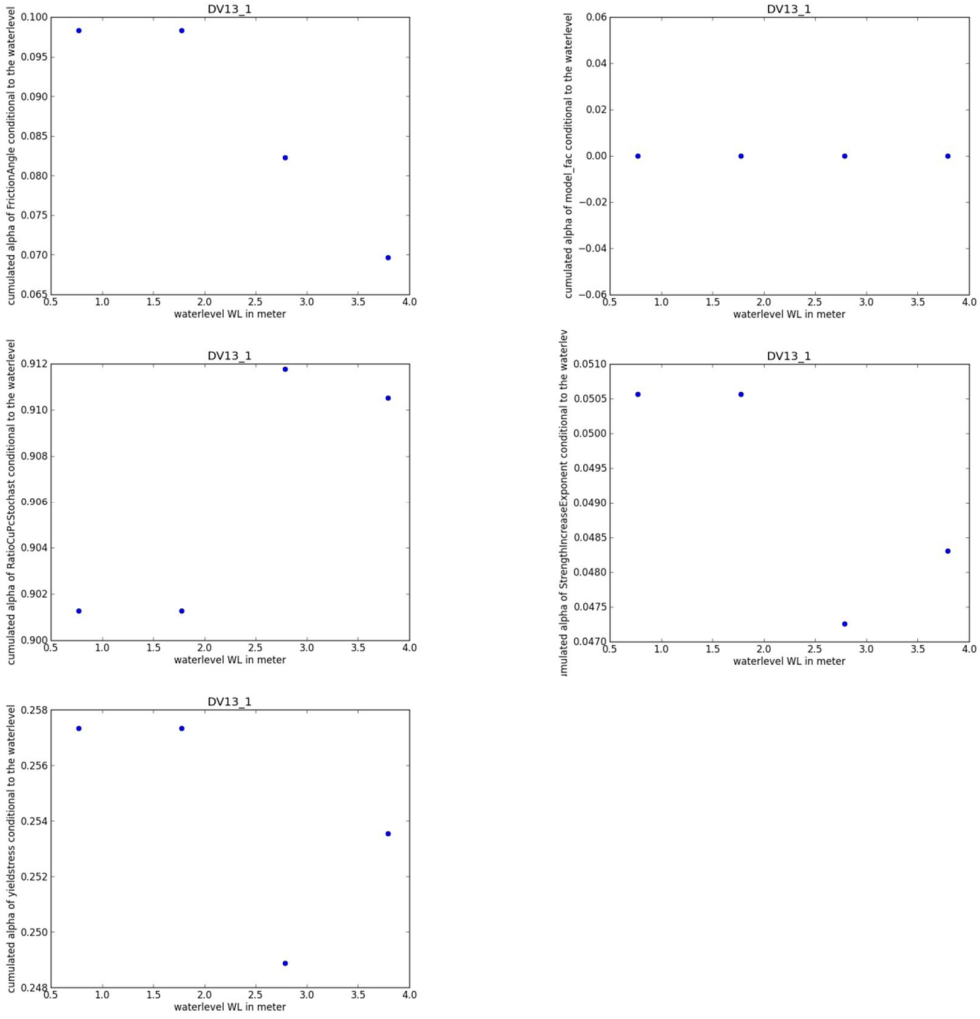

Figure C.73 Output case DV13

Basic geometry + 10 m berm

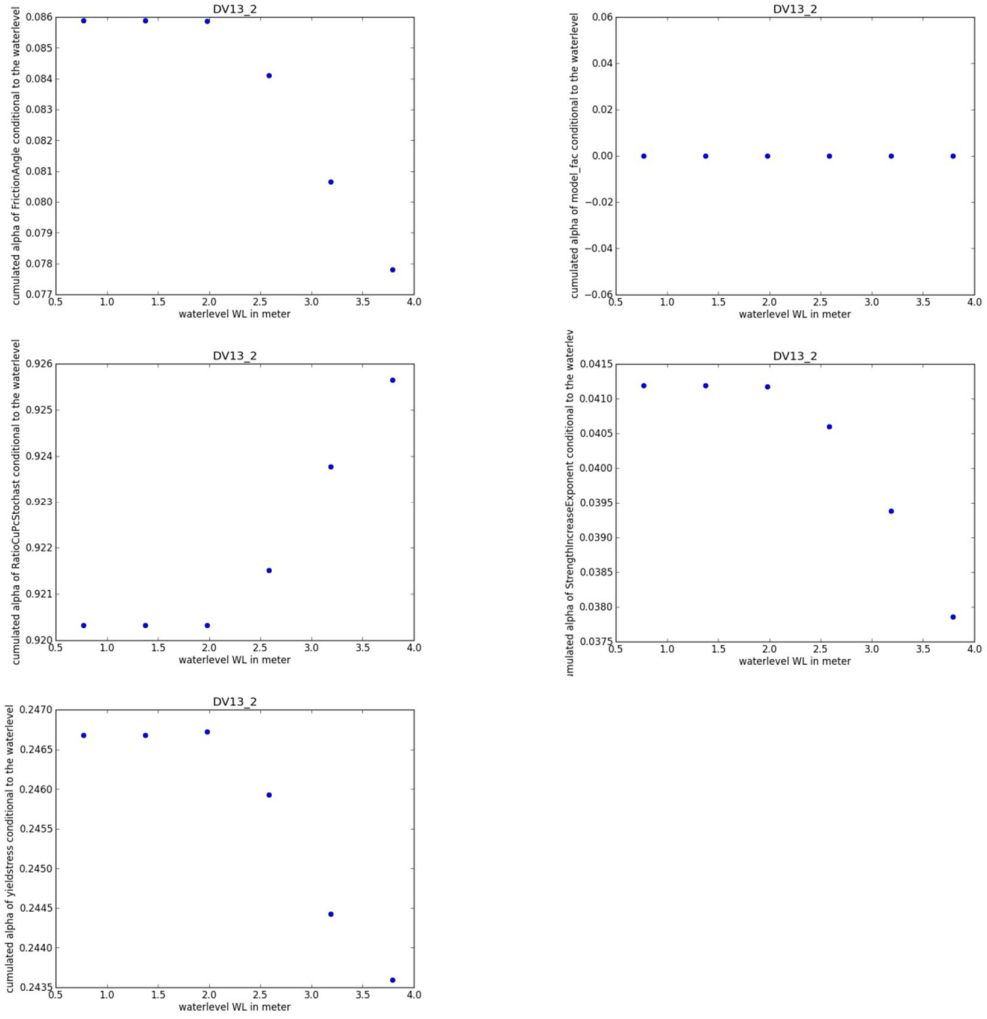

Figure C.74 Output case DV13

Basic geometry + 15 m berm

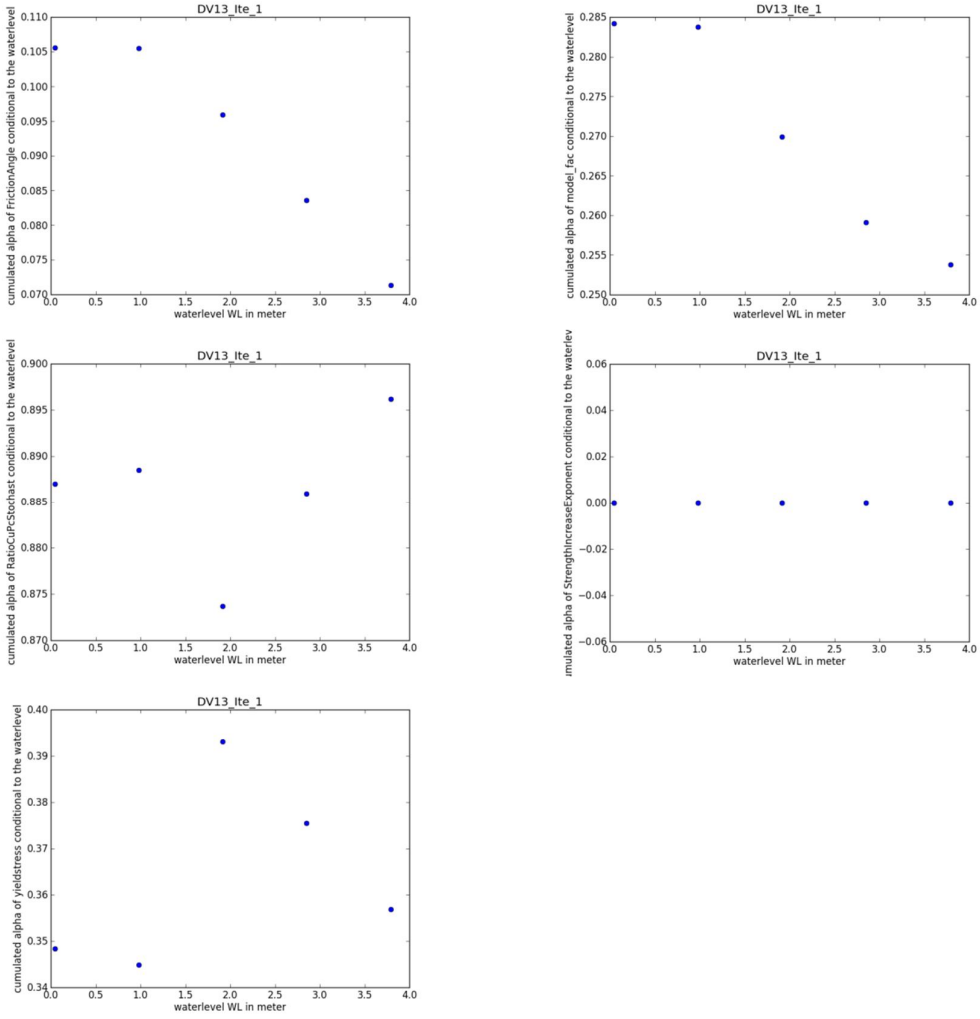

Figure C.75 Output case DV13

<u>Slip circle in design point</u>
Basic geometry + 0 m berm

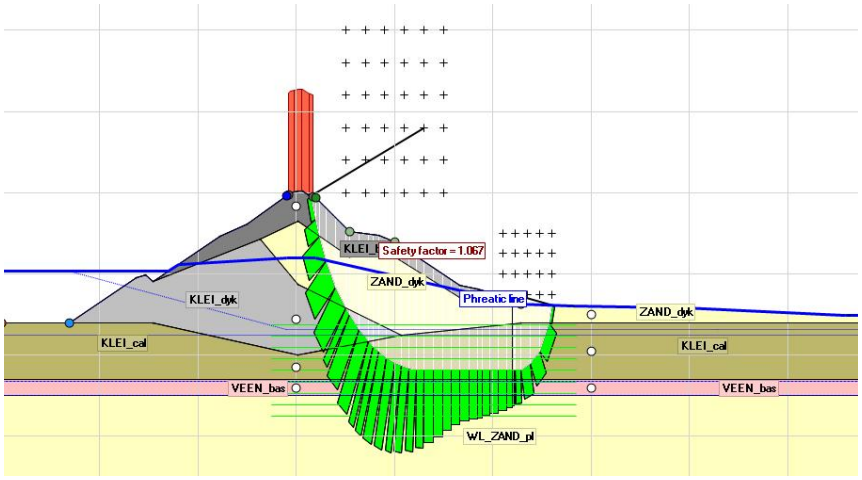

Basic geometry + 5 m berm

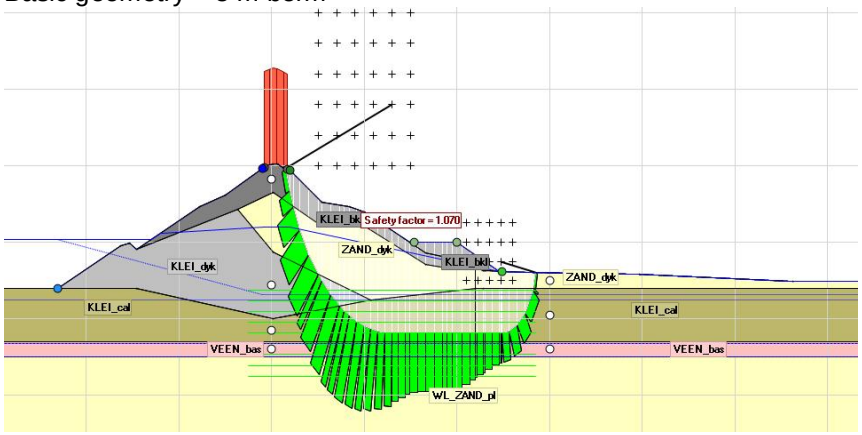

Basic geometry + 10 m berm

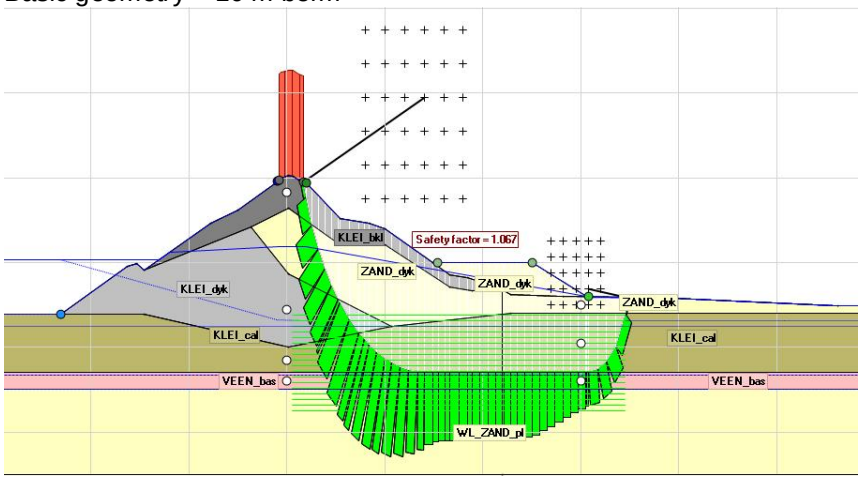

Basic geometry + 15 m berm

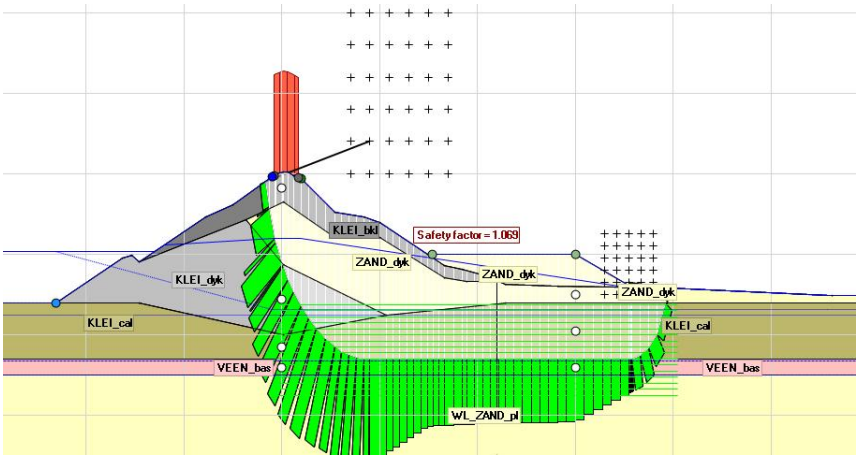

Figure C.76 Slip circle in the design point

C.11 Wsno_0161

This appendix describes the steps and decisions made in setting up and performing probabilistic calculations for slip failure of the inner slope for a specific cross section. Furthermore it summarizes the intermediate results for this case.

C.11.1 Setup

Location and geometry

The location of this cross section (VNK: WsNoo_Dp0161, PC-Ring ID 31001003) is at Zuid Beveland, Western Scheldt, near Kruiningen.

Stratification

The stratification of the subsoil schematization from the VNK-2 project. There is a separation between soils below and besides the dike.

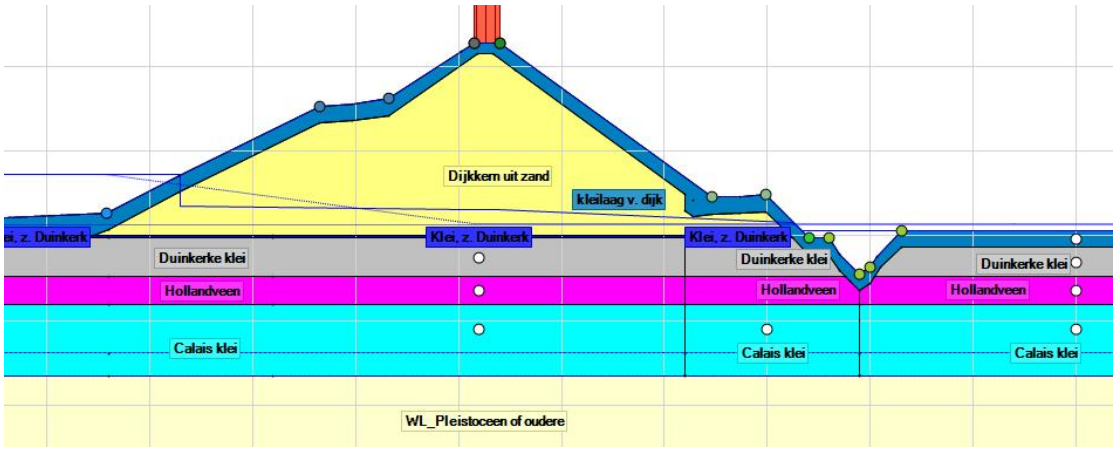

Figure C.77 Schematization

Material properties

Material properties for the soil types are taken from the original schematization (river undrained parameters). The distribution parameters for the random soil types are summed in the next table. This dataset already includes averaging from regional to local data and includes averaging along the slip plane.

The POP has a mean value of 25 kPa for all materials. The standard deviation is 6 kPa, according to the WTI-SOS database.

Table C.21 Material parameters

Soil type	Vol. weight	Friction angle		Su-ratio		Strength increase exp.	
		μ	σ	μ	σ	μ	σ
WL_Pleistoceen of oudere	19/17	34.26	2.36				
Calais klei	18/17			0.21	0.01	0.9	0.02
Hollandveen	10/10			0.32	0.02	0.9	0.02
Duinkerke klei	17.1/17.1			0.21	0.01	0.9	0.02
kleilaag v. dijk	17/17			0.22	0.02	0.9	0.02
Klei, z. Duinkerk	18.1/18.1			0.21	0.01	0.9	0.02
Dijkkern uit zand	19/17	38.02	2.47				
Jong zeezand	19/17	29.89	2.19				

Waternet

The creation of phreatic lines is done by D-Geo Stability, according to the following options.

Table C.22 Waternet Creation options

Option	Value
Creation method:	Create Waternet
Dike/soil material	Clay dike on clay
PL1 line creation method	Ringtoets WTI 2017

The decimate height and exceedance frequency are taken from the PC-Ring database:
h_{dec} = 0,674 m
$1/F_{exc}$ = 1/30000
MHW = NAP +6,715m

The average high outside water level GHW is taken as the tidal mean high water level for the Western Scheldt, NAP +2,75 m. The minimum phreatic line in the dike body is defined by the Dupuit water level: NAP +1,25m. The polder water level in the ditch is NAP +0,25m.

For the PL3 and PL2 schematization, the leakage length is used. In this case back calculated from WTI Piping calculations. λ_{out} 104 m and λ_{polder} 301 m.

The intrusion length is determined according to Schoofs en Van Duinen (2006). Based on the stratification and the duration of high water, the intrusion length is found to be 1,0 m. From the original schematization an intrusion length of 1,1 meter is found; therefore this intrusion length is used.

Traffic load

A uniform load of 13kN/m2 over a width of 2,5 m is applied as temporary load for traffic in emergency situations.

Yield stress points

The yield stress points are defined in each layer. The yield stress value is defined at daily water level by the next equation $\sigma_y = \sigma'_{v,i} + POP$. The used POP value is based on expert knowledge.

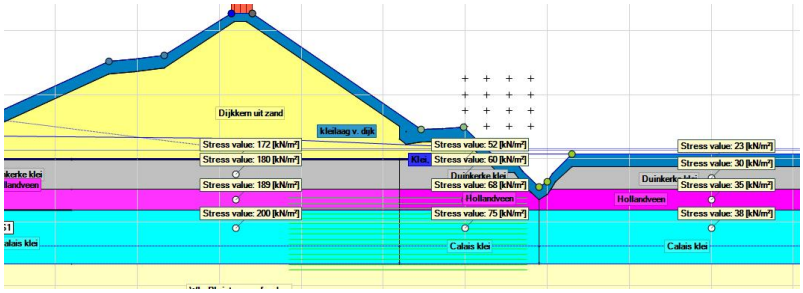

Figure C.78 Schematization of yield stress

Other information

The blanket layer is thicker than 4 metre, so uplift cannot occur; therefore the shear strength will never be reduced for uplift conditions.

Stability berms

In order to reach reliability numbers which are in the range of interest, stability berms are added. The material is the general “dijkkern uit zand”. The berm length (measured as the total berm top width) is 0 for the basic geometry, 10 m and 20 m.

C.11.2 Probabilistic prototype

Deterministic sanity check

Mean values

Characteristic values

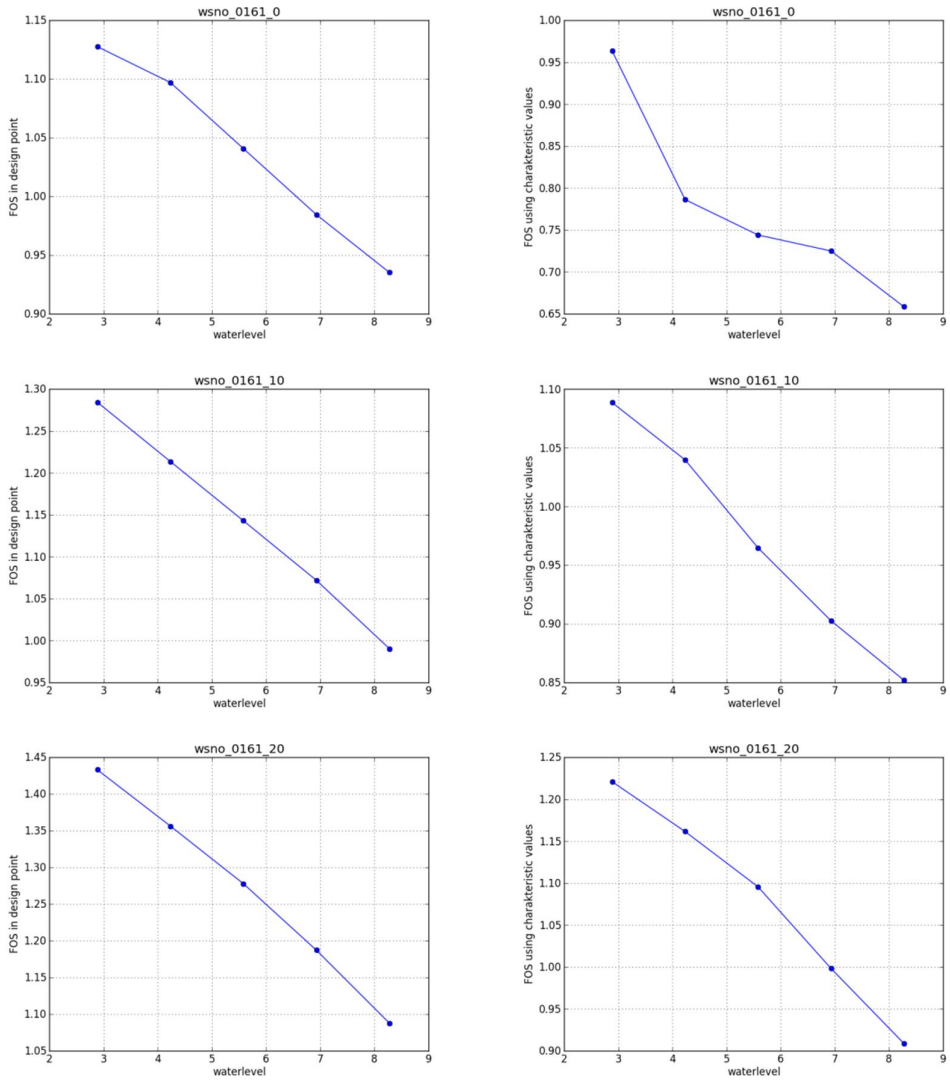

Figure C.79 Output case wsno_0161

Probabilistic fragility curve (Max_beta_interation_inner_loop = 0.05)

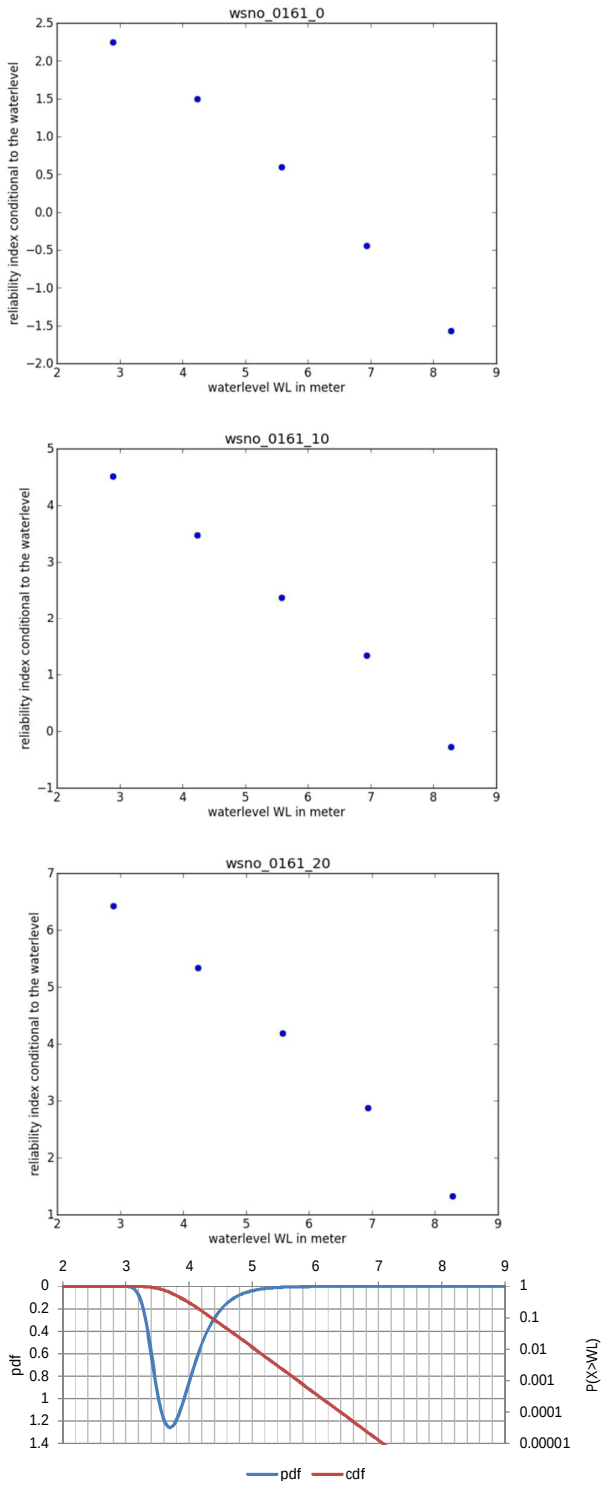

	dp	alpha^2
beta final	1.70	
SF char	0.730	
CuPc		0.314
m		0.005
yieldstress		0.215
cohesion		0.000
fric angle		0.032
model fac	1.042	0.390
water level	3.95	0.043

	dp	alpha^2
beta final	3.60	
SF char	0.920	
CuPc		0.323
m		0.002
yieldstress		0.158
cohesion		0.000
fric angle		0.009
model fac	1.075	0.310
water level	4.56	0.199

	dp	alpha^2
beta final	5.04	
SF char	1.020	
CuPc		0.149
m		0.001
yieldstress		0.126
cohesion		0.000
fric angle		0.004
model fac	1.071	0.143
water level	6.53	0.577

Figure C.80 Output case wsno_0161

Cumulative alpha values conditional to the water level

Basic geometry

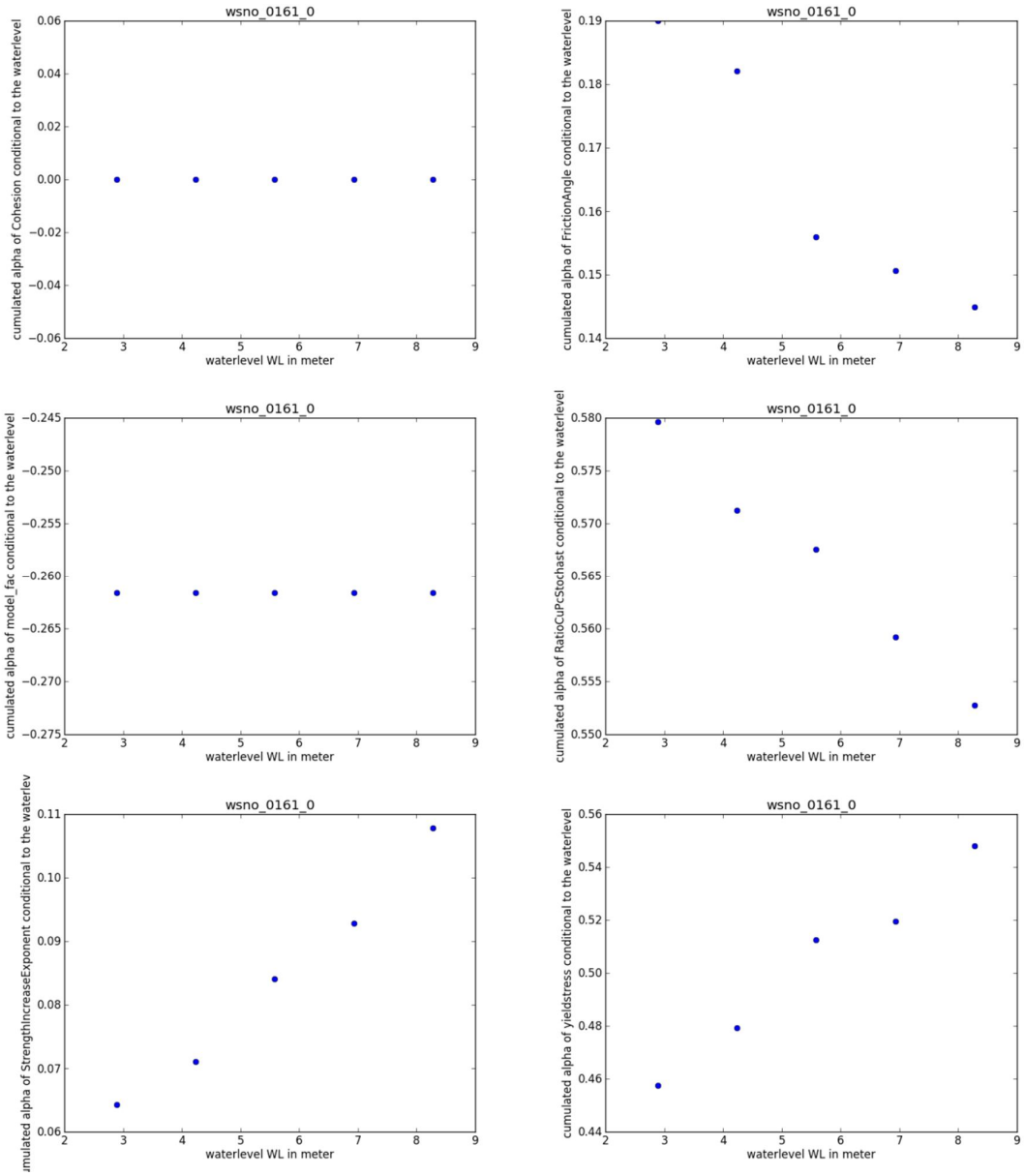

Figure C.81 Output case wsno_0161

Basic geometry + 10m berm

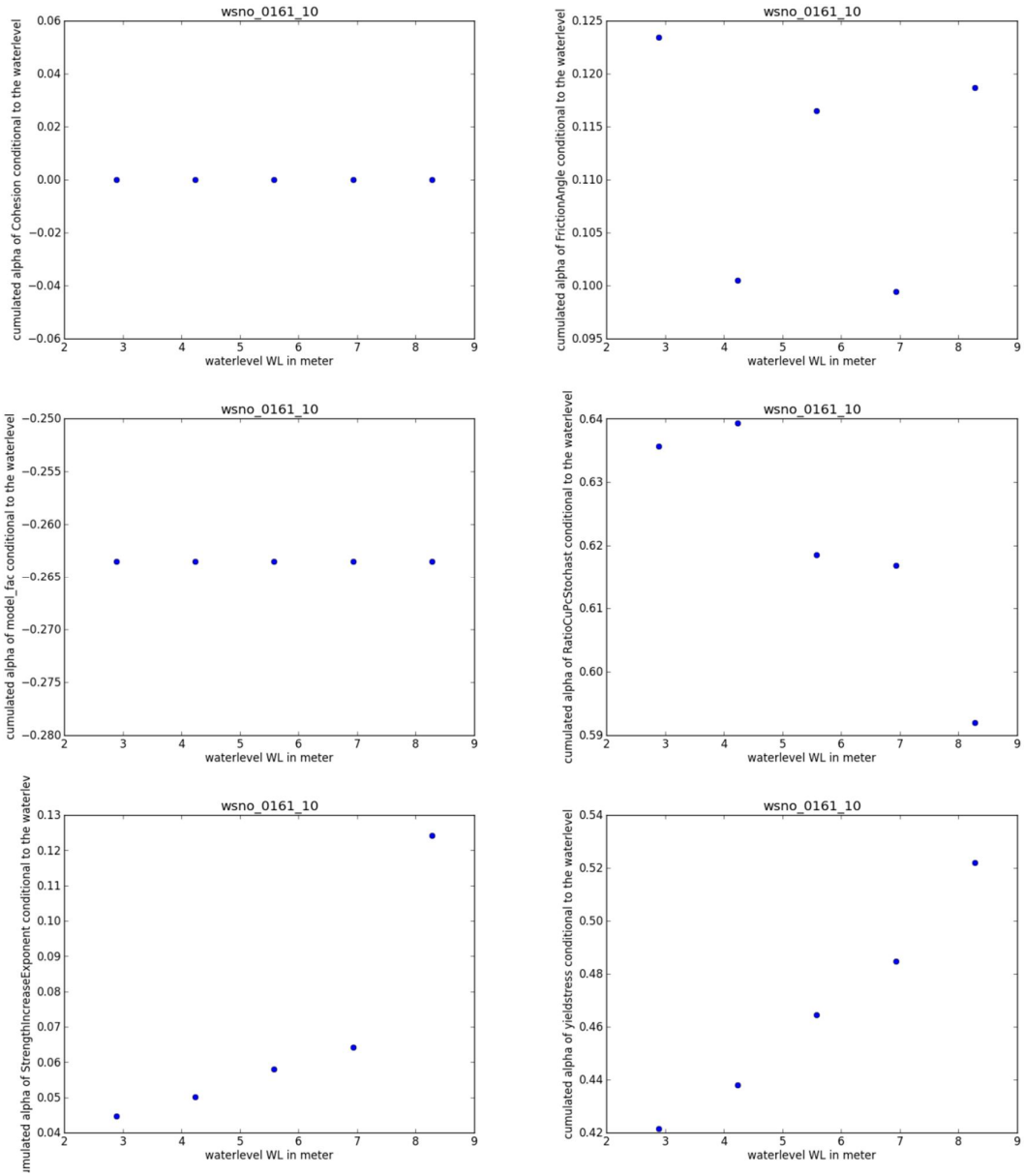

Figure C.82 Output case wsno_0161

Basic geometry + 20m berm

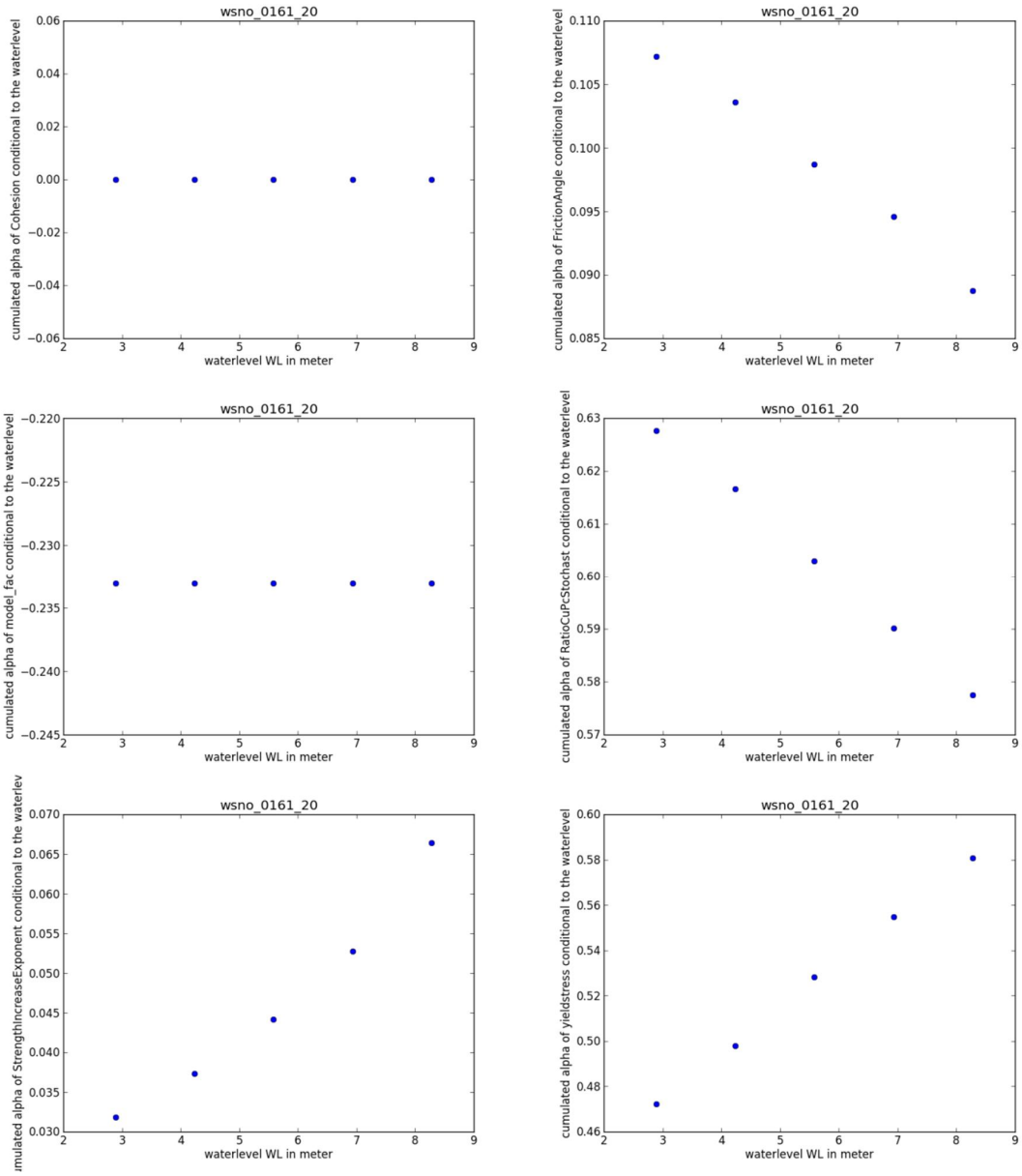

Figure C.83 Output case wsno_0161

Slip circle in design point

Basic geometry

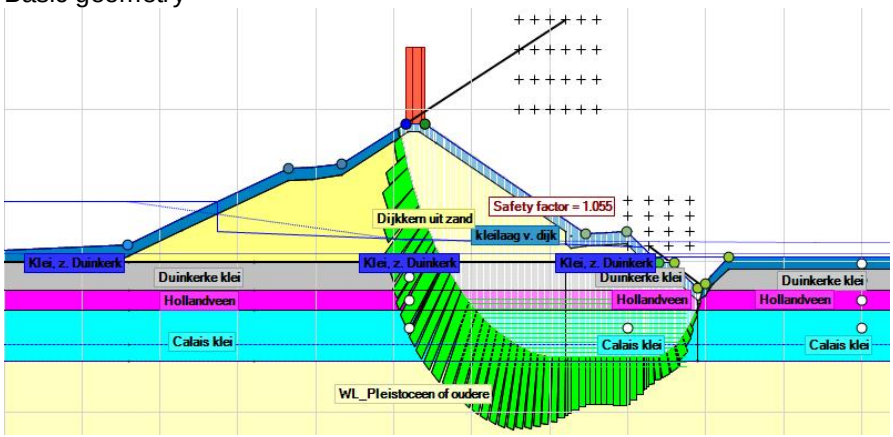

Basic geometry + 10m berm

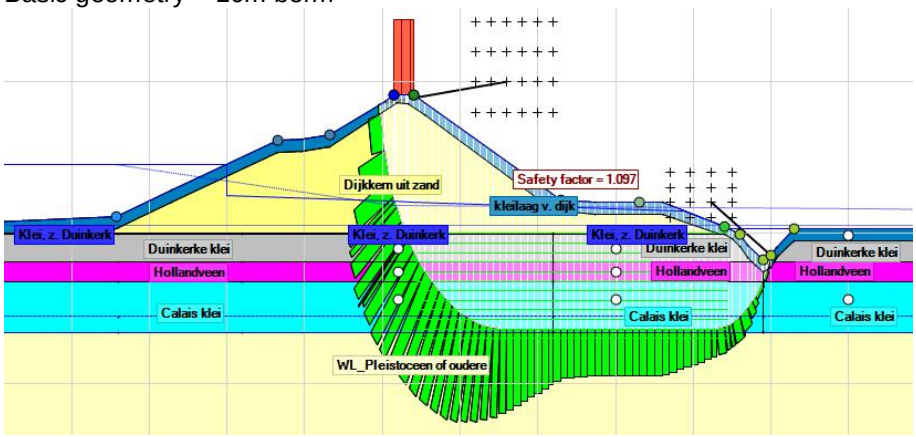

Basic geometry + 20m berm

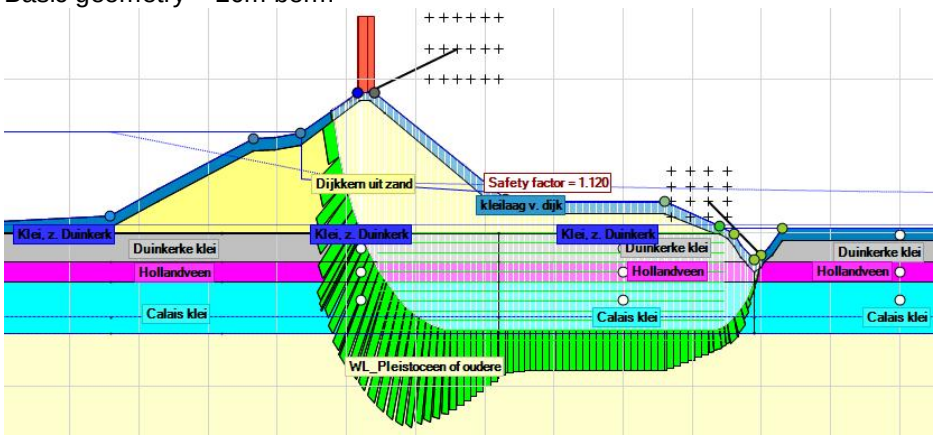

Figure C.84 Slip circle in the design point.

C.12 Dp_92

This appendix describes the steps and decisions made in setting up and performing probabilistic calculations for slip failure of the inner slope for a specific cross section. Furthermore it summarizes the intermediate results for this case.

C.12.1 Setup

Location and geometry

The location of this cross section (VNK: dp_92, PC-Ring ID 52001005) is at the river Ijssel, near Zutphen.

Stratification

The stratification of the subsoil schematization from the VNK-2 project. There is a separation between soils below and besides the dike.

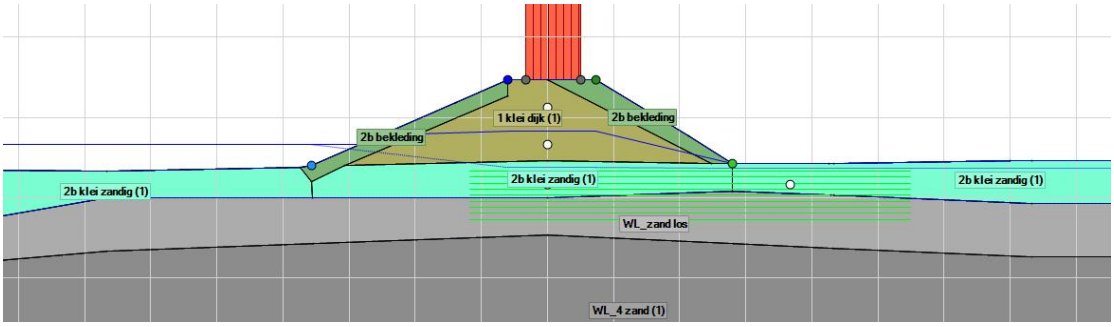

Figure C.85 Schematization

Material properties

Material properties for the soil types are taken from the original schematization (river undrained parameters). The distribution parameters for the random soil types are summed in the next table. This dataset already includes averaging from regional to local data and includes averaging along the slip plane. The POP has a mean value of 20 kPa for all materials. The standard deviation is 6 kPa, according to the WTI-SOS database.

Table C.23 Material parameters

Soil type	Vol. weight	Friction angle		Su-ratio		Strength increase exp.	
		μ	σ	μ	σ	μ	σ
WL_4 zand (1)	20/18	35.24	2.4				
WL_zand los	19/17	35.24	2.4				
2b klei zandig (1)	19/18.7			0.3	0.03	0.90	0.02
1 klei dijk (1)	20.2/19.9			0.3	0.03	0.90	0.02
2b bekleding	19/18.7			0.3	0.03	0.90	0.02
zand los	19/17	35.24	2.4				

Waternet

The creation of phreatic lines is done by D-Geo Stability, according to the following options.

Table C.24 Waternet Creation options

Option	Value
Creation method:	Create Waternet
Dike/soil material	Clay dike on clay
PL1 line creation method	Ringtoets WTI 2017

Since the MHW according to the new safety standards for this cross section is higher than the crest level, the MHW and water level distribution is “transposed” to a plausible value: 1,0 m below the crest. The decimate height and exceedance frequency are taken from the PC-Ring database:

h_{dec} = 0,664 m

$1/F_{exc}$ = 1/3000

MHW = NAP +10,84m

The average high outside water level GHW is taken as the water level at mean discharge for the river IJssel, NAP +5,37 m. The minimum phreatic line in the dike body is defined by the Dupuit water level: NAP +9,50m. The polder water level is in the ditch NAP +8,20m.

For the PL3 and PL2 schematization, the leakage length is used. In this case back calculated from WTI Piping calculations. λ_{out} 1084 m and λ_{polder} 3440 m.

The intrusion length is determined according to Schoofs en Van Duinen (2006). Based on the stratification and the duration of high water, the intrusion length is found to be 7,5 m. However, this length is larger than half the impermeable layer thickness; therefore this intrusion length is not realistic anymore. The intrusion length is taken as 0, so the phreatic line will be interpolated from PL3 to PL1.

Traffic load

A uniform load of 13kN/m2 over a width of 2,5 m is applied as temporary load for traffic in emergency situations.

Yield stress points

The yield stress points are defined in each layer. The yield stress value is defined at daily water level by the next equation $\sigma_y = \sigma'_{v,i} + POP$. The used POP value is based on expert knowledge.

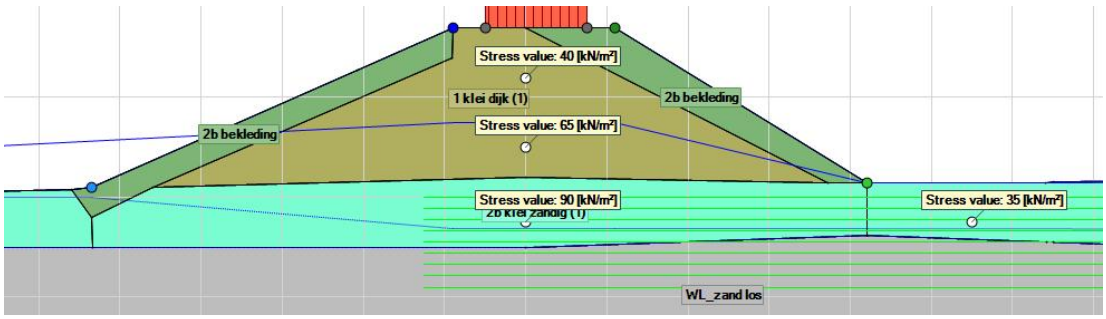

Figure C.86 Schematization of yield stress

Other information

The blanket layer is less thick than 4 metre, so uplift can occur; therefore the shear strength has to be reduced for uplift conditions:
No reduction of c-phi in case uplift potential n < 1,199
Full reduction of c-phi in case uplift potential n > 1,200

Stability berms

In order to reach reliability numbers which are in the range of interest, a stability berm is added. The material is the general “zand los”. The berm length (measured as the total berm top width) is 0 for the basic geometry and 5 m.

C.12.2 Probabilistic prototype

Deterministic sanity check

Mean values

Characteristic values

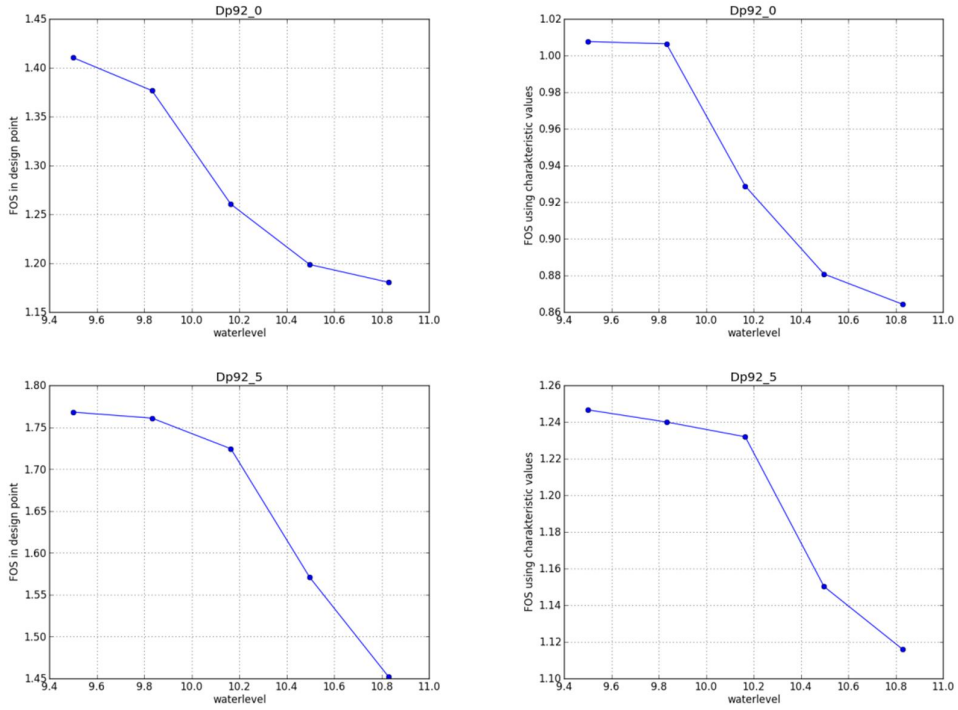

Figure C.87 Output case dp_92

Probabilistic fragility curve (Max_beta_interation_inner_loop = 0.05)

	dp	alpha^2
beta final	3.44	
SF char	0.840	
CuPc		0.507
m		0.003
yieldstress		0.380
cohesion		0.000
fric angle		0.000
model fac	1.044	0.110
water level	8.66	0.000

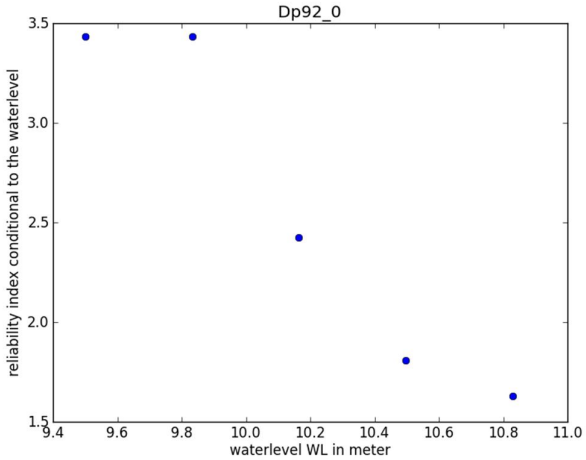

.

	dp	alpha^2
beta final	5.56	
SF char	1.060	
CuPc		0.516
m		0.001
yieldstress		0.376
cohesion		0.000
fric angle		0.000
model fac	1.068	0.106
water level	8.71	0.001

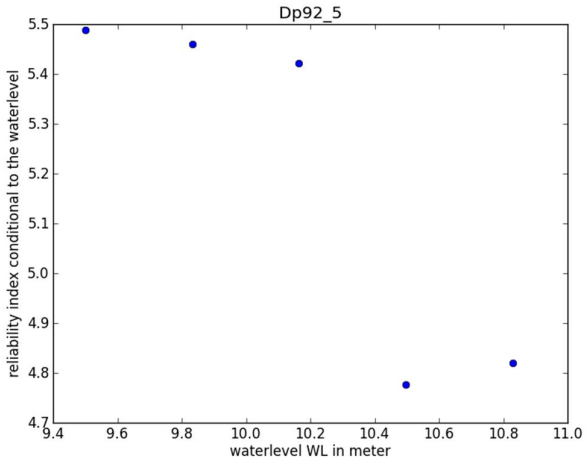

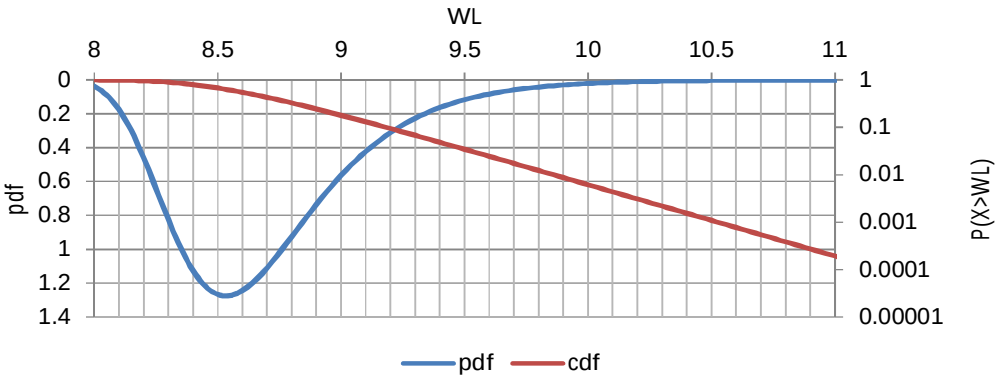

Figure C.88 Output case dp_92

Cumulative alpha values conditional to the water level

Basic geometry

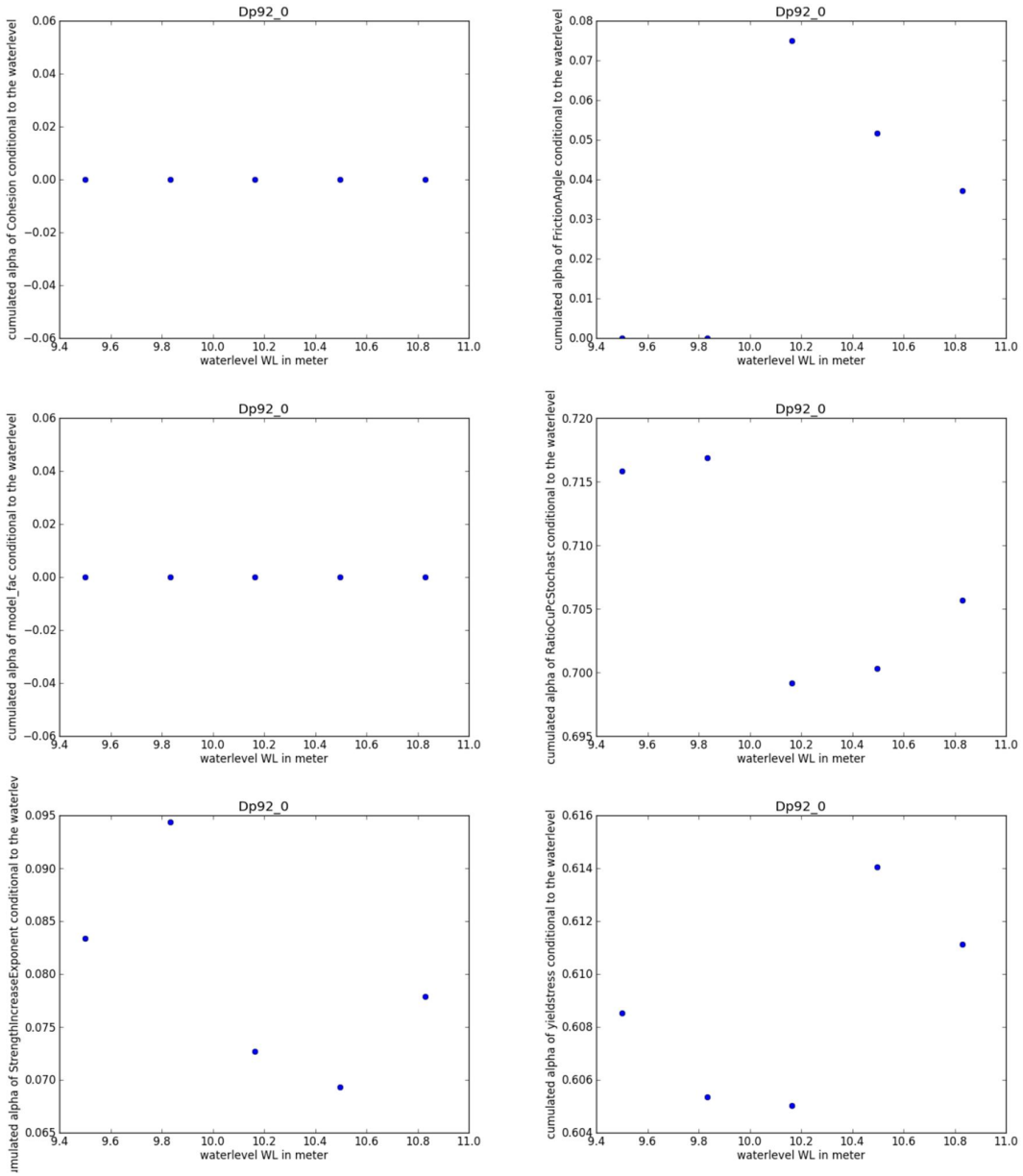

Figure C.89 Output case dp_92

Basic geometry + 5m berm

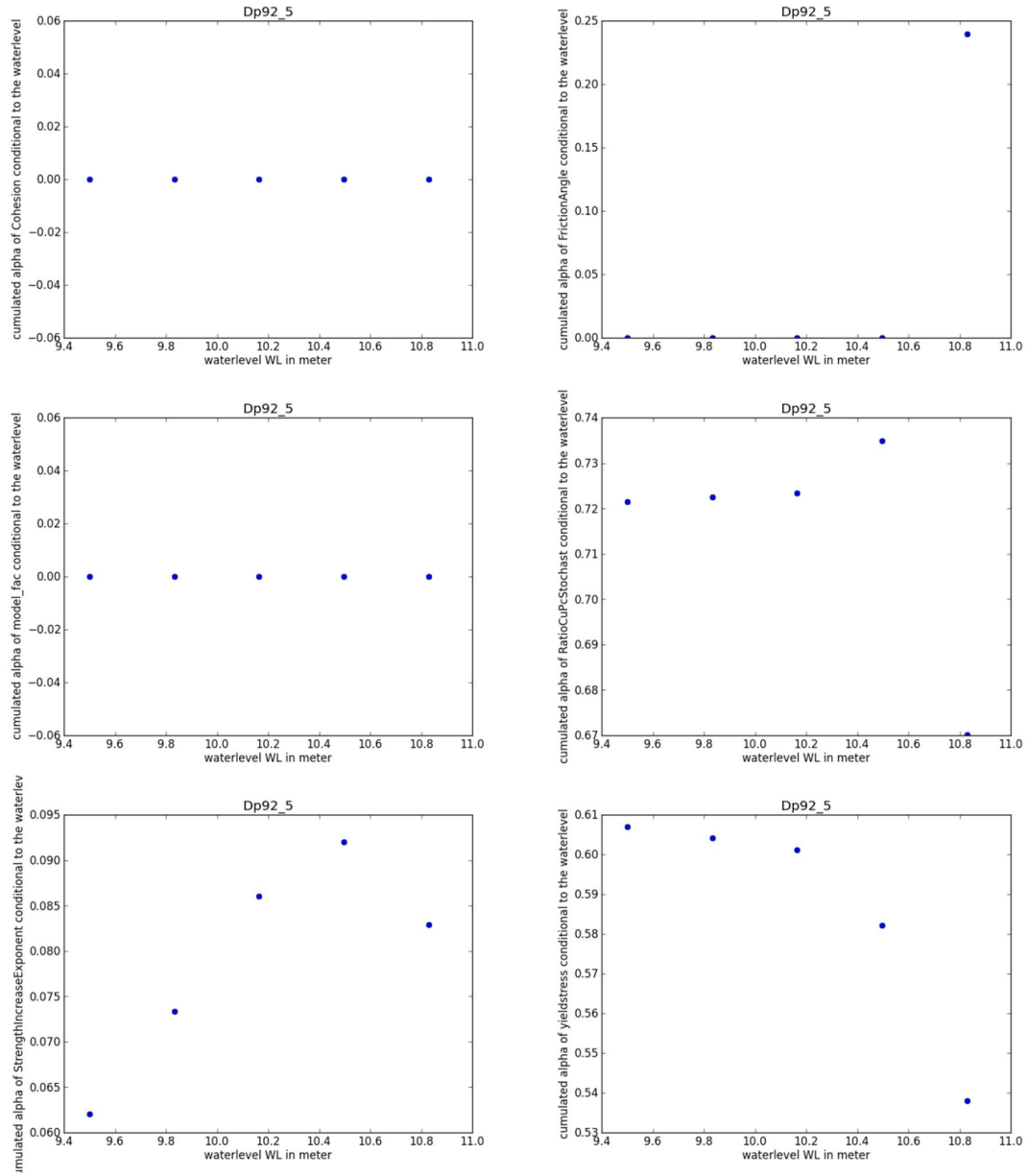

Figure C.90 Output case dp_92

Slip circle in design point

Basic geometry

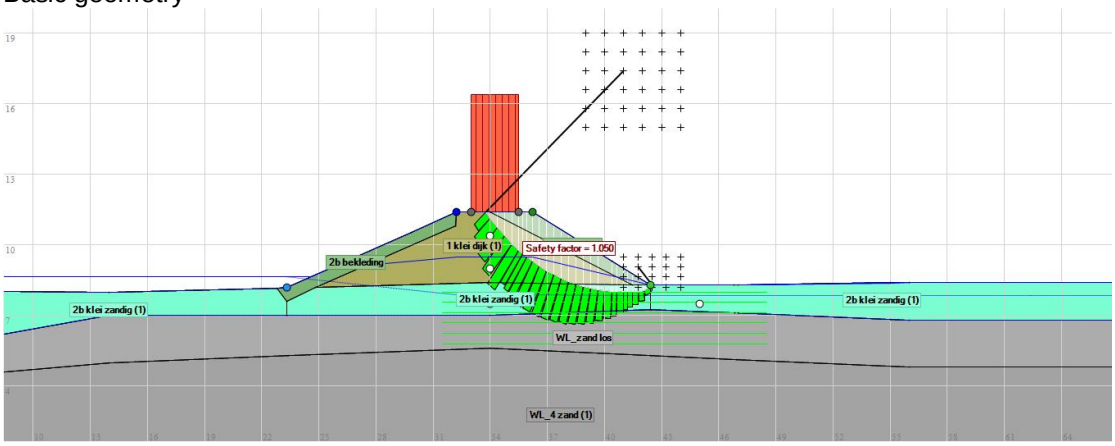

Basic geometry + 5m berm

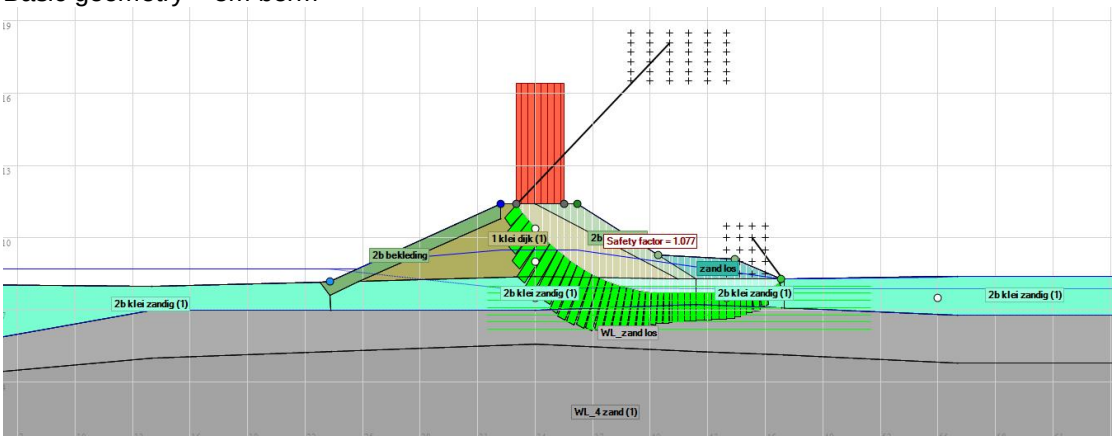

Figure C.91 Slip circle in the design point

D Appendix: Spatial averaging

D.1.1 Rationale

This appendix describes how averaging of uncertainties is implemented in the calibration of slope stability. Averaging can to be taken into account because the soil properties fluctuate rapidly in the vertical dimension relative to the dimension of the failure plane, resulting in averaging of the vertical part of the variance

D.1.2 Description averaging

There are various formulas circulating with respect to averaging in slope stability, e.g. the one from TRWG (2001):

$$\sigma(c_{u,G})^2 = \Gamma(G)^2 \cdot \sigma(c_u)^2 \quad (1)$$

Where $\sigma(c_{u,G})^2$ is the variance of the average shear strength along a slip circle, $\sigma(c_u)^2$ is the point variance of the slip circle and $\Gamma(G)^2$ is the variance reduction factor; see TRWG (2001) and below.

As we typically deal with regional datasets, a stochastic model was developed. This model basically says that a part of the regional variance ($\sigma_{reg}{}^2$) is due to local fluctuation of the shear strength ($\sigma_{loc}{}^2$) and part is due to regional fluctuations in of the local mean of the shear strength ($\sigma_{loc,aver}{}^2$).

There are three effects that determine the local, average standard deviation ($\sigma_{loc,aver}$), that should be input into the computation based on the measured data (σ_{reg})

1. Incorporate the relation between regional and local variability: the a factor
2. Incorporate local averaging along failure plane: the γ_d factor
3. Incorporate the effect of limited measurements: n

This can be summarized by eqn (4), an equation used in VNK2 and in the 'schematiseringshandleiding' (Van Deen and Van Duinen, 2015).

$$\sigma_{loc,aver} = \sigma_{reg}\sqrt{(1-a) + a\gamma_d + \frac{1}{n}} \quad (2)$$

where:

- σ_{reg} is the standard deviation of the regional variation
- a is the portion of the total variability stemming from local variability (and (1-a) the fluctuations of local means) [default: a = 0.75, Leidraad Rivieren]. In case of a local dataset, a =1.
- γ_d is the variance reduction factor: $\gamma_d = \min(D_v \sqrt{\pi}/d, 1)$
- Dv is vertical correlation length, d is layer thickness
- *n* is the number of samples [default: *n* = 10]. NB. Alexander says 20 would be better.

When it is assumed that all local variance averages, γ_d goes to 0 and eqn. 4 reduces to:

$$\sigma_{loc,aver} = \sigma_{reg}\sqrt{(1-a) + \frac{1}{n}} \quad (2)$$

This equation is found in e.g. TRWG (2001).

D.1.3 Including averaging in the WTI

Su data and m are the only parameters being currently considered for averaging. Yield stress is dominated by transformation uncertainty, which doesn't average, hence, averaging in yield stress is not considered. The inputs of the cases provided by Cluster Macrostrability already incorporate eqn. 2. Hence, there was already an implicit assumption of full local averaging (γ_d =0). Cluster Macrostability's input is based on a regional dataset, as is common. Due to the averaging already being incorporated, the Su data can be treated as mean and variances of the local average shear strength, and no more processing is necessary.

E Appendix: The insensitivity to the water level

E.1 Description low sensitivity water level

This section is based on internal memo's and meetings and discussions by e-mail between various WTI clusters.

The results of the calibration for inner slope stability (STBI) with the new undrained material model, show a limited influence of the outer water level on the factor of safety and reliability. This memo describes results and other observations, gives explanations and presents some questions which are the consequence of the undrained material model and specifically the calibration.

Results

The (preliminary) results are presented below

- The relation between factor of safety and reliability index shows low spreading.
- The influence factor of the outer water level is lower than 0.1 for the most cases, however a few of these resulted in high alpha values in the previous (VNK) study.
- The beta dependent relation is relatively gentle.
- Only case wsno_0161 shows a relatively large influence of the water level. However this is a case with sand core which is calculated drained.
- Both cases with and without uplift show a limited influence of the outer water level.
- To exclude the new D-GeoStabilty kernel and Waternet Creator from the discussion, one case is calculated with drained parameters. This indeed leads to a high alpha value for the water level, which is comparable with the results of VNK.

Possible explanations

Possible explanations for the relatively low influence of the water level are:

1. The undrained material model. Su is calculated with $su = \sigma'vi \cdot S \cdot OCR^m$ with $OCR = \sigma'vy / \sigma'vi$. The yield stress σ'vy is a fixed value which is not influenced by water levels or pore water pressures, as long as these have short durations. If the effective stress σ'vi decreases by an increase of water level, the OCR increases with the effective stress' σ'vi decrease. Consequently, the su only changes by the strength exponent $m<1$. If m would equal 1, the su would be fully insensitive for changes in effective stress and pore water pressures.
2. The phreatic level. Dikes have a initial phreatic level that is higher than the daily outer water level. So if the outer water level increases to a slightly higher level than on average, this does not lead to an increase of the phreatic level. A sufficiently high outer water level (with low probability of occurrence) is needed for the phreatic level to increase relative to the initial level. In case this initial phreatic level is relatively high (because of a rather impermeable dike or wide dike base), the influence of the outer water level on the phreatic level (and thus shear strength) is limited.
3. Typical location of the slip plane. If the slip plane goes through the aquifer, the deeper part of the slip plane is sensitive to changes of the outer water level and pore water pressures. In the sand, the drained material model is used, so the shear strength is directly dependent to the change of effective stresses. If the slip circle goes through clay only, the influence of the water level is low.
4. If the uncertainty of the strength parameters (Resistance) is high, it is evident that the influence of the water level is low (Load).

Implications

The largest implication is the difference with the past, when the strength of dikes (for slope stability) were assumed to be sensitive for the outer water level. This can result in acceptance questions. Another issue this how proven strength affects the safety philosophy.

Case 41_W_237_Ite

Uplift en α_h^2 is 0.1

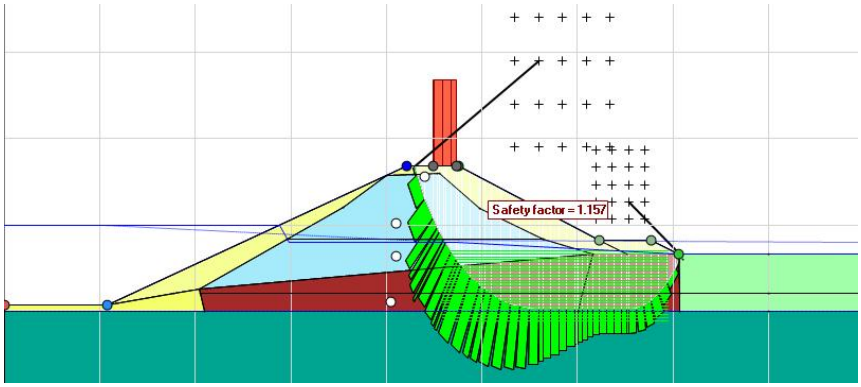

Figure E.1 Glijcirkel in het ontwerpunt:

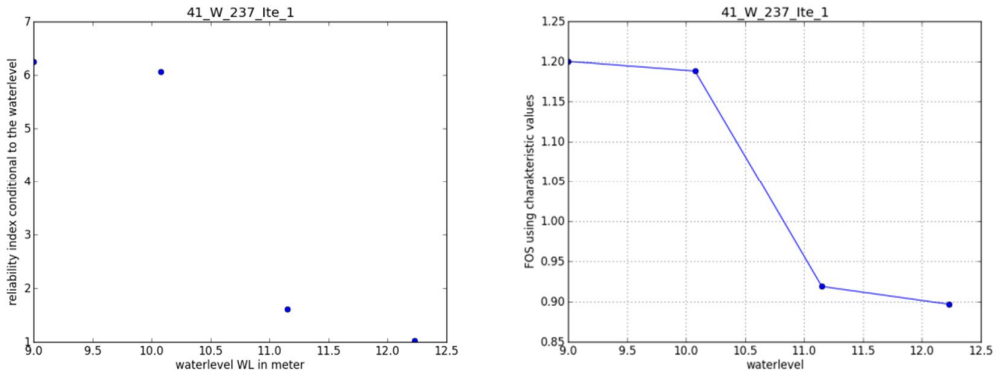

Figure E.2 Betrouwbaarheidsindex (links) en veiligheidsfactor (rechts) als functie waterstand

DP43
No uplift, low alpha

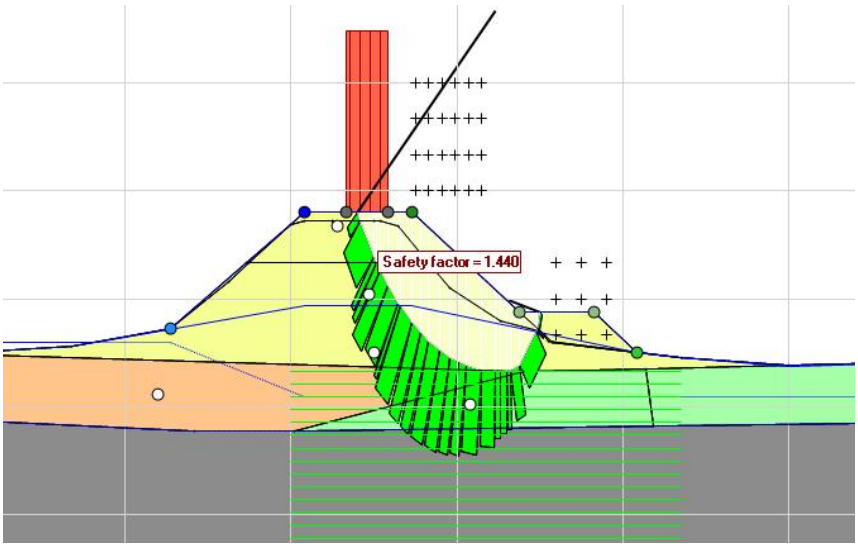

Figure E.3 Slip circle in the design point

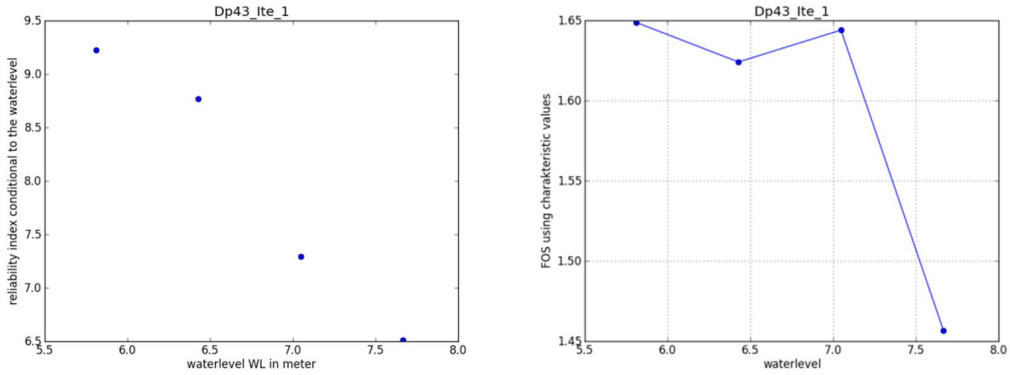

Figure E.4 Reliability index (left) and factor of safety (right) versus the water level.

dwp0_lte
Deep slip plane, low alpha.

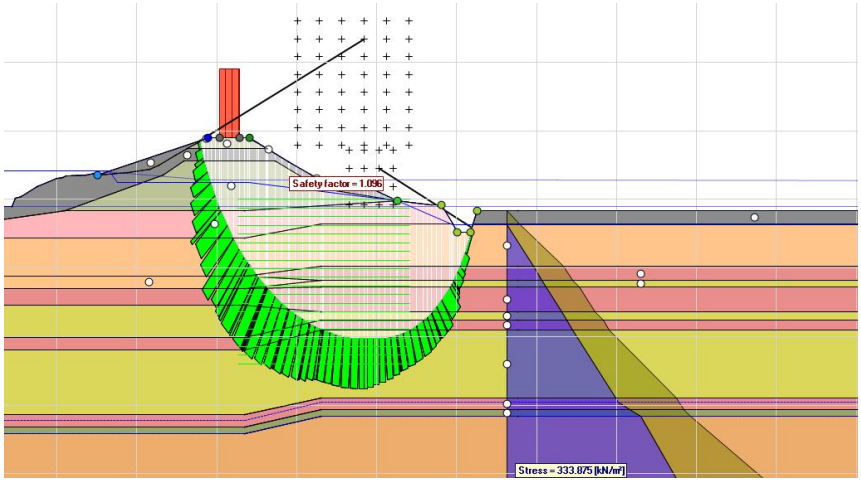

Figure E.5 Slip circle in the design point

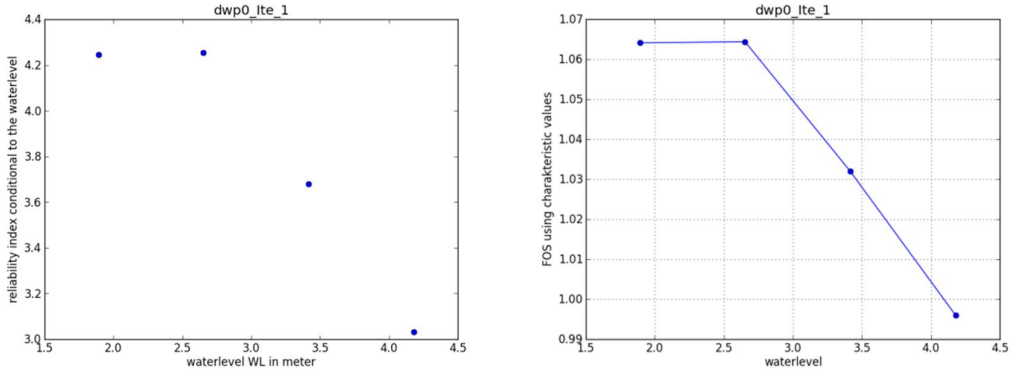

Figure E.6 Reliability index (left) and factor of safety (right) versus the water level.

E.2 Preliminary investigation implications proven strength

This section provides a preliminary investigation into proven strength (or performance observations). Proven strength becomes especially interesting when there is limited sensitivity for the water level, as seems the case for undrained shear strength computations. A very rough estimate is made for 11 cases. Similar approaches as for the Markermeerdijken are used. A main assumption is made that future conditions are the same as during the observation. This is an upper bound approach (not conservative), and would probably not hold for e.g. the phreatic line, that is not only influenced by the outside water level but also by e.g. rainfall. Therefore, only relatively low observed performances are considered. The results are presented in Figure E.7 The figure shows the decrease in failure probability after incorporating proven strength (the proven strength factor). This factor can be very large. A main limitation of the presented analysis is that the proven strength factor needs a high number of Monte Carlo simulations to be computed accurately. Due to time constraints, this was not possible. E.g. cases DV13 and 41_W_237_0 did not show any change for proven strength because of the limited amount of samples used. Hence, these have been omitted from the figure.

This, together with the used upper bound approach, justifies further study into proven strength. Since proven strength is very location dependent, the results shown below should not be interpreted as absolute values but merely as first indications.

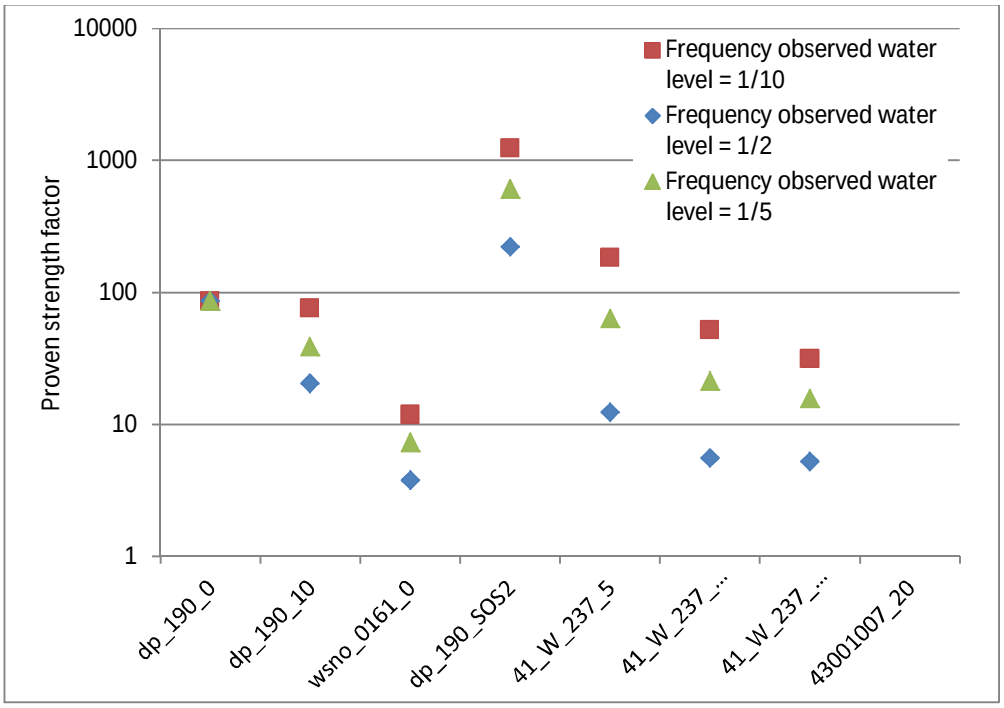

Figure E.7 Preliminary potential effects of proven strength.

E.3 Comparison calibration with drained analysis

This section presents a comparison between a drained and undrained analysis of cross-section 41_W_237. The computations are made with the prototype, hence the same version of D-Geo Stability, waternet creator, geometry, etc are used. The only difference is the material model. This allows differentiating between the material models, keeping all other factors except the material properties the same. Drained input parameters of VNK2 are used, which not necessarily correspond to the undrained parameters used in the calibration.

The results of the comparison are presented in the table and figures below. The main conclusion is that $\alpha^2_{water\ level}$ reduces from 0.89 to 0.11 when the transition is made from drained to undrained. This supports the idea the indeed it is the material model and/or the uncertainty related to the undrained material properties that causes the low $\alpha^2_{water\ level}$ (and very different Beta-values)

Table E.1 Comparison drained and undrained

	Calibration prototype	
	Drained	Undrained
β	4.33	2.06
α^2 CuPc	0	0.213
α^2_m	0	0.030
$\alpha^2_{yield\ stress}$	0	0.351
α^2_c	0.064	0.000
α^2_ϕ	0.031	0.002
$\alpha^2_{model\ fac}$	0.020	0.297
$\alpha^2_{water\ level}$	0.885	0.107
$\alpha^2_{material}$		

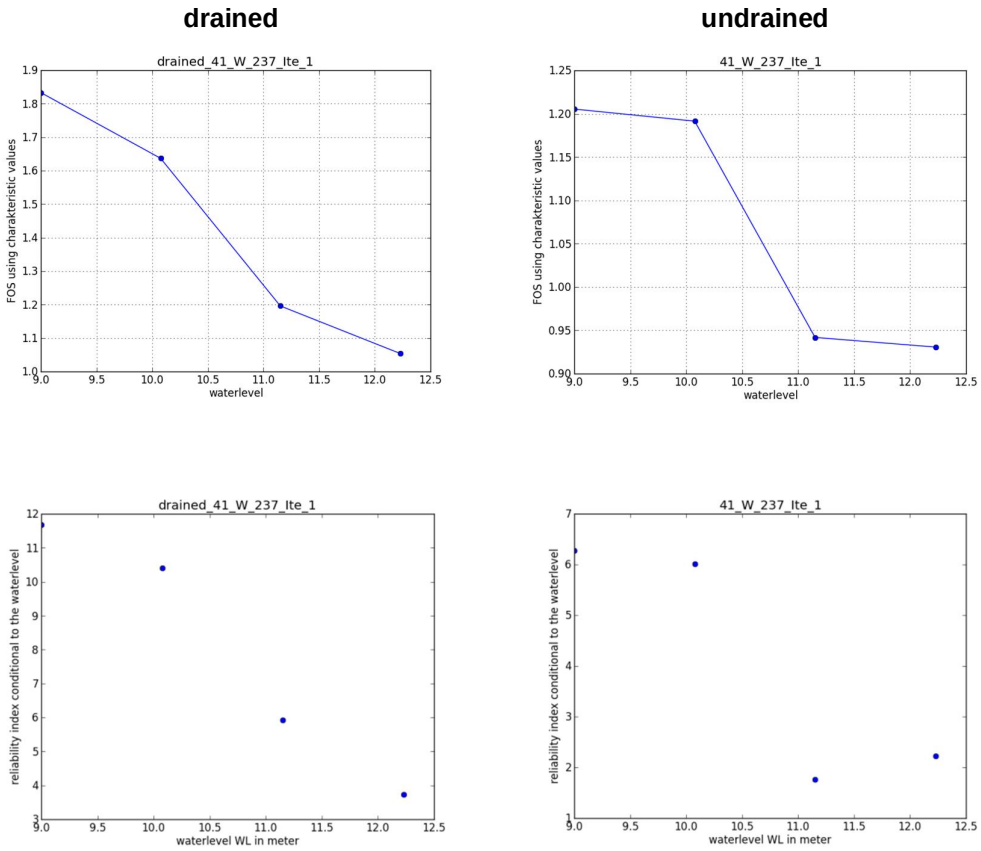

Figure E.8 Comparison drained and undrained analysis

F Appendix: The influence of traffic loads

F.1 Introduction

In all calibration calculations, a traffic load is taken into account: a uniformly distributed load of 13kN/m^2 over a width of 2,5m for traffic in emergency situations. A consequence analysis is made for the deterministic and probabilistic calculations of two cross sections with and without traffic load. The first involves a case with a small slip plane and the second involves a case with a large (deep) slip plane. In the next sections, the results are discussed.

F.2 Dp92_0

This case (without berm) has a relatively small slip plane, mainly through the dike core. Uplift can occur at high water levels. In the next figures the difference in FoS for mean and characteristic values is shown. It should be noted that the scale of the pictures is different. The difference in FoS is about 10%.

Dp92_0 without traffic load **DP92_0 with traffic load**

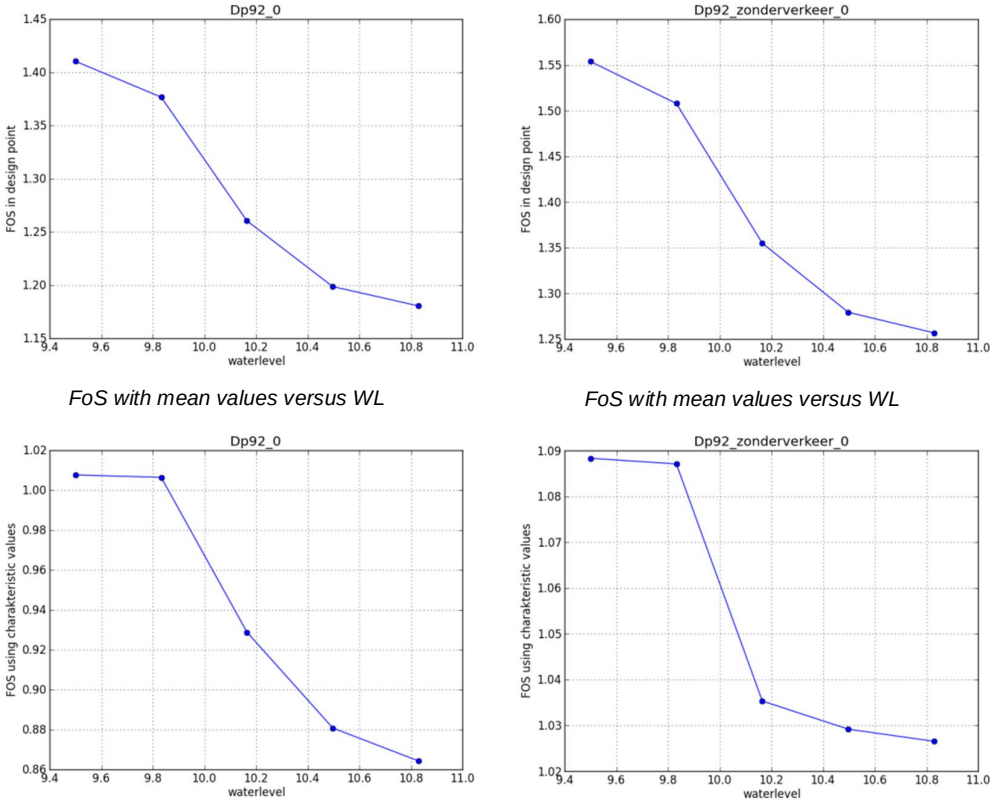

FoS with mean values versus WL *FoS with mean values versus WL*

FoS with characteristic values versus WL *FoS with characteristic values versus WL*

Figure F.1 Comparison safety factors with and without traffic load

In the next figure, the beta conditional water level is shown for both cases. As expected, the reliability indices conditional on a given water level are in general higher in case no traffic load is present. The final reliability is significantly higher; in case no traffic load is taken into

account, the probability of failure is about afactor 20 lower. The influence coefficients are in the same order.

Dp92_0 without traffic load **DP92_0 with traffic load**

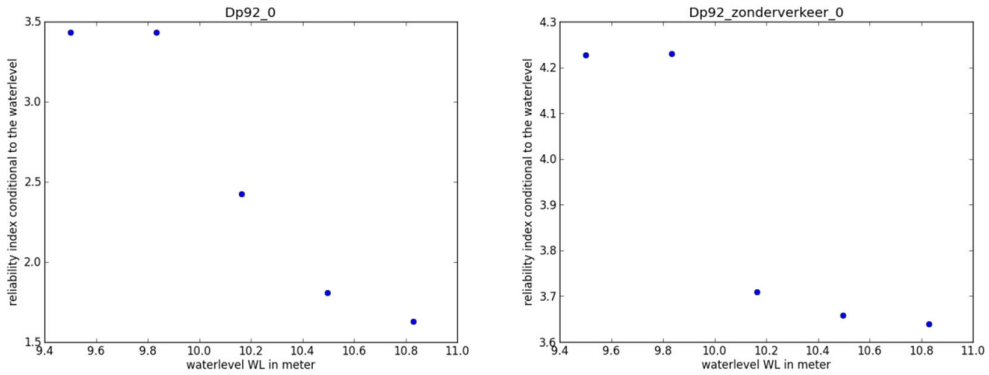

β | *WL versus WL* β_{final} = 3,44

β | *WL versus WL* β_{final} = 4,21

Figure F.2 Comparison beta's with and without traffic load

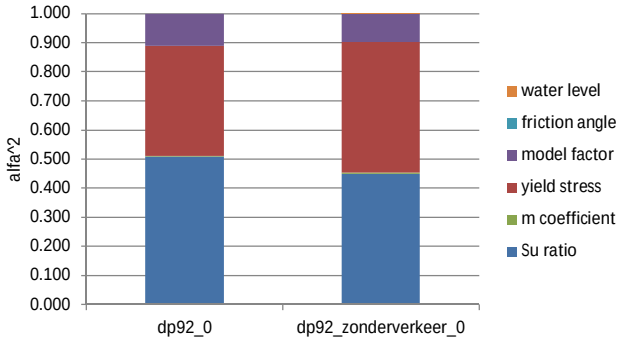

Figure F.3 Comparison influence factors with and without traffic load

F.3 43001007_10

This case (with a 10m berm) has a relatively large and deep slip plane. Uplift is not an issue in this case. In the next figures the difference in FoS for mean and characteristic values is shown. It should be kept in mind that the scale of the pictures is different. The difference in FoS is about 4%.

43001007_10 without traffic load **43001007_10 with traffic load**

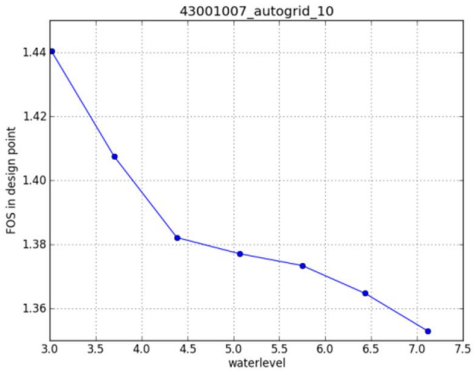

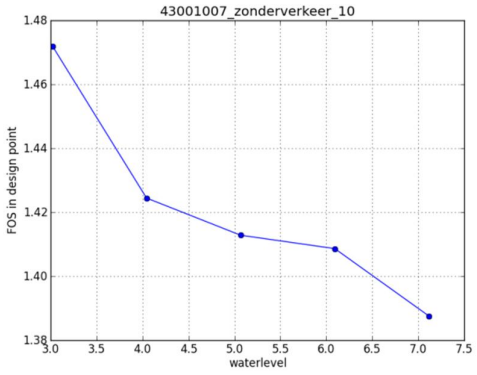

FoS with mean values versus WL *FoS with mean values versus WL*

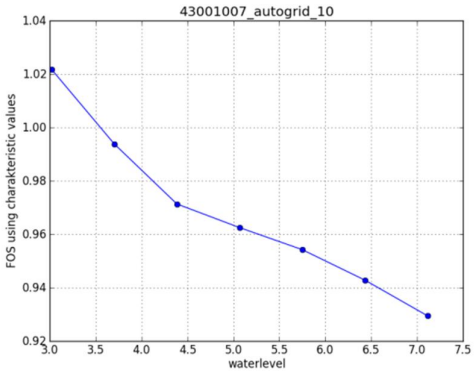

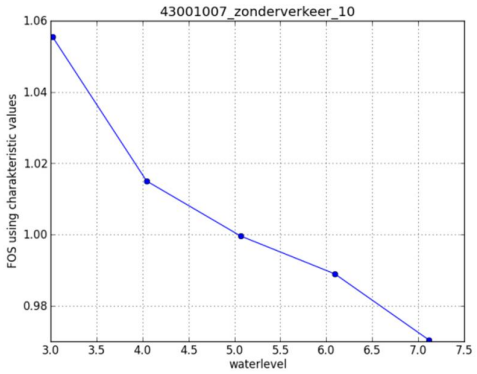

FoS with characteristic values versus WL *FoS with characteristic values versus WL*

Figure F.4 Comparison safety factors with and without traffic load

In the next figure, the beta conditional water level is shown for both cases. As expected, the reliability indices conditional a given water level are higher in case no traffic load is present. The final reliability is a bit higher in case no traffic load is taken into account, the probability of failure is in the order of a factor 4 lower. The influence coefficients are in the same order.

43001007_10 without traffic load **43001007_10 with traffic load**

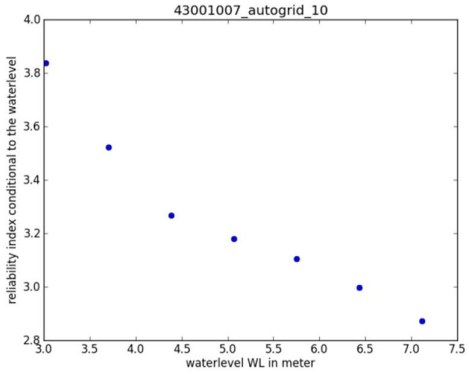

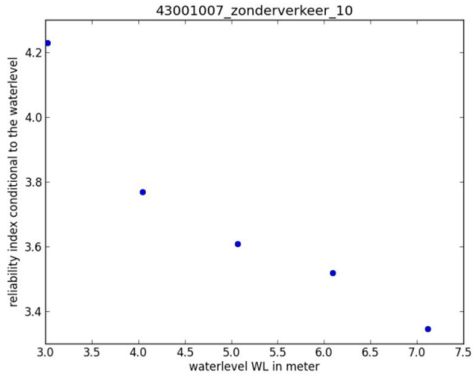

β | *WL versus WL* β | *WL versus WL*

β_{final} = 3,37 β_{final} = 3,76

Figure F.5 Comparison beta's with and without traffic load

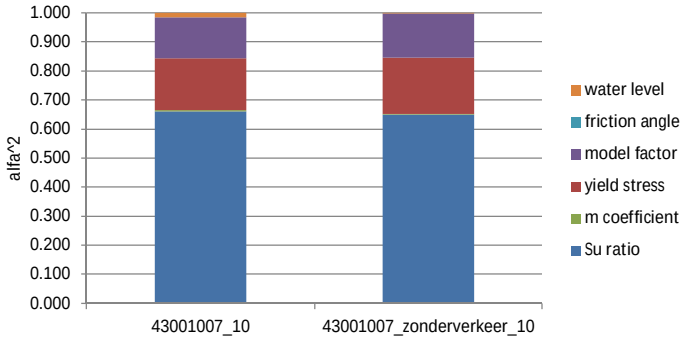

Figure F.6 Comparison influence factors with and without traffic load

F.4 Conclusions regarding the calibration fit

Both the cases with traffic load and without traffic load are depicted in the calibration graph. It is clearly seen that ignoring the traffic load leads to an increase in both the Factor of Safety (characteristic values) and the reliability index. The increase of the dp92 FoS is relatively larger than the FoS increase of 43001007, relative to the reliability index. In general the points are in the expected range of the scatter and the shift is in the same order as the calibration fit, so the traffic load does not influence results of the calibration. This may be explained by the fact that the influence coefficients are nearly the same.

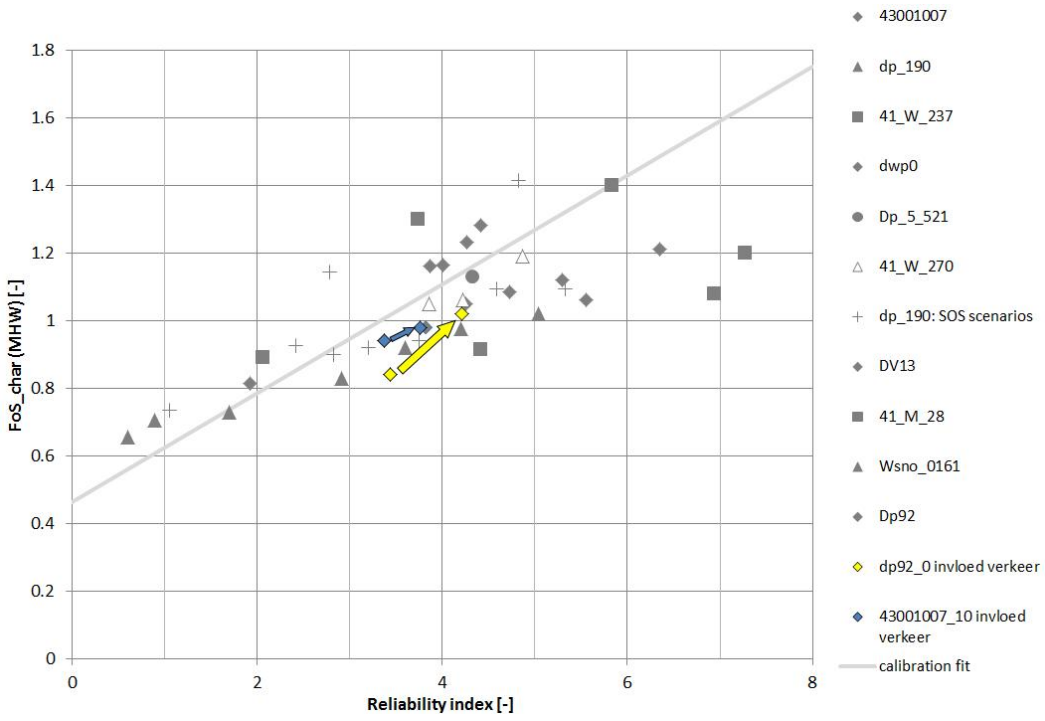

Figure F.7 Influence traffic load on reliability index and factor of safety